

# **Synthesis of Highly Fluorinated Diels-Alder Polyphenylenes**

Jessica Price Evans

Dissertation submitted to the faculty of the Virginia Polytechnic Institute and State University in partial fulfillment of the requirements for the degree of

Doctor of Philosophy  
In  
Chemistry

Paul A. Deck, Chair  
Karen J. Brewer  
Paul R. Carlier  
Richard D. Gandour  
Timothy E. Long  
S. Richard Turner

July 26, 2010  
Blacksburg, VA

Keywords: Diels-Alder reaction, fluorine, fluoroaromatic, cyclopentadienone synthesis, step-growth polymerization, perfluoroarene, polyphenylene

# Synthesis of Highly Fluorinated Diels-Alder Polyphenylenes

Jessica Price Evans

## Abstract

Fluoropolymers have useful properties including high thermal stability, chemical resistance, low dielectric constants, and both hydrophobic and oleophobic character, as compared to non-fluorinated analogues. Meanwhile, Diels-Alder polyphenylenes (DAPPs) are known for thermal stability as well as their rigid structure and glassy physical characteristics, which have led to a variety of film and membrane applications. This dissertation merges these two fields by demonstrating a novel and general synthetic approach to highly fluorinated DAPPs. These polymers are expected to retain the physical characteristics of glassy, non-fluorinated DAPPs while also incorporating the desirable attributes of fluoropolymers.

The polymer synthesis described herein is based on the well-established polycondensation of bis(cyclopentadienone) (CPD) monomers and dialkynes. Our first main scientific contribution is a general method for preparing CPDs containing both a fluoroaromatic linker and variable fluoroaromatic head-groups. Our CPD synthesis uses nucleophilic aromatic substitution reactions of cyclopentadienyl anions and perfluoroarenes, as well as a new catalytic method of converting cyclopentadiene methylene ( $\text{CH}_2$ ) groups into the corresponding ketones ( $\text{C}=\text{O}$ ) that is the primary dissertation subject of Brian S. Hickory in our laboratory. The overall synthesis is notable for its use of inexpensive starting materials, its efficiency, and its structural versatility.

Our second main contribution is the synthesis of novel highly fluorinated Diels-Alder polyphenylenes (DAPPs). Fluorinated DAPPs varied in their molecular weight, in the identity of the lateral fluoroaryl substituent (pentafluoro-phenyl or tetrafluoro-4-pyridyl), and in the structure of the aromatic dialkyne monomer. These polymers are glassy materials with high

glass transition temperatures and high thermal stability. Since the polyphenylene structure is intrinsically rigid, the polymers form brittle films even at molecular weights of over 30,000 ( $M_w$ ). Unlike many fluoropolymers, the fluorinated DAPPs are freely soluble in common organic solvents such as tetrahydrofuran and chloroform. An unknown side reaction competes with the polymer propagation and reduces the highest obtainable molecular weights, which limit the ability to form films. However, a stoichiometric imbalance leads to highly fluorinated polyphenylene oligomers terminated with either alkyne or CPD end groups ( $M_n = 9000$ ).

Because preliminary experiments had shown that the desired Diels-Alder propagation reaction was slower than expected, we also undertook a detailed model study of the reaction conditions needed for Diels-Alder reactions of fluorinated CPDs and aromatic alkynes. These experiments showed that protic polar solvents (e.g., *m*-cresol) and conventional heating at ca. 150 °C optimize reaction rate while minimizing side-reactions that can contribute to lower molecular weight in corresponding polymerization reactions.

*This dissertation is dedicated to my grandma, Inis Pruitt. I can only hope science will bring the cure for Alzheimer's disease to humankind one day.*

## Acknowledgements

I am thankful for my advisor, Dr. Paul Deck for his guidance, unique enthusiasm, and shared knowledge throughout my time at Virginia Tech. He is truly my most important inspiration and defines how I think of chemistry. I would also like to thank my committee members for their continued support, advice, and guidance. Dr. Carla Slebodnick is an excellent crystallographer and helpful instructor. I appreciate Prof. Gordon Yee for his always useful discussions, continuous support, insight and friendship. I would also like to extend my gratitude to Dr. Rebecca Brown and Mark Flynn for help with size exclusion chromatography. The outstanding university staff is vital to our department including: Angie Miller, Claudia Brodtkin, Geno Iannaccone, Hugo Azurmendi, Bill Bebout, Sr., Sharelle Dillon, Tom Wertalik, Emilie Shephard, Laurie Good, Mary Jane Smith, Valerie Owens, Judy Spicer, Roberta Gilbert and Patricia Angus.

I would also like to extend a more personal note of gratitude to my labmates in Dr. Deck's group for their continued help and support: Brian Hickory, Sanghamitra Sen, and Charles Carfagna. A special thanks should also go to my volleyball team including Prof. Gordon Yee, Prof. Alan Esker, Prof. Diego Troya, Lesley Owens, Leslie Adamczyk, Jeff Waldon, and Terry Whitesell for the extracurricular activities that kept me sane. I am sincerely grateful for the people who led me to choose this path, including Tom Wilson, Latanya Walker, and Gail Webb. Lastly and most importantly, I would like to thank my family, especially my husband, Adam, for love and support since I started on this long journey.

## Table of Contents

<b>Dissertation Overview</b>	<b>1</b>
<b>Chapter 1. Literature Review</b>	<b>2</b>
1.1 Introduction	2
1.2 Synthesis of Polyphenylenes	3
1.2.1 Oxidative Couplings (Kovacic Synthesis)	4
1.2.2 Metal-Enabled Sigma Couplings	7
1.2.3 Bergman Cyclization	13
1.2.4 Aromatization of Poly(cyclohexadiene)	14
1.3 Nucleophilic Substitution in Perfluoroarenes	14
1.3.1 General Overview of S <sub>N</sub> Ar	15
1.3.2 Trends in S <sub>N</sub> Ar Reactions of Perfluoroarenes	17
1.3.3 Alternative Substitution Mechanisms	18
1.4 Fluorinated Polymers by Nucleophilic Substitution	20
1.4.1 Linear Condensation Polymers	22
1.4.2 Perfluoroarylene Copolymers	27
1.4.3 Lateral Functionalization	30
1.4.4 Properties of Perfluoroarylene Condensation Polymers	32
1.4.5 Stability of Perfluoroarylene Condensation Polymers	34
1.5 Diels-Alder Polyphenylenes	35
1.5.1 Introduction to DAPPs	36
1.5.2 Hyperbranched or Dendritic Structures by Diels-Alder Polycondensation	41
1.5.3 DAPP Applications	42

1.6 Conclusions	45
<b>Chapter 2. Synthesis of Highly Fluorinated Biscyclopentadienone (CPD) Monomers</b>	<b>47</b>
2.1 Introduction	47
2.2. Monomer Design	47
2.2.1 Design Origins	47
2.2.2 A Generalized Monomer Synthetic Plan	50
2.2.3 A First-Generation Monomer Design	52
2.2.4 A Second-Generation Monomer Design	53
2.3 Results and Discussion	55
2.3.1 Monomer Synthesis by Plan 2	55
2.3.2 Monomer Synthesis by Plan 1	57
2.3.3 Creating a Family of Diketone Monomers	67
2.4 Crystallographic Analysis	71
2.5 Conclusions	76
2.6 Experimental	77
<b>Chapter 3. Model Diels-Alder Reactivity Studies of Highly Fluorinated Cyclopentadienones and Dialkynes</b>	<b>93</b>
3. 1 The Inverse Electron Demand DA Reaction	94
3.2 Model Reactivity Study of Monomer 1	96
3.3 Catalysis	98
3.3.1 Choice of Models	98
3.3.2 Basic Catalysis Concepts	99
3.3.3 Classical Lewis Acids: Background	99

3.3.4 Classical Lewis Acids: Results	100
3.3.5 Catalysis by Hydrogen Bonding: Background	100
3.3.6 Catalysis by Hydrogen Bonding: Results	102
3.4 Substituent Effects	105
3.4.1 Model Compound Synthesis	106
3.4.2 Analysis of Substituent Effects	107
3.5 Microwave Assisted Diels-Alder Reactions	108
3.5.1 Microwave Theory	109
3.5.2 Experimentally Observed Microwave Enhancement	112
3.6 Crystallographic Analyses	115
3.7 Conclusions	117
3.8 Experimental	117
<b>Chaper 4. Highly Fluorinated DAPPs by Diels-Alder Polycondensation</b>	<b>124</b>
4.1. Introduction	124
4.2. Experimental	125
4.3. Results and Discussion	128
4.3.1 From Models to Polymers	128
4.3.2 End Group Analysis	129
4.3.3 Testing the Step-Growth Model	130
4.3.4 Equivalent-Stoichiometric Polymerizations	133
4.4. Thermal characterization	138
4.4.1 Thermo-Gravimetric Analysis (TGA)	138
4.4.2 Differential Scanning Calorimetry (DSC)	139

4.5. Conclusions	141
<b>Chapter 5. Conclusions and Future Work</b>	<b>142</b>
5.1. Summary and Conclusions	142
5.2. Recommendations for future work	143
5.2.1 Achieving Higher Molecular Weights	143
5.2.2 Post-modification	143
5.2.3 Telomer Approaches	144
5.2.4 Triarylated Monomers	145
References	147
Appendix A NMR Spectra	154
Appendix B Copyright Permission	172

## List of Schemes

1-1	PPP can be synthesized from benzene and a Lewis acid.	4
1-2	Grigoras synthesized macromonomers from Suzuki coupling and polyphenylenes with PS arms by oxidative polymerization.	6
1-3	Two aryl halide compounds react with copper to form a new aryl-aryl bond and a copper halide.	7
1-4	Ullman coupling of 1,4-diiodo-2,3,5,6-tetrafluorobenzene produces fluorinated polyphenylenes.	8
1-5	Suzuki polycondensation typically involves C-C couplings of bifunctional aromatics and boron compounds.	10
1-6	SPC produced perfectly alternating polyphenylenes with PS and PEO arms.	11
1-7	There are side reactions associated with Pd catalysts.	13
1-8	Enedynes are tautomerized to aryene biradicals and recombined to form polyphenylenes.	14
1-9	Grubbs and coworkers synthesize PPP from an acetoxy precursor.	14
1-10	Single electron transfer is a valid alternative mechanism.	19
1-11	Fluorinated aromatics undergo side reactions with metals.	21
1-12	The generated arylcesium behaves as a nucleophile, forming a new C-C bond.	23
1-13	PAEs synthesized from DFB are typically more stable than	23

	those composed of DFBP or BPFPS.	
1-14	A creative variety of fluorinated monomers can be reacted with bisphenols to form PAEs.	25
1-15	Hougham and coworkers report the synthesis of fluorinated polyimides.	26
1-16	Guiver and coworkers produced random copolymers with both hydrophobic and hydrophilic segments.	28
1-17	McGrath demonstrates a convergent synthesis of a hydrophilic-hydrophobic block copolymer.	29
1-18	Lee controls the end group functionality by stoichiometric ratio.	30
1-19	Pendant groups improve solubility and provide a site for postmodification.	31
1-20	Carbonyls are sensitive heteroatoms because the generated radical is resonance stabilized.	34
1-21	Polymers with heteroatoms are more sensitive to scission mechanisms.	35
1-22	CPD-derived Diels-Alder polyphenylenes exhibit both <i>meta</i> and <i>para</i> catenation.	38
1-23	DAPPs containing alkylene chains have improved solubility and lower thermal stability.	40
1-24	The Diels-Alder polycondensation can also be applied to polyimide synthesis.	40

1-25	Müllen shows the synthesis of highly phenylated dendrimers by Diels-Alder cycloaddition.	42
1-26	SiLK resin is a partially polymerized oligomer.	43
1-27	Hibbs and coworkers produce cationic polymers from DAPPs.	44
2-1	Prof. Deck previously reported the synthesis of arylated cyclopentadienes from cyclopentadienyl anions.	49
2-2	Decafluorobiphenyl can connect two cyclopentadiene moieties	50
2-3	Dilthey and Schommer report the oxidation of arylated cyclopentadienes to the corresponding ketones using DMNA.	50
2-4	There are two general methods for the synthesis of fluorinated CPDs.	52
2-5	The <i>tert</i> -butyl group provides some steric regiocontrol in cyclopentadiene arylation.	54
2-6	The second-generation monomer synthesis provides a variety of fluorinated CPDs.	55
2-7	The arylation reaction produces an inseparable mixture of three tautomers from decafluorobiphenyl and <i>tert</i> -butyl cyclopentadiene.	59
2-8	The linked bis(cyclopentadiene) intermediate (1) reacts with hexafluorobenzene (HFB) to form a bis(cyclopentadiene) with pendant aryl groups.	61
2-9	Diarylated <i>tert</i> -butyl cyclopentadiene reacts with DMNA to form a mixture of nitron products which are then hydrolyzed to the corresponding ketone.	64
2-10	Several attempted oxidation methods failed to produce the	65

	corresponding ketone.	
2-11	The novel copper-catalyzed air oxidation is more efficient for the <i>tert</i> -butyl containing cyclopentadienes.	66
2-12	The arylation of bisdiene 1 with PFP was unsuccessful with NaH as the base.	68
2-13	The arylation of bisdiene 1 with PFP was successful with LiTMP as the base.	70
2-14	The cumylcyclopentadiene monomer behaves similarly to produce fluorinated biscyclopentadienes with a lateral phenyl group for selective post-sulfonation.	71
3-1	Monomer 1 reacts with PDEB to form a fluorinated polyphenylene.	93
3-2	Highly fluorinated cyclopentadienones and aromatic alkynes follow inverse electron demand.	96
3-3	The reaction between monomer 1 and phenylacetylene is a monofunctional model for the polymerization	96
3-4	Monofunctional model compounds are used to study the electronic substituent effects.	105
3-5	Perfluoroaryl-substituted cyclopentadienones can be synthesized by one-pot procedures.	106
4-1	CPDs react with monofunctional phenylacetylene for a simple model reaction.	128
4-2	Fluorinated DAPPs are synthesized from CPDO-C <sub>6</sub> F <sub>5</sub> and CPDO-C <sub>5</sub> F <sub>4</sub> N and a variety of dialkynes.	128

5-1	The pendant fluoroaromatic groups can be used as sites for postfunctionalization.	144
5-2	A monofunctional alkyne could react as an endcapping agent.	144
5-3	The alkyne terminated oligomer could be thermally cured or linked with other difunctional compounds (such as $N_3-R-N_3$ ).	145

## List of Figures

1-1	Several fluorine-containing oligomers are derived from 1,4-dibromotetrafluorobenzene.	8
1-2	Most metal-catalyzed couplings include oxidative addition, transmetallation, and reductive elimination.	10
1-3	High molecular weight polyphenylenes have properties similar to polycarbonate.	12
1-4	This figure shows a generic S <sub>N</sub> Ar mechanism.	16
1-5	Perfluoroarenes exhibit substitution preferences.	18
1-6	The most commonly used perfluoroarenes maintain a balance of cost, reactivity, and regioselectivity.	22
1-7	The <i>para</i> positions can be selectively displaced by various nucleophiles.	32
1-8	Pu compares polybenzimidazoles with varying fluorine content.	33
1-9	Zhu and Han reports fluorinated and nonfluorinated polyesters.	34
1-10	The Diels-Alder reaction proceeds through an aromatic transition state.	36
1-11	First-generation Diels-Alder homopolymers form reversibly.	36
1-12	Irreversible Diels-Alder reactions involve small-molecule extrusions.	37
1-13	Irreversible Diels-Alder reactions provide a basis for polymer synthesis.	37
1-14	Pyrone-derived Diels-Alder polyphenylenes are regioregular.	39

1-15	The lateral phenyl groups of DAPPs are sulfonated selectively.	44
1-16	Lateral phenyl groups on DAPPs can be sulfonated selectively.	42
2-1	The conceptual target (B) is similar to Stille's CPD monomer (A).	48
2-2	The arylation reaction is easily monitored by $^{19}\text{F}$ NMR.	58
2-3	$^1\text{H}$ NMR indicates the reaction is complete [bottom is starting material (A), middle is incomplete (B), and top is the crude product 3 (C)].	62
2-4	This figure shows a thermal ellipsoid plot (50% probability) of the molecular structure of bisdiene 1.	72
2-5	This figure shows a thermal ellipsoid plot 50% probability of the bisdiene 2.	73
2-6	This figure shows a thermal ellipsoid plot (50% probability) of bisdiene 3.	73
2-7	This figure shows a thermal ellipsoid plot (50% probability) of dioxime 8.	74
2-8	This figure shows a thermal ellipsoid plot (50% probability) of diketone 10.	75
2-9	This figure shows a thermal ellipsoid plot (50% probability) of bisdiene 12.	76
3-1	Electron deficient dienes react with electron rich dienophiles by inverse electron demand.	95
3-2	$^1\text{H}$ (a) and $^{19}\text{F}$ (b) NMR spectra of DA reaction products 2a, 2b, and 2c are consistent with 3 isomers.	98
3-3	Monofunctional diarylated <i>tert</i> -butyl cyclopentadienones and phenyl	99

	acetylene (right) are good models for the Diels-Alder reaction of fluorinated biscyclopentadienones and dialkynes (left).	
3-4	The energy diagram shows the stabilization of the first transition state by hydrogen bonding ( $R = CMe_3$ ).	101
3-5	Reaction rates increase with more electron withdrawing substituents.	108
3-6	Thermal imaging shows a distinct difference in temperature profiles after 1 min of microwave irradiation (left) versus oil bath (right).	110
3-7	$^{19}F$ NMR shows the conversion of the product (outlined) in reaction conducted in the microwave (A) is much higher than the oil bath (B) under the exact same reaction conditions.	113
3-8	The model reaction should produce these two compounds.	114
3-9	This figure shows a thermal ellipsoid plot (50% probability) of ketone 10.	115
3-10	This figure shows a thermal ellipsoid plot (50% probability) of arene 12.	116
4-1	The polymerization reaction progress is monitored by $^{19}F$ NMR.	127
4-2	Number-average molecular weight can be calculated by integration.	130
4-3	SEC shows oligomers with excess CPD end groups have the same molecular weight as oligomers with alkyne end groups.	132
4-4	A SEC trace indicates the presence of a low concentration of high molecular weight material.	135
4-5	Thermal stability was measured under $N_2$ up to 800 °C.	139
4-6	DSC (10 °C/min up to 200 °C) might suggest the presence of a glass	140

transition temperature with the second heating cycle (top, A)  
confirmed by the cooling cycle (bottom, B).

5-1 The triarylated bisdiene monomer precursor was synthesized on a preliminary (NMR) scale. 146

## List of Tables

3-1	Model studies were used to study catalysis of Diels-Alder reactions.	103
3-2	Superheating can occur with microwave irradiation to elevate solvent's boiling points.	111
4-1	A series of experiments show similar molecular weight data for several polymerizations.	133
4-2	Microwave heating produces polymers with relatively low molecular weights compared to conventional heating.	138

### Table of Abbreviations

BPAF	Bisphenol A-F
BPFPS	Bis-pentafluorophenylsulfide
CPD	Biscyclopentadienone
DAPP	Diels-Alder polyphenylene
DFB	Decafluorobiphenyl
DFBP	Decafluorobenzophenone
DMAc	Dimethyl acetamide
DMF	Dimethylformamide
DMSO	Dimethyl sulfoxide
DP	Degree of polymerization
HFB	Hexafluorobenzene
HOMO	Highest occupied molecular orbital
LED	Light emitting diode
LUMO	Lowest unoccupied molecular orbital
OLED	Organic light emitting diode
PAEK	Poly(arylene ether ketone)
PEO	Poly(ethylene oxide)
PEP	4-(phenylethynyl)phenol
PFN	Perfluoronaphthalene
PPP	Poly( <i>para</i> -phenylene)
S <sub>N</sub> Ar	Nucleophilic aromatic substitution
SPC	Suzuki polycondensation
TFB	1,2,4,5-Tetrafluorobenzene
THF	Tetrahydrofuran
TPT	Thiophene/phenylene/thiophene

## **Dissertation Overview**

This dissertation focuses on the synthesis and characterization of highly fluorinated Diels-Alder polyphenylenes (DAPPs). Chapter 1 reviews polyphenylene synthesis and fluoropolymers derived from fluoroaromatic compounds. Chapter 2 describes an efficient and versatile synthesis of fluorinated bis(cyclopentadienone) monomers (CPDs). Chapter 3 details our efforts to catalyze and optimize conditions for the Diels-Alder propagation reaction through a series of model reactions. Chapter 4 presents the results of our polymerization experiments, including detailed characterization of the polymeric materials. Chapter 5 summarizes the overall conclusions of this dissertation and the outlook for further research based on our findings.

## Chapter 1. Literature Review

### 1.1 Introduction

Fluorinated polymers are well suited for high performance applications because they possess unique thermal and mechanical stability compared to hydrogen analogues. Polyphenylenes also exhibit enhanced thermal and mechanical properties because they are composed of linked benzene rings. Merging these two areas of polymer science – to make fluorinated polyphenylenes – could therefore provide especially useful new substances, in addition to providing an interesting area of fundamental science.

Fluoropolymers exhibit unique properties because of the special features of the fluorine atom. Fluorine has a high electronegativity that results in strong bond polarization, e.g. [(C+)–(F–)]. This feature makes fluorinated organic compounds especially resistant to oxidants and acids. The C-F bond also has a particularly high bond strength ( $480 \text{ kJ mol}^{-1}$ )<sup>1</sup> which enhances stability overall. The presence of several fluorine atoms in an organic compound leads to truly unique physical properties. Perfluoroaliphatic compounds exhibit both hydrophobicity and oleophobicity,<sup>2,3</sup> partly because opposing local (C+)–(F–) dipoles cancel, and partly because the small size and high effective nuclear charge of fluorine weakens van der Waals interactions. While fluoroaromatic compounds do not show this “fluorous” behavior, their “inverted” charge densities do have supramolecular consequences.<sup>1</sup>

Most commercial fluoropolymers are aliphatics synthesized by free radical vinyl enchainment. Examples include Teflon™, Viton™, Kalrez™, and Nafion™. Nafion is a fluorinated aliphatic chain with pendant sulfonic acid groups with applications in ion exchange resins, especially proton exchange membranes for hydrogen fuel cells. While Nafion is thermally and chemically stable, the aliphatic backbone results in a low melting and glass

transition temperatures, which are detrimental to fuel cell stability (electrode poisoning) and performance (fuel crossover), especially above about 80 °C.<sup>4</sup>

Polyphenylenes tend to be glassy materials because of the rigidity that comes from having a backbone of linked benzene rings. Few known aromatic fluoropolymers, however, are true polyphenylenes. Instead they are usually poly(arylene ethers), polyesters, or other condensation polymers derived from fluoroaromatic monomers. Their thermal and chemical stability therefore depends more on the properties of the linking functional groups, and less on the fluoroaromatic moieties.

This dissertation shows how one particular method of preparing polyphenylenes (Diels-Alder polycondensation) can be adapted to access highly fluorinated *true* polyphenylenes. This chapter reviews the most relevant aspects of polyphenylene synthesis and aromatic fluoropolymers so that our contributions may be viewed in a proper scientific context.

## **1.2 Synthesis of Polyphenylenes**

Because of the significance of aromatic compounds throughout organic chemistry, many methods of preparing compounds containing coupled benzene rings (biphenyls, terphenyls, etc.) have been developed over the years. The idea of forming a polymer entirely from linked benzene rings (a polyphenylene) also seemed natural, because of the likelihood that the thermal and chemical stability of benzene would translate into desirable properties in the polymer. This section summarizes the most successful methods.

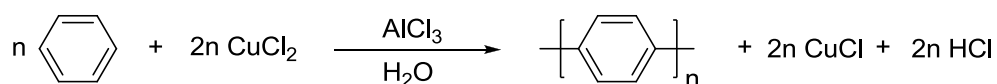
Polyphenylene synthesis can be divided roughly into two categories. The most conceptually simple approach is to couple existing aromatic rings into chains. Kovacic demonstrated oxidative coupling of benzene, but his method only forms oligomers with poor polymer properties (Section 1.2.1). The later discovery of palladium-catalyzed sigma couplings

(especially the Stille and Suzuki reactions) largely solved the molecular weight problem, but these methods require functionalized arylene monomers and expensive catalysts (Section 1.2.2). Between the oxidative Kovacic approach and the formally reductive sigma-coupling approach is the Bergman cyclization of enedynes, which affords an arylenediyl (a benzene 1,4-biradical) that can polymerize under the right conditions (Section 1.2.3).

The other main approach to polyphenylene synthesis is to find monomers or precursors that can couple efficiently, while aromatization is left to the end. Post-polymerization aromatization of poly(cyclohexadiene) is the simplest example (Section 1.2.4). Diels-Alder polymerization (to which a main section of this chapter is devoted) is somewhat more sophisticated because aromatization occurs as the last mechanistic step of the propagation reaction. This review is not intended to be exhaustive, but instead to describe the principles underlying each synthetic method and to discuss the suitability of each for preparing polyphenylenes with significant fluorine content. We will show that only Diels-Alder polymerization is suited for the synthesis of fluorinated polyphenylenes.

### 1.2.1 Oxidative Couplings (Kovacic Synthesis)

Under relatively harsh conditions (high temperature, aluminum chloride catalyst), benzene will undergo coupling with a single electron oxidant ( $\text{CuCl}_2$ ) (Scheme 1-1).<sup>5,6</sup> When  $\text{FeCl}_3$  is used, it serves in both the oxidant and Lewis acid roles. The mechanism of this reaction is still unclear and controversial.<sup>7</sup> The most interesting features of this reaction are its simplicity and its regioselectivity: only *para*-polyphenylene (PPP) is obtained. More generally, however, coupling of substituted arenes is not regioselective.<sup>7</sup>

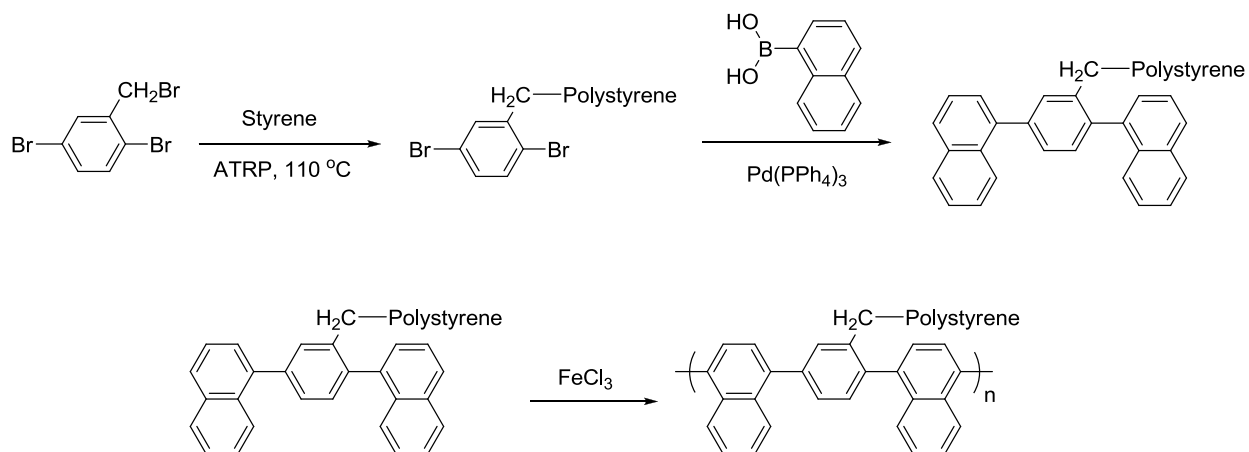


**Scheme 1-1. PPP can be synthesized from benzene and a Lewis acid.**

Although the ordered, rigid-rod structure of PPP is attractive for applications like liquid crystalline<sup>8,9</sup> or light emitting diode (LED) materials,<sup>10</sup> the substance is essentially intractable beyond a degree of polymerization of about 5.<sup>6</sup> This poor solubility limits other possible applications. Several groups have tried to work around this problem. One approach is to start with a polyaromatic monomer that has some built-in structural flexibility. Bilow and Miller used *ortho*- or *meta*-terphenyl with either AlCl<sub>3</sub>/CuCl<sub>2</sub> or FeCl<sub>3</sub>, in the melt, to synthesize tractable polyphenylenes up to 3000 g/mol.<sup>11</sup> The addition of pendant side groups (“lateral” substituents) also dramatically increases solubility, however usually at the expense of other attractive properties that depend on extended conjugation such as electrical conductivity.<sup>12</sup> Kaeriyama<sup>13</sup> and coworkers polymerized methyl 2,5-dibromobenzoate using nickel-catalyzed coupling of the Grignard reagent prepared *in situ*. Kovacic polymerization would have failed due to the incompatibility of the ester functional group. The product polyarylene was converted into PPP by hydrolysis and decarboxylation.<sup>14</sup> The condensation formed a soluble all-*para* carboxylated precursor, but decarboxylation to give PPP cannot efficiently occur in solid state, preventing the formation of films.<sup>13,14</sup>

Kovacic-type polymerization still finds occasional application in special instances. Grigoras and co-workers synthesized polystyrene bearing a dibromobenzyl head group using ATRP, and then replaced the C-Br bonds with naphthyl groups using a Suzuki coupling (Scheme 1-2).<sup>15</sup> The macromonomer was then polymerized using FeCl<sub>3</sub> as the oxidant to obtain oligomers ( $M_n \sim 28$  kg/mol,  $n = 6$ ) with brush-like structures.<sup>15</sup> The macromonomer contains many different aromatic rings, but selectivity is achieved in this example because naphthalene is much more reactive toward electrophilic aromatic substitution than either benzene or the phenyl groups of polystyrene.<sup>16</sup> This difference arises because only 105 kJ/mol of resonance energy must be

provided to disrupt one ring of a naphthalene molecule, whereas the resonance energy in benzene is around 150 kJ/mol. Also, carbocations in the *alpha* position of naphthalene enjoy more resonance stabilization than a cyclohexadienyl cation intermediate in a typical Friedel-Crafts type mechanism.<sup>16</sup>

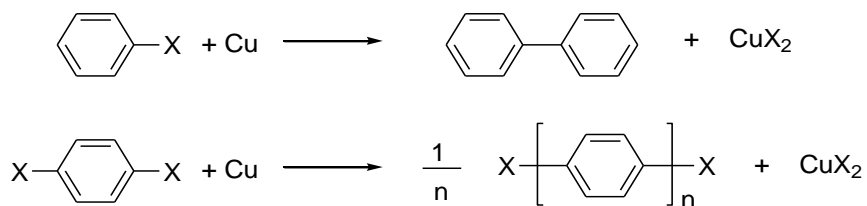


**Scheme 1-2. Grigoras synthesized macromonomers from Suzuki coupling and polyphenylenes with PS arms by oxidative polymerization.**

Electropolymerization is a closely related oxidative coupling technique that consists of oligomerizing aromatic monomers like benzene by removing electrons with an electrode rather than a chemical oxidant. Electrochemical oxidation of benzene or biphenyl gave powders and films of limited molecular weight, until Aeiyaeh reported an optimized electrochemical oxidation of benzene and biphenyl in SbF<sub>5</sub>-SO<sub>2</sub> medium.<sup>17</sup> The electrochemical anodic polymerization offers the opportunity to coat an electrode surface with a doped conducting polymer directly, eliminating the additional isolation and processing steps. Molecular weights are still low, but for many surface coating applications high molecular weight is not needed. The major disadvantage of this technique is the toxic, corrosive nature of the reaction medium. Early work with ionic liquids suggests there is hope for improvement in this field.<sup>18</sup>

### 1.2.2 Metal-Enabled Sigma Couplings

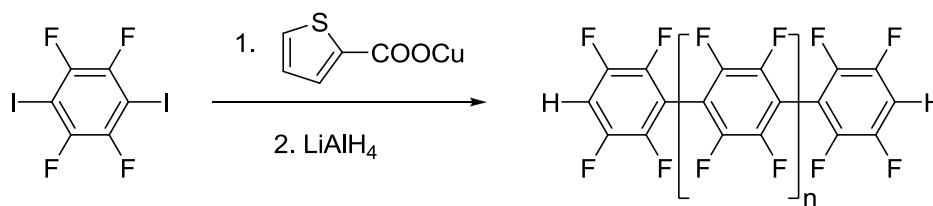
Ullmann Coupling. The conceptual opposite of the Kovacic synthesis is the Ullmann Coupling. Here, aryl halides are treated with copper, presumably to afford an arylcopper species that behaves like a metal-stabilized aryl radical. Coupling of two radicals gives the new C-C bond with elimination of a copper halide (Scheme 1-3). Thus the overall coupling process is a carbon-centered reduction.



**Scheme 1-3. Two aryl halide compounds react with copper to form a new aryl-aryl bond and a copper halide.**

This synthesis works well for symmetrical biaryls but is ill-suited to polyphenylene synthesis because its yield is too low (typically 70%),<sup>7</sup> and because it requires electronegative activating groups like NO<sub>2</sub>.<sup>19</sup> Best efforts have afforded only oligomers along with cyclic byproducts.<sup>7,19</sup> The other obvious problem with both the Ullmann and Kovacic methods is the need for *stoichiometric* metal-containing reagents. In addition to reagent costs, removal and disposal of the metal-containing by-products is difficult and expensive.

Ullman-type homocoupling produces a fluorinated oligophenylene from 1,4-diiodo-2,3,5,6-tetrafluorobenzene in the presence of copper thiophenecarboxylate in NMP.<sup>1,20</sup> Dehalogenation by lithium aluminum hydride converted the end groups into protons so that the material could be purified by column chromatography. Oligomers composed of five fluorinated benzene rings were obtained (Scheme 1-4).<sup>20</sup>



**Scheme 1-4. Ullman coupling of 1,4-diiodo-2,3,5,6-tetrafluorobenzene produces fluorinated polyphenylenes.**

Copper-catalyzed homocoupling was also used to make other fluorinated, linear oligophenylenes from 1,4-dibromotetrafluorobenzene in THF/dioxane/toluene mixture (Figure 1-1). This method produced a material with up to eight fluorinated benzene rings linked together covalently.<sup>10</sup> The oligomers were purified by sublimation and characterized by MS, DSC, and elemental analysis.<sup>10</sup> It is worth mentioning also that 1,4-dibromo- and 1,4-diiodotetrafluorobenzenes are expensive (\$7.5 g<sup>-1</sup> and \$19.9 g<sup>-1</sup> for Aldrich's largest package sizes).

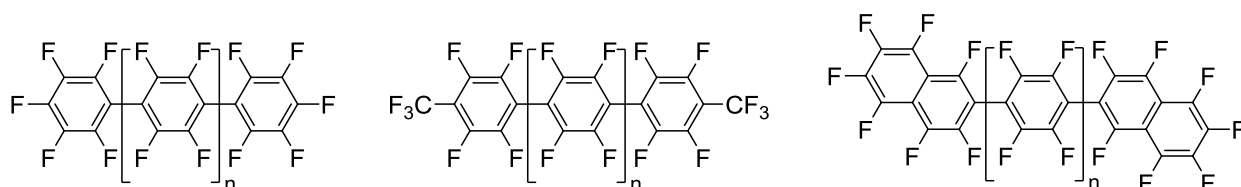


**Figure 1-1. Several fluorine-containing oligomers are derived from 1,4-dibromotetrafluorobenzene.**

Palladium-Catalyzed Couplings. The promise of species such as polyacetylene,<sup>21-23</sup> polythiophenes,<sup>9,24,25</sup> and polyfluorenes<sup>9,26</sup> in electronic materials has fueled the application of late-transition-metal catalyzed aryl couplings to the synthesis of polyarylenes and poly(arylene vinylene)s.<sup>27,28</sup> Virtually every “named” sigma-coupling reaction (e.g. the Kumada-Corriu, Stille, Heck, and Suzuki reactions) have been applied to this problem. This section highlights applications of the Stille and Suzuki reactions, which are the best developed coupling methods for the synthesis of polyphenylenes. Palladium-catalyzed couplings generally have much higher

yields than the Ullmann coupling; they use only catalytic quantities of metals (often around 1% on a mole basis), and they tolerate a much wider range of functional groups.<sup>29</sup>

Advantages and Disadvantages of Pd-Catalyzed Couplings. Through rational synthesis the functional groups needed for coupling reactions can be placed on aromatic compounds almost at will, which gives the polymer chemist great control over functionality and microstructure, particularly backbone and lateral substituent regiochemistry. One does still need, however, to remove the small amounts of colloidal metal impurities from the polymeric product, especially for polymers intended for electronics or optics applications. Another obvious drawback is the higher cost and lower atom economy associated with using sophisticated functional groups like stannyl or boryl groups in the monomers. There are also toxicity issues with phosphine ligands and with the organotin reagents and by-products associated with the Stille reaction. Finally the palladium catalysts are expensive and often air-sensitive, and there are often side reactions that can limit molecular weight or introduce polymer defects.<sup>29,30</sup>

Mechanism of Pd-Catalyzed Coupling. All of these Pd-catalyzed methods typically undergo the same general mechanism: oxidative addition, transmetallation, and reductive elimination. First, the first aryl group is connected to the transition metal (Pd) by oxidative addition of the aryl halide (monomer). Transmetallation from boron (specific to Suzuki coupling) or tin (Stille coupling) connects the second aryl group onto Pd. Reductive elimination of the two aryl groups forms a new aryl-aryl bond and regenerates the Pd catalyst (Figure 1-2).

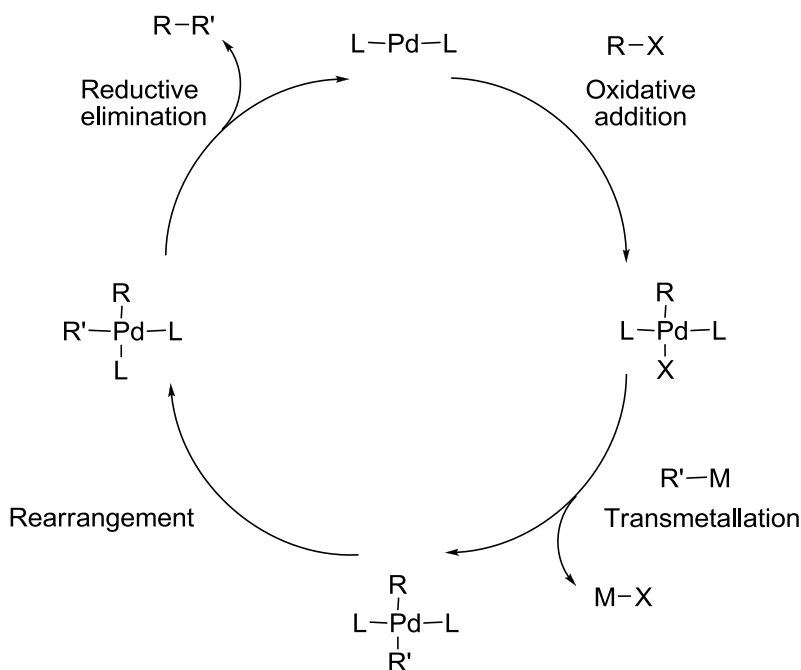
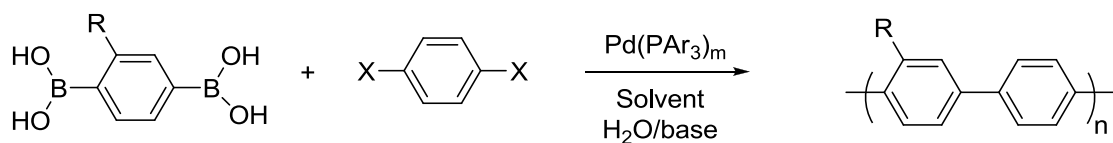


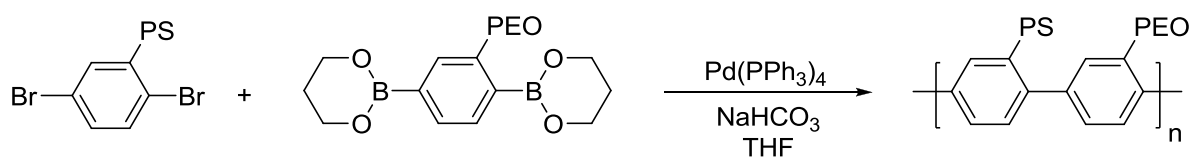
**Figure 1-2. Most metal-catalyzed couplings include oxidative addition, transmetalation, and reductive elimination.**

Suzuki Polycondensation involves C-C couplings of bifunctional aromatic monomers (Scheme 1-5).<sup>31</sup> The reaction requires a halogen (reactivity:  $I > Br \gg Cl$ ) and a boronic acid or a boronic ester. While it is possible to have a single “AB” type monomer containing both functional groups, in practice the corresponding “AA + BB” approach is always used because the difunctional AB monomer is more difficult to prepare. The halogen leaving group is typically bromide, which balances reactivity against synthetic convenience. Chlorides can be used, but the palladium needs a very electron-rich ligand array to force C-Cl oxidative addition.<sup>31</sup>



**Scheme 1-5. Suzuki polycondensation typically involves C-C couplings of bifunctional aromatics and boron compounds.**

Suzuki polycondensation, or SPC, has become a valuable method of polyarylene synthesis. Most efforts are aimed at applying SPC to aromatic monomers with flexible side chains because solubility and processability are the two fatal flaws associated with polyphenylenes. Substituents on macromonomers may help add functionality while resolving the problems associated with polyphenylenes. However, electronic conjugation is decreased by these side groups because the side groups increase the dihedral angle between the adjacent benzene rings. Polyphenylenes made by SPC exhibit molecular weights ranging from 15-30 kg/mol (DP = 30 to 60).<sup>30</sup> Yagei used SPC to make perfectly alternating amphiphilic polyphenylene graft copolymers with unique self-organization properties caused by the hydrophilic PEO arm combined with the hydrophobic PS arm (Scheme 1-6).<sup>32</sup> Schluter and coworkers showed that amphiphilic polyphenylenes with polar arms and apolar backbones have the ability to segregate lengthwise.<sup>33</sup> Wegner studied charged amphiphilic polyphenylene versions for polyelectrolyte applications.<sup>34</sup> Most amphiphilic copolymers are studied extensively because they have different surface activity and aggregate formation, while the lengthwise segregation could make these materials interesting for electro-optics or colloids.<sup>33</sup>



**Scheme 1-6. SPC produced perfectly alternating polyphenylenes with PS and PEO arms.**

A high molecular weight poly(*para-meta*-phenylene) was recently synthesized from dibromide and diboronic acid ester with properties similar to polycarbonate (Figure 1-3). This tough, amorphous material with alternating *para* and *meta* connected phenylene units has short butyloxy side groups for improved solubility and processability.<sup>31,34,35</sup>

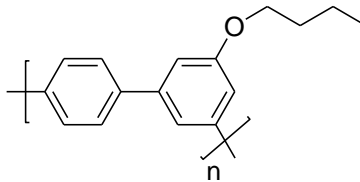
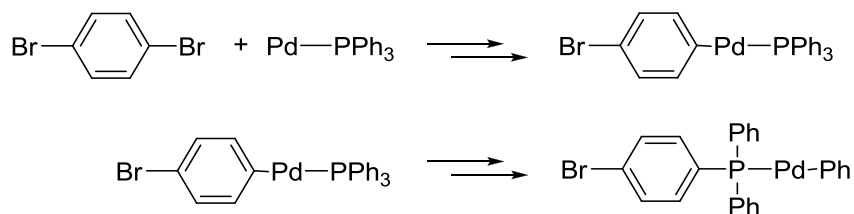


**Figure 1-3. High molecular weight polyphenylenes have properties similar to polycarbonate.**

These examples demonstrate that polyarylenes with useful molecular weights for high performance applications may be achieved by SPC. However the method has not been extended effectively to highly fluorinated polyphenylenes. Metal-catalyzed coupling reactions of perfluoroaryl halides can be slow because the M-aryl bond is so strong that catalytic steps, especially reductive elimination (see Figure 1-2), can have high activation barriers.

One particularly interesting side-reaction in Suzuki polymerization is oxidative addition of the C-P bonds of the triphenylphosphine ligand. Novak and co-workers<sup>29</sup> showed that  $\text{Ph}_3\text{P}$  can undergo aryl exchanges with the Pd-aryl group of the activated monomer (Scheme 1-7), with three main consequences. First, coupling of the Pd-Ph group (Ph arises from  $\text{Ph}_3\text{P}$ ) to the end of the polymer terminates (caps) the chain end. Second, continued exchange to form  $\text{PhP}(\text{C}_6\text{H}_4\text{Br})_2$  creates a new arylene dibromide monomer, which could create a chain defect because the phosphinediaryl unit is more flexible than a *p*-phenylene. Third, exhaustive exchange would afford  $\text{P}(\text{C}_6\text{H}_4\text{Br})_3$ , opening up a pathway to branching and cross-linking. Thus instead of forming a high-molecular-weight rigid-rod, one might actually form a branched, flexible, low-molecular weight polymer. These aryl-scrambling reactions of phosphorus-containing ligands make the polymer structure unpredictable.<sup>30</sup> There are even some reports of phosphorus incorporated into a polyphenylene backbone caused by these side reactions.<sup>30</sup> Adjustment of the phosphine substituents should allow some degree of optimization but has not been extensively investigated.



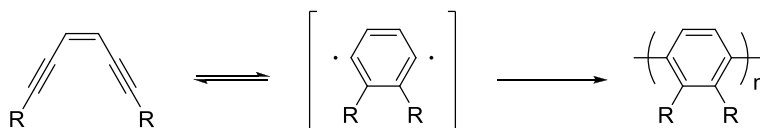
**Scheme 1-7. There are side reactions associated with Pd catalysts.**

Stille polycondensation is similar to Suzuki polycondensation, except the boron groups are replaced with stannyl groups. Stille coupling is most common for polythiophene<sup>24,25,36-41</sup> and poly(*p*-phenylenevinylene)<sup>42</sup> synthesis, but that topic is slightly outside the scope of this review. However, Stille coupling has been used to make soluble copolymers which combine thiophene and polyphenylene properties. Thiophene/phenylene/thiophene (TPT) polymers are an interesting variation of polyphenylene because they have good electronic properties for applications such as solar cells and other photovoltaics.<sup>38</sup> As conjugated materials, their orbital energy levels can be tuned by incorporating a variety of electron-withdrawing monomers with Stille coupling.<sup>38</sup> One advantage of Stille coupling is that it can be run under neutral conditions, whereas the Suzuki reaction requires a base to activate the boronic acid for transmetalation.<sup>43</sup> However, stannanes are less stable and more toxic compared to boronic acid compounds, so Suzuki coupling is somewhat preferred.

### 1.2.3 Bergman Cyclization

Bergman cyclization is a process in which enediynes are tautomerized to arylene biradicals and recombined to form polyphenylenes (Scheme 1-8).<sup>44</sup> The polyphenylene product suffers from broad molecular weight distributions and many defects. The yields ranged from 50-90% with average molecular weights around 2500 g/mol. Enediynes are expensive and known to form explosive materials. Although this route does not require metal catalysts or heteroatom coupling

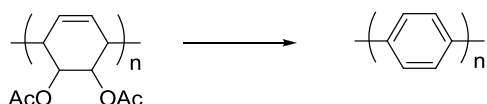
sites, the reaction requires high temperatures and other extreme conditions.<sup>44</sup> Thus it should be considered something of a novelty.



**Scheme 1-8. Enediyne are tautomerized to arylene biradicals and recombined to form polyphenylenes.**

### 1.2.4 Aromatization of Poly(cyclohexadiene)

Marvel and Hartzell first reported the synthesis of low molecular weight (ca. 5-10 kg/mol), amorphous powders by the polymerization of 1,3-cyclohexadiene using a Ziegler catalyst composed of triisobutylaluminum and titanium tetrachloride.<sup>45</sup> Dehydrogenation gave some PPP according to IR spectroscopic analysis and X-ray diffraction, but they were unable to isolate PPP in a pure form.<sup>45</sup> More recently Grubbs and coworkers prepared stereoregular PPP by first polymerizing a cyclohexadienediol diacetate with nickel, and then eliminating 2 equiv of acetic acid to obtain PPP (Scheme 1-9).<sup>14</sup> Since the side group elimination is required to form the polymer, there is not a good way to include substituents to increase solubility of the rigid rod product.



**Scheme 1-9. Grubbs and coworkers synthesize PPP from an acetoxy precursor.**

### 1.3 Nucleophilic Substitution in Perfluoroarenes

The major, characteristic bond-forming reaction of perfluoroarenes (and therefore the main reaction used to form polymers from perfluoroarenes, see Section 1.4) is nucleophilic aromatic substitution ( $S_NAr$ ), which can proceed to high conversion with high regioselectivity under mild conditions. These features suggest a prominent role for perfluoroarenes in step-growth

polymerization. However, unless the nucleophiles are aryl anion equivalents (e.g., 1,4-dilithiobenzene), the obvious drawback of nucleophilic substitution as a polymerization method is the incorporation of heteroatoms and other non-aromatic functionality into the polymer backbone, which changes the physical properties. Some of these changes might be desirable, such as increased solubility, but thermal stability and chemical resistance will be invariably worse (see section 1.4.4). Because this dissertation focuses on polymers derived from fluoroaromatic compounds, this section emphasizes fluoropolymers made by nucleophilic substitution and other modified techniques that use perfluoroarenes as building blocks in polymer synthesis. This section begins with a description of the  $S_NAr$  that is intentionally rather detailed because this reaction also is critical to the monomer syntheses described in Chapter 2.

### 1.3.1 General Overview of $S_NAr$

The most important feature of  $S_NAr$  as compared to binuclear aliphatic substitution ( $S_N2$ ) is that the  $S_NAr$  mechanism proceeds through two distinct steps, whereas  $S_N2$  is a one-step mechanism.<sup>46-48</sup> This difference has important consequences for trends in the activating substituents, the regioselectivity of substitution, and the role of the leaving group.<sup>49</sup>

Mechanistic Essentials. The generic  $S_NAr$  mechanism is shown in Fig. 1-4. The nucleophile (shown here as  $Nu^-$ ) attacks an activated aromatic ring, forming an intermediate “Meisenheimer complex,” in which both the leaving group (X) and the nucleophile ( $Nu^-$ ) are attached to the  $sp^3$ -hybridized carbon atom. Electron-withdrawing substituents (Y) activate the addition by increasing electrophilicity at the *ipso* carbon, and they also stabilize the intermediate by helping to disperse the charge of the cyclohexadienyl anion. Loss of the leaving group (X) restores aromaticity and forms the substitution product. All of the steps are reversible, so the formation of the product must be driven thermodynamically. Formation of a C–O or C–N bond is a

common driving force, because these bonds have some double-bond character when the carbon is part of an electron-poor aromatic ring.

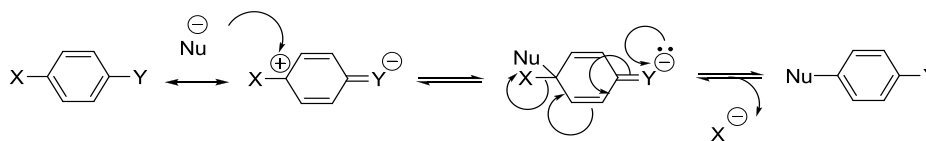


**Figure 1-4. This figure shows a generic  $S_NAr$  mechanism.**

Solvent Effects. Polar aprotic solvents (THF, DMSO, DMAc) favor the reaction by stabilizing the partial charge in the transition state without weakening the nucleophile through hydrogen bonding. This feature is one that the  $S_NAr$  and  $S_N2$  reactions do have in common.<sup>50</sup>

Leaving Groups. In  $S_N2$  reactions, alkyl iodides react faster than other halides because the C–I bond is the weakest of the carbon-halogen bonds. Less energy is needed to partially break the C–I bond in the five-coordinate transition state. In the  $S_NAr$  mechanism, aryl fluorides react fastest because the C–F bond is highly polarized, making the *ipso* carbon more electrophilic and more reactive toward the incoming nucleophile.<sup>51</sup> This trend is more important than the relative strengths of the carbon-halogen bonds, because the initial addition step is rate-limiting. Other good leaving groups (triflate and nitro groups) are sometimes used, but they can also serve as oxidants toward electron-rich nucleophiles, causing unwanted side-reactions.<sup>51-55</sup>

Activating Groups. Increasing the partial positive charge on the *ipso* carbon (labeled Y in Fig. 1-1) accelerates nucleophilic attack.<sup>56</sup> Hammett  $\sigma$  values are probably the most convenient indicator of whether a group should be activating.<sup>57</sup> Among several possibilities,<sup>58</sup> sulfones, carbonyls,<sup>59</sup> and heterocyclic rings are the most common activating groups for  $S_NAr$  in polymer synthesis, because these groups can also link two aromatic rings to form difunctional monomers.<sup>57</sup> Commercial polymers, including PPO, PAES, PEEK, and others, are based on this approach. Knauss has broadened the category of “electron-withdrawing” substituents to include

sulfide,<sup>57</sup> azomethine,<sup>60</sup> and a variety of unusual heterocyclic moieties,<sup>61,62-64</sup> for the synthesis of poly(arylene ether)s. Activation by fluorine on the aromatic ring is discussed later in more detail, but CF<sub>3</sub> groups also activate inductively. Because fluoride is commonly used as a leaving group, some authors have discussed the use of the <sup>19</sup>F NMR chemical shift of the electrophilic CF bond to indicate how activated the bond is.<sup>65</sup>

Regiochemistry. The effect of an activating group is also a function of its location on the aromatic ring relative to the leaving group. Activating groups are located at the *ortho* or *para* position so that they can stabilize the negative charges in Meisenheimer intermediates. Fig. 1-4 shows an example of stabilization by a *para* substituent. Regioselectivity arises if an aromatic ring has two leaving groups. The leaving group that is either *ortho* or *para* to the activating group will be substituted. This issue does not arise often in polymer synthesis, except in the case of polyfluorinated aromatic compounds, which have several potential leaving groups. This issue is discussed in Section 1.4.

### 1.3.2 Trends in S<sub>N</sub>Ar Reactions of Perfluoroarenes

Perfluoroarenes have the best possible leaving group (fluoride), while the other fluorines have an overall inductive activating effect. The most interesting issue, then, is *regiochemistry*. Nucleophilic substitution in polyfluoro-aromatic compounds usually occurs at the site that has the most fluorine atoms in the *ortho* and *meta* positions.<sup>66</sup> From left to right in Figure 1-5, pentafluorobenzenes react mainly at the *para* position, especially when X = CF<sub>3</sub>, Ph, CH<sub>3</sub>, C<sub>6</sub>F<sub>5</sub>, or CN. When a strong donor group is present (X = OH or NH<sub>2</sub>), mixtures of *para* and *meta* substitution products are formed. These trends are important in polymer synthesis when two C<sub>6</sub>F<sub>5</sub> groups are connected by a linking group (G). *Para*-selectivity is essentially perfect with G = C(O) and SO<sub>2</sub>, but poor with G = O.

Chambers proposed that a fluorine *para* to the leaving group *destabilizes* the Meisenheimer complex by p( $\pi$ )-donation, whereas it is too far away to have an inductive stabilizing effect. For example, C<sub>6</sub>F<sub>6</sub> reacts only 75% as fast as C<sub>6</sub>F<sub>5</sub>H with sodium methoxide in methanol at 50 °C.<sup>67</sup> Presumably for fluorine atoms in *ortho* and *meta* positions, the inductive activating effects overcome the deactivating effects of p( $\pi$ )-donation.

Pentafluoropyridine reacts first in the 4 position,<sup>68</sup> but when that position is blocked (e.g., R = Ph), the normal preference of pyridines to react at the 2-position with strong nucleophiles takes over.<sup>69</sup> Octafluoronaphthalene substitutes first at a  $\beta$  position, but then the second substitution often gives a mixture of 2,6 and 2,7 isomers, which would contribute to polymer regioirregularity. The substitution preferences of aromatic rings having combinations of fluorine and hydrogen, fluorine and chlorine, etc., are documented. However the systems shown in Figure 1-5 are, by far, used the most in polymer synthesis.

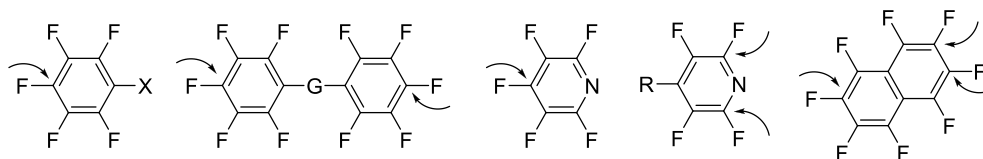
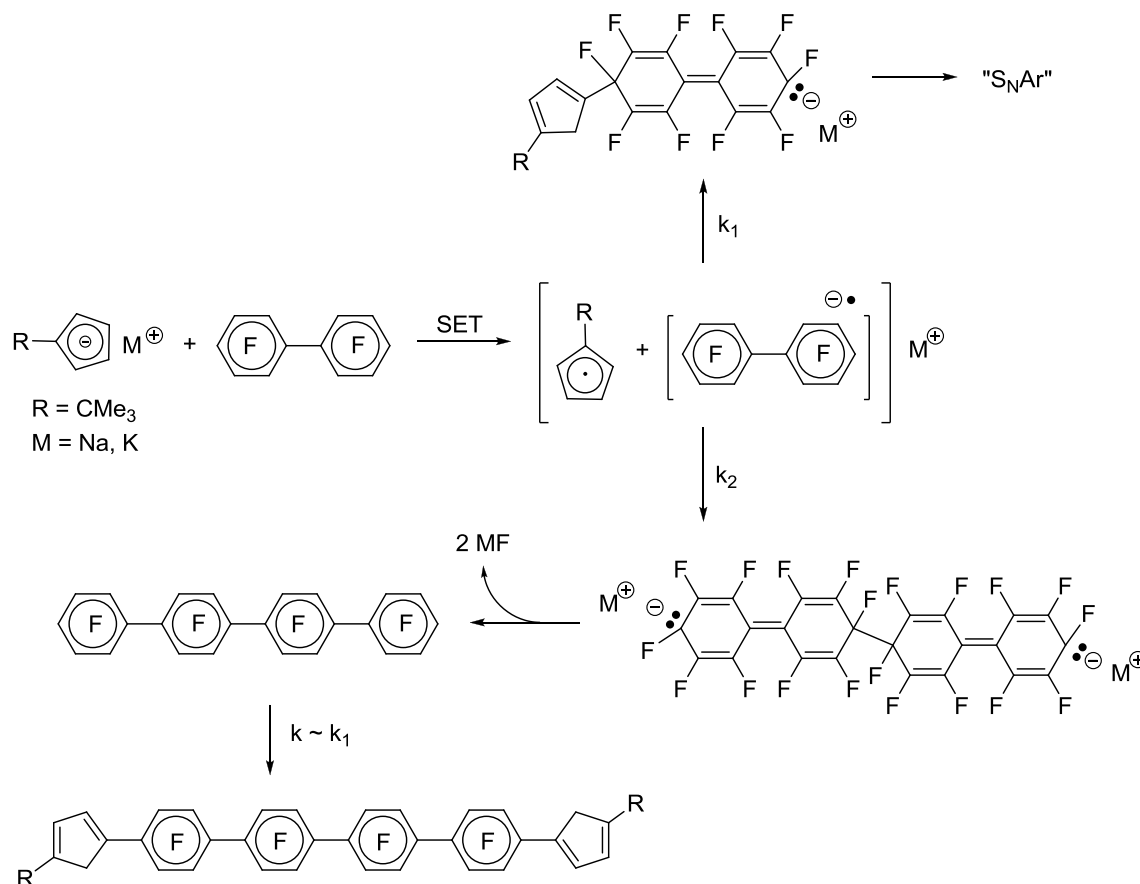


**Figure 1-5. Perfluoroarenes exhibit substitution preferences.**

### 1.3.3 Alternative Substitution Mechanisms

While the proposed polar mechanism of S<sub>N</sub>Ar rationalizes the empirical facts well, there is evidence the initial addition step might not be a two-electron process. Because perfluoroarenes are electron-poor, single-electron transfer (SET) from the nucleophile to the arene to form an arene radical anion seems reasonable too.<sup>64,70</sup> However if the solvent-caged radicals combine quickly, the end result will typically be the same. This almost always is the case, which is why SET is usually not discussed explicitly as an alternative. Normally, the [solvent-caged radicals] would simply couple, and the rest of the reaction would be the same as S<sub>N</sub>Ar, with the same

products, for much the same reasons. But if the radicals live long enough to escape the solvent cage, they could couple with one another to form different products.



**Scheme 1-10. Single electron transfer is a valid alternative mechanism.**

Scheme 1-10 shows an example from my own research that suggests a SET mechanism operating in a nucleophilic substitution. When  $M^+ = K^+$ , the tetraphenylene derivative was isolated in 3% yield and characterized by crystallography. However, when  $M^+ = Na^+$ , the coupled product was not observed. Thus the ratio  $k_2/k_1$  depends on the identity of the alkali cation, possibly indicating a role of the cation in stabilizing the caged radical anion species through ion pairing (solvent = THF). The coupled by-product was only an annoying diversion here, but in a polymerization it would lead to structural defects. Control studies ruled out the

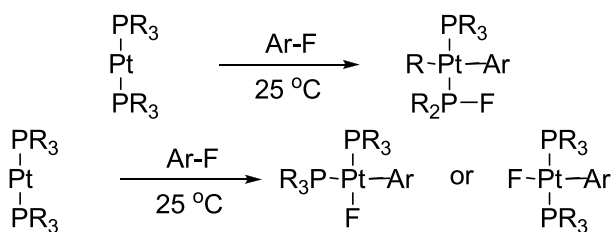
possibility that the tetraphenylene derivative is formed by first coupling decafluorobiphenyl with potassium, which is sometimes found as an impurity in potassium hydride.

#### **1.4 Fluorinated Polymers by Nucleophilic Substitution**

There are two approaches for synthesizing fluorine-containing polymers: polymerization of fluorine-containing monomers or fluorination of non-fluorine-containing polymers. Direct fluorination of polyphenylenes is relatively unsuccessful because it is difficult to control fluorine content: fluorination of polystyrene converts C-H bonds into C-F, C-F<sub>2</sub>, or C-F<sub>3</sub> groups.<sup>71-73</sup> Direct fluorination of polymers is a heterogeneous reaction with gaseous F<sub>2</sub> and the polymer surface.<sup>74</sup> Even optimized methods with mild fluorinating agents can have unpredictable results because fluorination seems to occur preferentially on the surface rather than the bulk.<sup>72</sup> The formation of a completely fluorinated polymer could take weeks or months.<sup>74</sup> On the other hand, polymerization of perfluoroarenes without a heteroatom may also be considered relatively unsuccessful so far. Fluorinated PPP oligomers with DP = 2-8 were made by metal-promoted couplings in low yields as described above. In general, metal-mediated coupling methods used for making polyphenylenes are poorly-suited for incorporating fluorine. Stille and Suzuki coupling methods have been used to make some polyphenylenes, albeit with limited fluorine content.<sup>1,75-78</sup>

Fluorinated polyphenylenes are scarce in the literature because most successful polyphenylene syntheses involve metal catalysis. Unfortunately, fluoropolymers undergo unwanted side-reactions with some metals, and fluoroaromatics especially show a strong tendency to undergo oxidative C-F bond addition to metals in the nickel group.<sup>79,80</sup> Oxidative addition competes with phosphine assisted C-F activation, in which rearrangement may occur in

the presence of phosphine ligands.<sup>80,81</sup> These problems ultimately lead to poor catalyst turnover and selectivity issues (Scheme 1-11).<sup>80-82</sup>



**Scheme 1-11. Fluorinated aromatics undergo side reactions with metals.**

On the other hand, perfluoroarenes react readily with nucleophiles as described in the preceding sections. Combining a perfluoroarene that can be selectively substituted exactly twice (AA) and a difunctional nucleophile (BB) should therefore give a linear polymer by nucleophilic substitution. High conversion is vital to achieving high molecular weights for step growth condensation polymerizations according to the Carothers equation. Not surprisingly, the most important monomers (Figure 1-6) represent the best balance of cost, reactivity, and regioselectivity. This figure also summarizes some abbreviations that will be used in the rest of the review.

The use of the compounds in Figure 1-6 is so convenient that the alternative approach of making a single monomer having both nucleophilic and electrophilic components (AB) remains essentially unexplored. The subsections below illustrate some of the variations in synthetic approaches leading to a wide array of linear polymers (Section 1.4.1), copolymers (Section 1.4.2), and polymers modified using lateral perfluoroarene groups (1.4.3). Section 1.4.4 addresses stability issues characteristic of perfluoroarylene polymers and Section 1.4.5 discusses the instability of polymers containing heteroatoms.

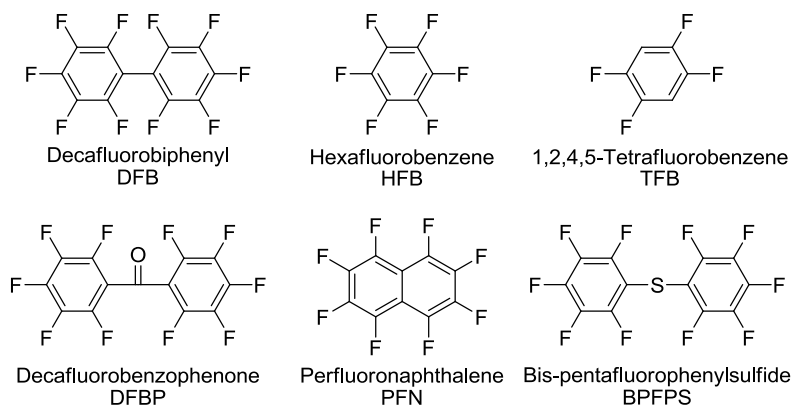


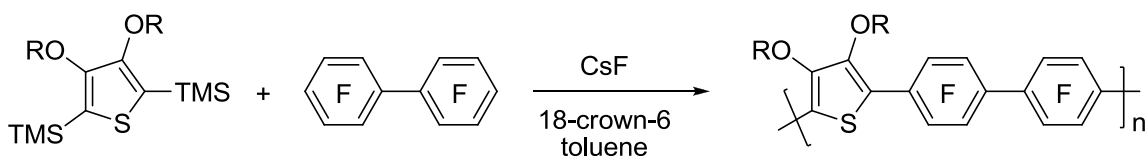
**Figure 1-6. The most commonly used perfluoroarenes maintain a balance of cost, reactivity, and regioselectivity.**

### 1.4.1 Linear Condensation Polymers

As mentioned above, combining a stoichiometric ratio of two comonomers, a perfluoroarene (AA) and a difunctional nucleophile (BB) is by far the most common approach in aromatic fluoropolymer synthesis. Subsections describe variations on this general strategy with a few examples to illustrate the central concepts.

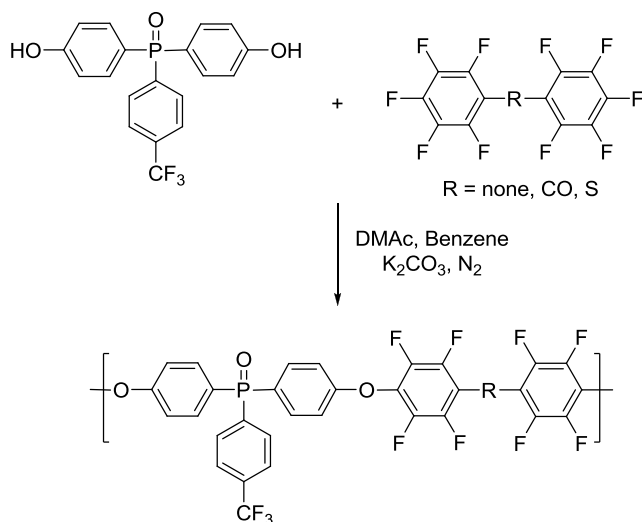
Carbon Nucleophiles. One could try to make polyarylenes by reacting perfluoroarenes with difunctional carbon nucleophiles. The resulting polymer would be connected entirely by carbon-carbon bonds and could be very stable. However, because carbon nucleophiles are strongly basic, they generally cannot be isolated to ensure the purity and precise assay needed for step-growth polymerization. The use of carbon nucleophiles is therefore relatively sparsely explored,<sup>37</sup> but some known examples include lithiated ferrocenes,<sup>83</sup> thiophenes,<sup>37</sup> acetylenes,<sup>84</sup> and indenes.<sup>85</sup> Scheme 1-12 shows a clever fluorodesilylation approach to generating the needed carbanions *in situ*. CsF cleaves the Si-aryl bonds, and the resulting arylcesium reacts as a nucleophile, forming a new C-C bond.<sup>37,86,87</sup> Fluoride is displaced, so the process is catalytic in

CsF. Generally the polymers formed from these nucleophiles are oligomeric species that may have useful electronic applications ( $M_n = 17 \text{ kg/mol}$ ,  $DP = 31$ ,  $T_g = 96 \text{ }^\circ\text{C}$ ).<sup>37</sup>



**Scheme 1-12. The generated arylcesium behaves as a nucleophile, forming a new C-C bond.**

Poly(arylene ether)s. Lee and co-workers synthesized fluorinated poly(arylene ether phosphine oxide)s from DFB, DFBP, and BPFPS, as well as some fluorinated dihydroxy(arylphosphine oxide)s in DMAc with an excess of anhydrous potassium carbonate, the most common base in these systems (Scheme 1-13).<sup>88</sup> The DFB-based polymers are generally more thermally stable than those derived from the ketone DFBP or the sulfide BPFPS.<sup>88,89</sup>



**Scheme 1-13. PAEs synthesized from DFB are typically more stable than those composed of DFBP or BPFPS.**

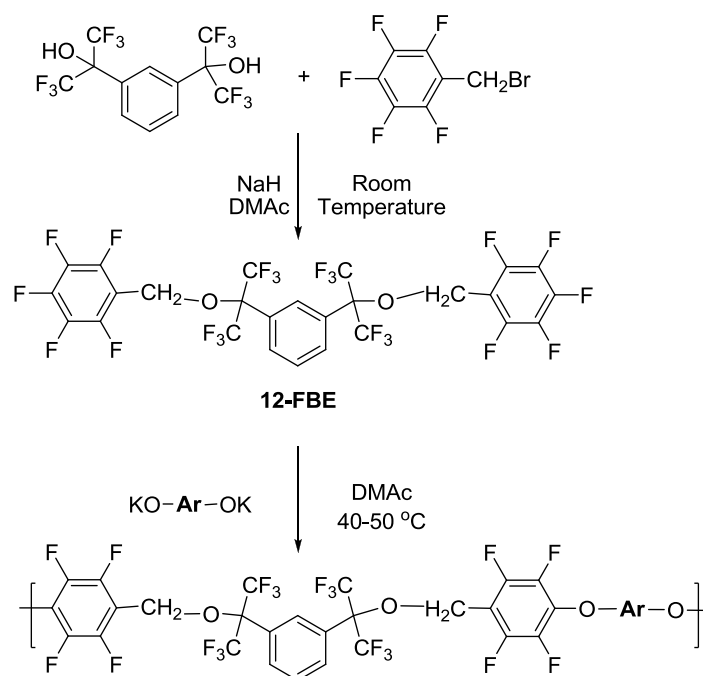
DFB generally undergoes nucleophilic substitutions at the 4- and 4'-positions, but if the conditions are not controlled carefully, substitution at a 2- or 3-position can occur, forming hyperbranched and crosslinked polymers and make processing more difficult.<sup>88,90</sup> Apparently,

the ketone DFBP and the sulfide BPFPS are even more prone to these kinds of unwanted side-reactions.<sup>90</sup> Switching to a less reactive perfluoroarene can sometimes enhance regioselectivity and prevent cross-linking.<sup>90</sup>

Cassidy and co-workers also studied highly fluorinated aromatics such as 1,2,4,5-tetrafluorobenzene (TFB), hexafluorobenzene (HFB) and decafluorobiphenyl (DFB) and their reaction with bisphenols like bisphenol-A (BPA) and bisphenol-AF (BPAF) in a DMAc/toluene medium.<sup>91</sup> BPA and BPAF reacted slowly with DFB to produce clear, colorless, flexible polymers that were soluble in ordinary solvents and showed low solution viscosity.<sup>91,92</sup> TFB was not reactive enough and did not form polymers, while HFB gave unfilterable gels. The first substitution at HFB introduces a pentafluorophenyl ether, which does not react regioselectively and may indeed react at two more positions to form crosslinked products.<sup>91</sup> Cassidy proposed to control this problem by changing the stoichiometry or the reaction conditions.<sup>91</sup>

In principle, any diol might react with a perfluoroarene like DFB. Accordingly, many research groups have built their own diols with wide-ranging functionality between the two OH moieties.<sup>93,94</sup> Usually the OH groups themselves are phenols because alkyl perfluoroaryl ethers are not particularly stable, but diaryl ethers are very stable.

As expected, there has also been some creativity on the side of the perfluoroarene monomers. Fitch and coworkers synthesized an interesting highly fluoroaromatic monomer (12F-FBE, Scheme 1-14).<sup>95</sup> In general, hexafluoroisopropylidene units impart useful properties like flame resistance, good solubility, thermo-oxidative stability, low color, low dielectric constant, crystallinity, and decreased water absorption.<sup>95-97</sup> The monomer 12F-FBE reacts with diphenols to form soluble, hydrophobic polyethers with glass transition temperatures ranging between 89 and 110 °C.<sup>95</sup>

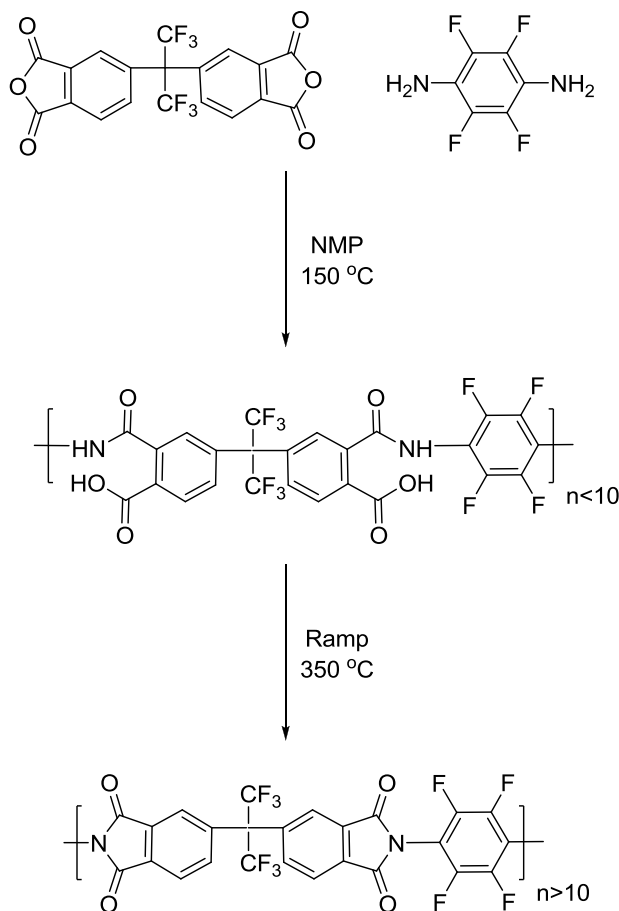


**Scheme 1-14. A creative variety of fluorinated monomers can be reacted with bisphenols to form PAEs.**

Poly(arylene ether)s are thermoplastics with excellent chemical, physical, and mechanical properties. Fluorinated poly(arylene ether)s are often especially soluble in common aprotic organic solvents, thermally stable, oxidatively stable and have low water absorption, refractive index, and optical loss.<sup>98</sup> Applications of fluorinated poly(arylene ether)s include engineering plastics,<sup>99</sup> membrane materials<sup>99</sup>, microelectronics (dielectrics),<sup>98,100</sup> optical waveguide devices,<sup>88</sup> organic light emitting diodes (OLEDs),<sup>101</sup> proton exchange membranes for fuel cells, and many other high performance applications.

Polyimides. Hougham and co-workers combined fluorinated phenylenediamines with anhydrides to prepare several highly fluorinated polyimides in a typical two-step procedure involving the synthesis of a polyamic acid followed by thermal imidization.<sup>102</sup> This example also illustrates the incorporation of the perfluoroarylene group into the nucleophilic monomer. The drawback of this approach is that fluorinated groups can reduce the reactivity of the

nucleophilic reactant, but Hougham and co-workers formed a precursor poly(amic acid) first (Scheme 1-15). The electron donating effect of the amine and the native electron deficiency of the anhydride control the rate of reaction. Normally, polyimides synthesized from fluorinated diamines have to be forced to high molecular weight, but fluorinated dianhydrides are readily reactive.<sup>102</sup> In fact, the reactivity of these fluorinated dianhydrides can cause problems in synthesis.<sup>102</sup> The incorporation of fluorine into polyimides have shown to lower the dielectric constant and water absorption, while improving optical properties and thermal stability in most cases.<sup>102</sup> In his review of low-*k* dielectrics,<sup>94</sup> Maier concluded that polyimides synthesized from a mixture of fluorinated and non-fluorinated monomers can achieve a low dielectric constant along with other desirable properties.



**Scheme 1-15. Hougham and coworkers report the synthesis of fluorinated polyimides.**

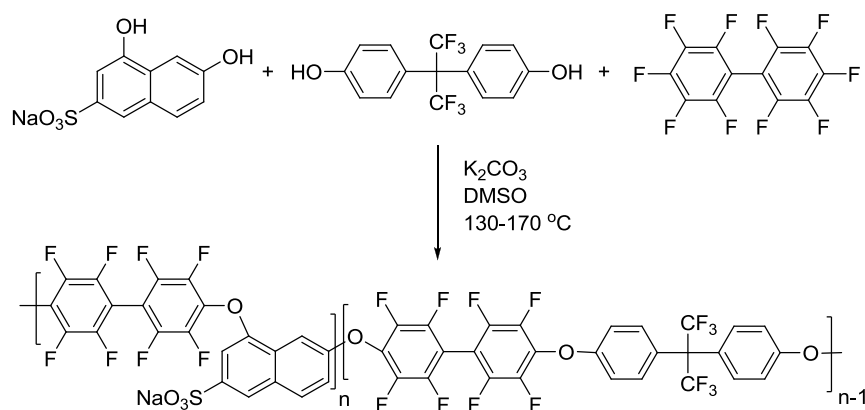
### 1.4.2 Perfluoroarylene Copolymers

A copolymer is a polymer with two different repeat units. Alternating copolymers have the monomeric units distributed in an alternating fashion, while block copolymers have these units distributed in larger groupings of homopolymer. In a random copolymer the monomer units are distributed in no particular order; composition is determined statistically. Graft copolymers have one homopolymer branching away from the backbone of another. Fluoroaromatic compounds play useful roles in the synthesis of these different microstructures and topologies, as illustrated in the next few sections.

Random Copolymers. In a reaction involving multiple monomers (generally  $AA + A'A' + BB + B'B'$ ), the tendency toward alternating, random, or block character is influenced strongly by *reactivity ratios* among the reactive groups. If a truly random copolymer is desired, then AA needs to have the same reactivity as  $A'A'$ , and so on. This criterion is not well met by mixing-and-matching among the fluoroaromatic monomers shown in Figure 1-6. Moreover the point of copolymerization is usually to tune features such as chain flexibility and the concentrations of lateral functional groups. Therefore the most common approach in fluoroaromatic polymers is to “co” the other monomer (e.g., the diol).

A good example of copolymerization involving two diols is shown in Scheme 1-16. Guiver and co-workers reacted DFB with varying amounts of BPAF and sodium 2,8-dihydroxynaphthalene-6-sulfonate to form random polymers intended for fuel cell applications.<sup>103</sup> Sulfonate content, a key parameter in PEM fuel cell materials, was under stoichiometric control. The authors claim a random co-monomer distribution, but from the structures of the two diols it is not obvious that they should have strictly identical nucleophilicities, even though both are

aromatic diols. Although the naphthalene moiety is desirable because of its low cost, the polymer suffers from poor solubility due to the rigid ring in the backbone.<sup>103</sup>

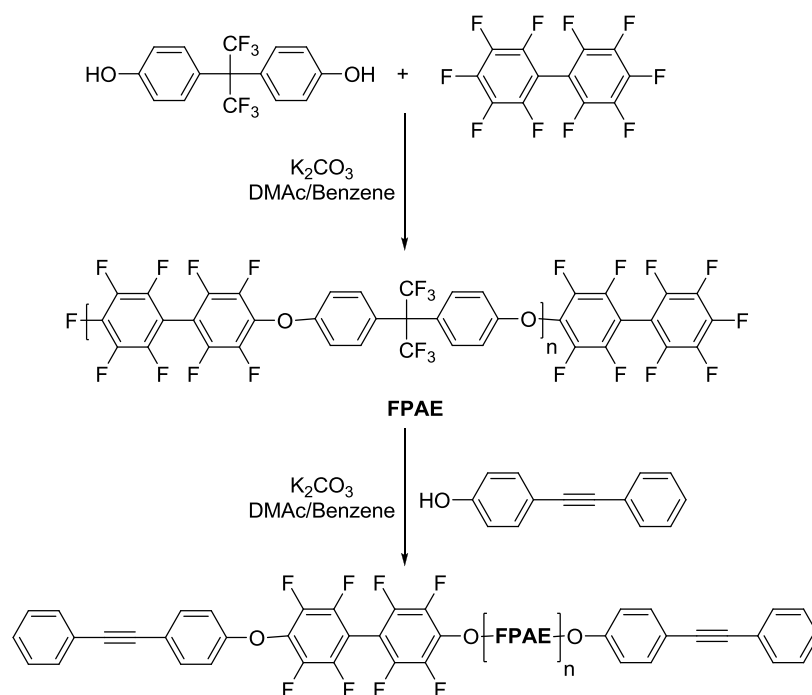


**Scheme 1-16. Guiver and coworkers produced random copolymers with both hydrophobic and hydrophilic segments.**

Segmented Copolymers. Another function that fluoroaromatic groups commonly serve is to link telomers together into larger, blocky (segmented) structures.<sup>104</sup> These copolymers are synthesized in order to combine the properties of both homopolymers that compose the newly synthesized copolymer. Block copolymers are also well known for their tendency toward micro-phase separation into distinct morphologies on the submicron scale.

McGrath and co-workers synthesized a variety of multiblock sulfonated fluoropolymers intended for use in proton exchange membrane fuel cells. A decafluorobiphenyl terminated poly(arylene ether) is synthesized and reacted with a hydroxy-terminated sulfonated poly(arylene ether sulfone) to yield a multiblock copolymer seen in Scheme 1-17.<sup>104</sup> The perfluorinated poly(arylene ether) acts as hydrophobic segment while the highly sulfonated poly(arylene ether sulfone) behaves as a hydrophilic segment in the newly formed highly phase separated material. The hydrophobic segment provides good mechanical properties and the hydrophobic segment enhances proton conductivity.<sup>104</sup>

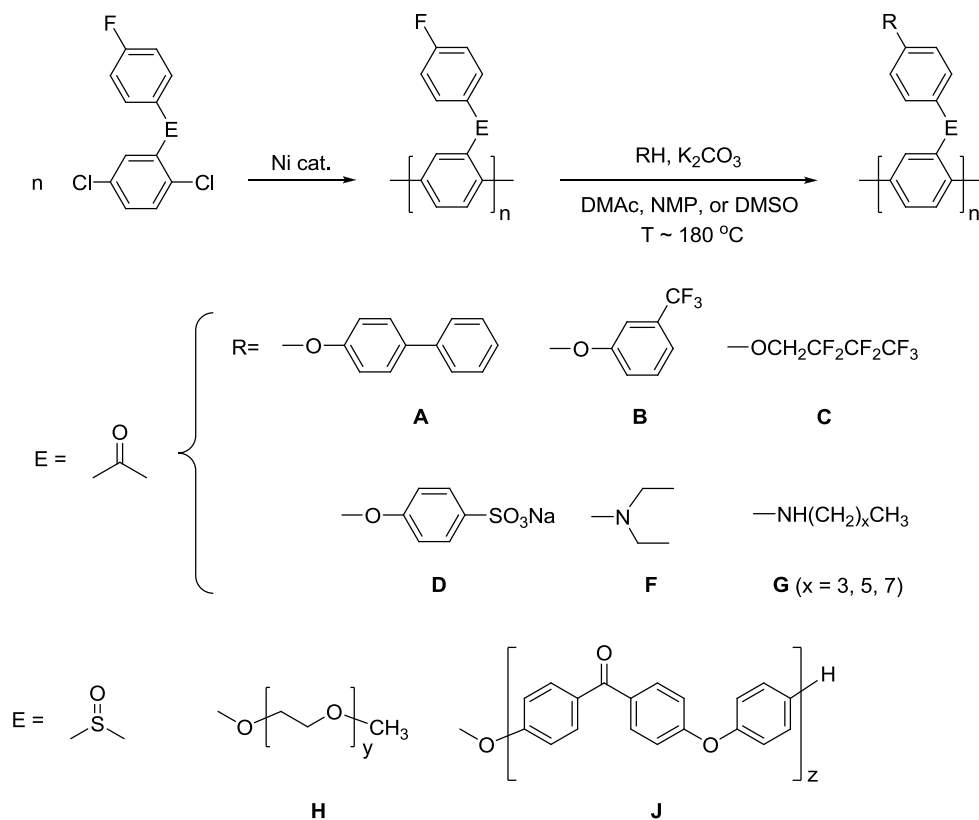




**Scheme 1-18.** Lee controls the end group functionality by stoichiometric ratio.

### 1.4.3 Lateral Functionalization

As discussed above, a main problem with (PPPs) is their poor solubility, which can be improved by adding pendant groups.<sup>106</sup> In addition, the predictable reactivity of fluoroaromatic groups enables controlled post-functionalization of a polymer containing those groups. Pendant (lateral) fluoroaryl groups are more commonly used for chemical modification, graft copolymerization, and crosslinking,<sup>106</sup> than backbone fluoroarylene groups. Even 4-fluorophenyl groups are reactive enough to allow efficient functionalization through  $\text{S}_{\text{N}}\text{Ar}$  when attached via an electron-withdrawing linker (Scheme 1-18).<sup>50,107</sup> This approach allows control over solubility, hydrophobicity,  $T_g$ , thermo-oxidative stability, and other physical properties of the polymer.<sup>50</sup>



**Scheme 1-19. Pendant groups improve solubility and provide a site for postmodification.**

This synthetic approach offers a way to design more variations into a polymer system with relatively few monomers (Scheme 1-19). Bloom and Sheares<sup>50,107</sup> used this approach to obtain polymers with modified hydrophobicity (**A**), fluoro-aliphatic content (**B**, **C**), and amine functionality (**F**, **G**), as well as graft copolymers with PEO (**H**) and PAEK (**J**).<sup>106</sup> Ghassemi and McGrath adapted this approach to prepare sulfonated polyphenylenes (**D**) for fuel cell applications.<sup>108</sup>

Pendant pentafluorophenyl groups enable post-polymerization substitution reactions to be effected under relatively mild conditions. Zolotukhin confirmed that the *para* position of the  $C_6F_5$  group reacts regioselectively with nucleophiles under basic conditions in polar aprotic solvent (Figure 1-7).<sup>109</sup> In this approach, it is important also to confirm (e.g., using SEC) that the post-functionalization reaction has not changed the overall DP.<sup>108</sup>

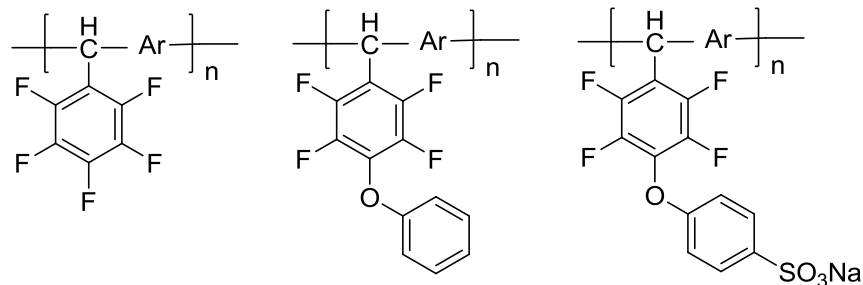


**Figure 1-7.** The *para* positions can be selectively displaced by various nucleophiles.

#### 1.4.4 Properties of Perfluorophenylene Condensation Polymers

Several discussions in the preceding paragraphs have referred to the superior physical properties of fluoropolymers, especially thermal stability.<sup>110-112</sup> These characteristics are often associated with saturated aliphatic fluoropolymer chains. For example it is known that changing BPA monomer to BPAF will enhance certain polymer properties, even though the added fluorine content is not really enough to consider the BPAF-derived polymers “fluorous.” Comparing fluoroaliphatic and fluoroaromatic structures is not simple though. Since this dissertation is about fluoroaromatic polymers, the goal of this section is to summarize the effects of introducing fluoroaromatic groups on physical properties. However, one unfortunately finds that information in this particular topic in the open literature is relatively sparse.

Kameshima and coworkers synthesized an array of fluorine-containing fluorene-based polymers for OLED applications (A in Figure 1-8).<sup>113</sup> The polymers with fluorinated benzene segments have decreased intermolecular interactions and lower main chain aggregation due to an increased free volume and large atomic radius of the fluorinated materials.<sup>113</sup> The polymers also showed higher fluorescence quantum yields (due to the distortion of planar structure with large fluorine atoms) and better thermal stability with increasing fluorine content.<sup>113</sup>

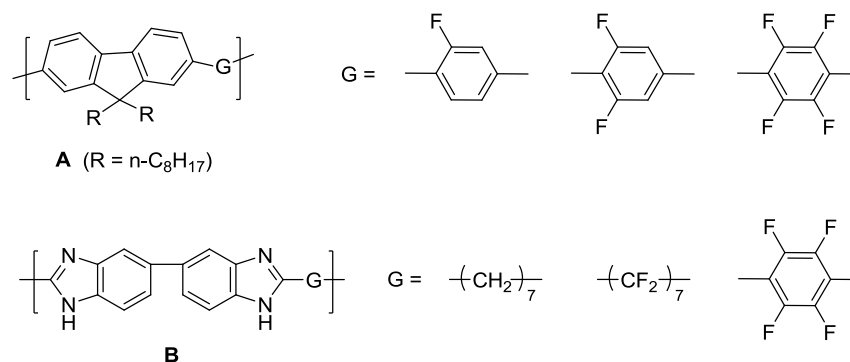


**Figure 1-8. Pu compares polybenzimidazoles with varying fluorine content.**

Pu et al. synthesized and compared fluorine-containing and nonfluorinated polybenzimidazoles for PEM applications (**B** in Figure 1-8).<sup>114,115</sup> The thermal stability, solubility, and radical oxidative stability is increased by introducing fluorine content into the structure. However, the modulus decreases slightly with more fluorine content due to the decreased intermolecular forces.<sup>114</sup> In both studies, the most noticeable characteristic owing to fluorine content is the decreased intermolecular interactions.

Zhu and Han synthesized both fluorinated (**C**) and nonfluorinated (**D**) aromatic polyesters to study the effect of fluorine on crystallization (Figure 1-9).<sup>116</sup> Material **C** was insoluble in most organic solvents at room temperature, but soluble in polar organic solvents such as DMF, DMSO, and DMAc. The increased solubility in polar solvents is caused by the local polarities within the fluorinated segments.<sup>116</sup> Material **D** did not show any crystalline behavior, while **C** was highly crystalline. The reduced intermolecular forces in the fluorinated polyester allowed higher mobility of the polymer chains, facilitating crystallization. The authors also suggest that the dipolar interactions deriving from C-F bonds can also act as a driving force for crystallization.<sup>116</sup> The increased fluoroaromatic content allow more freedom to align into ordered crystalline structures by reducing intermolecular chain interactions.<sup>116</sup>

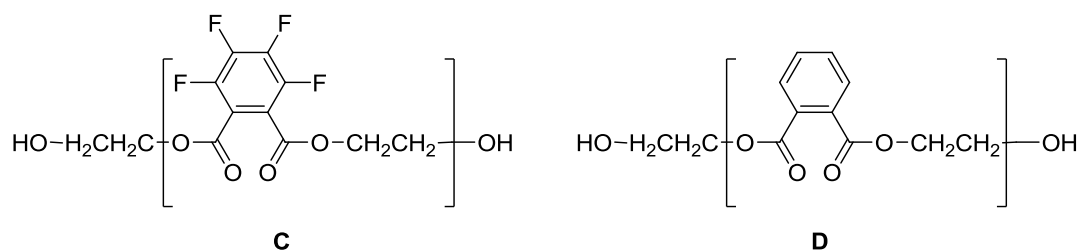
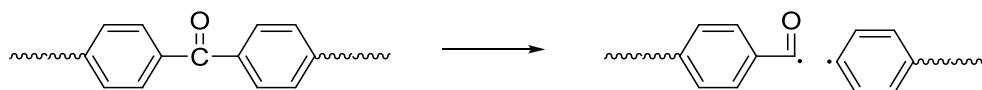


**Figure 1-9. Zhu and Han reports fluorinated and nonfluorinated polyesters.**

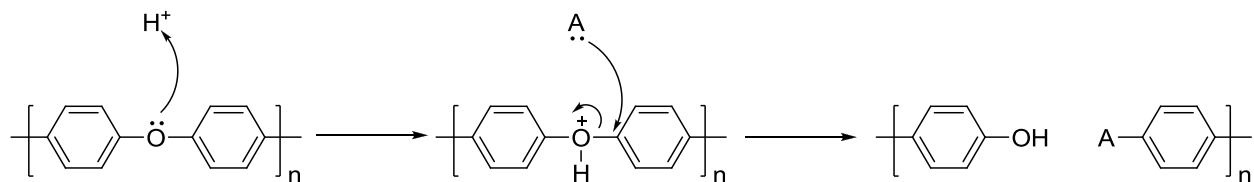
### 1.4.5 Stability of Perfluoroarylene Condensation Polymers

Polymers containing heteroatoms in their backbone structures are more susceptible to chain scission and other methods of degradation than polymers having entirely aromatic backbones (polyphenylenes). For example, studies conducted in a fuel cell environment demonstrate hydroxyl and superoxide radicals formed from oxygen crossover can either recombine or cause chain scission.<sup>117,118</sup> Scission mechanisms are dependent on the heteroatom within the backbone.<sup>4</sup> For example, polymers with carbonyl groups in the backbone are sensitive to scission because the newly generated radical is resonance stabilized (Scheme 1-20).<sup>119</sup> Poly(arylene ether)s easily undergo scission as well because phenoxy radicals are resonance stabilized.



**Scheme 1-20. Carbonyls are sensitive heteroatoms because the generated radical is resonance stabilized.**

Mitov and coworkers reviewed several possible mechanisms of degradation of fuel cell membranes for polysulfones, polyetherketones, polybenzimidazoles, polyethersulfones, polyetherimides, *etc.*<sup>117,118</sup> Free radical processes can induce chain scission, but some proposed degradation routes include protonation as a first step. A mechanism of degradation of poly(arylene ether)s proposed by Sanchez shows that the hydrochloric acid byproduct induces chain scission when polymer size increases (Scheme 1-21).<sup>120</sup>



**Scheme 1-21. Polymers with heteroatoms are more sensitive to scission mechanisms.**

### 1.5 Diels-Alder Polyphenylenes

Section 1.2 showed that polyphenylenes are interesting for their thermal and chemical stability, and for their rigid structures, which makes them suitable candidates for applications when glassy polymers are needed. Section 1.4.4 showed how fluorination, in the form of fluoroaromatic moieties, imparts interesting physical properties to condensation polymers. Fluoroaromatic groups especially provide new opportunities for functionalizing, grafting, and segmenting to form new polymers with a wide range of potential applications.

Combining the stable, semi-rigid architecture of polyphenylenes with the desirable attributes of fluoroaromatics would be a natural research avenue. However, there is not, in the open literature, a general way to make polyphenylenes that are highly fluorinated. Palladium-catalyzed coupling reactions, which are otherwise quite applicable to the synthesis of polyphenylenes, are not generally useful for fluoroaromatic substrates. While  $S_NAr$  is a successful route to polymers containing fluoroarylene subunits, it is not applicable to the synthesis of true polyphenylenes without heteroatoms.

However there is one method of polyphenylene synthesis that could be adapted to fluoroaromatic analogues. This method is Diels-Alder polycondensation. This section will review this synthetic approach, and the rest of this dissertation will show how we have developed monomer chemistry and polymerization methods to adapt Diels-Alder polycondensation to the synthesis of highly fluorinated polyphenylenes. Nucleophilic substitution reactions play a key

role in my research plans in two ways: First in monomer synthesis, and second in post-polymerization functionalization chemistry.

### 1.5.1 Introduction to DAPPs

The Diels-Alder reaction is a [4+2] cycloaddition in which a diene reacts with a dienophile (usually an alkene or alkyne), forming two new C-C bonds simultaneously (Figure 1-10).

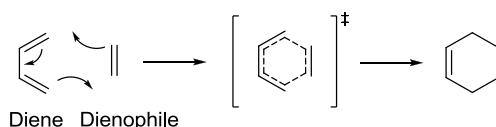


**Figure 1-10. The Diels-Alder reaction proceeds through an aromatic transition state.**

Stille initially used the Diels-Alder reaction to form polymers from 1, $\omega$ -bis(cyclopentadienyl)alkanes (Figure 1-11).<sup>121</sup> The idea is simple because the cyclopentadiene serves as both the diene and dienophile, and the reaction needs no catalyst and forms no by-products.<sup>121,122</sup> However, the monomers were difficult to purify and the polymer reverts to monomer starting at about 120 °C. Although the idea of reversibility is interesting for self-mending or recyclable polymers,<sup>123,124</sup> that feature is undesirable for a thermally stable polymer.

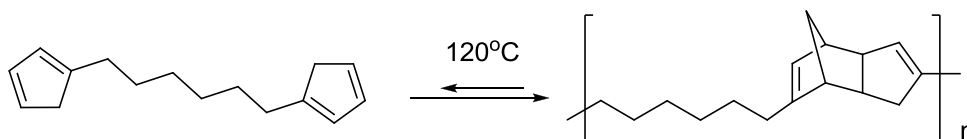


**Figure 1-11. First-generation Diels-Alder homopolymers form reversibly.**

Stille solved these problems by taking advantage of an interesting, irreversible Diels-Alder reaction involving an alkyne and cyclopentadienone (CPD), a 2-pyrone<sup>125</sup>, or a thiophene dioxide.<sup>126-128</sup> The reaction proceeds through an unstable bicyclic intermediate, extrudes the small molecule (CO, CO<sub>2</sub>, or SO<sub>2</sub>), and forms a new aromatic ring (Fig 1-12).<sup>126</sup> Moreover the loss of the extruded molecule adds to the entropic driving force, and the reaction is

thermochemically irreversible.<sup>129</sup> The Diels-Alder polycondensation follows a second-order rate law and requires a low  $\Delta H$  ( $\Delta H^\ddagger = 12.4$  kcal/mol) and a large negative  $\Delta S$  ( $\Delta S^\ddagger = -48$  eu).<sup>130</sup>

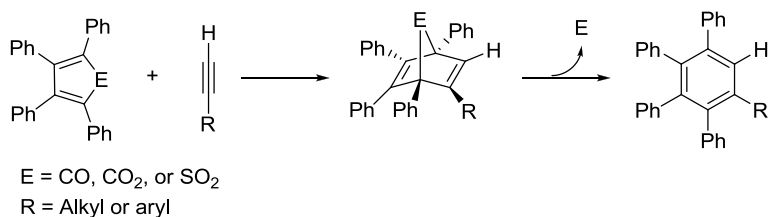


**Figure 1-12. Irreversible Diels-Alder reactions involve small-molecule extrusions.**

By reacting dialkynes and CPD monomers, Stille converted this reaction into a platform for polyphenylene synthesis (Figure 1-13). If the dialkyne and CPD linkers ( $L_1$  and  $L_2$ ) are aromatic, then the product is a wholly aromatic polymer composed of a benzene backbone, which makes it mechanically and thermally stable.<sup>127,128</sup>

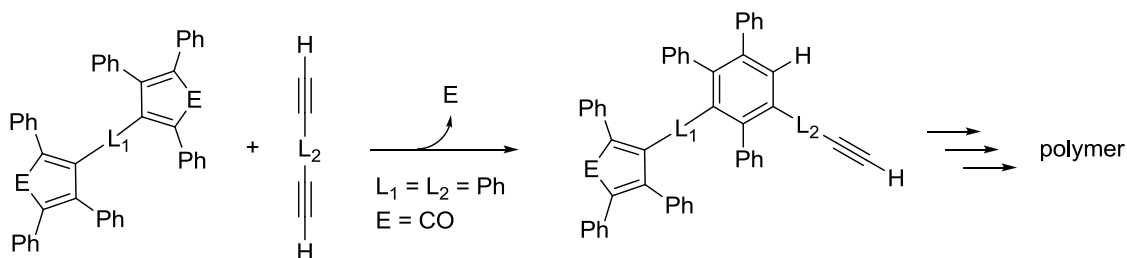
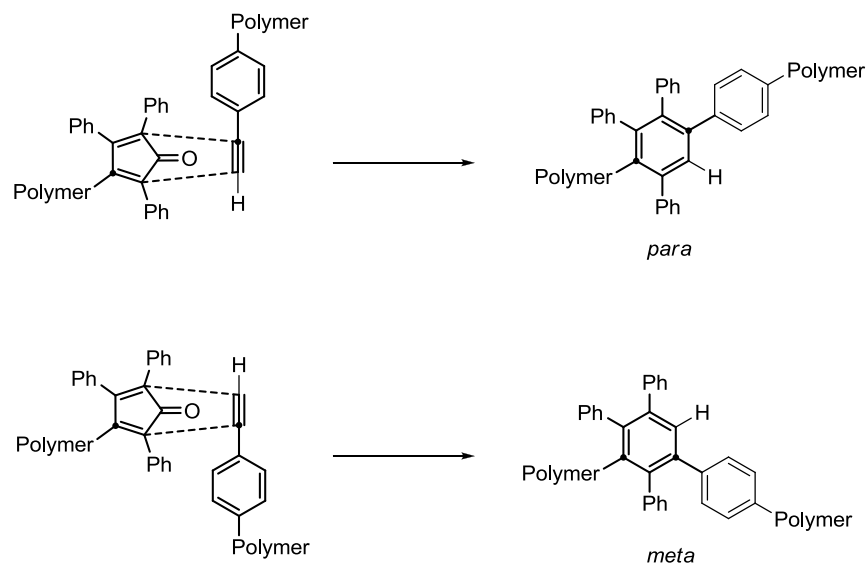


**Figure 1-13. Irreversible Diels-Alder reactions provide a basis for polymer synthesis.**

Diels-Alder polyphenylenes are more soluble than typical polyphenylenes because the reaction forms both *meta*- and *para*- linkages, so the chains are not true rigid rods (Scheme 1-22).<sup>131,132</sup> The reaction between CPDs and alkynes is generally not regioselective; Stille and Noren reported a ratio of *para*- to *meta*-catenation of approximately 57:43.<sup>131,132</sup> In general the materials become more amorphous (more soluble, lower melting point) with increasing *meta* linkage content.<sup>127</sup>



**Scheme 1-22. CPD-derived Diels-Alder polyphenylenes exhibit both *meta* and *para* catenation.**

Stille used phenyl-substituted CPD monomers simply because they were synthetically accessible through aldol chemistry. These phenyl substituents become “lateral” substituents in the resulting polymer. Since the size of the lateral groups prevent arene stacking, the phenylated polyphenylenes are less crystalline compared to other phenylene derivatives. The lateral groups also twist the polymer into nonplanar biaryl conformations and disrupt the phenylene conjugation along the backbone.<sup>132</sup> The result is a Diels-Alder polyphenylene (DAPP) that is not only soluble in chloroform and thermally stable to 550 °C in air (at which temperature lateral phenyl groups begin to cleave), but also electrically insulating (see subsequent section on DAPP properties).

The advantage of using pyrones (Figures 1-12 and 1-13, E = CO<sub>2</sub>) over cyclopentadienone monomers is their superior regioselectivity. 5-Substituted 2-pyrones react with alkynes to form only the *para* isomer of the new aromatic ring (Figure 1-14). Stille showed that poly(*p*-phenylene) could be made from 5,5'-*p*-phenylenebis-2-pyrone and *p*-diethynylbenzene to produce PPP, which of course has very different properties compared to phenylated

polyphenylenes.<sup>133</sup> The phenylated polyphenylenes were yellow amorphous powders with good solubility, while the PPP was intractable.<sup>133</sup> Pyrone-derived PPP had significantly higher thermal stability than the phenylated polyphenylene structure with 10% weight loss at 650 °C.<sup>133</sup> Stille took advantage of the excellent regiocontrol to prepare a regio-alternating polyphenylene as well (Figure 1-14).

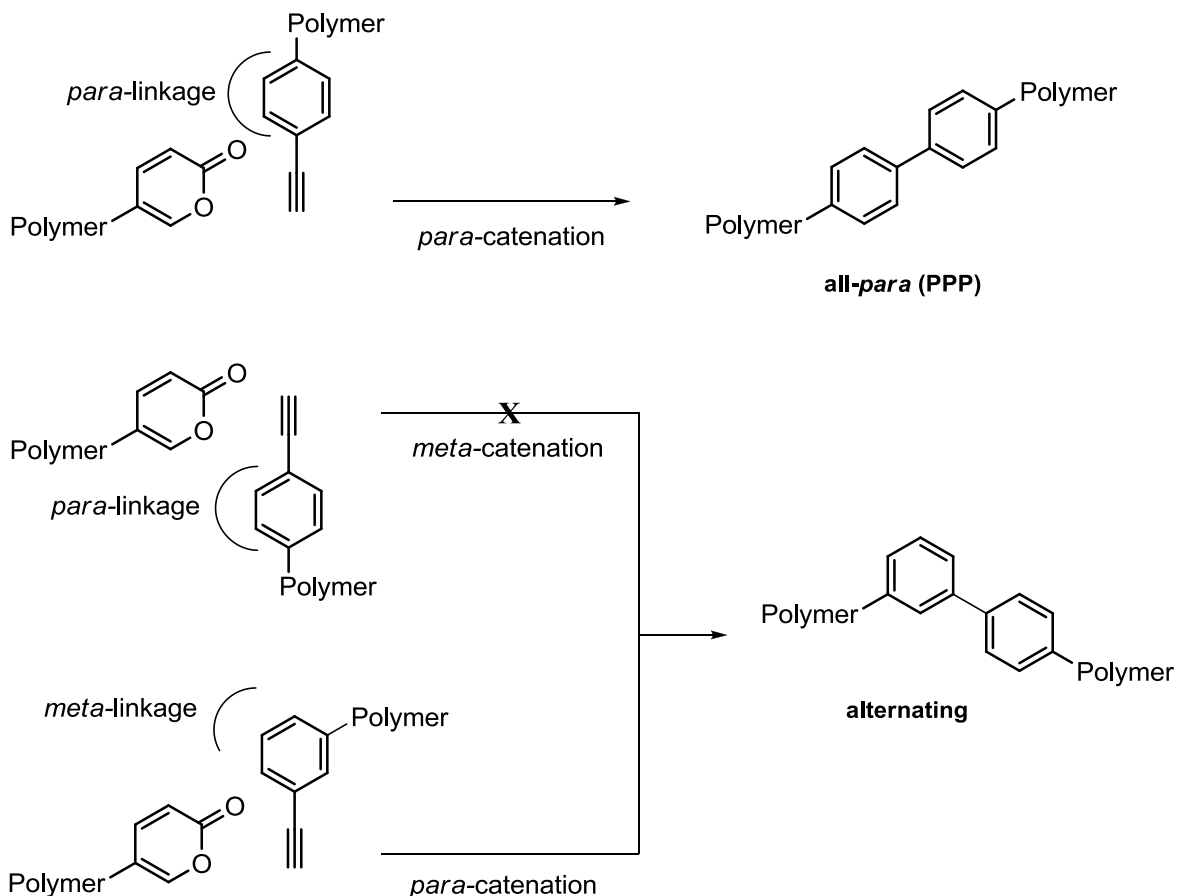
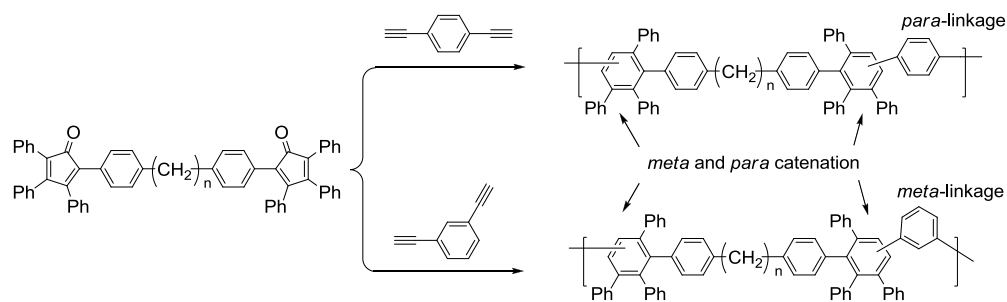


**Figure 1-14. Pyrone-derived Diels-Alder polyphenylenes are regioregular.**

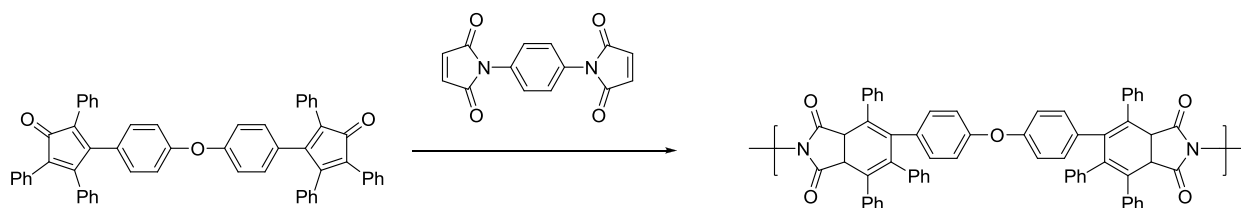
Like other types of polycondensation, Stille's Diels-Alder approach has the advantage that either the CPD (or pyrone) monomer or the dialkyne can be modified, giving rise to many structural variations. For example, Stille polymerized alkyne-linked CPD monomers with diethynylbenzene (Scheme 1-23).<sup>126</sup> The resulting polymers (DP = 30-60) were more soluble

than the all-benzene-backbone analogues, but they also had lower degradation temperatures (465 °C). Clear films of these polymers were cast from chloroform.<sup>126</sup>



**Scheme 1-23. DAPPs containing alkylene chains have improved solubility and lower thermal stability.**

Stille also applied the Diels-Alder approach to polyimides.<sup>134</sup> A bis(maleimide) reacts with the difunctional CPD monomer to form a polyimide that is soluble in DMF and forms clear, slightly yellow films (Scheme 1-24). The polymer can be dehydrogenated (aromatized) at elevated temperatures.<sup>134,135</sup> Rusanov and co-workers extended this work with several different tetracyclone monomers and anhydrides to form phenylated polyimides.<sup>135</sup>



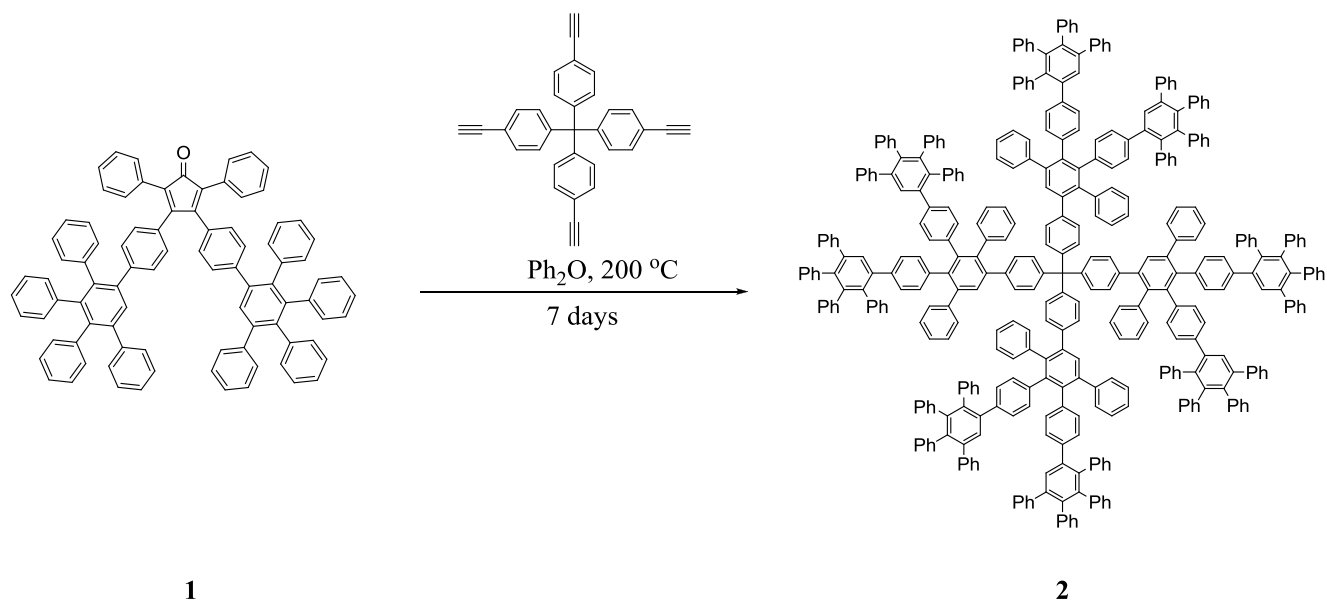
**Scheme 1-24. The Diels-Alder polycondensation can also be applied to polyimide synthesis.**

Kumar and Neenan extended Stille's work, varying both the CPD and dialkyne structures, to make several substituted DAPPs. The polymers are generally soluble in common organic solvents.<sup>135</sup> These authors found that that the polymerization reaction is strongly dependent on concentration of the reactants. This phenomenon is difficult to explain and these types of results have been seen before.<sup>135,136</sup> The polymers with molecular weights ranging from 5-140 kg/mol (DP = 6 to 175) with glass transition temperatures ranging from 245 to 270 °C and

decomposition temperatures from 310 to 480 °C.<sup>137</sup> The fluorinated dialkyne, 1,3-diethynyltetrafluorobenzene, reacted with a CPD to form polymers with high glass transition temperatures (up to 285 °C) and very high decomposition temperatures (543 °C under argon) compared to the non-fluorinated analogs.<sup>137</sup> These polymers form strong, transparent films and were studied for dielectric applications.<sup>135,137</sup>

### 1.5.2 Hyperbranched or Dendritic Structures by Diels-Alder Polycondensation

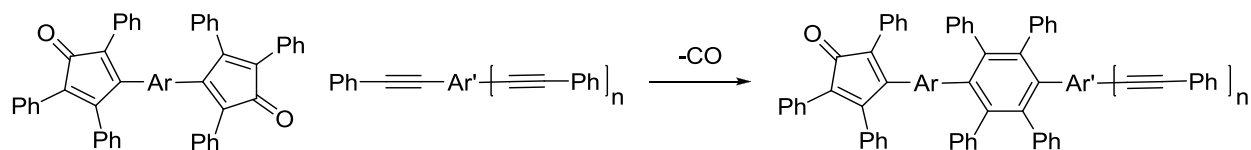
The main advantage of hyperbranched or dendritic structure is increased solubility and processability over linear analogs, while maintaining excellent chemical and thermal stability from the aromatic structure. Müllen showed the synthesis of thermally and chemically stable dendrimers by DA condensation of a highly phenylated cyclopentadienone dendron (**1** in Scheme 1-25).<sup>138</sup> Dendron **1** reacts with multifunctional alkynes to produce dendrimers with over 60 benzene rings. The highly phenylated dendrimers possess excellent thermal stability and chemical stability. Dendrimer **2** (Scheme 1-24) decomposed under air at temperatures higher than 550 °C. The dendrimers did not decompose after exposure to boiling concentrated HCl or 30% KOH solutions.<sup>138</sup> More sterically hindered multifunctional alkynes require higher reaction temperatures or longer reaction times. Different shapes may be obtained by changing to a less sterically hindered core or modifying the cyclopentadienone dendron structure.<sup>139,140</sup> Müllen also explored polyphenylenes for organic electronic applications<sup>140</sup> and spherical, monodisperse polyphenylene dendrimers<sup>139,140</sup> that may be oxidized to generate well-defined graphite disks.<sup>141</sup>



**Scheme 1-25. Müllen shows the synthesis of highly phenylated dendrimers by Diels-Alder cycloaddition.**

### 1.5.3 DAPP Applications

DAPPs have been pursued as high performance materials since their discovery. Variations on Stille's original theme were commercialized by Dow Chemical Company as spin-on dielectric coatings for microchips<sup>142,143</sup> under the trade-name SiLK.<sup>TM</sup> SiLK dielectric was synthesized by reacting polyfunctional cyclopentadienone and acetylene-containing materials to produce crosslinked polyphenylenes.<sup>143</sup> The processability issues can be resolved by forming soluble oligomers followed by spin coating. The oligomers further react on wafers to make the crosslinked polyphenylene coating, a technique known as b-staging. SiLK resin is a partially polymerized oligomer with molecular weights less than 10,000 g/mol in high purity organic solvents (Scheme 1-26).<sup>143</sup> Spin coating and thermal curing (400-470 °C) produce durable thin films.<sup>143</sup>



**Scheme 1-26. SiLK resin is a partially polymerized oligomer.**

DAPPs have been investigated as novel dielectrics due to high molecular weight, high glass transition temperature, thermal and mechanical stability, high solubility in common organic solvents, good film forming ability, and ease of incorporating organic substituents by utilizing simple changes in the polymerization chemistry.<sup>63,143</sup> The cured SiLK films have low dielectric constants (2.65), high glass transition temperature (490 °C), high fracture toughness (0.62 MPa m<sup>1/2</sup>), and 0.7%/h isothermal weight loss at 450 °C.<sup>143</sup> DAPPs possess unique low dielectric properties because they have high free volume and the absence of polar groups along the polymer chain.<sup>63</sup>

Sandia National Laboratories showed that the lateral phenyl groups on DAPPs may be sulfonated (Figure 1-15) to form proton conductive materials for applications as proton exchange membranes with good thermal and oxidative stability.<sup>144,145</sup> The pendant phenyl rings allow the incorporation of up to six sulfonic acid groups per repeat unit.<sup>144</sup> The post-sulfonated DAPP or SDAPP possesses proton conductivity similar to Nafion.<sup>144,146</sup> The introduction of sulfonic acid groups make the DAPP proton conductive and more hydrophilic at the same time, so sulfonic acid content was carefully monitored to maintain good mechanical properties. These materials had molecular weights ranging from 55 to 82 kg/mol with an average polydispersity around 2. The unsulfonated polymer had a glass transition temperature of 388 °C, but thermal decomposition of the sulfonic groups prevented measurement of the glass transition temperature of the sulfonated DAPP. The glass transition temperature was anticipated to be higher than the nonsulfonated material because of more intermolecular interactions like hydrogen bonding.

SDAPP formed creasable films. Although the material is composed of rigid chains, the SDAPP possessed properties that are attractive for PEM application with high glass transition temperature, high thermochemical stability, and high modulus.<sup>144,145</sup>

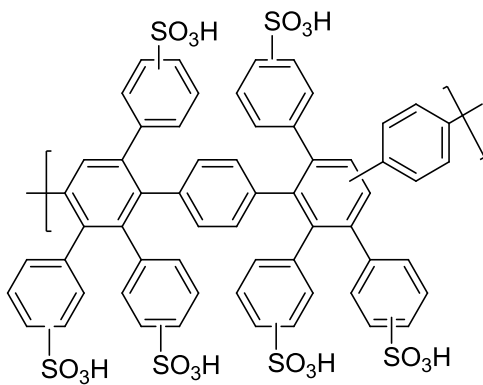
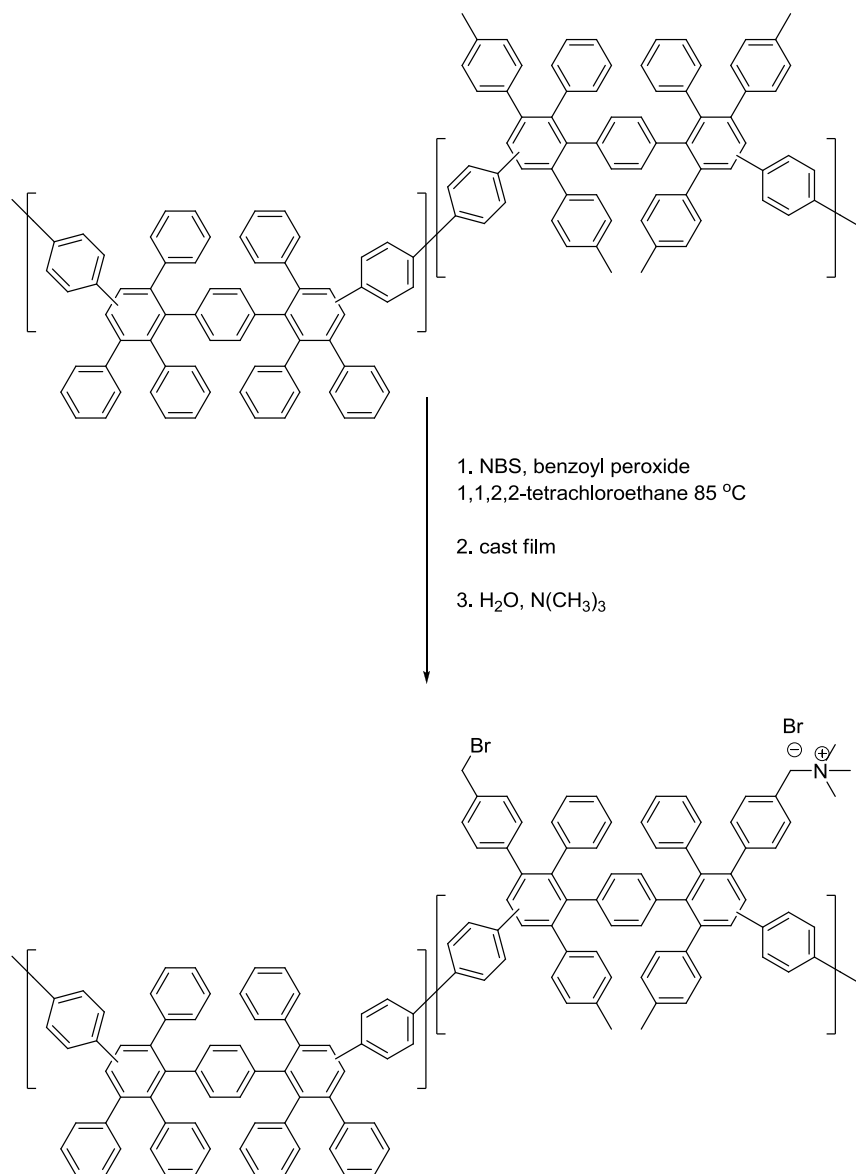


**Figure 1-15. The lateral phenyl groups of DAPPs are sulfonated selectively.**

The same sulfonated material was studied for gas separation membranes. Most gas separation membranes are made up of high free volume, glassy polymers with void regions that help gas transport through the membrane.<sup>147</sup> The rigid aromatic backbone and lateral phenyl groups of DAPPs make them good candidates for gas separation membrane materials.<sup>63,148</sup> The lateral phenyl rings are aligned out-of-plane with the backbone. This orthogonal orientation prevents conjugation, and the steric interactions cause high free volume, which allows gas permeability.<sup>148</sup> Reduced mobility as a result of the rigid aromatic backbone leads to good selectivity.<sup>63,148</sup> The ability to selectively modify the arylene polymers, mechanical properties, thermal stability, and high free volume make these materials ideal candidates for gas separation.<sup>131,148,149</sup>

Hibbs, Fujimoto and Cornelius investigated DAPPs for anion exchange membranes for use in alkaline fuel cells and other electrochemical devices. Methyl-substituted DAPPs were converted into cationic polymers by bromination and amination (Scheme 1-27). The resulting cationic polymers are robust, creasable films with high ion conductivity and better properties compared to

polysulfone rivals. These materials are excellent candidates for anion exchange membranes because they exhibit high conductivity and good stability at high pH conditions.<sup>131</sup>



**Scheme 1-27. Hibbs and coworkers produce cationic polymers from DAPPs.**

## 1.6 Conclusions

The goal of this work is to combine the thermal and chemical stability of fluoropolymers and polyphenylenes. However, the synthesis of a fluorinated polyphenylenes is not trivial. Oxidative coupling methods form oligomers with poor solubility because *para*-catenation is favored.

Metal-catalyzed coupling methods are not suitable for fluorinated polyphenylene synthesis because fluorine undergoes side reactions with metals and catalyst retrieval from a polymer system can be expensive. Although several fluorine-containing polymers are synthesized by nucleophilic substitution, most condensation polymerizations involve the incorporation of a heteroatom into the polymer backbone, weakening the thermal and chemical stability. The literature review shows the Diels-Alder polymerization is an ideal method to form highly fluorinated polyphenylenes with a true aromatic backbone. Also, the *meta*- and *para*- catenation of Diels-Alder polyphenylenes improves overall solubility for synthesis and processing compared to other approaches to polyphenylenes.

## Chapter 2. Synthesis of Highly Fluorinated Biscyclopentadienone (CPD) Monomers

### 2.1 Introduction

Like many types of condensation polymer, Diels-Alder polyphenylenes (DAPPs) can have wide variations in structure and physical properties. As described in Chapter 1, both the bis(cyclopentadienone) (CPD) and dialkyne monomers can be varied in their structure to obtain polymers with a wide range of physical properties. We envisioned an efficient synthesis of highly fluorinated CPD monomers using cyclopentadiene chemistry developed almost entirely within Prof. Deck's laboratories since 1995. It was really this insight that led us into the exploration of fluorinated DAPPs, which is the main subject of this dissertation. The present chapter discusses the origins of our approach, our overall synthetic strategy, and the details of our monomer synthesis.

### 2.2. Monomer Design

2.2.1 Design Origins. Stille's original CPD monomer (**A**) has two main skeletal features: Pendant aryl groups on the cyclopentadienone rings and an aromatic group linking two cyclopentadienes (Fig. 2-1).<sup>126</sup> These features are not arbitrary. First of all, the linker has to be aromatic if the resulting polymer is to have a polyphenylene structure, which was Stille's main goal. Stille's CPD monomer syntheses used base-catalyzed aldol condensation reactions (Fig. 2-1). Functional group tolerance under the necessarily harsh conditions is very limited. Selectivity for the cyclopentadienone product is much higher if the only elimination reactions possible are within the five-membered ring (endocyclic). In addition, the product cyclopentadienones are only stable (e.g., with respect to dimerization) if the core five-membered ring is highly substituted (three or four attached groups).<sup>150</sup> Therefore, Stille was essentially limited to benzils (diphenylethanediones), dibenzyl ketones, and their ring-substituted analogues.

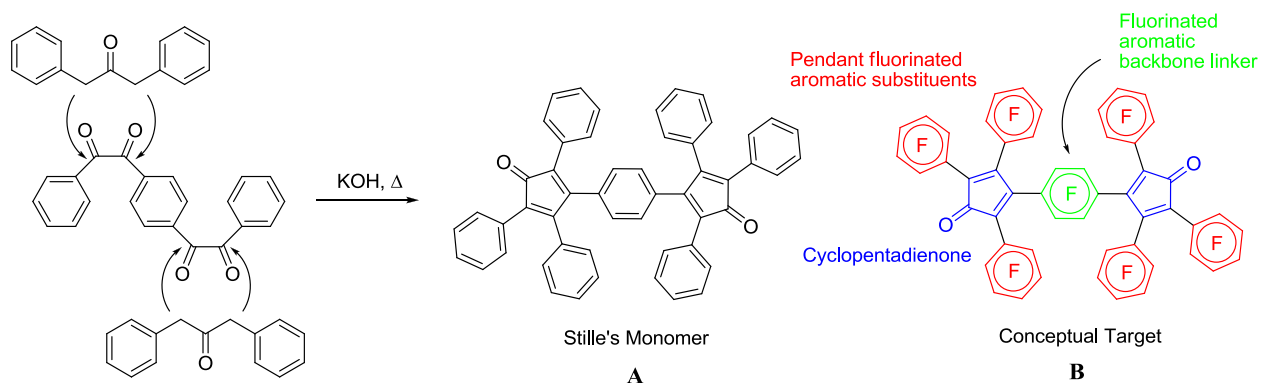
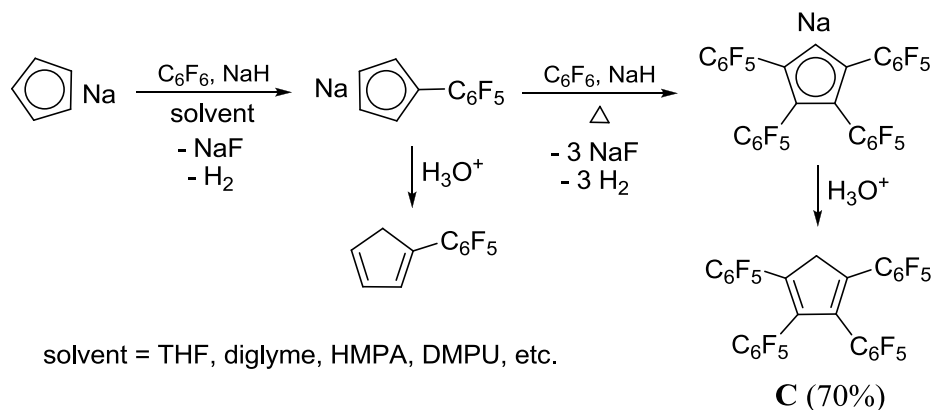


**Figure 2-1. The conceptual target (B) is similar to Stille's CPD monomer (A).**

Our proposed conceptual target (**B**) retains the features of Stille's monomer while maximizing fluorine content in the pendant aryl groups and arylene linker. However, synthetic limitations specifically rule out the aldol approach to our target **B**. Highly fluorinated aromatic groups undergo nucleophilic substitution readily (Section 1.3), and the conditions of the aldol condensation are functionally incompatible. One could envision an acid-catalyzed variant, and the needed starting materials are known. (Perfluorobenzil<sup>151</sup> may be prepared from  $C_6F_5Cu$  and oxalyl chloride, while 1,3-bis(pentafluorophenyl)acetone<sup>152</sup> is made from pentafluorobenzyl bromide and  $Fe_2(CO)_9$ .) However, as shown below we envisioned an alternative synthetic approach to perfluorinated CPD monomers, all the while keeping an open mind about the possibility that we might have to modify the “dream” structure shown in Fig. 2-1.

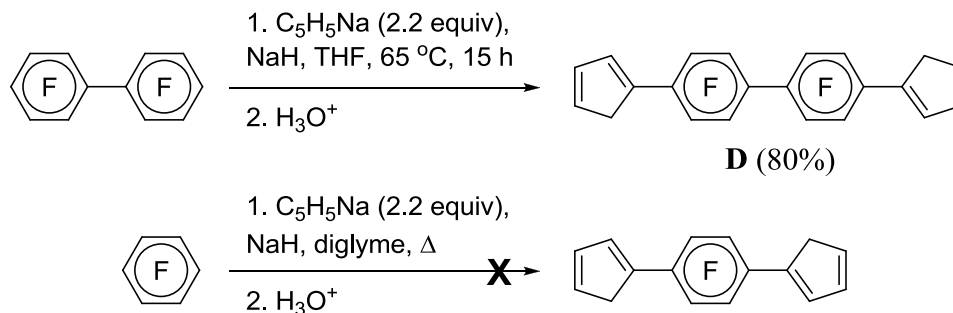
Deck and co-workers previously reported an interesting and efficient synthesis of fluoroarylated cyclopentadienes (Scheme 2-1), in which cyclopentadienyl anions react with perfluoroarenes ( $S_NAr$ ).<sup>83,85,151,153</sup> Multiple positions of the cyclopentadienyl anion may be substituted (often in one pot) and selectivity for the number of aryl groups attached is obtained by varying the stoichiometric ratio. The reaction is clean and proceeds in high yields. The perfluoroarenes may be hexafluorobenzene (shown in Scheme 2-1), octafluorotoluene (selective for substitution *para* to the  $CF_3$  group)<sup>154</sup> or pentafluoropyridine (selective for substitution at the 4-position).<sup>155</sup> The

number of fluorinated aromatic groups posted on the cyclopentadienyl anion varies with reaction conditions. Interestingly, even under forcing conditions no pentaarylated products are observed; diene **C** is obtained selectively.



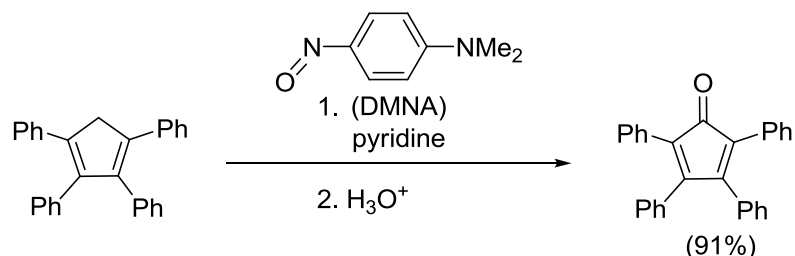
**Scheme 2-1. Prof. Deck previously reported the synthesis of arylated cyclopentadienes from cyclopentadienyl anions.**

A resemblance of diene **C** to the conceptual target **B** is obvious. However two important differences are apparent. First, the target **B** bears *two* linked five-membered rings, whereas **C** is a mono-diene. Second, **B** has ketone oxygens in place of the methylene hydrogens of **C**. Deck and co-workers showed previously that two cyclopentadienes may be connected through a fluoroarylene by the reaction of cyclopentadienyl anion (2 equiv) with decafluorobiphenyl (Scheme 2-2). The linked compound **D** is obtained in over 80% yield, however it is unstable toward dimerization of the cyclopentadiene units and must be stored as its conjugate base. Note that this reaction places two arylene groups between the cyclopentadiene groups, whereas the conceptual target **B** has only one. However hexafluorobenzene does not react with 2 equiv of  $\text{NaC}_5\text{H}_5$  even under forcing conditions, so if a single arylene linker is required, one would need to find different chemistry to achieve it.



**Scheme 2-2. Decafluorobiphenyl can connect two cyclopentadiene moieties.**

The other difference between target **B** and diene **C** is the oxidation state of the ring carbon that does not bear a substituent. There are methods in the literature for converting substituted cyclopentadienes to the corresponding cyclopentadienones,<sup>150</sup> most notably that shown in Scheme 2-3, which uses *N,N*-dimethylnitrosoaniline (DMNA).<sup>156</sup> While it was not clear which of the available oxidation methods would work for fluoroaryl-substituted cyclopentadiene derivatives, we attempted to adapt them to our needs.

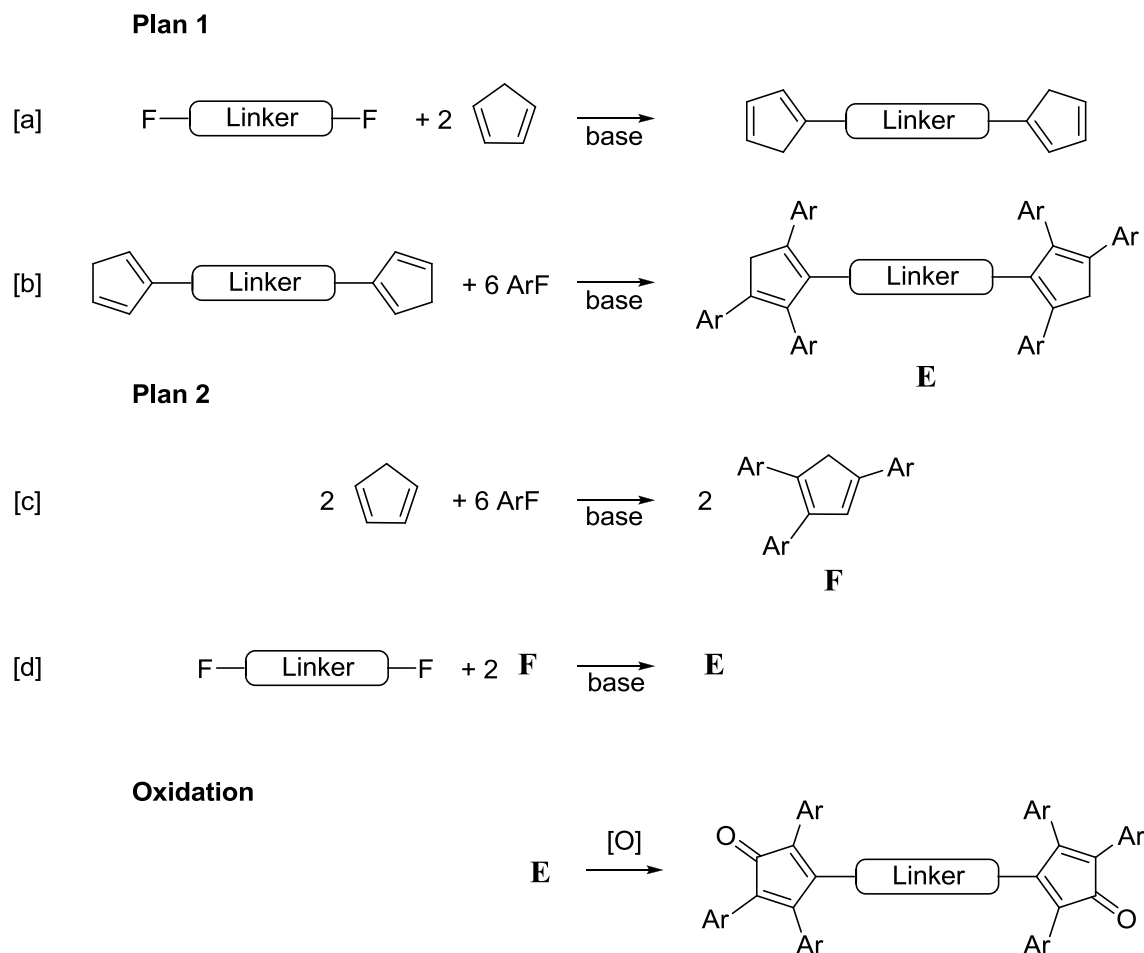


**Scheme 2-3. Dilthey and Schommer report the oxidation of arylated cyclopentadienes to the corresponding ketones using DMNA.**

**2.2.2 A Generalized Monomer Synthetic Plan.** The preceding section shows how we could meet the three basic requirements for the preparation of target **B** or a substantially similar compound: (1) Attaching multiple fluoroaryl groups to stabilize the cyclopentadienone and contribute additional fluorine content to the monomer, (2) Linking two cyclopentadienes using a

fluorinated arylene group, and (3) Oxidation of the unsubstituted carbon atoms of a substituted cyclopentadiene. This section describes the order in which these steps might occur.

Scheme 2-4 shows a pair of general synthetic pathways. Because the carbon skeleton is assembled using nucleophilic substitution reactions of cyclopentadienyl anions, oxidation to the ketone has to be last. In the first pathway (Plan 1), the cyclopentadienes are linked first (e.g., with decafluorobiphenyl, **linker** = C<sub>12</sub>F<sub>8</sub>), followed by attachment of the pendant fluoroaromatic substituents (Ar) and then oxidation [O] of the common intermediate **E**. In the second pathway (Plan 2), the pendant groups are attached before the linker. The second pathway has both a major advantage and a disadvantage. The advantage comes in the final step, [**d**], where only two CC bond-forming reactions need to happen. Convergence often helps minimize the number of side reactions and simplifies product purification, often critical in monomer synthesis. Plan 1 requires six CC bond-forming reactions, obviously a divergent synthetic approach. The disadvantage of Plan 2 comes from the need to prepare the intermediate **F** selectively, leaving places both for attachment of the linker and for oxidation. Deck and co-workers have found that this selectivity does not always come easily.<sup>153</sup> A further disadvantage of Plan 1, which will be explained in more detail below, is that **E** is obtained as a mixture of three skeletal regioisomers, whereas Plan 2 should afford **E** as a single species.



**Scheme 2-4. There are two general methods for the synthesis of fluorinated CPDs.**

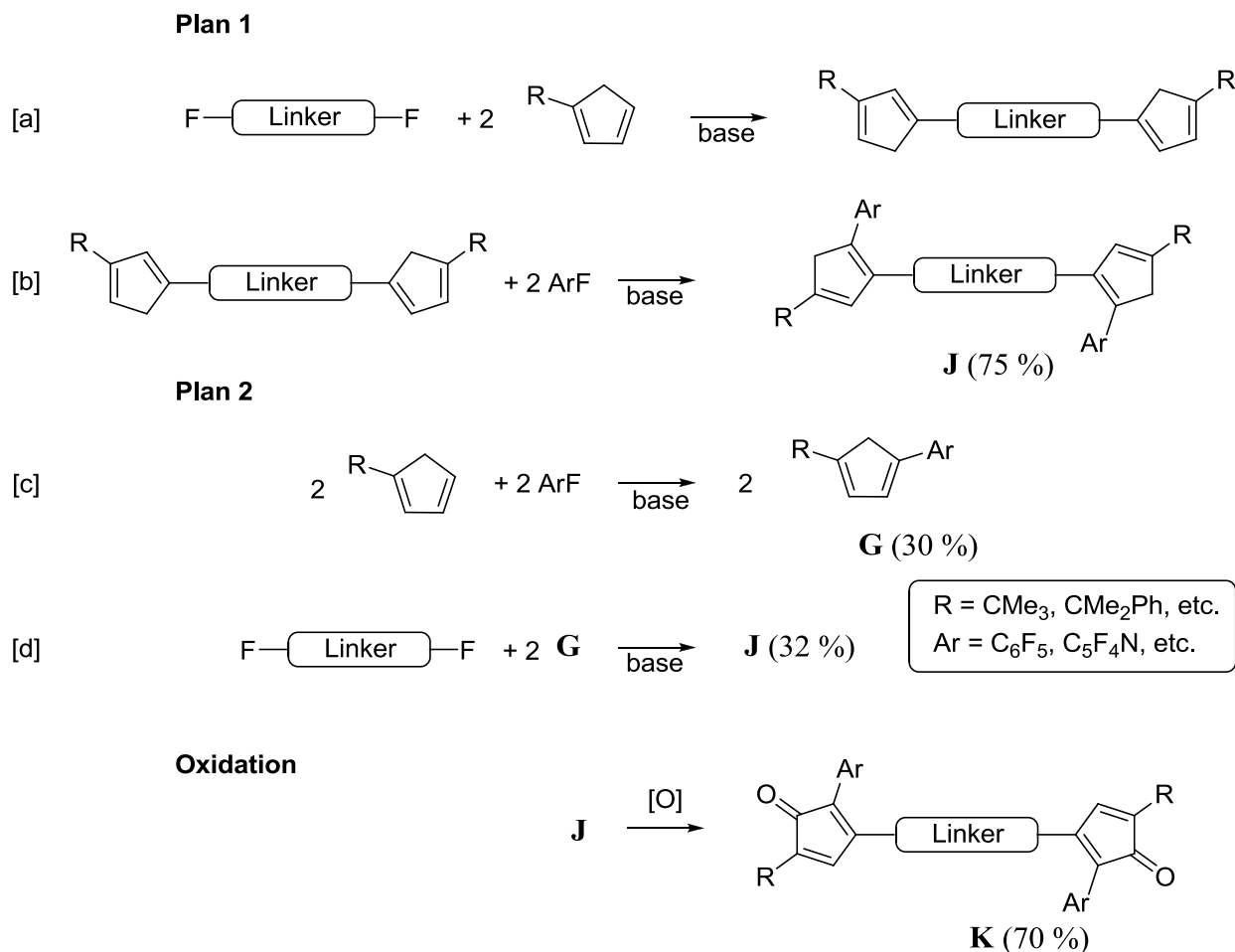
2.2.3 A First-Generation Monomer Design. The pathways shown in Scheme 2-4 could be executed with little modification, using decafluorobiphenyl as the linking reagent (Linker =  $C_{12}F_8$  in Scheme 2-4) and a simple pendant arylating reagent such as hexafluorobenzene (Ar =  $C_6F_5$  in Scheme 2-4). In fact, a small variant of that very monomer design is the doctoral dissertation topic of my colleague, Ms. Sanghamitra Sen. Summarizing briefly, she has found that Plan 1 in Scheme 2-4 works best, and that octafluorotoluene (Ar =  $C_6F_4CF_3$ ) arylates cleanly in step [b].<sup>157</sup> She and an undergraduate co-worker, Mariam M. Konaté, found that analogous reactions of hexafluorobenzene were not clean enough to pursue. Plan 2 with Ar =  $C_6F_5$  also failed because the reaction did not succeed in displacing both of the linker fluorides. The oxidation step seems to be highly effective with hydrogen peroxide (catalytic  $SeO_2$ ), which was

surprising considering the failure of peroxide-based oxidants to convert non-fluorinated cyclopentadienes to the corresponding cyclopentadienones.<sup>150</sup> Her monomer does undergo Diels-Alder reactions with dialkynylarenes to afford fluorinated DAPPs. While Ms. Sen has overcome most of the serious technical problems that her project has posed, in the early stages there were problems with selectivity and purity arising from the sixfold arylation step. As is typical in such divergent synthetic approaches, ensuring complete conversion of all six arylations is not only a synthetic challenge but an analytical problem as well. Furthermore purification by liquid chromatography is more difficult because of the low solubility of the highly fluorinated synthetic intermediates.

2.2.4 A Second-Generation Monomer Design. Based on the difficulties that Ms. Sen initially experienced in realizing Scheme 2-4, we wanted to modify the monomer design, mainly so that fewer concurrent arylations would be required in a single pot. We understood that this simplification might initially decrease the amount of overall fluorine content that we could achieve, but we hoped to see advantages in terms of synthetic efficiency and possibly even monomer purity. We also hoped that these advantages would translate into synthetic flexibility – the ability to create a “modular” family of monomers around a common synthetic approach.

Fortunately, Deck and co-workers had previously shown that *tert*-butylcyclopentadiene reacts with hexafluorobenzene to afford either the monoarylated diene **G** or the diarylated diene **H** (Scheme 2-5). Evidently the *tert*-butyl group directs arylation away from the vicinal positions (steric approach control). Importantly, Deck found that only diene **H** could be prepared selectively; diene **G** always contained diene **H** as a side-product. The observation of **G** as an inseparable mixture of tautomers will become important as well.



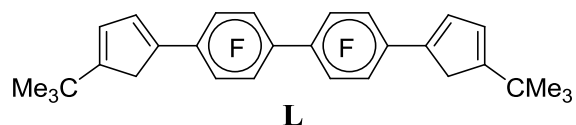


**Scheme 2-6. The second-generation monomer synthesis provides a variety of fluorinated CPDs.**

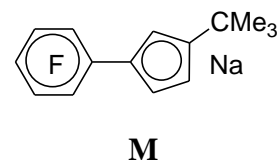
## 2.3 Results and Discussion

2.3.1 Monomer Synthesis by Plan 2. We attempted initially to prepare the targeted second-generation monomer (**K** in Scheme 2-6 with R = CMe<sub>3</sub> and Ar = C<sub>6</sub>F<sub>5</sub>) using Plan 2 in Scheme 2-6. First, we attempted to improve upon the published reaction shown in Scheme 2-5 in order to obtain the needed intermediate **G** selectively (without forming the diarylated analogue **H**), but even reactions with limiting hexafluorobenzene at low temperature showed poor selectivity. The reaction may be monitored by working up small aliquots and analyzing them using <sup>1</sup>H NMR spectroscopy. Deck and co-workers have previously shown that the ring methylene (CH<sub>2</sub>) resonances provide a convenient diagnostic tool for determining product ratios in crude mixtures.

The major isomer of **G** shows methylene (ring CH<sub>2</sub>) hydrogens at 3.47 ppm, while the methylene hydrogens of **H** correspond to a signal at 3.55 ppm. The <sup>19</sup>F NMR spectra were consistent with these assignments. Products exhibited characteristic *ortho* [-141.2 to -141.7 ppm range], *para* [-157.6 to -159.1 ppm range], and *meta* [-163.5 to -164.1 ppm range] signals. The *para* region is often well-resolved and shows separate signals for the three isomers of **G** and the two equally-integrating signals for **H**. In an experiment where KH was used in place of NaH, we were surprised to see a trace of the coupled byproduct **L**, confirmed by <sup>1</sup>H and <sup>19</sup>F NMR, as well as MS (*m/z* = 538, corresponding to C<sub>30</sub>H<sub>26</sub>F<sub>8</sub>). An explanation for the origins of these “coupled” products was provided in Chapter 1 (see Scheme 1-10).



Several other technical problems frustrated our efforts to prepare the intermediate **G**. Separation of **G** from other reaction products by liquid chromatography on a useful preparative scale was more difficult than expected, which led to relatively poor yields of sample pure enough to carry forward. Furthermore **G** is an oil, not a solid, which makes it harder to handle. In addition, we found that **G** begins to spontaneously polymerize within a few days even when stored in a freezer. Thus we knew that storing **G** would really mean storing its conjugate base as the sodium salt **M** and would require all subsequent handling to be carried out anaerobically (e.g., in a glove box).



Despite these problems we continued with the second step (Scheme 2-6, Plan 2, step [d] with R = CMe<sub>3</sub> and Ar = C<sub>6</sub>F<sub>5</sub>). Under optimized conditions, however, we were only able to obtain a 32% yield of the bis(diene) **J** after chromatographic purification. The low yield surprised us, considering the much higher yield (over 80%) of analogous reactions with NaC<sub>5</sub>H<sub>5</sub>. However,

we rationalized the observation by noting that the electron-withdrawing  $C_6F_5$  group probably makes the substituted cyclopentadienyl anion **M** much less nucleophilic and less reactive toward decafluorobiphenyl. Also, reactions using  $NaC_5H_5$  are easier to work up, because the excess  $NaC_5H_5$  needed to ensure complete substitution of both fluorides (4 and 4') from decafluorobiphenyl can be removed by evaporation during the workup (b.p. of  $C_5H_6$  is 45 °C), whereas the excess amount of diene **G** must be separated on a column. In view of these problems (low yield of diene **G**, difficulty in handling **G**, and low yields of bis-diene **J**), we abandoned this synthetic approach before even attempting the final oxidation step.

2.3.2 Monomer Synthesis by Plan 1. For the reasons described in the previous section, we returned to Plan 1 shown in Scheme 2-6 for the synthesis of **J** ( $R = CMe_3$ ,  $Ar = C_6F_5$ ). Because we ultimately found Plan 1 to be successful, we explored it in much more detail, and each reaction is described in a separate subsection with schemes showing specific compounds rather than generalized structures.

*Linking the Two Dienes.* As shown in Scheme 2-7, the first step involves coupling the two cyclopentadiene groups through an arylene linker. Decafluorobiphenyl (DFB) was chosen for its commercial availability, its high reactivity toward nucleophiles, and its relatively strict 4,4'-regioselectivity for substitution. Sodium *tert*-butylcyclopentadienide reacts with DFB in the presence of sodium hydride to produce **1**. This reaction is conveniently monitored by  $^{19}F$  NMR, with or without workup of each aliquot. (If the aliquot is not worked up, then it must be transferred to an NMR tube using a syringe in an apparatus that protects the sample from air by means of a nitrogen counterstream. Then, ca. 0.1 mL of  $C_6D_6$  is added to enable locking and shimming before acquiring the  $^{19}F$  NMR spectrum. The disappearance of the well-resolved *para*

C<sub>6</sub>F<sub>5</sub> signals of DFB (and of the monosubstituted intermediate) at -150 ppm indicate that the reaction is complete (Figure 2-2).

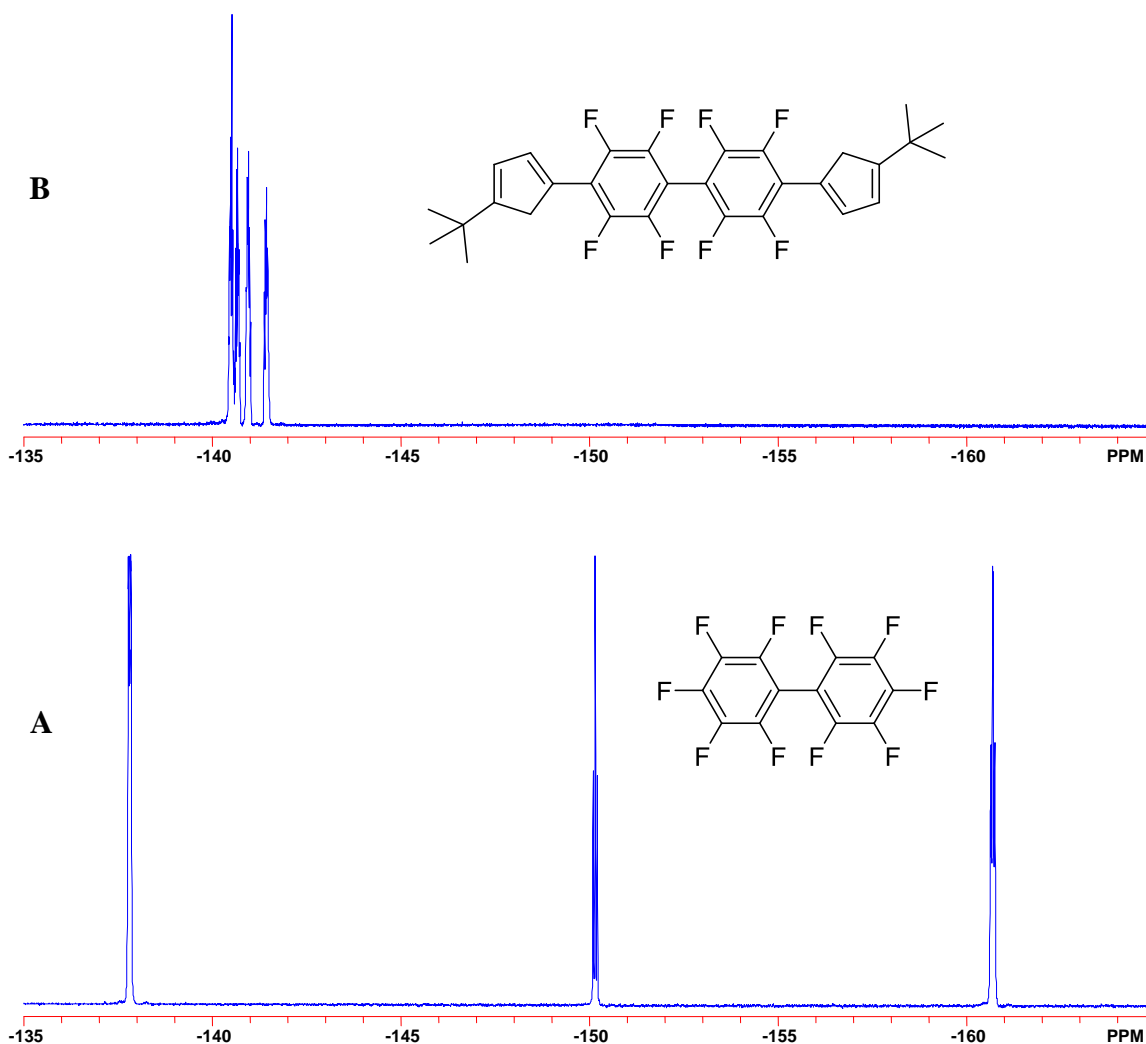
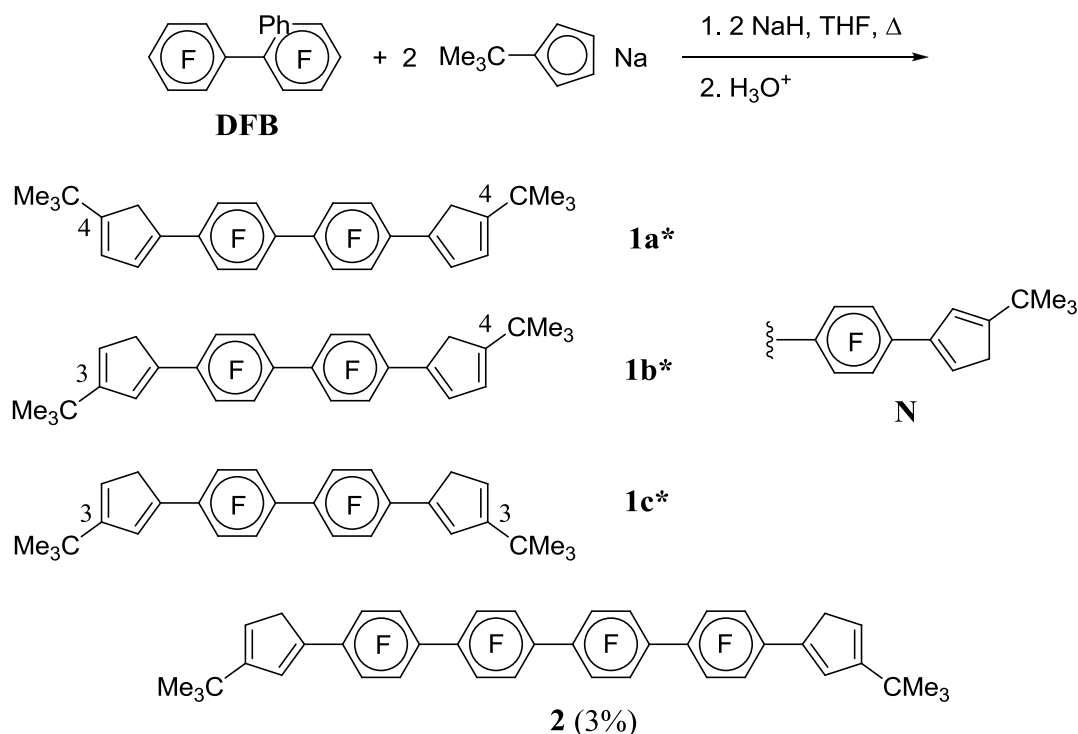


**Figure 2-2. The arylation reaction is easily monitored by <sup>19</sup>F NMR. The disappearance of the *para* fluorine signals in DFB (A) indicate conversion to 1(B).**

To minimize the formation of byproducts in which *tert*-butylcyclopentadiene is connected to two aryl groups, the reaction is optimally initiated at -20 °C with inverse addition of DFB to a solution of the organosodium compound. The temperature is then gradually increased to the point of reflux. A glassy yellow solid is obtained after an aqueous workup. Purification involves

filtering a hexane solution through silica gel and then recrystallization from hot hexanes. The product is a white solid and is obtained in an 85% yield.

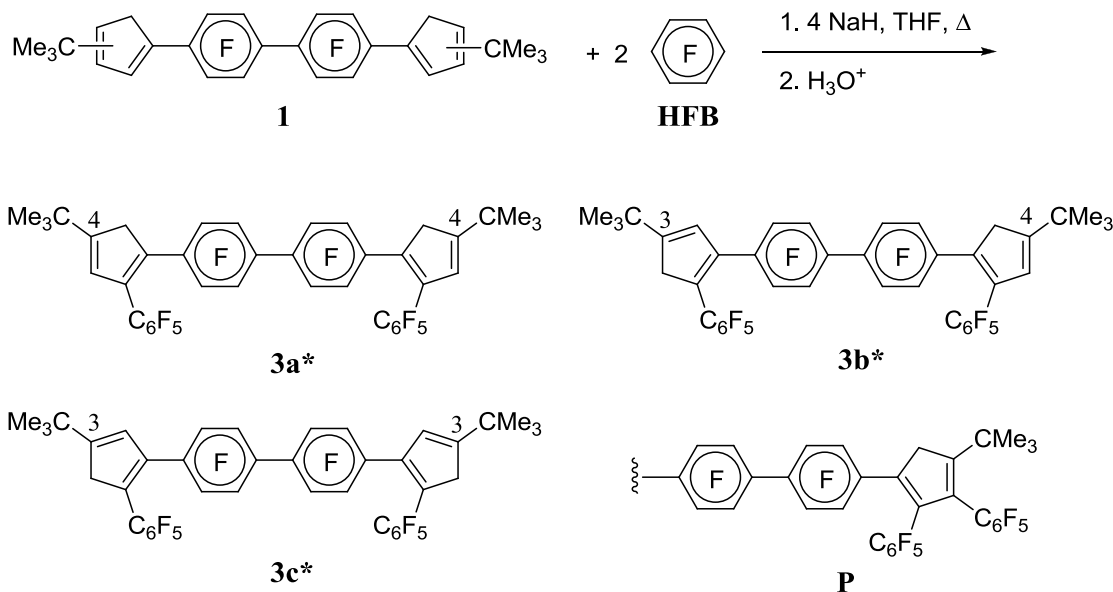


**Scheme 2-7. The arylation reaction produces an inseparable mixture of three tautomers from decafluorobiphenyl and *tert*-butyl cyclopentadiene; (\*) Total yield of **1** (all isomers) was 85%.**

One feature of this chemistry that needs additional discussion is the formation of the product **1** as a mixture of inseparable tautomers (Scheme 2-7). The aryl group is attached to the five-membered ring at the 1-carbon (where it participates in extended conjugation with the diene), but the *tert*-butyl group may be attached to either the 4-carbon or the 3-carbon of the diene. Each isomeric form of the diene should give two signals in the vinylic CH region of the <sup>1</sup>H NMR spectrum. There are two pairs of signals have approximately equal intensities, suggesting that

the *tert*-butyl group has no preference for either the 3- or 4-position of the diene moiety. The methylene CH<sub>2</sub> resonance is insensitive to the position of the *tert*-butyl group and all three isomers have overlapping signals at 3.6 ppm. In some of the crude product spectra, trace quantities of other cross-conjugated tautomers (see **N** in Scheme 2-7) were identified by additional, small vinylic CH signals and a ring CH<sub>2</sub> signal at 3.2 ppm, consistent with the observation of three isomeric products for **G** (Scheme 2-5). However these cross-conjugated tautomers are not observed after purification. As described in Chapter 1.3, certain reactions in which KH was used as the base resulted in the formation of the tetraphenylene-linked byproduct **2** (ca. 3%). However the use of KH was abandoned because it is more dangerous to handle and it did not improve yields or shorten reaction times. This byproduct (**2**) did not present problems for any of the further chemistry. Both **1a** and **2** were characterized crystallographically as described in a separate section below.

*Adding the Pendant (Lateral) Aryl Groups.* Returning to the general synthetic plan (Scheme 2-6, Plan 1), the second step (step [b]) is a substitution reaction in which one more perfluoroaryl group is attached to each five-membered ring of compound **1**. The specific reaction is shown in Scheme 2-8. Pendant fluorinated aromatic groups will add fluorine content to eventual polyphenylene structure, while twisting the backbone, decreasing conjugation length, improving redox stability, and increasing solubility. Some evidence for this additional twisting can be seen in the crystallographic analysis of **3**, which is presented in a separate section below. Lateral C<sub>6</sub>F<sub>5</sub> groups should also provide sites for post-modification of the polyphenylene (see Sections 1.4.4 and 5.1).



**Scheme 2-8. The linked bis(cyclopentadiene) intermediate (1) reacts with hexafluorobenzene (HFB) to form a bis(cyclopentadiene) with pendant aryl groups. HFB may be exchanged for other perfluoroaryl groups to create a family of monomer synthetic intermediates; (\*) Total yield of 3 (all isomers) was 86%.**

The reaction shown in Scheme 2-8 is most conveniently monitored by <sup>1</sup>H NMR spectroscopy (Fig. 2-3). The downfield vinylic signals (terminal diene CH) disappear, while the other signals (internal diene CH) shift slightly in response to the electron-withdrawing effect of the newly attached pentafluorophenyl group. The selectivity implied by Scheme 2-5 was observed. There was no spectroscopic evidence for species containing overarylated cyclopentadienes (see structure **P** in Scheme 2-8), although in subsequent model chemistry (see Chapter 3), we learned that under certain conditions a third aryl group can be attached to *tert*-butylcyclopentadiene, vicinal to the *tert*-butyl group. We therefore suggest that others pursuing the chemistry shown in Scheme 2-8 will need to be watchful for this possibility if they change the reaction conditions.

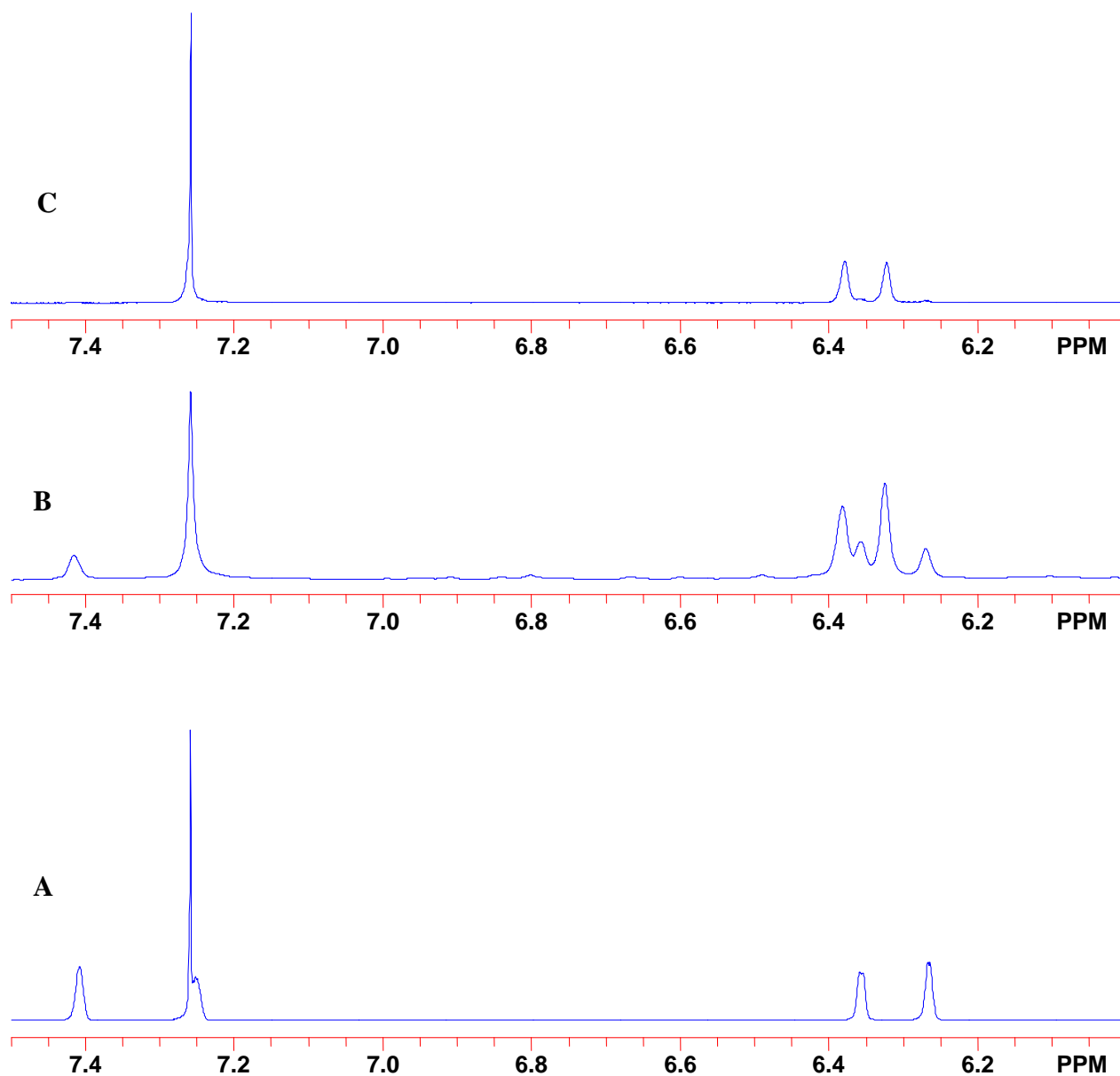
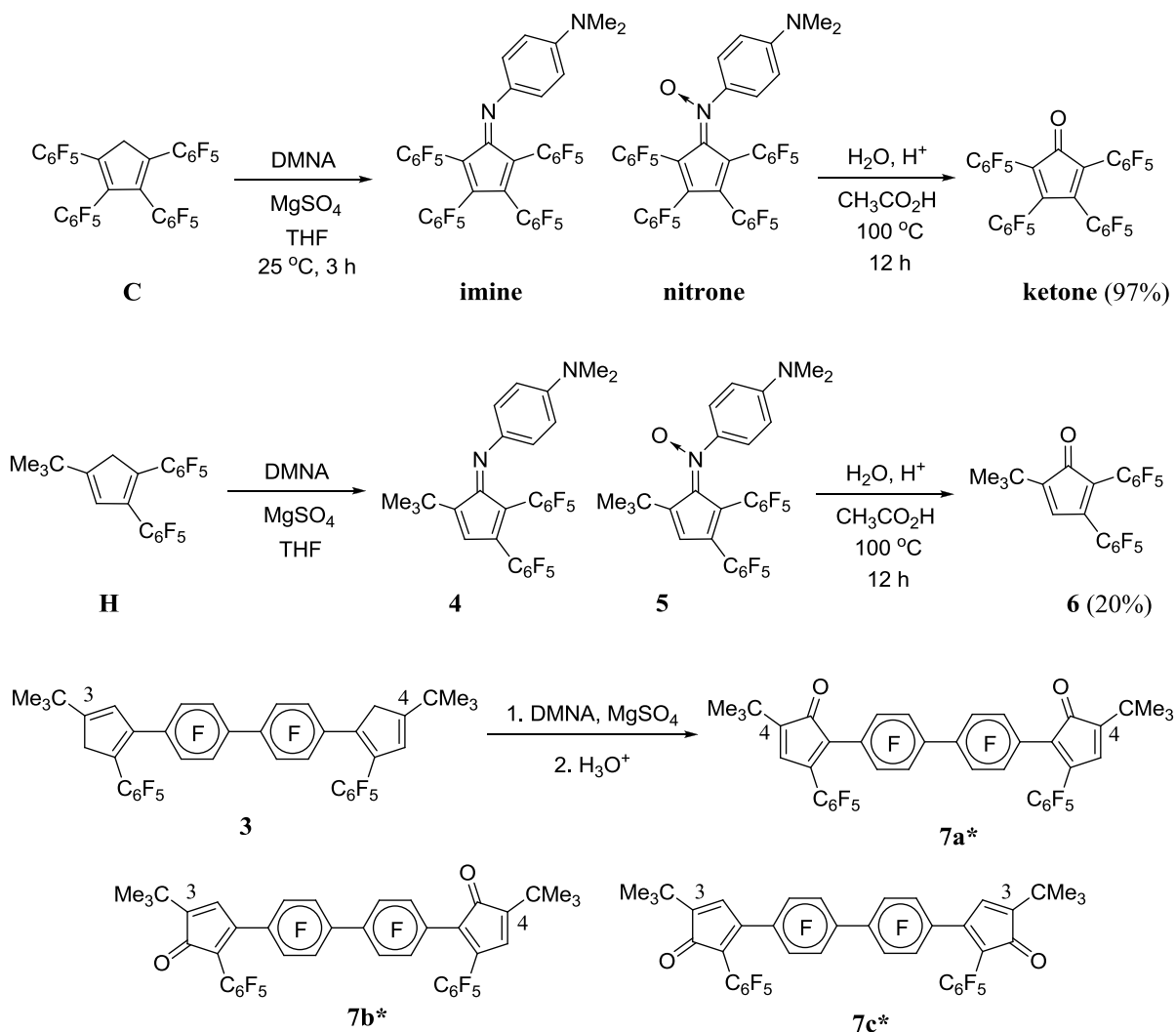


**Figure 2-3.  $^1\text{H}$  NMR indicates the reaction is complete [bottom is starting material (A), middle is incomplete (B), and top is the crude product 3 (C)].**

As with intermediate **1**, the diarylated intermediate **3** is obtained as an inseparable mixture of three tautomers, which differ in the placement of the  $\text{C}_6\text{F}_5$  vs. the octafluorobiphenylene linker on the 1- and 2-carbons of the cyclopentadiene. This assignment accounts for the presence of two vinylic CH signals in the  $^1\text{H}$  NMR spectrum. As with **1**, the  $\text{CH}_2$  resonances of the three tautomers are coincident.

*Oxidation.* Returning to Scheme 2-6, the final step in the monomer synthesis is the oxidation of the ring methylenes to the corresponding ketones. This step was very troublesome and gave low yields until two of my lab-mates, Sanghamitra Sen and Brian Hickory, discovered superior alternative methods, as described below. (Both of these coworkers have devoted sections of their dissertations to the subject of cyclopentadiene oxidation.) We used the mono-diene **H** as a model compound to work out reaction conditions for the oxidation of the monomer intermediate **3**. Both **H** and **3** have cyclopentadiene structures bearing a *tert*-butyl group and two aryl groups.

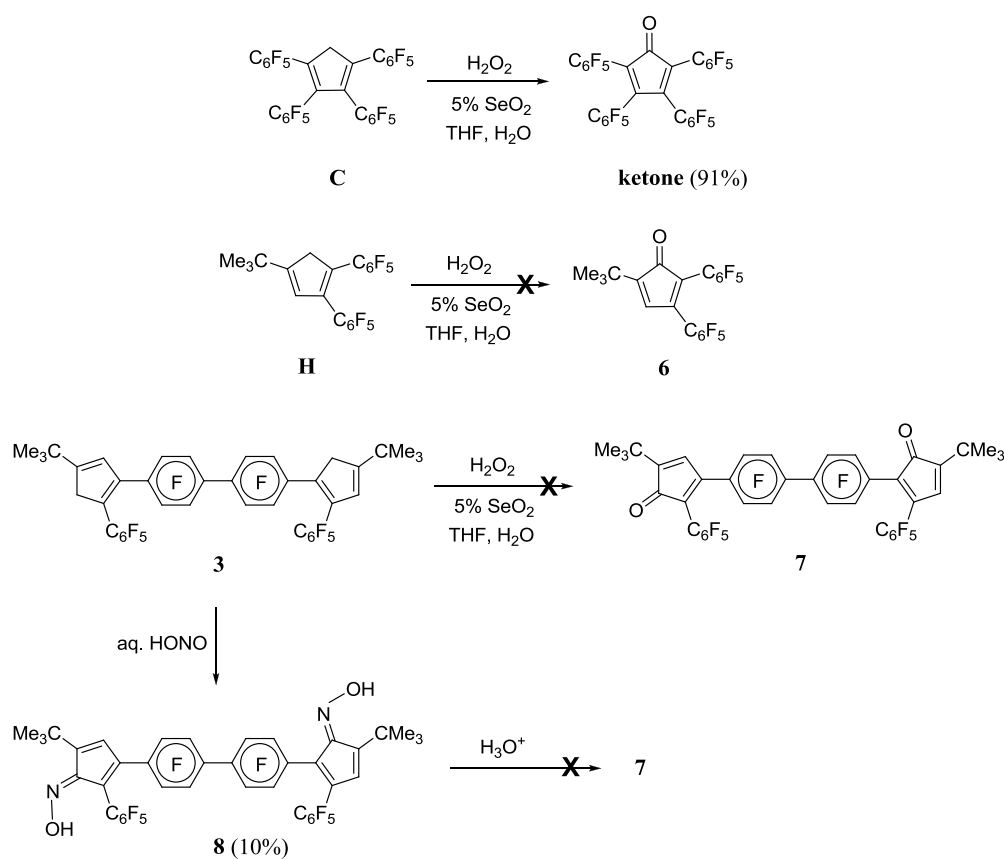
The use of DMNA as a reagent was discussed in a previous section (see Scheme 2-3). This method has been available since the 1930s and is robust. The general approach (Scheme 2-9) involves a condensation reaction to form, in general, a mixture of an imine and a nitron. Formation of the imine requires removal of one equiv of water, and Prof. Deck found that anhydrous magnesium sulfate promotes the reaction. The mechanism of formation of the nitron is less clear. Brian Hickory and Prof. Deck reported<sup>158</sup> that tetrakis(pentafluorophenyl)cyclopentadiene reacts with DMNA, followed by acid hydrolysis of the imine/nitron mixture, to give a 97% yield of the analytically pure corresponding ketone. DMNA also reacts with diene **H** to form a mixture of an imine (**4**) and a nitron (**5**), in combined yields surpassing 90%. The problem with this method is the low yield (ca. 20%) of the hydrolysis to give the ketone **6**. Oxidation of **3** was attempted, but the best yield obtained for the desired CPD monomer **7** was about 30%, and the purity of the product was also questionable (less than 98% even after column chromatography).



**Scheme 2-9.** Diarylated *tert*-butyl cyclopentadiene reacts with DMNA to form a mixture of nitron products which are then hydrolyzed to the corresponding ketone. Compound **3** is arbitrarily drawn as isomer **3b**. The material was reacted as a mixture of tautomers as described in Scheme 2-8; (\*) Total yield of **7** (all isomers) was 30%.

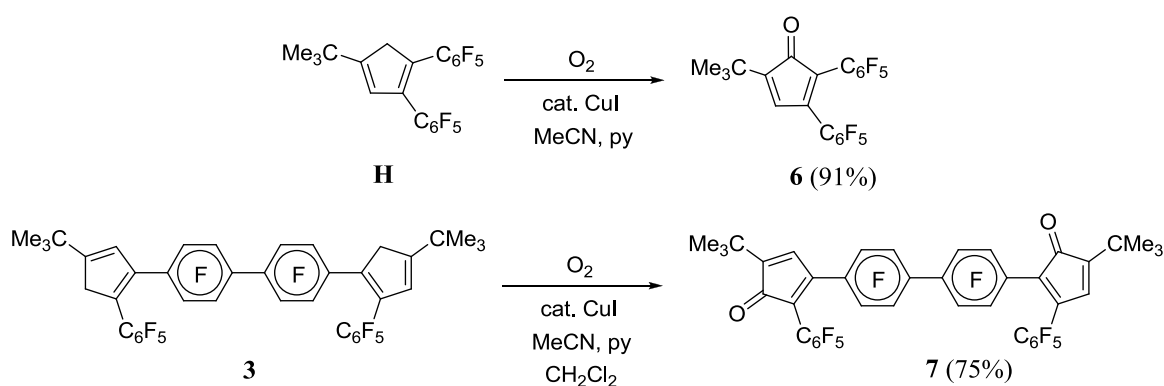
My lab-mate, Sanghamitra Sen, proposed a new oxidation technique using *tert*-butyl hydroperoxide as the oxidant and catalytic selenium dioxide (Scheme 2-10). These methods also were shown to be successful for tetraarylated cyclopentadienes such as diene **C**. However, my efforts to convert either the model diene **6** or the monomer precursor **3** were futile; less than 5% of the desired ketone products were obtained with complete loss of the starting materials.

The compositions of the products were not pursued further. Another reagent that we explored briefly was nitrous acid. My lab-mate, Brian Hickory, reasoned that the structure of nitrous acid was analogous to DMNA, with the large aryl group of DMNA (Ar–N=O) replaced by a simple hydroxyl group (HO–N=O). His idea was that the simple oxime might hydrolyze more readily than either the imine or especially the nitron. The reaction afforded the expected dioxime **8** in low yield (the structure was confirmed by NMR spectroscopy and by preliminary X-ray data), but the purity was poor and the ease of hydrolysis was not improved. Both methods were deemed failures for this particular system.



**Scheme 2-10. Several attempted oxidation methods failed to produce the corresponding ketone. Compounds 3, 7, and 8 are mixtures of isomers as described in the text.**

As part of his dissertation research, my lab-mate, Brian Hickory, developed a copper catalyzed air-oxidation method for fluoroaryl-substituted cyclopentadienes. His discovery is complementary to the existing literature methods because his method does not work for non-fluorinated compounds such as tetramethylcyclopentadiene or tetraphenylcyclopentadiene. The details of his methodology will be described in his dissertation. The *tert*-butyl containing cyclopentadienes are still the most difficult substrates, but finally under carefully optimized conditions (Scheme 2-11) we were able to obtain yields of approximately 75%.

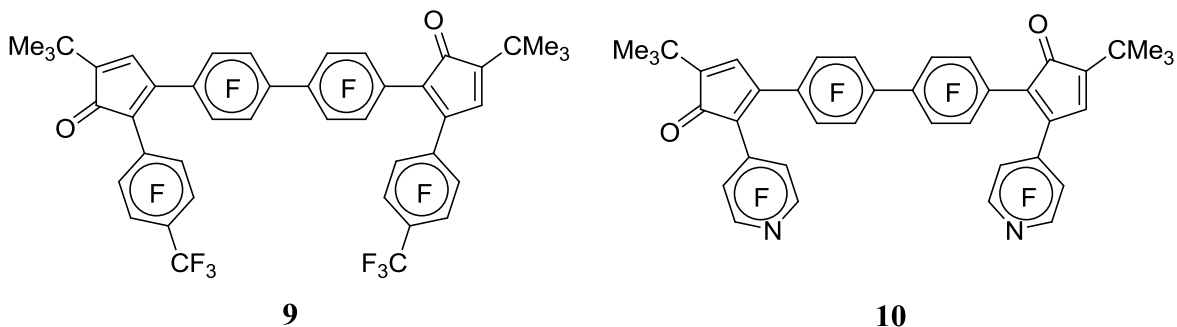


**Scheme 2-11. The novel copper-catalyzed air oxidation is more efficient for the *tert*-butyl containing cyclopentadienes. Compound 3 is arbitrarily drawn as isomer 3b. The material was reacted as a mixture of tautomers as described in Scheme 2-8.**

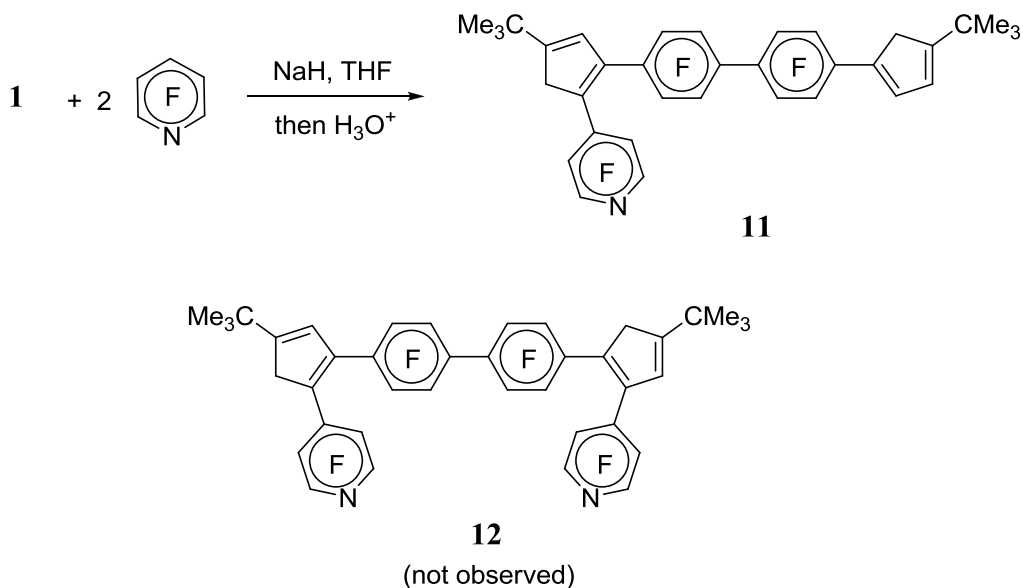
First, CuI and pyridine are combined in acetonitrile to form either a copper(I) or copper(II) catalyst *in situ*. (Oxidation states in the active catalytic species are not always the same as the oxidation state in the precatalytic reagent. Brian Hickory will address these issues in his dissertation.) The catalyst “cocktail” is then added to an acetonitrile solution of either the model **6** or the monomer intermediate **3** that is continuously aerated. Lower yields are obtained if the CuI reagent is added directly to a solution of the substrate (the lost mass is retained as a dark residue at the top of a silica gel column). Interestingly, we found that the intermediate in which only one CH<sub>2</sub> group of **3** has been oxidized precipitates from the reaction, but the addition of

dichloromethane solved that problem. The reaction is monitored by  $^1\text{H}$  NMR until the methylene signals at 3.6 ppm are gone. Filtration through silica gel removes copper species to obtain a crude product, which is purified by column chromatography. Typically traces of partially oxidized material are removed. As shown in Scheme 2-9, diketone **7** is also obtained as a mixture of isomers in the same statistical ratio as both **1** and **3**. Unlike the bisdienes **1** and **3**, the isomers of **7** cannot interconvert. Assuming that the tautomers of **3** can exchange rapidly under the conditions of the oxidation reaction (which seems reasonable in the presence of a base like pyridine), the observation of three isomers of **7** in the same ratio also means that the different tautomeric forms of **3** oxidize at approximately the same rate. We believe the pendant  $\text{C}_6\text{F}_5$  group and the fluorinated linking group have similar electronic and steric properties. Diels-Alder model reactions of diketone **7** and phenylacetylene are described in Chapter 3. Polymerization reactions of diketone **7** and diethynylarenes are described in Chapter 4.

2.3.3 Creating a Family of Diketone Monomers. As Scheme 2-6 suggests, the monomer synthesis described in the previous section can be made modular by changing the structures of the different components. The most convenient modification is changing the perfluoroarenes in the step [**b**] of Plan 1, because other perfluoroarenes are commercially available. Using this approach one could obtain new monomers that differ in their fluorine content. For example, if hexafluorobenzene were replaced by octafluorotoluene (OFT), the monomer (**9**) would have two additional  $\text{CF}_3$  groups. My lab-mate, Charles Carfagna, reported monomer (**9**) in his MS thesis. If pentafluoropyridine (PFP) were used instead (**10**), then there could be more opportunities for polymer post-functionalization through nucleophilic substitutions at the 2- and 6- positions. It also turns out that both **9** and **10** are more reactive toward Diels-Alder reactions for reasons that will be described in Chapter 3. The synthesis of **10** is described below.



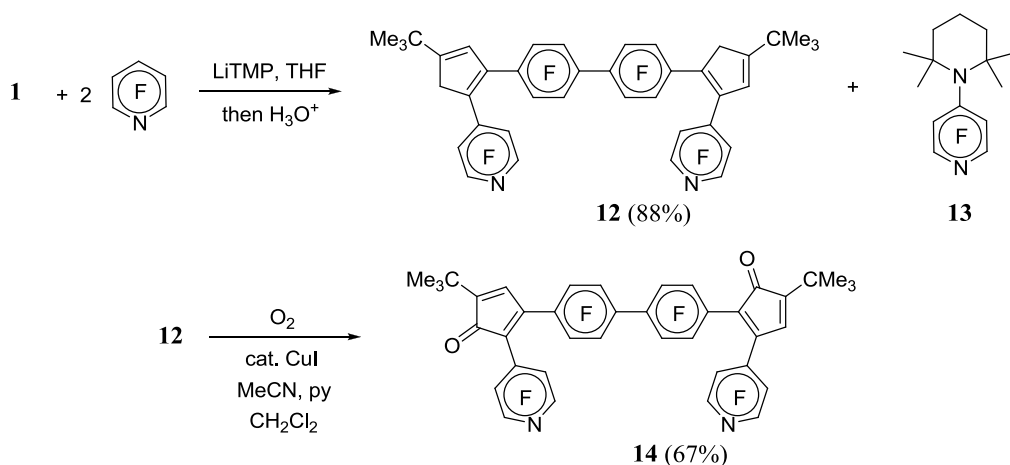
Unfortunately, arylation of bisdiene **1** with pentafluoropyridine with NaH as the base failed (Scheme 2-12). Several studies indicated the reaction stops at the stage of the monoarylated intermediate **11**. Only traces of the desired bisdiene **12** were observed. The reasons for this unusual behavior, which we have not observed in any other related system, remain unclear. Sodium hydride is a heterogeneous base in THF, and we considered the possibility that **11** or its conjugate base is insoluble, but we do not see the formation of a precipitate. Other proposed reasons include the formation of an unusually tight ion pair between the sodium atom and the either singly or doubly deprotonated intermediate.



**Scheme 2-12.** The arylation of bisdiene **1** with PFP was unsuccessful with NaH as the base.

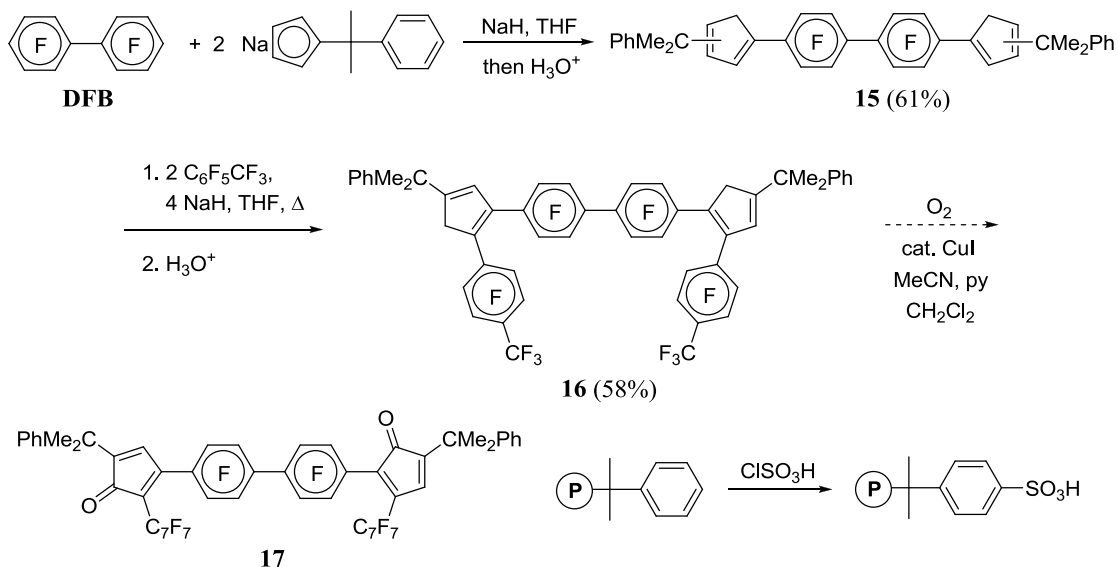
We considered the use of other bases, but perfluoroaromatic compounds, especially PFP, are so reactive toward nucleophiles that our other choices were limited. Lithium tetramethylpiperidide (LiTMP) is often touted as a soluble, non-nucleophilic base. In addition, lithium is well-solvated by THF which should weaken ion-pairing with the intermediate cyclopentadienyl anions so that they become more available as the nucleophile. To confirm the effect of ion pairing with  $\text{Na}^+$  versus  $\text{Li}^+$ , I synthesized both LiTMP and NaTMP and reacted each base with **1** and hexafluorobenzene at the same concentrations. No reaction occurred with NaTMP as the base. At first, I thought the NaTMP was unreactive, but the same NaTMP reacted with sodium *tert*-butyl cyclopentadiene and pentafluoropyridine to form diarylated *tert*-butyl cyclopentadiene. The rates of reaction suggest the LiTMP is much more efficient than NaTMP at the same concentrations.

Coming back to the synthesis of monomer **10**, the arylation of **1** with PFP with LiTMP as the base (Scheme 2-13) gave bisdiene **12** in 88% yield after silica gel chromatographic purification. One clear disadvantage of using LiTMP is that some 4-(tetramethyl-piperidyl)tetrafluoropyridine (**13**) can be formed as a byproduct, but this compound is easily separated on a silica column. This by-product shows how reactive PFP is as an electrophile. Copper-catalyzed air-oxidation gave the corresponding diketone **14** in 67% purified yield. Both the bisdiene **12** and the diketone **14** were each obtained as inseparable mixtures of three isomers.



**Scheme 2-13. The arylation of bisdiene 1 with PFP was successful with LiTMP as the base.**

Returning to Scheme 2-6, Plan 1, Kelly Daly, an undergraduate researcher, showed that cumylcyclopentadiene ( $R = \text{CMe}_2\text{Ph}$ ) can replace *tert*-butylcyclopentadiene ( $R = \text{CMe}_3$ ) in the monomer synthesis (Scheme 2-14). Under my direct supervision, Daly used the same steps as in the synthesis of monomer **7** and obtained pure products in comparable yields. Early studies suggest the oxidation **16** is promising, but **17** has not been synthesized and characterized completely. Although this seems like a small change, a new phenyl group could be important for functionalizing a polymer. The lateral non-fluorinated phenyl ring acts as a convenient sulfonation site that may be useful for incorporating sulfonic acid groups into this fluorinated DAPP system. Sulfonated materials are commonly used for fuel cell proton exchange membranes. McGrath, et al. show that sulfonated membranes have good conductivity while a fluorinated segment can increase thermal and mechanical stability. Note that she also changed the arylation reagent from hexafluorobenzene to octafluorotoluene, because my lab-mate, Charles Carfagna, had found that arylations using OFT are unusually efficient and clean. The  $\text{CF}_3$  groups will help polymers derived from monomer **17** to be more compatible with Nafion™.



**Scheme 2-14. The cumylcyclopentadiene monomer behaves similarly to produce fluorinated bis(cyclopentadienes) with a lateral phenyl group for selective post-sulfonation.**

## 2.4 Crystallographic Analysis.

Bisdiene **1**, **2**, and **3**, dioxime **8**, diketone **10**, and bisdiene **12** were analyzed crystallographically. The structures of **2** and **8** were helpful in conclusively identifying them. The other structures were obtained partly to learn something about crystallography (I had an opportunity to attend a workshop) and partly to explore variations in chain twisting in poly(fluoroarylene) species.

The structure of bisdiene **1** is shown in Fig. 2-4. One can see that in the absence of pendant aryl substituents on the cyclopentadiene moieties (proxy for a benzene ring in a polyphenylene), the rings are able to adopt nearly coplanar structures. The  $\text{C}_6\text{F}_4\text{-C}_6\text{F}_4$  torsional angle is  $53^\circ$ , somewhat non-coplanar, because of the repulsive van der Waals interactions of neighboring *ortho* fluorine atoms.  $\text{C}_6\text{H}_4\text{-C}_6\text{H}_4$  torsional angles vary widely, but  $30^\circ$  is an approximate average.

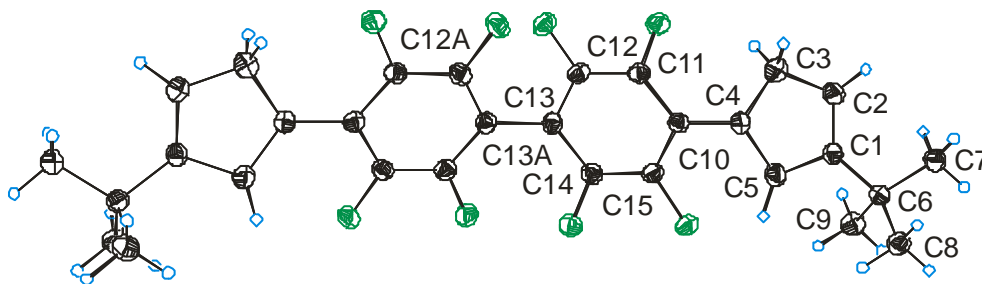


**Figure 2-4.** This figure shows a thermal ellipsoid plot (50% probability) of the molecular structure of bisdiene **1**. Fluorines are numbered the same as the carbon atoms to which they are attached. Selected bond distances (Å): C1-C2, 1.338(2); C1-C5, 1.480(2); C1-C6, 1.516(2); C2-C3, 1.477(2); C3-C4, 1.441(2); C4-C5, 1.424(2); C4-C10, 1.465(2). Selected bond angles (deg): C1-C6-C7, 110.73(13); C1-C6-C8, 109.88(12); C7-C6-C8, 109.21(13); C1-C6-C9, 108.76(12); C7-C6-C9, 108.66(13); C8-C6-C9, 109.57(13). Selected torsional angles (deg): C2-C1-C6-C7, 6.9(2); C3-C4-C10-C11, 22.8(2); C12-C13-C13A-C12A, 53.0(2).

The structure of bisdiene **2** is shown in Figure 2-5. Again the Cp-C<sub>6</sub>F<sub>4</sub> torsional angles are relatively low at 18(1)°, while the C<sub>6</sub>F<sub>4</sub>-C<sub>6</sub>F<sub>4</sub> torsional angles are higher, presumably due to F—F interactions.

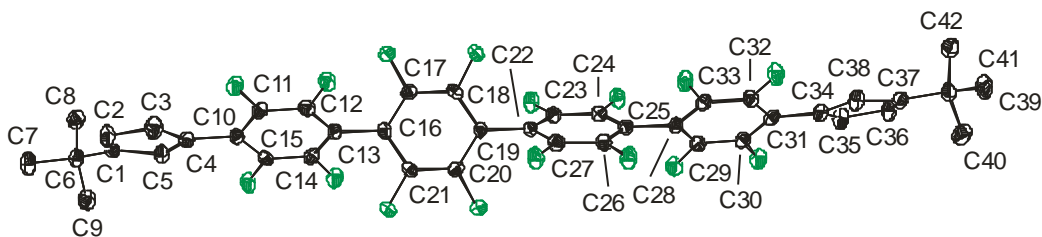


**Figure 2-5.** This figure shows a thermal ellipsoid plot 50% probability of the bisdiene **2**.

Fluorines are numbered the same as the the carbon atoms to which they are attached.

Selected bond distances (Ang): C1-C2, 1.352; C2-C3, 1.470; C3-C4, 1.406; C4-C5, 1.436;

C5-C1, 1.478. Selected torsional angles (deg): C3-C4-C10-C11, 17.1; C12-C13-C16-C17,

64.7; C18-C19-C22-C23, 57.3; C26-C25-C28-C33, 54.0; C30-C31-C34-C35, 19.1.

The structure of the bisdiene **3** is shown in Figure 2-6. Here all of the absolute Cp-C<sub>6</sub>F<sub>4</sub> dihedral angles are in the range 40-50°, with the C<sub>6</sub>F<sub>4</sub>-C<sub>6</sub>F<sub>4</sub> dihedral angle slightly larger at 53°, again owing to F-F interactions.

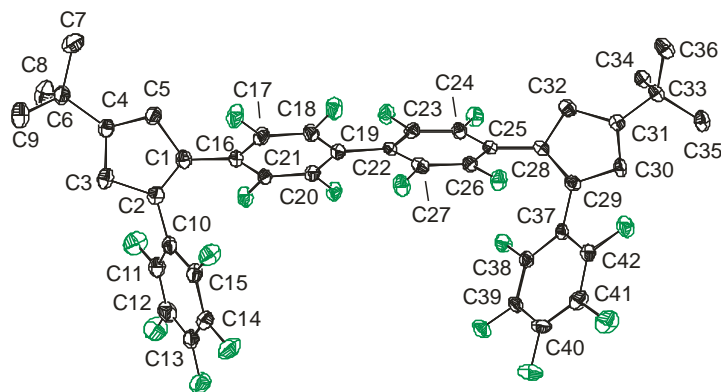


**Figure 2-6.** This figure shows a thermal ellipsoid plot (50% probability) of bisdiene **3**.

Fluorines are numbered the same as the the carbon atoms to which they are attached.

Selected bond distances (Ang): C1-C2, 1.349; C2-C3, 1.488; C3-C4, 1.449; C4-C5, 1.389;

C5-C1, 1.480; C28-C29, 1.355; C29-C30, 1.467; C30-C31, 1.385; C31-C32, 1.464; C32-C28,

1.503. Selected torsional angles (deg): C1-C2-C10-C11, -132.2; C2-C1-C16-C17, -138.0;

C18-C19-C22-C23, -127.8; C26-C25-C28-C29, 42.9; C28-C29-C37-C38, 49.4.

The structure of the dioxime **8** is shown in Figure 2-7. This structure is important because it reveals the stereochemistry of the oximes, with the OH oxygens directed away from the bulky *tert*-butyl groups. A single isomer (presumably the same isomer) about the N=OH bond is observed in solution NMR spectrometry. All of the biaryl (including aryl-Cp) torsions are at angles greater than 50°, possibly because of the greater torsional strain introduced by the oxime oxygen on the pendant C<sub>5</sub>F<sub>4</sub>N groups, although the observation of similar angles in the diketone **10** (see below) argues against that reasoning.

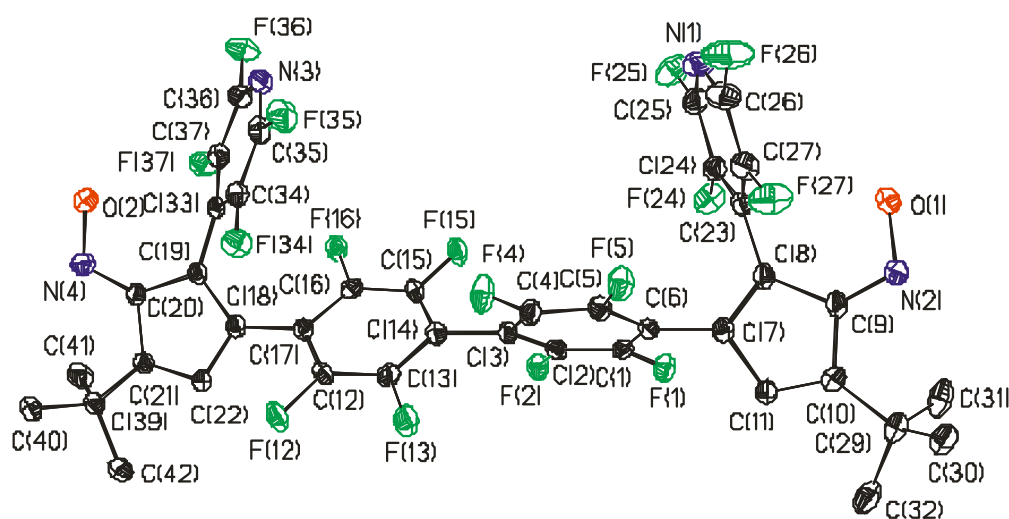


**Figure 2-7.** This figure shows a thermal ellipsoid plot (50% probability) of dioxime **8**. Hydrogen atoms are omitted for clarity. Selected bond distances (Å), bond angles (deg), and torsional angles (deg). C9-N2 1.280, N2-O1 1.386, C9-N2-O1 113.7, C8-C9-N2-O1 0.1, C20-N4 1.283, N4-O2 1.380, C20-N4-O2 112.3, C19-C20-N4-O2 3.6. C7-C8-C23-C24 – 62.3, C8-C7-C6-C5 –56.1, C4-C3-C14-C15 114.0, C16-C17-C18-C19 –55.5, C18-C19-C33-C34 –55.2.

The structure of diketone **10** is shown in Figure 2-8. All of the ring-ring torsion angles are in the range 50-60°.

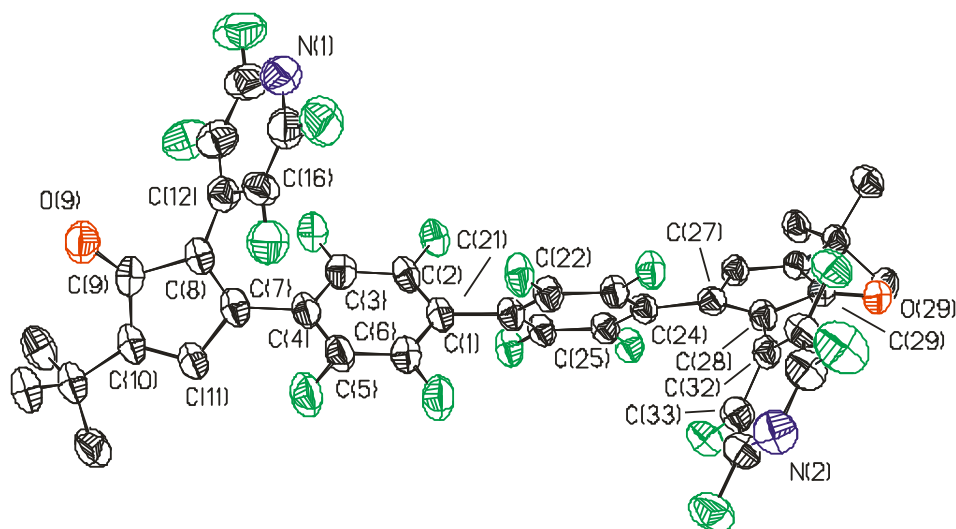


**Figure 2-8.** This figure shows a thermal ellipsoid plot (50% probability) of diketone **10**. Hydrogen atoms are omitted for clarity. Selected bond distances (Å), bond angles (deg), and torsional angles (deg). C29-O-29 1.214, C9-O9 1.218, C16-C12-C8-C7  $-58.1$ , C8-C7-C4-C3  $-59.4$ , C2-C1-C21-C22  $113.5$ , C25-C24-C27-C28  $-140.7$ , C27-C28-C32-C33  $50.7$ .

The structure of bisdiene **12** is shown in Figure 2-9. All ring-ring torsional angles are in the range  $40$ - $54^\circ$ . One of the pendant aryl groups adopts an angle of  $41^\circ$ , indicating that a slightly more coplanar arrangement is possible in the diene **12** as compared to the ketone **10**, possibly indicating steric repulsion of the pendant aryl group *ortho* fluorines and the heteroatom attached to the five-membered ring. That repulsion would also account for the angles in oxime **8**.

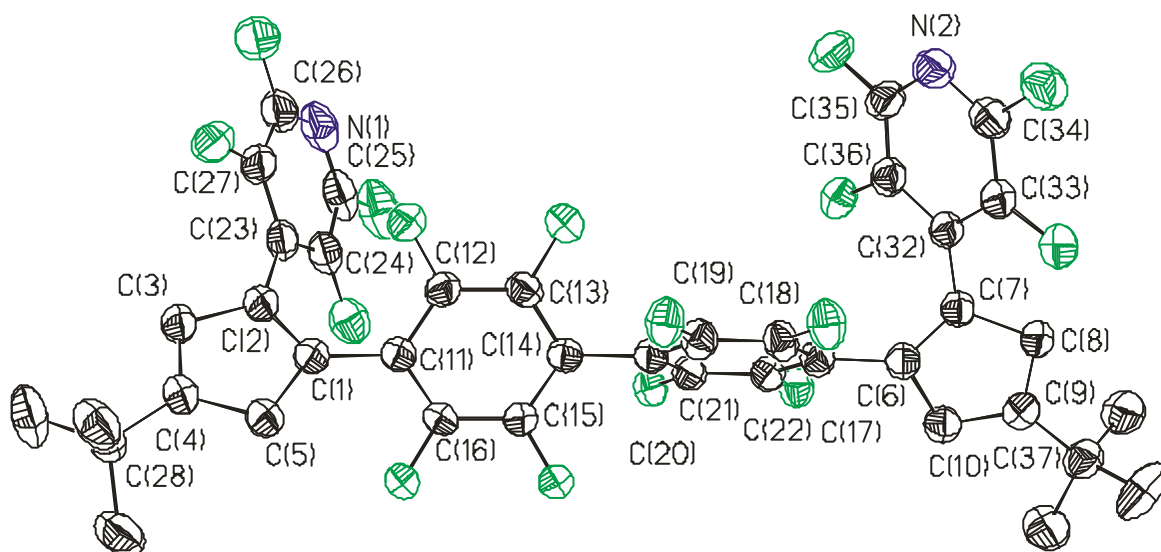


**Figure 2-9.** This figure shows a thermal ellipsoid plot (50% probability) of bisdiene 12.

Hydrogen atoms are omitted for clarity. Selected torsional angles (deg): C1-C2-C23-C24 51.2, C2-C1-C11-C12 53.5, C13-C14-C20-C19 53.8, C18-C17-C6-C7 -44.8, C6-C7-C32-C36 -40.5.

## 2.5 Conclusions

Highly fluorinated bicyclopentadienone monomers were synthesized by nucleophilic aromatic substitution of perfluoroarenes and cyclopentadienyl anions. The three-step monomer synthesis tolerates a wide variety of cyclopentadienyl anions or perfluoroarene compounds. Retroanalysis shows arylation of the linked cyclopentadienes (Plan 1 Scheme 2-4) is more favorable compared to linking arylated cyclopentadienes (Plan 2 Scheme 2-4). The *tert*-butyl groups impart solubility and regiodirection without hindering the success of the synthesis of fluorinated CPDs. The materials are isolated and characterized as an inseparable mixture of three isomers. The second step required an optimization of the base. Sodium hydride was not efficient for a wide variety of fluoroaromatics. Lithium tetramethylpiperadide was most effective for the arylation. Finally, oxidation methods developed by Brian Hickory converts arylated cyclopentadienes to the corresponding ketones.

## 2.6 Experimental

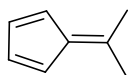
**General procedures.** Standard inert-atmosphere techniques were used for most reactions with the exception of oxidations. All chemicals and solvents were reagent grade and purchased from Aldrich, Alfa Aesar, or Matrix Scientific. Perfluoroaromatic compounds were used as received from Matrix or Oakwood. Sodium hydride was purchased as a 60% dispersion in mineral oil from Aldrich, washed with hexanes several times, dried under vacuum and stored in a glove box. The *tert*-butylcyclopentadiene was prepared by the method of Vladimirskaya, Koshutin, and Smirnov,<sup>159</sup> converted to its sodium or potassium salt by treatment with NaH or KH, and stored in a glove box.<sup>160</sup> Tetrahydrofuran was purified by the method of Pangborn et al.<sup>161</sup>

**Measurements and Characterization.** All new compounds were characterized by <sup>1</sup>H NMR and <sup>19</sup>F spectroscopy performed on Varian Unity 400 or Varian Inova 400 instruments. Chemical shifts are referenced to external C<sub>6</sub>F<sub>6</sub> in CDCl<sub>3</sub> for the <sup>19</sup>F NMR spectra (-163 ppm). Elemental analyses were determined by Desert Analytics (Tucson, Arizona). Mass spectra were collected on an Agilent 6220 instrument (direct infusion APCI). X-ray crystallographic data was collected on Oxford Diffraction Xcalibur and Gemini diffractometers. Melting points were determined using a Büchi B-540 melting point apparatus.

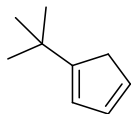
Two techniques used to samples reactions for NMR analyses are described here. Aliquot Method A. A 0.30-mL sample of a reaction mixture is transferred directly to a J-Young NMR tube using a needle and syringe under a nitrogen purge. The addition of benzene-d<sub>6</sub> (0.30 mL) enables frequency locking and magnetic field homogeneity adjustments. If any solids are present, such as sodium hydride, the sample is centrifuged upside down so that the solids are spun into the cap. The sample is analyzed by <sup>19</sup>F NMR and <sup>1</sup>H NMR spectroscopy. This method

is more appropriate for following crude reactions by  $^{19}\text{F}$  NMR since solvent peaks overcome other signals in the  $^1\text{H}$  NMR.

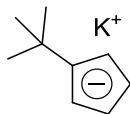
Aliquot Method B. Using a syringe, a 0.25-mL sample of a reaction mixture was transferred to a vial containing dichloromethane (3 mL) and water (1 mL). The vial was shaken and the allowed to stand until the layers separated. The lower organic layer was drawn out using a pipette. The organic layer was then washed with water (2 x 1 mL), dried over  $\text{MgSO}_4$ , filtered, and evaporated to afford a residue. The residue was then dissolved in  $\text{CDCl}_3$  (0.60 mL) and analyzed using  $^1\text{H}$  and  $^{19}\text{F}$  NMR spectroscopy. This method is appropriate for reactions in which hydrolyzed shifts need to be compared directly or solvent peaks interfere with the spectra.



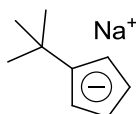
**6,6-Dimethylfulvene.** Following the published procedure,<sup>162</sup> freshly cracked cyclopentadiene (160 mL, 1.96 mol) was transferred to a 500-mL 3-neck flask and cooled with an ice bath to prevent dimerization. A reflux condenser (precaution), nitrogen inlet, and rubber septum were attached, and the apparatus was flushed with nitrogen. Acetone (144 mL, 1.96 mol) was added in one portion, and then 40% aqueous methyl amine (31 mL, 11 g of  $\text{MeNH}_2$ , 0.34 mol) was added dropwise with stirring, while cooling the reaction flask in an ice bath. The solution was then stirred and warmed to room temperature overnight. The organic layer was separated, washed with brine (4 x 50 mL), dried over  $\text{Na}_2\text{SO}_4$ , and filtered to afford a brownish orange liquid (185 g, 89%) crude product, which was then fractionally distilled (72 °C at 50 mmHg,; 76.8 °C at 50 mmHg<sup>163</sup>) to yield a bright orange, foul-smelling liquid (138 g, 1.31 mol, 67%).  $^1\text{H}$  NMR (400 MHz,  $\text{CDCl}_3$ )  $\delta$  (ppm): 6.55 (d, 2H), 6.52 (d, 2H), 2.22 (s, 6H). Notebook reference = JBP\_1\_34\_11b . NMR spectra are shown in Appendix A.



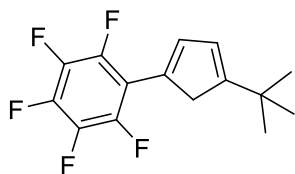
***tert*-Butylcyclopentadiene.** This method was reported by Vladimirskaya et al.<sup>159</sup> Anhydrous diethyl ether (1 L) was added to a nitrogen-flushed 2-L 3-neck round bottom flask fitted with a mechanical stirrer and a nitrogen inlet. Methylithium (1.6 M in ether, 170 mL, 0.27 mol) was measured into a graduated addition funnel and then run into the reaction flask in one portion. The turbid solution was cooled using an ice bath. With stirring, 6,6-dimethylfulvene (26 g, 0.25 mol) was added under a nitrogen counterstream in small portions using a pipette. With each addition, a transient yellow color is observed, followed by the formation of a white precipitate (lithium *tert*-butylcyclopentadienide). After stirring an additional 0.5 h, cold water (150 mL) was added slowly to quench the excess MeLi and the intermediate organolithium. Ammonium chloride (10 g) was added in one portion to neutralize the resulting lithium hydroxide in the aqueous layer. The organic layer was separated, washed with cold water (3 x 150 mL) and brine (1 x 150 mL), dried over MgSO<sub>4</sub>, and filtered. Ether was removed by short-path distillation at atmospheric pressure. Vacuum distillation (62 °C at 75 mm Hg; lit.<sup>164</sup> bp 53 °C at 42 mmHg) afforded a colorless oil (21 g, 0.17 mol, 76%). Note that if the ether is removed by rotary evaporation, the final yield of diene decreases significantly. The product is a mixture of tautomers. NMR data was consistent with literature data.<sup>164</sup> <sup>1</sup>H NMR (400 MHz, CDCl<sub>3</sub>) δ (ppm): 5.98, 6.17, 6.27, 6.43, 6.62 (m, 3H), 2.95 (m, 2H), 1.18, 1.19 (s, 9 H). Notebook reference = JBP\_1\_7\_15 or JBP\_1\_173\_12.



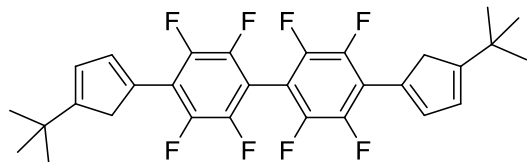
**Potassium *tert*-Butylcyclopentadienide.** A literature procedure<sup>160</sup> was adapted. A 250 mL Schlenk flask was charged with potassium hydride (6.9 g, 0.17 mol) and THF (80 mL). *tert*-Butylcyclopentadiene (21 g, 0.17 mol) was added in small portions by syringe. The reaction was monitored using a mineral oil bubbler to see hydrogen evolution. When the reaction was complete, the potassium hydride was consumed, and the solution turned clear. THF was evaporated to a liquid nitrogen trap using a vacuum pump. A solid white powder was recovered (26 g, 93%). <sup>1</sup>H NMR (400 MHz, THF-d<sub>8</sub>) δ (ppm): 5.37 (t, 2H), 5.27 (t, 2H), 1.19 (s, 9H). Notebook JBP\_1\_13\_13.



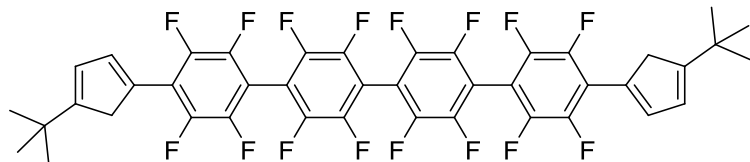
**Sodium *tert*-Butylcyclopentadienide.** A literature procedure<sup>160</sup> was adapted. A three-neck flask (1000 mL) was charged with sodium hydride (3.6 g, 0.15 mol) and THF (500 mL). To the suspension was added *tert*-butylcyclopentadiene (18 g, 0.15 mol) slowly under nitrogen purge. A condenser was fitted, and the reaction was stirred under reflux for 12 h. The resulting clear, brownish solution was evaporated using a vacuum pump to leave a pale solid. The crude product was collected on a coarse fritted filter under nitrogen, rinsed with pentane, and vacuum-dried to afford a white solid (16.9 g, 0.12 mol, 80 % yield). <sup>1</sup>H NMR (400 MHz, THF-D<sub>8</sub>) δ (ppm): 5.59 (t, 2H), 5.50 (t, 2H), 1.20 (s, 9H). Notebook JBP\_1\_55 or JBP\_1\_171\_9.



**1-Pentafluorophenyl-4-*tert*-butylcyclopentadiene (and isomers thereof).** Our own literature procedure<sup>160</sup> was adapted. Hexafluorobenzene (4.0 g, 0.022 mol) was added dropwise to a stirred suspension of potassium hydride (1.004 g, 0.025 mol) and potassium *tert*-butylcyclopentadiene (3.2 g, 0.020 mol) in THF (50 mL) maintained at 0 °C. The solution turned brownish and purple in color. After 2 h, the reaction was subjected to a routine aqueous workup (NMR JBP\_1\_15\_7). A second, identical reaction was stirred 24 h before workup (JBP\_1\_25\_18). The solvent was evaporated using a vacuum pump, and the residue was dissolved in hexane. Water was added slowly and made acidic with 10% H<sub>2</sub>SO<sub>4</sub>. After an aqueous work up, the organic layer was washed with water (5 x 15 mL), dried with MgSO<sub>4</sub>, filtered and rotary-evaporated. The product was purified using silica gel chromatography (5 cm x 22 cm, hexanes) to yield four fractions. Clean product was obtained from the first fraction. (1.7 g, 0.006 mol, 30%) <sup>1</sup>H NMR (400 MHz, CDCl<sub>3</sub>) δ (ppm): 7.22 (s, 1H) 7.14 (s, 1H), 6.25 (s, 1H), 6.19 (s, 1H), 3.42 (s, 2H), 1.22 (s, 9H), 1.21 (s, 9H). <sup>19</sup>F NMR (376 MHz, CDCl<sub>3</sub>) δ (ppm): -141.23 (d, 2F), -141.365 (minor, d, 2F), -141.722 (d, 2F), -157.64 (minor, t, 1F), -159.068 (t, 1F), -159.750 (t, 1F), -163.512 (m, 2F), -163.804 to -164.080 (m, 4F) Notebook JBP\_1\_25\_18a and JBP\_1\_49\_18\_a. The third fraction afforded a small amount of **1** (0.14 g) as determined by <sup>1</sup>H NMR and mass spectrometry (APCI<sup>+</sup> *m/z* 538) [Notebook JBP\_1\_25\_19].

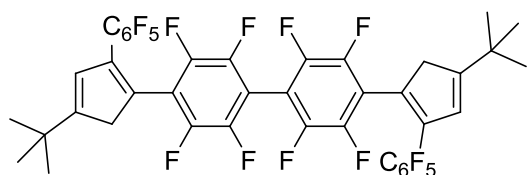


**4,4'-Bis(*q*-*tert*-butylcyclopentadien-1-yl)octafluorobiphenyl (*q* = 3,4) (1).** A mixture of sodium *tert*-butylcyclopentadienide (4.3 g, 0.031 mol) and sodium hydride (0.86 g, 0.037 mol) in THF (100 mL) was stirred under nitrogen and cooled using an ice bath. A solution of decafluorobiphenyl (4.1 g, 0.012 mol) in THF (30 mL) was added dropwise over several hours. The mixture was then stirred at 75 °C in for 24 h. Aliquot analysis by Method A revealed the absence of *para* fluorine signals (-152 ppm) in the <sup>19</sup>F NMR spectrum, indicating complete conversion. The THF was evaporated and hexane was added to form a slurry. Water was added to hydrolyze excess sodium hydride and organosodium intermediates. The organic layer was separated, washed, dried over MgSO<sub>4</sub>, filtered, and evaporated to afford a pale yellow solid (92% crude yield). Silica gel chromatography (2% dichloromethane in hexane) afforded a white crystalline powder (5.6 g, 0.010 mol, 86%). The compound is a mixture of 3 tautomers of *tert*-butyl cyclopentadiene. mp 123-126 °C. <sup>1</sup>H NMR (400 MHz, CDCl<sub>3</sub>) δ (ppm): 7.39 (s, 2H), 7.22 (s, 2H), 6.35 (s, 2H), 6.22 (s, 2H), 3.56 (br s, 8H), 1.26 (s, 18 H), 1.24 (s, 18H). <sup>19</sup>F NMR (CDCl<sub>3</sub>) δ (ppm): -140.5 (m, 4F), -140.7 (m, 4F), -140.9 (m, 4F), -141.4 (m, 4F). Anal. Calcd (found) for C<sub>30</sub>H<sub>26</sub>F<sub>8</sub> C, 66.91 (66.57); H, 4.87 (4.83). MS (APCI negative, *m/z*) calcd [M-H]<sup>-</sup> (found) 537.1834 (537.1845). Notebook JBP\_1\_35\_17a, JBP\_1\_83\_1, JBP\_4\_44\_2, JBP\_2\_39\_12.



**4,4'-Bis(*q*-*tert*-butylcyclopentadien-1-yl)hexadecafluorotetra(1,4-phenylene) (*q* = 3,4) (2).**

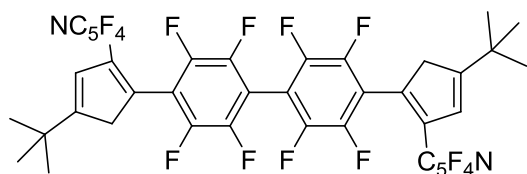
Potassium hydride (0.62 g, 15 mmol) and potassium *tert*-butylcyclopentadienide (2.0 g, 12 mmol) were suspended in THF (50 mL). A solution of decafluorobiphenyl (1.7 g, 5.0 mmol) in THF (10 mL) was added in small portions. The solution formed a brownish red color. The reaction was stirred overnight at 50 °C. Workup was carried out similar to the procedure for **1**. Silica gel chromatography (55 mm x 20 cm) of the crude product afforded **1** (43%) in the first band ( $R_f = 0.65$ , silica/hexanes). A subsequent band ( $R_f = 0.40$ , silica/hexanes) afforded a white solid (0.11 g, 0.13 mmol, 4%). mp 215-219 °C.  $^1\text{H}$  NMR (400 MHz,  $\text{CDCl}_3$ )  $\delta$  (ppm): 7.43 (s, 1H), 7.27 (s, 1H), 6.35 (s, 1H), 6.26 (s, 1H), 3.56 (br s, 4H), 1.24 (s, 9H), 1.22 (s, 9H). Anal. Calcd (found) for  $\text{C}_{42}\text{H}_{26}\text{F}_{16}$  C, 60.44 (60.69); H, 3.14 (3.57). Notebook JBP\_1\_33\_17, JBP\_1\_35\_17, JBP\_1\_35\_17c.



**4,4'-Bis[2-(pentafluorophenyl)-4-*tert*-butyl-1,*q*-cyclopentadiene-1-yl]-octafluorobiphenyl (*q* = 3,4) (3).**

A solution of bisdiene **1** (4.6 g, 8.5 mmol) in THF (30 mL) was added to a stirred suspension of sodium hydride (1.2 g, 51 mmol) in THF (90 mL), under nitrogen. After gas evolution ceased, hexafluorobenzene (4.7 g, 0.025 mol) was added, and the reaction was stirred under reflux for 32 h. The reaction was monitored by  $^1\text{H}$  NMR with hydrolyzed aliquots (Method B). The disappearance of the proton signals at 7.2 and 7.4 ppm indicated complete conversion. The THF was evaporated using a vacuum pump, and the residue was slurried in

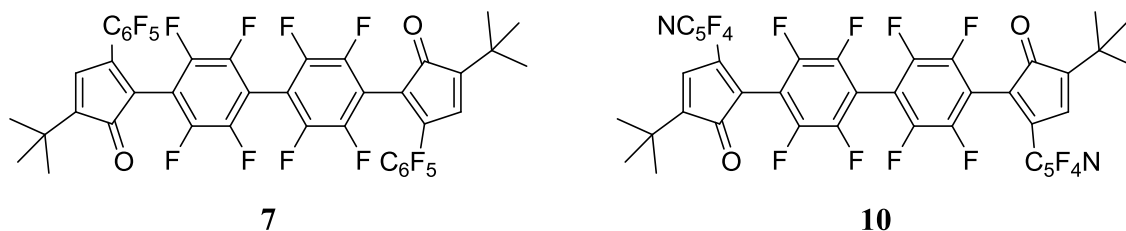
hexanes (50 mL), hydrolyzed cautiously with water (30 mL) and acidified with 10% aqueous sulfuric acid solution. The organic layer was separated, washed with water, dried over MgSO<sub>4</sub>, filtered, and rotary-evaporated to afford a foamy (glassy) yellow solid (95% crude yield). Silica gel chromatography (50 mm x 15 cm, hexanes, 300 mL forerun) afforded a white microcrystalline solid (6.4 g, 7.3 mmol, 86%). mp 98-126 °C. <sup>1</sup>H NMR (400 MHz, CDCl<sub>3</sub>) δ (ppm): 6.39 (s, 2 H), 6.32 (s, 2 H), 3.64 (s, 4H), 3.58 (s, 4 H), 1.28 (br s, 36 H). <sup>19</sup>F NMR (376 MHz, CDCl<sub>3</sub>) δ (ppm): -138.2 (m, 4 F), -138.4 (m, 4 F), -140.0 (m, 4 F), -140.4 (m, 4F), -140.7 (m, 4 F), -141.1 (m, 4 F), -154.7 (t, 2 F), -155.4 (t, 2F), -163.2 (m, 8 F). Anal. calcd (found) for C<sub>42</sub>H<sub>24</sub>F<sub>18</sub> C, 57.94 (57.92); H, 2.78 (2.79). Notebook JBP\_1\_81\_24, JBP\_2\_123\_1



**4,4'-Bis[2-(tetrafluoro-4-pyridyl)-4-tert-butyl-1,q-cyclopentadiene-1-yl]octafluorobiphenyl (q = 3,4) (12).** LiTMP (11 g, 0.074 mol, prepared from TMP and n-BuLi in hexane, see below) was dissolved in THF (110 mL) in a Schlenk flask (250 mL). Compound **1** (5.0 g, 9.3 mmol) was added to the solution in one portion. The solution was cooled using an ice bath, and pentafluoropyridine (9.4 g, 6.2 mL, 0.056 mol) was added slowly by syringe. Then the reaction was allowed to warm to room temperature over 0.5 h. The disappearance of the proton signals at 7.2 and 7.4 ppm indicated complete conversion after only 30 minutes. The THF solution was slowly added to a mixture of hexanes and 10% aqueous sulfuric acid. The organic layer was separated, washed with water, dried over MgSO<sub>4</sub>, and rotary-evaporated to afford a microcrystalline yellow solid. Silica gel chromatography (50 mm x 20 cm, hexanes) afforded a white crystalline powder (6.8 g, 8.2 mmol, 88%). <sup>1</sup>H NMR (400 MHz, CDCl<sub>3</sub>) δ (ppm): 6.44 (s, 1 H), 6.38 (s, 1H), 3.68 (br, 4 H), 1.29 (br s, 18 H). <sup>19</sup>F NMR (376 MHz, CDCl<sub>3</sub>) δ (ppm): -90.62

to -91.05 (m, 4 F), -137.67 to -137.87 (m, 4F), -139.5 to -140.2 (m, 4 F), -141.8 to -142.6 (m, 4 F). Anal. calcd (found) for  $C_{40}H_{24}F_{16}N_2$  C, 57.43 (57.69); H, 2.89 (3.04) N, 3.35 (3.19).

Notebook reference = JBP\_3\_9\_11 or JBP\_3\_93 or JBP\_2\_151\_12



**General Oxidation Method.** A solution of CuI (19 mg, 0.1 mol%) in acetonitrile (17 mL) and pyridine (3 mL) was added to a solution of a cyclopentadiene (nominally 1 mmol) dissolved in dichloromethane (10 mL). The combined solution was aerated for 1h during which time the reaction turns dark brown. After evaporation of the solvent, purification by silica gel chromatography (hexane) affords pure products as orange microcrystalline solids in about 75% yield. The reaction can be monitored by  $^1H$  NMR. The disappearance of the  $CH_2$  peaks and the downfield shift of the CH peaks indicate the reaction is complete.

**CPD Monomer 7 (Ar =  $C_6F_5$ ).** 75% yield. mp 130-160 °C.  $^1H$  NMR (400 MHz,  $CDCl_3$ )  $\delta$  (ppm): 6.87 (s, 1 H), 6.81 (s, 1 H), 1.26 (s, 18 H).  $^{19}F$  NMR (376 MHz,  $CDCl_3$ )  $\delta$  (ppm): -135.5 to -138.5 (several signals, some exchange-broadened, 24 F comprising 8 F from *ortho* of  $C_6F_5$  and 16 F from  $C_6F_4C_6F_4$  moieties), -149.5 (t, 2F), -149.7 (t, 2 F), -152.1 (t, 2 F), -152.3 (t, 2 F), -159.9 (m, 8 F), -161.4 (m, 8 F). Anal. calcd (found) for  $C_{40}H_{20}F_{18}O_2$  C, 56.14 (56.12); H, 2.24 (2.05). MS (APCI negative,  $m/z$ ) calcd  $[M^*]^-$  (found) 898.1181 (898.1198). Notebook JBP\_4\_101, JBP\_1\_95\_33

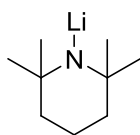
**CPD Monomer 10 (Ar =  $C_5F_4N$ ).** 67-93% yield. mp 167-172 °C.  $^1H$  NMR (400 MHz,  $CDCl_3$ )  $\delta$  (ppm): 6.95 (s, 1 H), 6.93 (s, 1 H), 1.29 (br s, 18 H).  $^{19}F$  NMR (376 MHz,  $CDCl_3$ )  $\delta$  (ppm):

–88.5 to –90.2 (m, 4F), –135.2 to –139.8 (m, 12 F). ). Anal. calcd (found) for  $C_{40}H_{20}F_{16}N_2O_2$ , 55.57 (56.37); H, 2.33 (1.86) N, 3.24 (3.18). MS (APCI negative,  $m/z$ ) calcd  $[M]^-$  (found) 864.1275 (864.1291). Notebook JBP\_3\_117\_6 or JBP\_181\_9 or JBP\_4\_4\_4

**Alternate (Inferior) Synthesis of CPD Monomer 7 Using DMNA.** *Step 1: Oxidation.* A mixture of **3** (2.05 g, 2.35 mmol), DMNA, 1.55 g, 10.4 mmol), anhydrous magnesium sulfate (2.8 g, 24 mmol), and THF (100 mL) was stirred under nitrogen. The reaction was initially a dark olive-green color and darkened slowly. After 5 h at room temperature, TLC analysis (silica, 4:1 hexane/toluene) showed the presence of unreacted starting material (**2**). After 18 h at reflux,  $^1H$  NMR analysis suggested nearly complete conversion. The reaction mixture was filtered to remove the magnesium sulfate, which was rinsed with additional THF (20 mL). Evaporation of the solvent afforded a purple residue. The crude product was dissolved in toluene (5 mL) and loaded onto a column (5.5 cm x 15 cm) of silica. A forerun (120 mL) was discarded, and then a purple band was collected and evaporated to afford 2.32 g (2.02 mmol) of a dark purple solid. Because the product was expected to be a complex mixture of regioisomeric diimines and dinitrones, complete characterization was not attempted.  $^1H$  NMR (acetone- $d_6$ )  $\delta$  7.4 to 6.4 (several multiplets, CH), 3.1 to 2.7 (several singlets,  $NMe_2$ ), 1.42 (tBu).  $^{19}F$  NMR (acetone- $d_6$ )  $\delta$  –140 to –144 (complex multiplet), –157.2 (t), –157.9 (t), –164 to –166 (multiplet).

*Step 2: Dinitrone hydrolysis.* To a solution of the intermediate diimine/dinitrone mixture (0.498 g, 0.433 mmol presumed) in glacial acetic acid (20 mL) was added 10% aqueous sulfuric acid (2 mL). After 5 h at reflux, the mixture was cooled and diluted with water (200 mL). Sodium bicarbonate (about 1 g) was added to neutralize the sulfuric acid. The mixture was extracted with dichloromethane (150 mL). The organic layer was washed with water and saturated sodium bicarbonate solution, dried over  $MgSO_4$ , filtered, and evaporated. The crude

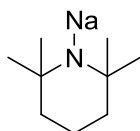
orange-brown product was dissolved in toluene (5 mL) and loaded onto a column (4 cm x 15 cm) of silica (that was loaded as a hexane-only slurry) and then eluted with an 8:1 hexane/toluene mixture. An orange band was collected and evaporated to afford 210 mg, (0.23 mmol, 54%) of a red solid. TLC and  $^1\text{H}$  NMR spectroscopic analyses revealed small amounts of impurities. An analytical sample was obtained by subjecting the red solid to chromatography on silica gel (3 cm x 10 cm column). A yellow band slowly eluted (3.5 L of hexane) and was discarded. Then a bright orange band was eluted with dichloromethane (250 mL) and evaporated to afford about 10% of pure **6** as a glassy, red-orange solid, mp 130-160 °C.



#### **Lithium 2,2,6,6,-Tetramethylpiperadide (LiTMP).**

The synthesis was adapted from Lappert et al.<sup>165</sup> This strong, yet non-nucleophilic base is not commercially available. 2,2,6,6-Tetramethylpiperidine (22 g, 0.16 mol) is slowly added to a solution of n-BuLi (100 mL, 1.6 M, 0.16 mol) in hexane held at -78 °C (dry ice acetone bath) under nitrogen. The solution slowly warms to room temperature and stirs overnight. After cooling the solution to 0 °C, the white precipitate is collected on a medium Schlenk frit. (The powder flows freely through a coarse frit.) The solid is rinsed with pentane (2 x 20 mL aliquots) and the white powder is dried by vacuum to afford 88% yield and stored in a glove box.

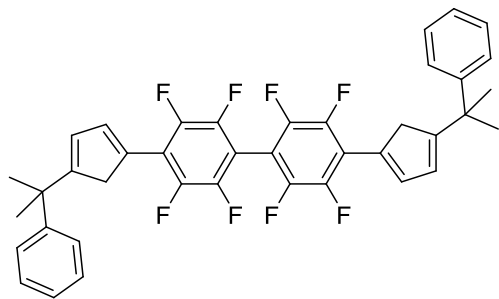
Notebook JBP\_4\_60



#### **Synthesis of NaTMP**

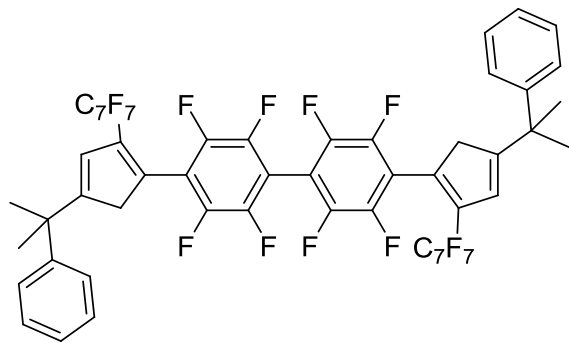
NaTMP was prepared by the methods reported by Gehrhus et al.<sup>166</sup> LiTMP (2.8 g, 19 mmol) is dissolved in hexanes (25 mL) to form a transparent solution. Sodium *tert*-butoxide (1.831 g, 19 mmol) is added all at once to the LiTMP in hexanes. The reaction stirs at room temperature overnight. A white precipitate is formed and collected using a medium frit. A fine white powder was retrieved after rinsing with pentane (5 x 10 mL) and dried by vacuum (2.5 g, 82%). Flame test (yellow) of the final product indicates the metal exchange occurred. Notebook reference = JBP\_4\_79

The following compounds were prepared by Kelly M. Daly under the supervision of J.P. Evans.



#### 4,4'-Bis(3,4-cumylcyclopentadien-1-yl)octafluorobiphenyl

The synthesis of compound 1 can be applied more generically other cyclopentadiene salts. Lithium cumylcyclopentadiene (from 6,6-dimethylfulvene and PhLi)<sup>167</sup> (3.4 g, 18 mmol) was suspended in THF (20 mL) and cooled to 0 °C. Decafluorobiphenyl (2.0 g, 5.9 mmol) dissolved in THF (5 mL) was added dropwise over several hours. The reaction warmed to room temperature and was subsequently heated for 36 h at reflux. The reaction was monitored by <sup>19</sup>F NMR. The disappearance of the *para* signals indicates the reaction is complete. The residue was dissolved in diethyl ether and a standard aqueous workup afforded a brown oil. The excess cumylcyclopentadiene is more difficult to remove because it is less volatile than *tert*-butyl cyclopentadiene. The presence of unreacted cumylcyclopentadiene can cause a poor separation, so the crude product was evaporated using a vacuum pump for several hours to separate most of the cumylcyclopentadiene that way. Purification by column (40 mm x 10 cm, hexanes) provides a white microcrystalline powder in 61% yield. <sup>1</sup>H NMR (400 MHz, CDCl<sub>3</sub>) δ (ppm): 7.39 (m, 10H), 7.21 (s, 1H), 7.18 (s, 1H), 6.50 (s, 1H), 6.40 (s, 1H), 3.62 (s, 2H), 3.40 (s, 2H), 1.62 (s, 12 H). <sup>19</sup>F NMR (CDCl<sub>3</sub>) δ (ppm): -142.0 (m, 4F), -142.5 (m, 4F). Notebook reference KMD-41-14 or KMD-53-4-1



**4,4'-Bis[2-(perfluorotolyl)-4-cumyl-1,q-cyclopentadiene-1-yl]-octafluorobiphenyl (q = 3,4).**

Octafluorotoluene (2.6 g, 10.9 mmol) was added to a slurry of sodium hydride (0.20 g, 8.3 mmol) and 4,4'-Bis(3,4-cumyl-cyclopentadien-1-yl)octafluorobiphenyl (1.1 g, 1.7 mmol) in THF (25 mL). The reaction stirred under nitrogen at reflux for 48 hours. The residue was taken up in diethyl ether after the THF was removed by vacuum. The organic layer was extracted, dried over MgSO<sub>4</sub>, filtered and evaporated to afford a glassy yellow solid. Silica gel chromatography (5'' x 1.5'', hexanes) yielded a pale yellow solid (0.65 g, 58%). <sup>1</sup>H NMR (400 MHz, CDCl<sub>3</sub>) δ (ppm): 7.40 (m, 10H), 6.58 (s, 1H), 6.46 (s, 1H), 3.50 (br s, 4H), 1.68 (s, 12 H). <sup>19</sup>F NMR (CDCl<sub>3</sub>) δ (ppm): -56.5 (s, 6F), -135.0 to -140.0 (m, 12F). Notebook reference KMD-55-11

**General Crystallographic Procedure.** Crystals of both **1** and **2** were grown by cooling hexane solutions to -10 °C. Crystals of **5** were grown from a concentrated hexane solution at room temperature. Orange prisms of dioxime **8** were obtained by slow evaporation of a CH<sub>2</sub>Cl<sub>2</sub> solution at room temperature. Orange-red crystals of diketone **10** were obtained by slow evaporation of a 10% CH<sub>2</sub>Cl<sub>2</sub> in hexanes solution at room temperature. Colorless plates of diene **12** were obtained by cooling pentane solutions to -10 °C.

With assistance from Dr. Carla Slebodnick, I collected, solved, and refined the data for compounds **1**, **2**, and **3** during an X-ray crystallography workshop at Virginia Tech. Dr. Slebodnick collected, solved, and refined the data for the remainder of the compounds. Each

chosen crystal was mounted on a nylon CryoLoop™ (Hampton Research) with Krytox® Oil (DuPont) and centered on the goniometer of an Xcalibur or Gemini diffractometer manufactured by Oxford Diffraction (a part of Varian, which part of Agilent), equipped with a CCD detector. The data collection routines, unit cell refinements, and data processing were carried out with the program CrysAlis or CrysAlisPro. (CrysAlisPro v171.33.55, Oxford Diffraction: Wrocław, Poland, 2009). The structures were solved by direct methods and refined using the SHELXTL NT software package.<sup>168</sup> The final refinement models involved anisotropic displacement parameters for non-hydrogen atoms and a riding model for all hydrogen atoms, except as indicated below. Molecular graphics generation used SHELXTL NT software or OLEX-2 software.<sup>168</sup> Data is archived in CIF format at Virginia Tech.

The solution and refinement of **2** were somewhat difficult because of a disordered solvent. The packing diagram reveals open, infinite channels along the crystallographic **a** axis, and a hexane molecule appears to be randomly positioned throughout this channel; however solvent loss was not observed. Despite this difficulty, the molecule of interest was modeled well.

The solution of diketone **10** revealed two molecules of the main species and 0.5 molecules of CH<sub>2</sub>Cl<sub>2</sub> in the asymmetric unit. A 4-position disorder model (2 positions further disordered across an inversion center) was used for the CH<sub>2</sub>Cl<sub>2</sub> with relative occupancies that refined to 0.372(5), 0.372(5), 0.173(5) and 0.173(5). Disordered atoms were refined isotropically.

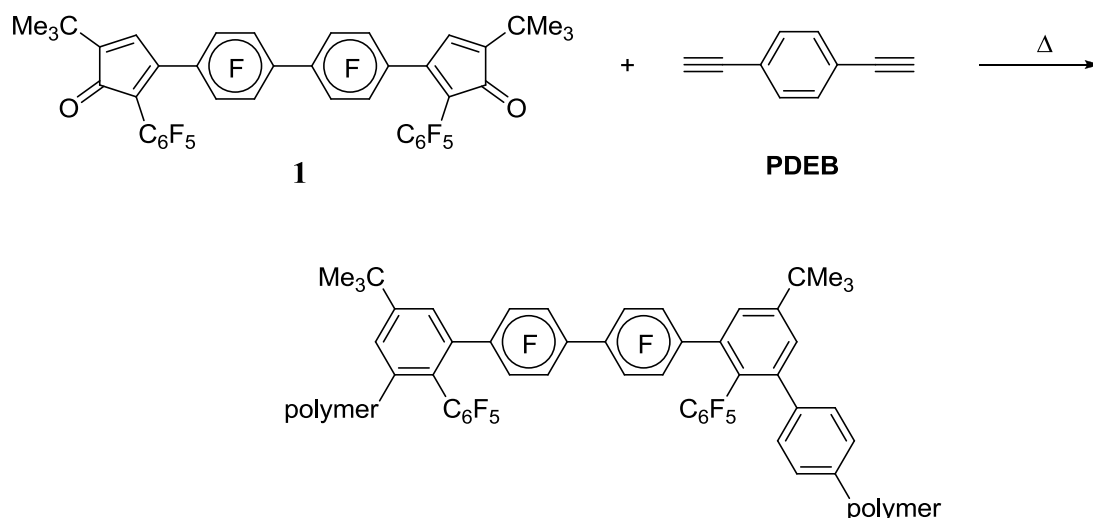
The solution of bisdiene **12** revealed one molecule of the main species and 0.5 molecules of pentane in the asymmetric unit. A 2-position disorder model was used for the *tert*-butyl methyl groups and the pentane solvate. The relative occupancies of the methyl positions refined to 0.699(15) and 0.301(15). The relative occupancies of the two pentane conformations refined to

0.624(19) and 0.376(19). One methyl hydrogen was omitted in the disorder model for the pentane. Disordered atoms were refined isotropically.

The solution of dioxime **8** revealed one molecule of the main species and one molecule of CH<sub>2</sub>Cl<sub>2</sub> in the asymmetric unit. Residual electron density maps suggested positional disorder in the CH<sub>2</sub>Cl<sub>2</sub> molecule. This disorder was modeled as 2-position disorder with refined occupancies of 0.637(3) and 0.363(3). In the minor CH<sub>2</sub>Cl<sub>2</sub> molecule, 3 approximately equal residual electron density peaks 1.5-1.8 Å from the carbon suggested additional disorder. These peaks were assigned as chlorine atoms with occupancies fixed at 2/3 the occupancy of the attached carbon. Only one hydrogen position was assigned to this CH<sub>2</sub>Cl<sub>2</sub> molecule, accounting for the discrepancy in the calculated and reported chemical formulas. Disordered solvent atoms were refined isotropically.

### Chapter 3. Model Diels-Alder Reactivity Studies of Highly Fluorinated Cyclopentadienones and Dialkynes

The synthesis of our first “second generation” highly fluorinated CPD monomer (**1**) was described in Chapter 2 (see Scheme 2-11 in Ch. 2). Naturally we wanted to use this monomer right away in the synthesis of polyphenylenes, for example, through a reaction with 1,4-diethynylbenzene (Scheme 3-1). Other studies conducted in our laboratories had suggested that such a polymerization reaction might proceed at an appreciable rate, in non-polar solvents, at temperatures less than 120 °C. That prediction was surprising, considering the temperatures that Stille needed (200-280 °C) for his polymerizations with non-fluorinated monomer analogues. We quickly learned that this prediction was “too good to be true.” Facing the prospects of long reaction times and decomposition side-reactions at high temperatures, we set out to learn more about these kinds of Diels-Alder (DA) reactions and find ways to accelerate them. Those studies are the subject of this chapter.



**Scheme 3-1. Monomer 1 reacts with PDEB to form a fluorinated polyphenylene.**

Section 3.1 explores the molecular orbital theory of the DA reaction and rationalizes the observed “inverse electron demand” effect. Results obtained by Brian Hickory in our group are

presented that suggested high reactivity of fluorinated cyclopentadienones in DA reactions with alkynes. Section 3.2 will demonstrate, through a model study, that monomer **1** is indeed reactive toward aromatic alkynes, but not nearly as reactive as we had anticipated based on Mr. Hickory's data. Section 3.3 presents model reactivity data to demonstrate that the "inverse" DA reaction can be accelerated by solvent catalysis. Section 3.4 shows how changing the lateral C<sub>6</sub>F<sub>5</sub> substituent in monomer **1** to C<sub>6</sub>F<sub>4</sub>CF<sub>3</sub> or C<sub>5</sub>F<sub>4</sub>N can accelerate its DA reactivity, again through model studies. Section 3.5 demonstrates the effects of microwave heating on model DA reactions.

### **3. 1 The Inverse Electron Demand DA Reaction**

The Diels-Alder reaction typically involves an electron rich diene and an electron poor dienophile. The HOMO of the diene overlaps with the LUMO of the dienophile (Figure 3-1). The reaction is accelerated by electron withdrawing substituents on the dienophile, because the LUMO level is lowered, making a more favorable HOMO-LUMO interaction.<sup>169</sup> However, in principle, an electron deficient diene can also react with an electron poor dienophile. In this "inverse electron demand" case, the HOMO of the dienophile overlaps with the LUMO of the diene.<sup>169</sup> This type of DA reaction is favored by electron withdrawing groups on the diene and electron donating groups on the dienophile.

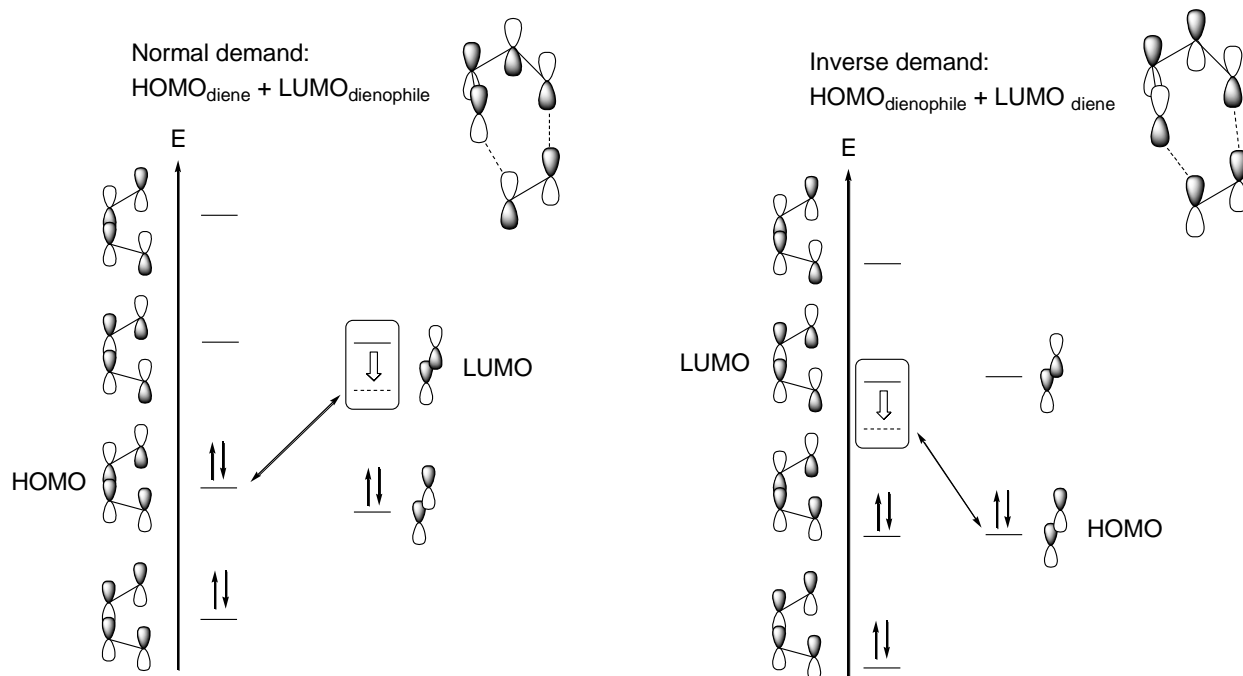
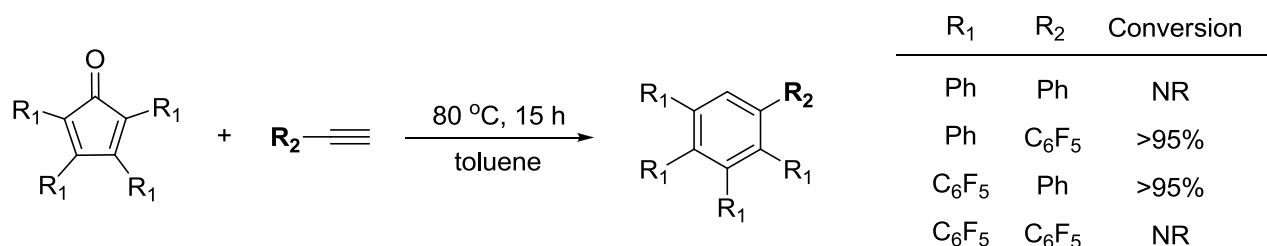


**Figure 3-1. Electron deficient dienes react with electron rich dienophiles by inverse electron demand.**

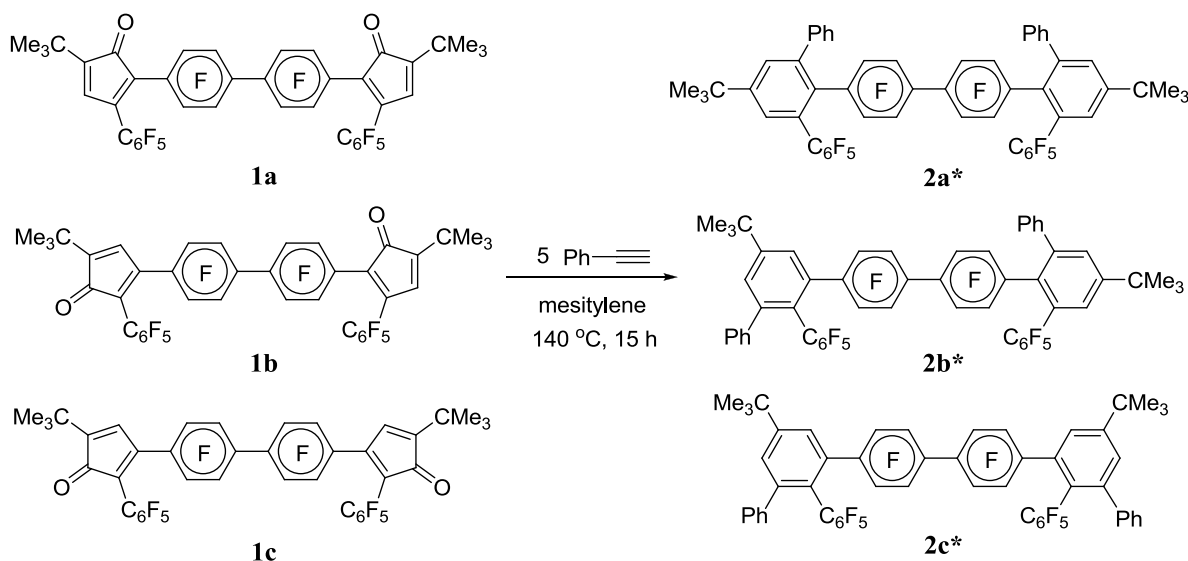
Brian Hickory in our research group obtained convincing evidence that reactions of highly fluorinated cyclopentadienones and non-fluorinated aromatic alkynes follow the inverse electron demand model. Scheme 3-2 shows qualitative reactivity data for four model reactions conducted at 80 °C in toluene solution, all with a large excess (20 equiv) of the alkyne. These data clearly indicate that both normal *and* inverse demand pathways can operate in this system.



**Scheme 3-2. Highly fluorinated cyclopentadienones and aromatic alkynes follow inverse electron demand. Data was provided by Brian Hickory.**

### 3.2 Model Reactivity Study of Monomer 1

Knowing that pentafluorophenyl substituents could accelerate DA reactions of cyclopentadienones and phenylacetylene, we attempted the reaction of **1** with phenylacetylene (Scheme 3-3). We discovered, however, that the reaction was slower than the analogous reaction shown in Scheme 3-2 (third table entry). With 5 equiv of phenylacetylene, the reaction was complete (> 98% conversion) after 15 h at 140 °C in mesitylene as the solvent. The product was an off-white solid, obtained in 96% yield after silica gel chromatography.



**Scheme 3-3. The reaction between monomer 1 and phenylacetylene is a monofunctional model for the polymerization; (\*) The total yield of 2 (a,b, and c) was 96%.**

Because monomer **1** is a statistical mixture of three isomers (**1a:1b:1c** = 1:2:1), the product arene **2** is also obtained as a mixture. Only three isomers are obtained. The  $^1\text{H}$  NMR spectrum of the product mixture shows eight doublets in the region 7.7-7.4 ppm (Figure 3-2a). Each symmetrical isomer (**2a** and **2c**) should exhibit two signals, while the unsymmetrical isomer (**2b**) should exhibit four. The lower symmetry of **2b** should give signals of half the intensity, but the double statistical concentration of **2b** compensates. Four of the doublets are in an upfield region (7.40-7.50 ppm, probably hydrogens between  $\text{CMe}_3$  and Ph groups), while four are in a downfield region (7.59 to 7.64 ppm, probably hydrogens between  $\text{CMe}_3$  and perfluoroaryl groups). Only two of the doublets are coincident (twofold integration at 7.62 ppm). All of the doublets exhibit a coupling constant of 2 Hz, consistent with a *meta* structural assignment for two hydrogens on a benzene ring. These spectroscopic features are consistent with **2** as the structure. Note that no isomers are observed in which Ph and  $\text{CMe}_3$  groups are adjacent, indicating perfect steric approach control (the phenyl group avoids the  $\text{CMe}_3$  group in the initial approach of diene and dienophile). The  $^{19}\text{F}$  NMR spectrum of the mixture shows four equally integrating triplets in the *para* region corresponding to the pendant  $\text{C}_6\text{F}_5$  groups, one signal for **2a** and **2c**, and two signals for the unsymmetrical isomer **2b**. Despite the interesting selectivity and isomerism issues, the reaction seemed too slow to be useful as a propagation reaction. We wanted to bring the temperature of the reaction down to around 100 °C if possible, to avoid known side-reactions of the aromatic alkynes. We wanted to understand these types of DA reactions and we needed to find ways to accelerate them.

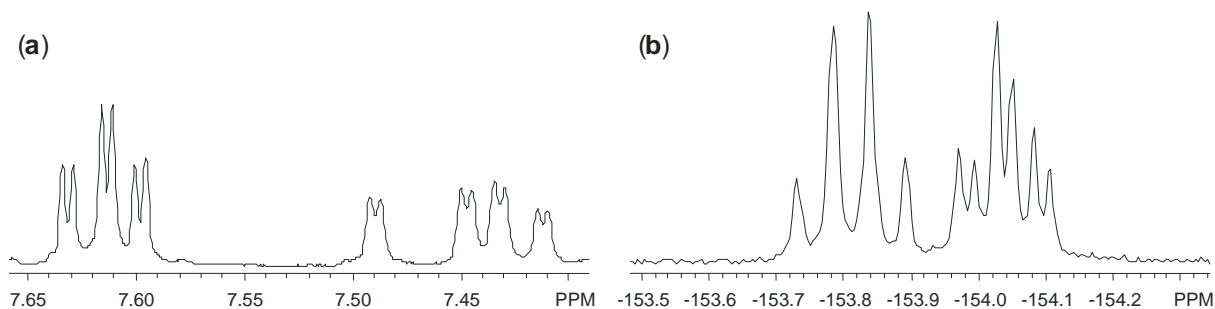


**Figure 3-2.  $^1\text{H}$  (a) and  $^{19}\text{F}$  (b) NMR spectra of DA reaction products 2a, 2b, and 2c are consistent with 3 isomers.**

### 3.3 Catalysis

3.3.1 Choice of Models. We wanted to explore these DA reactions in more detail, but not using monomer compounds such as **1**. First of all, the isomerism of **1** leads to multiple products (Scheme 3-3), which would make reactions hard to follow by NMR spectroscopy. Second, when we started our model studies, monomer compounds were still very precious because we hadn't yet developed the copper-catalyzed oxidation chemistry that made their synthesis much easier. Recalling the reaction schemes in Chapter 1, we realized that we could easily prepare cyclopentadienes and cyclopentadienones bearing one *tert*-butyl group and two  $\text{C}_6\text{F}_5$  groups, which would be structurally similar to each "end" of the monomer compound (Fig. 3-3). As for the alkyne, we stayed with phenylacetylene, also for the sake of simplicity, although in hindsight it might have been better to have a crystalline solid; phenylacetylene is a liquid at room temperature. For most of the work described in the rest of this chapter, the exact model compounds shown in Figure 3-3 will serve well. Only in the section on substituent effects (3.4) are different model reactants needed. Their synthesis will be described in that section. As we

became more proficient at synthesizing monomer **1**, we started to conduct some of our model studies (e.g., solvent effects) using **1** and phenylacetylene.

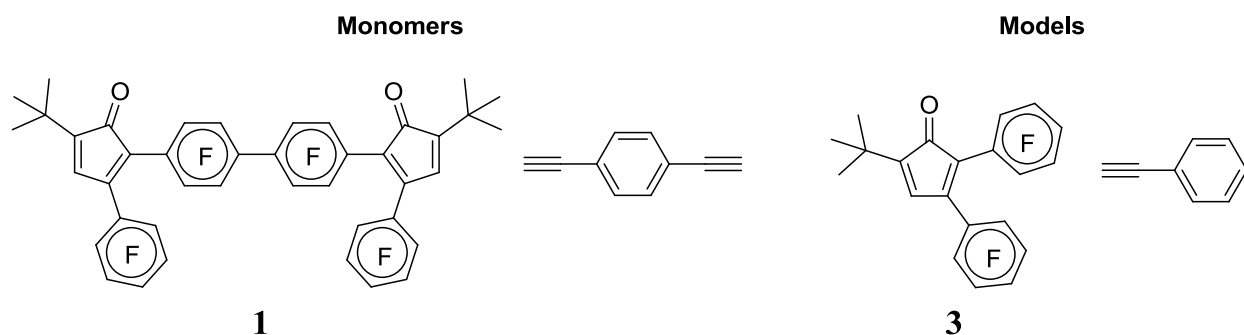


**Figure 3-3. Monofunctional diarylated *tert*-butyl cyclopentadienones and phenyl acetylene (right) are good models for the Diels-Alder reaction of fluorinated biscyclopentadienones and dialkynes (left).**

3.3.2 Basic Catalysis Concepts. Several methods of catalyzing the Diels-Alder reaction have been reported. Usually, a Lewis acid coordinates to a lone pair of electrons on the dienophile (such as acrolein), further lowering its LUMO energy and accelerating normal electron-demand reactions, as described in Section 3.1.<sup>170</sup> Here the term “Lewis acid” must be construed broadly. We thought we could achieve a similar result with our inverse-demand reactions because the only basic lone pair of electrons is the oxygen of the cyclopentadienone (our DA diene). We were aware, however, of reports in the literature suggesting that the acceleration effect of Lewis acids for inverse electron demand DA is much less pronounced.<sup>169</sup>

3.3.3 Classical Lewis Acids: Background. Walborsky and coworkers found that the DA reaction could be catalyzed by strong molecular Lewis acids.<sup>171</sup> The presence of  $\text{AlCl}_3$ ,  $\text{SnCl}_4$ , or  $\text{TiCl}_4$  catalyzes the reaction between dimethyl fumarate and butadiene.<sup>171</sup> Salts, especially lithium and magnesium perchlorates, are also popular.<sup>172-178</sup> Many research groups have pursued catalysis of DA reactions in order to control regio- and stereochemistry, but those details are outside the scope of this dissertation. One disadvantage of using metals to catalyze

polymerization reactions is the need to separate the metal from the product, as discussed in more depth in Chapter 1.

3.3.4 Classical Lewis Acids: Results. We tested the reaction of diene **3** with phenylacetylene. Reactions were carried out on small scales and monitored by  $^{19}\text{F}$  NMR spectroscopy. No workup or solvent removal is required because only **3** and the DA product are visible in the  $^{19}\text{F}$  NMR spectrum. A control without catalyst was always prepared from the same stock solutions and heated under identical conditions (e.g., in the same oil bath). Neither magnesium perchlorate nor lithium perchlorate had either an activating or deactivating effect on this model reaction. Initially the solvents we tried included butyl ether, diethyl ether, and diglyme. These salts are not soluble in hydrocarbon solvents, but we were concerned that the oxygen atoms of the ethers were competing with the dienone **3** for the coordination of the metal ion. We tried toluene and xylene but obtained the same negative result.

Because of the issue of competition from ether solvents, we wanted to find a Lewis acid that would be soluble in a hydrocarbon solvent. We ruled out  $\text{TiCl}_4$  and  $\text{SnCl}_4$  because they are hard to handle on a small scale without introducing  $\text{HCl}$ , which we knew would decompose the phenylacetylene reactant. Terminal alkynes are initiated toward cationic polymerization by strong Bronsted acids. In a moment of desperation, we tried tris(pentafluorophenyl)borane,  $(\text{C}_6\text{F}_5)_3\text{B}$ , an aggressive organo-Lewis acid. But this reagent immediately turned the reaction solution black. Workup and  $^1\text{H}$  NMR analysis showed that the phenylacetylene was oligomerized. The presence of the highly acidic hydrate  $(\text{C}_6\text{F}_5)_3\text{B}(\text{OH}_2)$  as the cause of the decomposition could not be ruled out.

3.3.5 Catalysis by Hydrogen Bonding: Background. Rawal and coworkers have shown that unactivated ketones can become activated toward Diels-Alder reactions in a hydrogen bonding

environment.<sup>179-183</sup> DA reaction rates can be increased through hydrogen bonding of the substrates with alcohols,<sup>184</sup> TADDOL derivatives,<sup>185,186</sup> ureas,<sup>187-189</sup> or water.<sup>190,191</sup> The H-bond donor essentially behaves as a Lewis acid toward one of the reactants, and the theory of the rate increase is the same. For the inverse electron demand DA reaction, the diene must be a good H-bond acceptor.<sup>183</sup> An alternate theory suggests that hydrogen-bonding solvents can also specifically stabilize charge-polarized transition states even though interactions with the ground state substrate molecules may be weak.<sup>184,192</sup> This concept is illustrated in Figure 3-4 using our model compounds.

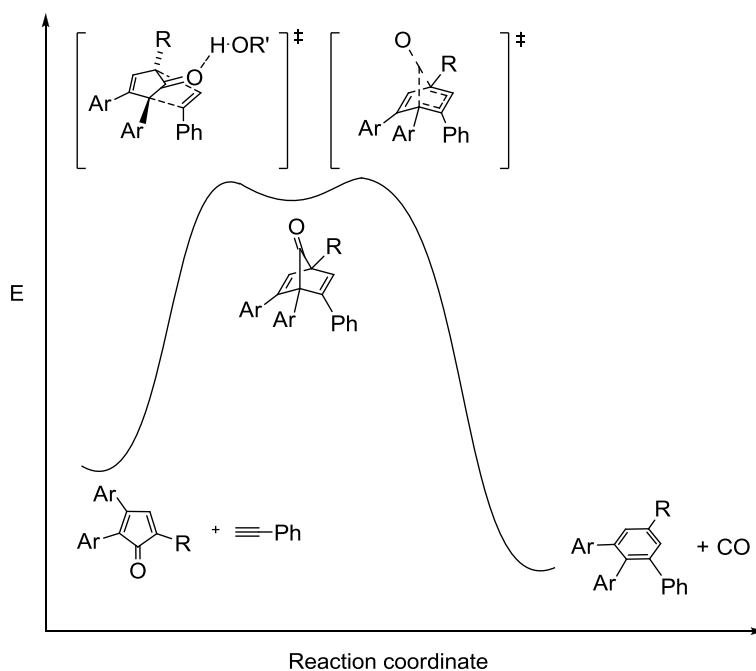


**Figure 3-4. The energy diagram shows the stabilization of the first transition state by hydrogen bonding (R = CMe<sub>3</sub>).**

Others have suggested that “enforced hydrophobic interactions” are also responsible for rate acceleration of DA reactions in aqueous media.<sup>192-195</sup> One simple interpretation is that hydrophobic aggregation of the organic reactants are responsible for the rate enhancement.<sup>196</sup> However, Engberts used the term “enforced” to distinguish generalized aggregation from

specific interactions that lead to the activated complex.<sup>192,193,197,198</sup> Engberts claimed that “enforced hydrophobic interactions” can destabilize the reactant ground state, while hydrogen bonding stabilizes the activated complex, leading to faster reactions.<sup>193</sup> Therefore, DA reactions are catalyzed by the combination of enforced hydrophobic interactions and hydrogen bonding. One limitation of the hydrophobic aggregation theory is that one would expect aggregation to be important only in solvents that are primarily aqueous, with just enough organic solvent to ensure that the substrates are dissolved.

3.3.6 Catalysis by Hydrogen Bonding: Results. Regardless of the underlying theory, we decided to test our model reactions (a diene such as **3** + phenylacetylene; or monomer **1** + phenylacetylene) in hydrogen-bonding media. The control solvent was xylenes or toluene. Hydrogen bonding agents that we tested included 1,4-butanediol, guanidinium hydrochloride, pentafluorophenol, trifluoroethanol, *m*-cresol, and water. The fluorinated cyclopentadienones are not soluble in highly polar media such as water, so in those cases the hydrogen bonding agent was used as an additive with an organic solvent like *N,N*-dimethylacetamide (DMAc) or toluene. In those cases a parallel control was run under identical conditions, but without the additive.

**Table 3-1. Model studies were used to study catalysis of Diels-Alder reactions.**  
**“Reaction time” is the amount of time needed to reach ca. 95% conversion.**

Solvent	Temperature °C	Lewis acid	Results/Reaction Time
Toluene	120	-	8 days
Xylenes	140	-	6 days
Dichlorobenzene	160	-	2 days
Xylenes	80	-	8 days
Xylenes	25	B(C <sub>6</sub> F <sub>5</sub> ) <sub>3</sub>	Alkyne decomposed
Xylenes + diglyme	140	Mg(ClO <sub>4</sub> ) <sub>2</sub>	4 days
Xylenes + diglyme	140	-	4 days
<i>m</i> -cresol	125	-	18 hours
<i>m</i> -cresol	80	-	4 days
Trifluoroethanol	80	-	9 days Precipitation
Pentafluorophenol	25	-	Alkyne decomposed

Butyl ether	110	-	2 days
Butyl ether	110	Mg(ClO <sub>4</sub> ) <sub>2</sub>	Intractable black material
Butyl ether	100	-	2 days
Butyl ether	100	LiClO <sub>4</sub>	2 days
DMAc	100	-	2 days
DMAc	100	Guanidinium HCl	2 days
<i>m</i> -cresol	80	-	1 day
DMAc	100	LiClO <sub>4</sub>	2 days
DMAc	100	10% H <sub>2</sub> O	40 hours
DMAc	100	25% H <sub>2</sub> O	30 hours
DMAc	100	50% H <sub>2</sub> O	Precipitation

Table 3-1 summarizes most of the experiments focused on catalysis by hydrogen bonding. Guanidinium HCl is poorly soluble in most organic solvents but soluble in DMAc. The reaction rate was not increased much with guanidinium HCl in DMAc. Since the idea is to add hydrogen bonding to organic solvents, I also tried water in DMAc. Water and DMAc are miscible. The model studies with diene **3** and phenylacetylene showed significant rate enhancement with water in DMAc compared to DMAc alone. However, later when I applied this technique to the polymerizations, I discovered some of the pendant perfluoroaryl groups (specifically C<sub>5</sub>F<sub>4</sub>N) react slowly with freshly distilled DMAc, giving rise to defects. We learned that perfluorophenyl-substituted model compounds like **3** or even the monomer **1** are not always good models for the perfluoropyridyl containing monomers in terms of susceptibility to nucleophilic side-reactions.

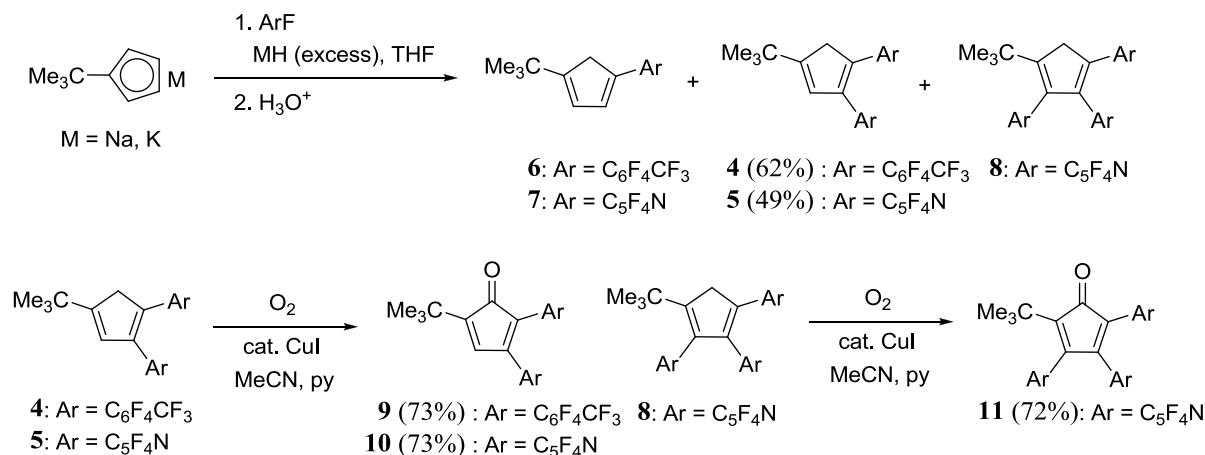
Strongly acidic hydrogen bonding agents failed. Pentafluorophenol (pKa 5.5) was a strong enough acid to initiate oligomerization of phenylacetylene. However, trifluoroethanol (pKa 12.5) and *m*-cresol (pKa 10.1) showed promising results. Trifluoroethanol has a much lower boiling point (78 °C) than *m*-cresol (bp 202 °C) which make it easier to remove, but the low boiling point limits the temperature range of the reaction. The reaction is clean in both trifluoroethanol and *m*-cresol, but we knew *m*-cresol would allow us to conduct reactions in realistic temperature ranges (120-180 °C). In addition, the product from the model reactions of diene **3** (or monomer **1**) with phenylacetylene also precipitated from trifluoroethanol. Although the precipitation of product in the model systems is convenient for isolating the final product, precipitation in a polymerization can lead to low conversions and low molecular weights.

My efforts quickly focused on *m*-cresol because it is a hydrogen bonding solvent with a high temperature range and does not react with either monomer. We figured we could try



### 3.4.1 Model Compound Synthesis. The two new CPDs shown in Scheme 3-4 (**9** and **10**)

were prepared in analogy to compound **3**, as shown in Scheme 3-5.

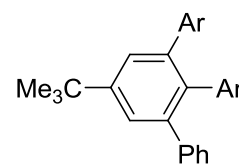


#### Scheme 3-5. Perfluoroaryl-substituted cyclopentadienones can be synthesized by one-pot procedures.

The syntheses of dienes **4** and **5** were carried out in one-pot arylation procedures analogous to the procedure used to prepare diene **3**.<sup>83</sup> The key variables that govern the number of aryl groups attached are the reaction temperature, reaction time, number of equivalents of perfluoroarenes (ArF) added, and the reactivity of the perfluoroarenes. In the case of hexafluorobenzene, the monoarylated diene can be prepared with moderate selectivity (see Scheme 2-5 in Chapter 2), whereas attachment of the second C<sub>6</sub>F<sub>5</sub> group is relatively slow, requiring several hours at reflux in THF. Excesses (> 2 equiv) of more reactive perfluoroarenes give the disubstituted dienes easily (**5** is obtained at room temperature), however yields are only moderate (40-60%) after chromatographic purification. Only traces of the monoarylated or triarylated dienes **6**, **7**, and **8** are observed by NMR spectroscopy under mild conditions, so the reason for the loss of yield is not known. Neither **6** nor **7** has been isolated. Interestingly, when 1.2 equiv of octafluorotoluene is used, a 60% crude yield of the diarylated diene **4** is still obtained.

The biggest surprise in this chemistry was the observation of the triarylated diene **8** (60%) after extended heating (8 d in THF at reflux with 4 equiv of C<sub>5</sub>F<sub>5</sub>N). This result shows clearly that the steric bulk of the *tert*-butyl group does not completely prevent vicinal arylation. Oxidation of dienes **4**, **5**, and **8** using Hickory's copper-catalyzed air oxidation method gave good yields (>70%) of the corresponding ketones **9**, **10**, and **11**, respectively. The ketones are orange to red-orange crystalline solids. Ketone **10** has been characterized crystallographically (see below).

3.4.2 Analysis of Substituent Effects. Earlier work in the Deck Group<sup>153</sup> suggested that the perfluoro-4-tolyl group is about 1.5 times as electron-withdrawing as the pentafluorophenyl, while the tetrafluoro-4-pyridyl group is about twice as electron withdrawing as C<sub>6</sub>F<sub>5</sub>, based on electrochemical measurements on substituted ferrocenes and infrared spectra of substituted



**12**: Ar = C<sub>6</sub>F<sub>5</sub>

**13**: Ar = C<sub>6</sub>F<sub>4</sub>CF<sub>3</sub>

**14**: Ar = C<sub>5</sub>F<sub>4</sub>N

CpM(CO)<sub>3</sub> complexes (M = Mn, Re). With ketones **9**, **10**, and **11** available, we had an opportunity to test this trend in terms of chemical reactivity. Solutions of each ketone and an excess of phenylacetylene were heated in NMR tubes. In the <sup>19</sup>F NMR spectrum the disappearance of the ketones and the appearance of the arene products (**12**, **13**, and **14**, respectively) could both be monitored without requiring any workup. Each sample contained some C<sub>6</sub>D<sub>6</sub> to allow locking and shimming of the NMR probe. Arene **12** was also prepared on a preparative scale characterized crystallographically (see below).

The results are shown in Figure 3-5. While there were some outlying data points, these curves show that the ratio of rates for Ar = C<sub>6</sub>F<sub>5</sub> (**12**) : Ar = C<sub>7</sub>F<sub>7</sub> (**13**) : Ar = C<sub>5</sub>F<sub>4</sub>N (**14**) is about 1:2:4. Although this ratio seems small, it could mean the difference between a polymerization that takes a few days compared to one that is finished overnight. However the goal is not

convenience; the goal is to eliminate any side reactions that prevent propagation. It is difficult to know what effect, if any, the substituent effects might have on unwanted side reactions.

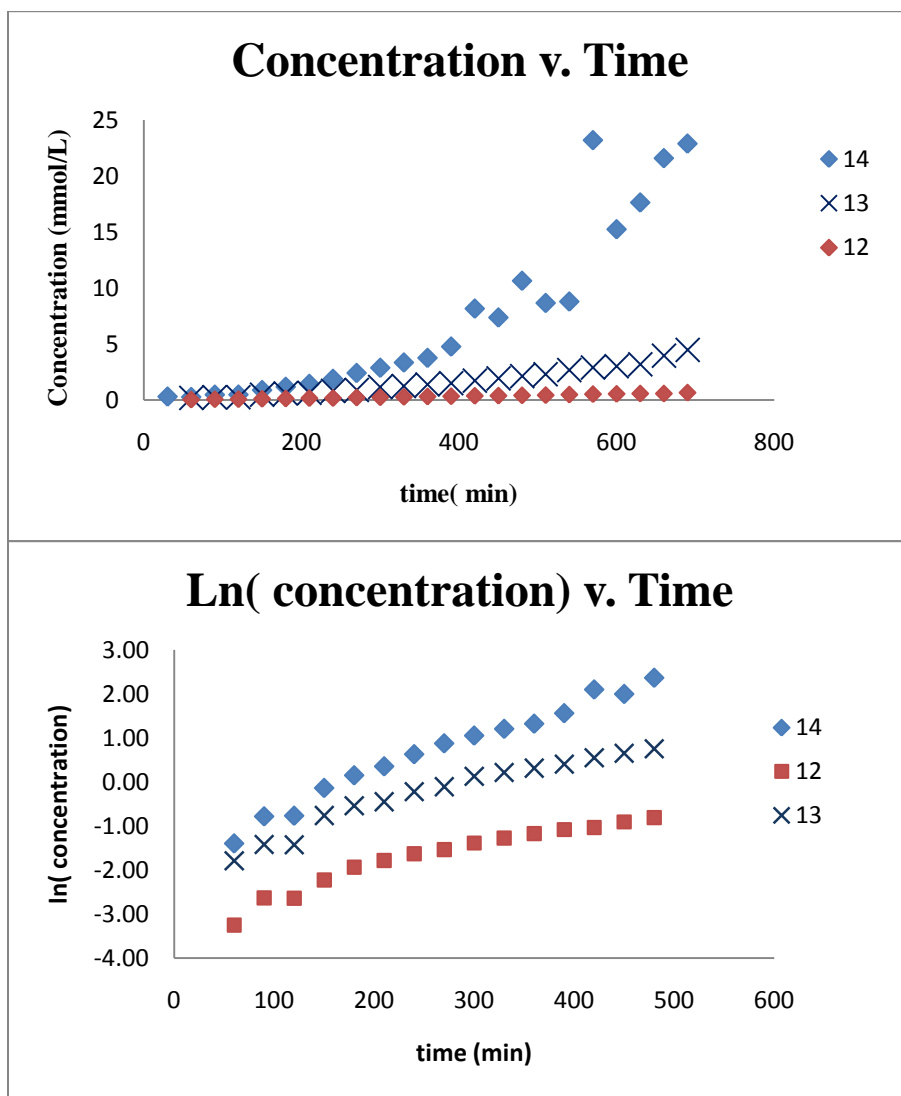


**Figure 3-5. Reaction rates increase with more electron withdrawing substituents. The graphs show the formation of arene products 12, 13, and 14 as a function of time. The ln(concentration) v. time plot shows a rate difference of approximately 1:2:4 for 12:13:14.**

### 3.5 Microwave Assisted Diels-Alder Reactions

Since the first reports of chemistry using modified kitchen microwaves for chemical reactions in 1986, over 2000 articles and several reviews have been published regarding

microwave chemistry,<sup>199-201</sup> and good commercial equipment is now readily available.<sup>199,200,202</sup> Microwave heating can reduce reaction times from hours to minutes while increasing yields and reproducibility. After a brief introduction of microwave theory, this section will discuss how microwave heating affects the Diels-Alder reaction of highly fluorinated CPDs and alkynes.

3.5.1 Microwave Theory. Microwave irradiation cannot induce chemical reactions directly, because the energy of a microwave photon is not high enough to break chemical bonds.<sup>199</sup> However, microwave heating is more efficient than conventional heating. Microwave enhancement can be described by widely accepted thermal effects and controversial nonthermal effects. The combination of these effects is the so-called “microwave effect”.<sup>203-205</sup>

Microwave heating is essentially just a more homogeneous, reproducible method compared to conventional heating. Microwaves induce faster heating from within the sample, rather than slow heating from outside the sample. As a result, the faster, homogenous heating accelerates reactions without side reactions on the surface of reaction vessels. The efficiency of microwave heating depends on the ability of a material to absorb microwave energy and convert it to heat. First, an electromagnetic field is applied and heating is caused by dipolar polarization and ionic conduction. The microwave absorbent material moves in order to align with the applied electric field. Molecular friction, rotation, and collisions cause heat generation from within the sample.<sup>206</sup> Therefore, the amount of heat produced in this process depends on how well the material is able to align itself with the frequency of the applied field (dielectric). The key result is that the heat comes from within the sample,<sup>199,201</sup> in contrast to external (e.g., oil bath) heating. This difference is illustrated in Figure 3-6,<sup>200</sup> in which the temperature profile of a sample after 60 s of each type of heating has been applied.

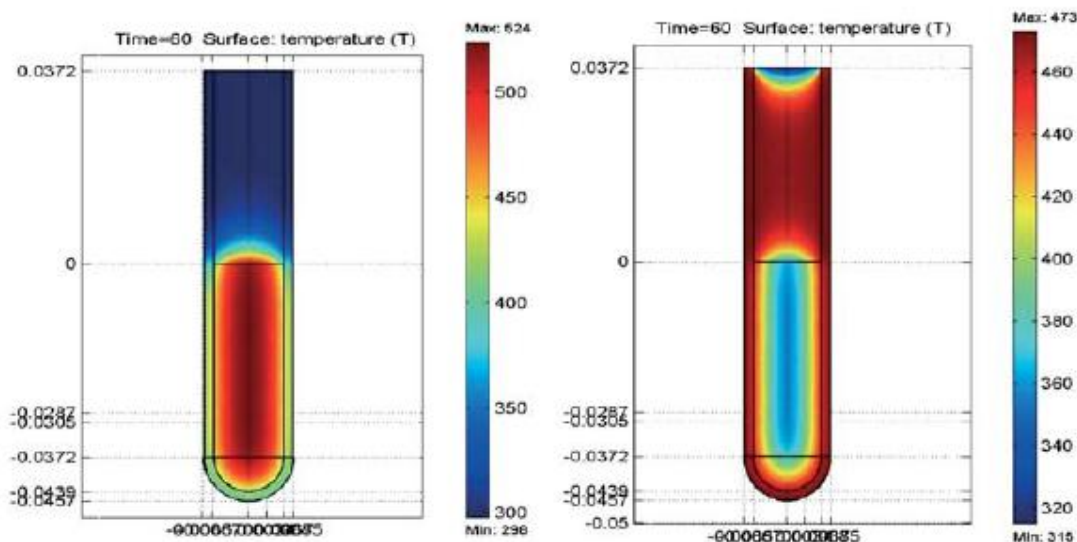


**Figure 3-6. Thermal imaging shows a distinct difference in temperature profiles after 1 min of microwave irradiation (left) versus oil bath (right).<sup>199,206</sup> Microwave heating raises the sample temperature homeogeneously while the oil bath heats the reaction vessel wall before the bulk.**

Reprinted "with kind permission from Springer Science+Business Media: Molecular Diversity, Microwave synthesis solutions from Personal Chemistry, 7, 2003, 294, Jon-Sverre Schanche, Figure 2," 2010.

Another, more controversial thermal effect is superheating,<sup>203,205,206</sup> which refers to raising the temperature of reaction above the normal boiling point of the solvent. Table 3-2 demonstrates some solvents have elevated boiling points with microwave exposure compared to normal conventional heating.<sup>203</sup> (In contrast, when the microwave experiments are performed in closed reaction vessels, the elevated boiling points are more likely derived from the increased pressure.<sup>206</sup>) The "superheating effect" has been explained by the slower nucleation in microwave heating.<sup>203,205,206</sup> Boiling nuclei are formed at the liquid surface with microwave heating rather than the imperfections of the reaction vessel in conventional heating.<sup>205</sup> Therefore, the overheating of polar solvents can be explained because of the inverted heat transfer since it

takes higher temperatures to form nucleation sites on the solvent's surface.<sup>205</sup> The superheating effect is minimized in well-stirred solutions or using low microwave power.<sup>203</sup>

<b>Table 3-2. Superheating can occur with microwave irradiation to elevate solvent's boiling points.</b>			
<b>Solvent</b>	<b>Conventional (°C)</b>	<b>Microwave (°C)</b>	<b>Difference (°C)</b>
Water	100	105	5
1-Butanol	117	138	21
2-Butanol	98	127	29
Methanol	65	84	19
1-Pentanol	136	157	21
1-Heptanol	176	208	32
Acetone	56	89	33
Ethyl acetate	77	102	25
Tetrahydrofuran	67	103	36
Acetonitrile	82	120	38

A third thermal effect is the "hot spot."<sup>205</sup> Hot spots are areas or zones within a sample with much greater temperatures than the bulk of the sample.<sup>205</sup> Theories explain that hot spots arise from an inhomogenous applied field or the selective heating of polar materials over apolar molecules.<sup>205</sup> For a mixture, the polar molecules get hotter than apolar molecules, leading to hot spots. For the inhomogenous applied field, the area with direct contact obtains a higher temperature than the areas not directly exposed to the microwave irradiation. These hot spots can obtain temperatures 100-200 K higher than the bulk of the sample with sizes estimated from 90 to 1000  $\mu\text{m}$ .<sup>205,207</sup> Current microwave equipment is designed to prevent hot spots by applying a more homogenous applied field.

The early microwave studies demonstrated rate accelerations and different product distributions compared to oil bath heating. Most scientists agree that these results can be clearly defined by kinetics and thermal effects mentioned above.<sup>208</sup> In other words, the same reaction conditions should be able to be reproduced by heating with an oil bath if the same temperature with fast homogenous heating could occur. However, some authors have published theories

about microwave enhancement to explain results atypical of purely thermal rate accelerations. The review by de la Hoz<sup>205</sup> summarizes the controversial theories of nonthermal effects.

3.5.2 Experimentally Observed Microwave Enhancement. Until recently, microwave enhancement has not been extensively explored for polymer applications. Schubert and coworkers demonstrate MW heating is an impressive tool for some polymerizations including step-growth condensations, ring opening polymerizations, or radical polymerizations.<sup>201</sup> This work inspired my efforts to use microwave irradiation to catalyze my Diels-Alder polymerizations. Microwave heating significantly enhances the DA reaction of fluorinated cyclopentadienones and alkynes.

Model studies were used to compare microwave and conventional heating for the reaction between the model compounds mentioned previously and phenylacetylene. My experiments demonstrate the reactions under the same conditions are moderately accelerated by microwave heating compared to conventional heating. In addition to rate enhancement, the reactions appear much cleaner visually, but there will be more to say about that below. Conventional heating is much slower because the heat was being conducted through the reaction vessel and into the reaction medium, with a buildup of heat on the vessel walls. Sometimes, the reactions in oil baths would produce an insoluble brown material on the sides of the Schlenk tubes. In contrast the microwave reactions give white products.

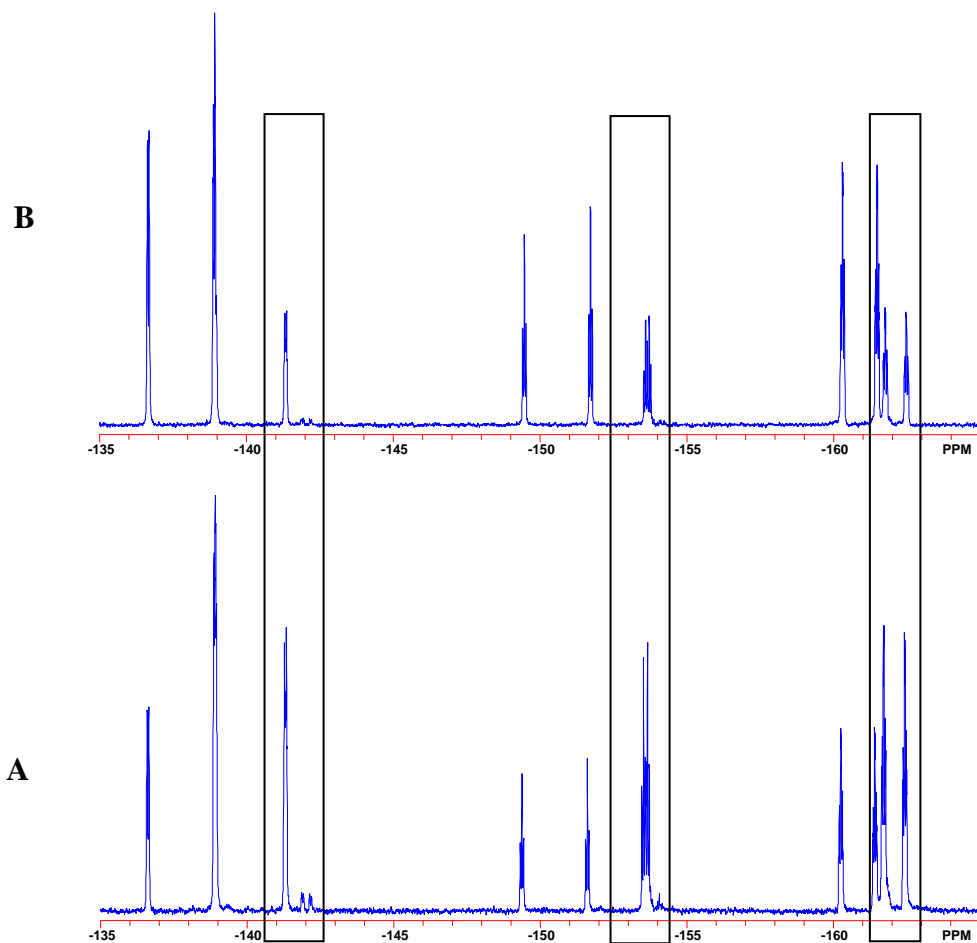


**Figure 3-7.  $^{19}\text{F}$  NMR shows the conversion of the product (outlined) in reaction conducted in the microwave (A) is much higher than the oil bath (B) under the exact same reaction conditions.**

Side by side reactions (controlled reactivity studies) confirm the conversion is much higher with microwave irradiation. A solution of CPD and PhCCH was divided into two portions. One was heated in a Schlenk tube in an oil bath at 80 °C and the other reaction was heated using a 12 mL reactor vessel in a Milestone Start<sup>TM</sup> microwave, also regulated at 80 °C using the infrared sensor in the instrument. Aliquots were removed simultaneously and analyzed by NMR. At the same concentrations and the reaction time, the conversion in the microwave is much higher than

reactions in an oil bath (Figure 3-7). The figure demonstrates the reaction conducted in the oil bath has much less product compared to the microwave.

There is a noticeable amount of a side-product in these spectra (see the small signals at  $-142$  ppm and  $-154$  ppm in Fig. 3-7), and the microwave seems to enhance the production of this byproduct. At first, I thought this minor product was an isomer of the product arising from incomplete steric control in the addition of phenylacetylene to the CPD (Figure 3-8).

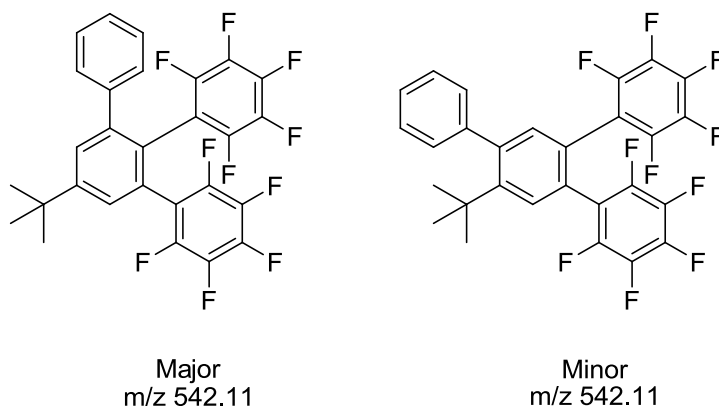


**Figure 3-8. The model reaction should produce these two compounds.**

However, a small amount of the “minor isomer” was isolated in an impure form (after exhaustive efforts to get it pure by flash chromatography or TLC) and submitted for mass spectrometry. The side product was not the “minor isomer” (m/z of 542.1), but rather the byproduct has a m/z of 610.2. This species has not yet been identified. A combination of studies tried to reproduce this side reaction including the CPD heated alone, the CPD in solvent with heat, the PhCCH heated alone, and the PhCCH in solvent with heat. These experiments show the side reaction only occurs in the presence of both CPD and alkyne. If the side reaction is competing with the DA reaction, the formation of this byproduct could cause problems with stoichiometric balance in the polymerization.

### 3.6 Crystallographic Analyses

Ketone **10** and arene **12** were analyzed crystallographically. The structure of ketone **10** is shown in Figure 3-9. As we have shown in other arylated cyclopentadiene systems, vicinal perfluoroaryl groups are forced into a propeller-type conformation by the steric effects of neighboring *ortho* fluorine atoms. Not surprisingly, the oxygen O1 has a larger steric effect than the vinylic hydrogen H4 (attached to C4, not shown in the figure), so the aryl ring vicinal to the oxygen atom adopts a less coplanar conformation with the five-membered ring. Normally in a cyclopentadiene there are two C—C bonds (to the  $sp^3$  carbon of the ring) that are somewhat longer, but in the ketone, this carbon (C1) is also  $sp^2$  hybridized, so the adjoining bonds are only slightly longer than the C3-C4 bond, which is shortened because the C—C bond order is slightly higher between the middle two carbons of a diene system due to resonance.

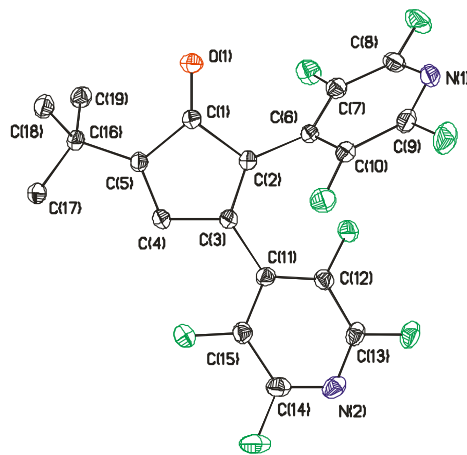


**Figure 3-9.** This figure shows a thermal ellipsoid plot (50% probability) of ketone **10**. Hydrogen atoms are omitted for clarity. Fluorine atoms are numbered the same as the carbon atoms to which they are attached. Selected bond distances (Å), bond angles (deg), and torsional angles (deg). C1=O1 1.205, C1-C2 1.520, C2=C3 1.344, C3-C4 1.505, C4=C5 1.342, C5-C1 1.516, C1-C2-C6-C7  $-54.1$ , C2-C3-C11-C12  $-40.2$ .

The structure of arene **12** is shown in Figure 3-10. This structure is interesting because it serves as a structural model for the conformations within the repeat unit of the targeted polyphenylenes. The presence of three vicinal aromatic rings on a central ring gives rise to torsional angles that are nearly perpendicular (ca. 75°). While twisting in the polymer should aid solubility, it is good that the angles are not rigidly 90°, otherwise there would be less torsional freedom in the repeat unit and possibly a longer critical entanglement molecular weight. Even the observation of a 75° dihedral angle makes us wonder if mutual movement of these aryl groups is conformational restricted.

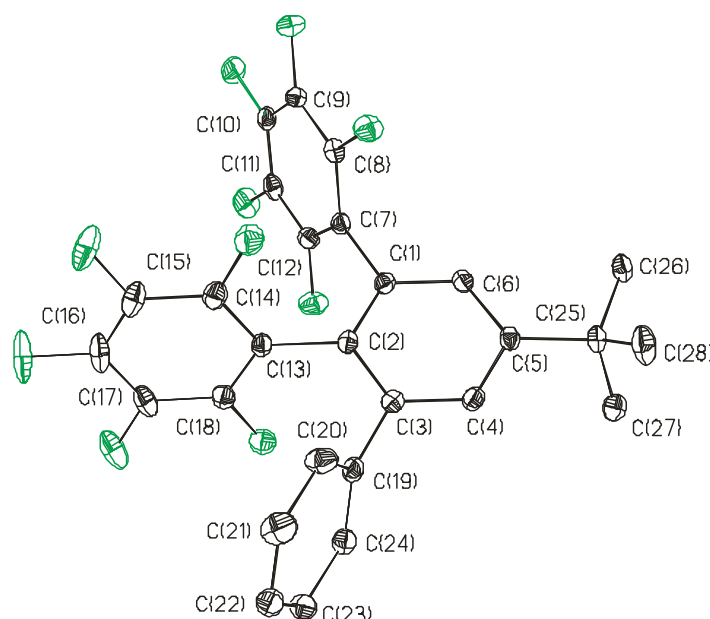


**Figure 3-10.** This figure shows a thermal ellipsoid plot (50% probability) of arene **12**. Hydrogen atoms are omitted for clarity. Fluorine atoms are numbered the same as the carbon atoms to which they are attached. Selected bond distances (Å), bond angles (deg), and torsional angles (deg). C1-C2 1.394, C2-C3 1.405, C3-C4 1.390, C4-C5 1.399, C5-C6 1.395, C6-C1 1.394, C2-C1-C7-C12 -74.2, C1-C2-C13-C14 -77.4, C2-C3-C19-C20 -76.7.

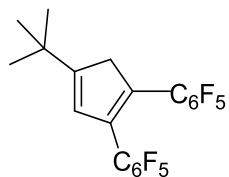
### 3.7 Conclusions

Reactions conditions of fluorinated cyclopentadienones and phenylacetylene were thoroughly studied and optimized. Catalysis by Lewis acids and hydrogen bonding has been explored. Studies indicate Lewis acids are inefficient as catalysts, but hydrogen bonding combined with more electron deficient substituents are highly effective. We also show the reaction rate is enhanced by more electron withdrawing substituents. Kinetic studies suggest the perfluoropyridine as a substituent make the diene more reactive compared to perfluorophenyl or perfluorotolyl side groups. Acidic conditions lead to decomposition of the terminal alkynes and the fluorinated cyclopentadienones have poor reactivity with internal or aliphatic alkynes.

The key message from these reactivity studies is that catalysis and substituent effects do not provide a “silver bullet” type of solution to the reactivity of our monomers, but we decided to move ahead with *m*-cresol as the solvent and continue with both C<sub>6</sub>F<sub>5</sub> and C<sub>5</sub>F<sub>4</sub>N-substituted CPD monomers. Finally, there is an unknown side reaction that appears to compete with the desired Diels-Alder reaction, possibly limiting the overall success of my project. The next chapter will focus on the polymerization efforts based on these model studies.

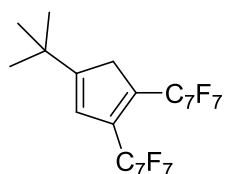
### 3.8 Experimental

**General Procedures.** Commercial sources of starting materials, purification of solvents, instrumentation and analytical services are described in the experimental section of Chapter 2.



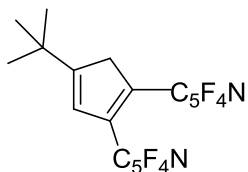
**3,4-Bis(pentafluorophenyl)-1-*tert*-butylcyclopentadiene.** Our own literature procedure<sup>160</sup> was adapted. Hexafluorobenzene (5.2 g, 0.028 mol) was added to a suspension of sodium hydride (1.0 g, 0.042 mol) and sodium *tert*-butylcyclopentadienide (1.0 g, 0.0069 mol) in THF (50 mL).

The reaction turned purple and stirred at reflux for 72 h. THF was removed by vacuum and the residue was taken up in hexanes. After a standard aqueous workup, the organic layer was extracted, dried over MgSO<sub>4</sub>, filtered and evaporated to afford pale yellow powder. Silica gel chromatography (20 cm x 40 mm, 300 mL of hexanes then 10% dichloromethane in hexanes) yields a fine white crystalline solid (2.7 g, 86%). <sup>1</sup>H NMR (400 MHz, CDCl<sub>3</sub>) δ (ppm): 6.28 (s, 1 H), 3.53 (s, 2H), 1.26 (s, 9H). <sup>19</sup>F NMR (376 MHz, CDCl<sub>3</sub>) δ (ppm): -140.38 to -140.62 (m, 2F), -141.07 to -141.15 (m, 2F), -154.67 (t, 1F), -155.36 (t, 1F), -161.93 to -162.24 (m, 4F).  
Notebook reference = JBP\_2\_5\_10 or JBP\_2\_79

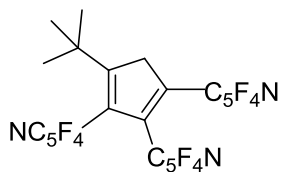


**3,4-Bis(perfluoro-4-tolyl)-1-tert-butylcyclopentadiene (9).** To a stirred, ice-cold mixture of potassium hydride (1.00 g, 0.025 mol), potassium *tert*-butylcyclopentadiene (3.2 g, 0.020 mol) and THF (50 mL) was added octafluorotoluene (5.9 g, 0.025 mol) in small portions over 15 min. The reaction turned dark orange and brown in color. The reaction stirred for 15 min at 0 °C and 1 h at room temperature. TLC showed *tert*-butylcyclopentadiene after 1 h. This reaction was intended to make the mono-arylated *tert*-butylcyclopentadiene, but the reaction immediately formed diarylated material instead. The reaction stirred or over 24 hours until TLC indicated an absence of starting material. The THF was evaporated from the black, viscous solution by cold trap. The residue was dissolved in hexane (50 mL) and water (50 mL) was added. Sodium bicarbonate was added for better phase separation. Some black solid was present and was removed by celite filtration. The organic layer was extracted, dried over MgSO<sub>4</sub>, filtered, and evaporated. The product was purified using silica gel chromatography (10 cm x 2.5 cm, hexanes). The hexane was evaporated to yield a pale yellow solid (4.2 g, 62%). <sup>1</sup>H NMR (400

MHz, CDCl<sub>3</sub>)  $\delta$  (ppm): 6.35 (s, 1H), 3.64 (s, 2H), 1.28 (s, 9H). <sup>19</sup>F NMR (376 MHz, CDCl<sub>3</sub>)  $\delta$  (ppm): -56.6 (m, 6F), -138.6 (m, 2F), -139.4 (m, 2F), -140.2 (m, 2F), -140.6 (m, 2F). Notebook reference = Jbp-27-15 or JBP\_bis\_cf3\_tbu\_cp



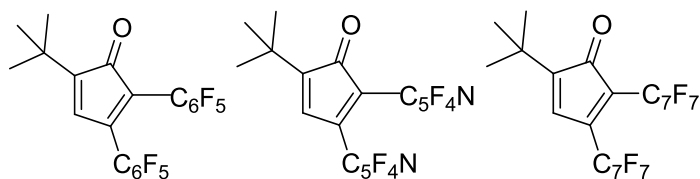
**3,4-bis(perfluoropyridyl)-1-tert-butyl cyclopentadiene (10).** Pentafluoropyridine (12 g, 0.071 mol) was added to a suspension of sodium hydride (2.5 g, 0.107 mol) and sodium *tert*-butyl cyclopentadiene (2.5 g, 0.0179 mol) in THF (100 mL) at -15 °C. The reaction warmed to room temperature and stirred for 18 hours. THF was removed by vacuum and the residue was taken up in hexanes. After a standard aqueous workup, the organic layer was extracted, dried over MgSO<sub>4</sub>, filtered and evaporated to afford a yellow solid. Silica gel chromatography (15 cm x 3.8 cm, hexanes) yields a fine white crystalline solid (3.7 g, 49%). <sup>1</sup>H NMR (400 MHz, CDCl<sub>3</sub>)  $\delta$  (ppm): 6.40 (s, 1 H), 3.71 (s, 2H), 1.30 (s, 9H). <sup>19</sup>F NMR (376 MHz, CDCl<sub>3</sub>)  $\delta$  (ppm): -90.05 (m, 2F), -90.47 (m, 2F), -141.74 (m, 2F), -142.59 (m, 2F). Notebook reference = JBP\_2\_101 or JBP\_2\_19\_9.



**2,3,4-tris(perfluoro-4-pyridyl)-1-tert-butylcyclopentadiene (8).**

Pentafluoropyridine (10.8 g, 0.064 mol) was added to a suspension of sodium hydride (1.5 g, 0.064 mol) and sodium *tert*-butyl cyclopentadiene (3.0 g, 0.021 mol) in THF (80 mL) at 25 °C. The reaction changed from pale brown to light green in color. The reaction was heated to reflux for 8 days. THF was removed by vacuum and the residue was taken up in hexanes. After a

standard aqueous workup, the organic layer was extracted, dried over MgSO<sub>4</sub>, filtered and evaporated to afford a yellow solid. Silica gel chromatography (10 cm x 2.5 cm, hexanes) yields a fine white crystalline solid (60%). <sup>1</sup>H NMR (400 MHz, CDCl<sub>3</sub>) δ (ppm): 4.00 (s, 2H), 1.23 (s, 9H). <sup>19</sup>F NMR (376 MHz, CDCl<sub>3</sub>) δ (ppm): -88.01 (m, 2F), -89.16 (m, 4F), -139.08 (m, 2F), -141.26 (m, 2F), -141.88 (m, 2F). Mass spectrometry APCI negative Calcd [M-H]<sup>-</sup> (found) 568.0689 (568.0718). Notebook reference = JBP\_4\_43.

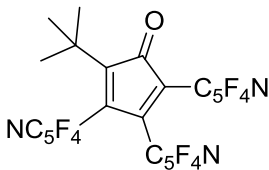


**C<sub>9</sub>H<sub>10</sub>Ar<sub>2</sub>O** (Ar = C<sub>6</sub>F<sub>5</sub>, C<sub>5</sub>F<sub>4</sub>N, or C<sub>7</sub>F<sub>7</sub>). The diene precursors **3**, **9**, and **10** are oxidized with the same copper catalyzed method shown previously for the difunctional CPD monomers (see Chapter 2).

**Ar = C<sub>6</sub>F<sub>5</sub>**. 91.3% yield. <sup>1</sup>H NMR (400 MHz, CDCl<sub>3</sub>) δ (ppm): 6.80 (s, 1 H), 1.27 (s, 9H). <sup>19</sup>F NMR (376 MHz, CDCl<sub>3</sub>) δ (ppm): -136.17 to -136.22 (m, 2F), -138.18 to -138.26 (m, 2F), -149.88 (t, 1F), -152.40(t, 1F), -160.03 (m, 2F), -161.44 (m, 2F). Anal. calcd (found) for C<sub>21</sub>H<sub>10</sub>F<sub>10</sub>O C, 53.86 (54.72); H, 2.15 (1.63). Notebook reference = JBP\_2\_7\_8 or JBP\_4\_86\_6 or JBP\_2\_177\_1 or JBP\_2\_11\_10\_a

**Ar = C<sub>5</sub>F<sub>4</sub>N**. 73% yield. <sup>1</sup>H NMR (400 MHz, CDCl<sub>3</sub>) δ (ppm): 6.92 (s, 1 H), 1.30 (s, 9H). <sup>19</sup>F NMR (376 MHz, CDCl<sub>3</sub>) δ (ppm): -87.83 (m, 2F), -89.38 (m, 2F), -138.04 (m, 2F), -139.64 (m, 2F). Anal. calcd (found) for C<sub>19</sub>H<sub>10</sub>F<sub>8</sub>N<sub>2</sub>O C, 52.55 (52.77); H, 2.32 (1.76); N 6.45 (6.22). Notebook reference = JBP\_2\_93 or JBP\_2\_101 or JBP\_2\_19\_9 or JBP\_2\_25\_15\_1.

**Ar = C<sub>7</sub>F<sub>7</sub>**. 73% yield. <sup>1</sup>H NMR (400 MHz, CDCl<sub>3</sub>) δ (ppm): 6.86 (s, 1H), 1.29 (s, 9H). <sup>19</sup>F NMR (376 MHz, CDCl<sub>3</sub>) δ (ppm): -56.78 (m, 6F), -135.01 (m, 2F), -136.80 (m, 2F), -138.94 (m, 2F), -140.01 (m, 2F). Notebook reference = JBP\_3\_67\_3

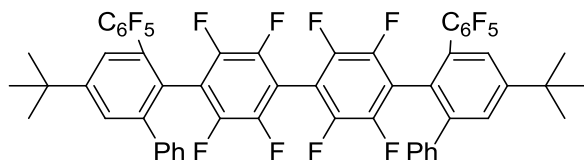


**2,3,4-trisperfluoropyridyl-1-tert-butyl cyclopentadienone (11).** 72% yield.  $^1\text{H}$  NMR (400 MHz,  $\text{CDCl}_3$ )  $\delta$  (ppm): 1.26 (s, 9H).  $^{19}\text{F}$  NMR (376 MHz,  $\text{CDCl}_3$ )  $\delta$  (ppm): -86.03 (m, 2F), -87.55 (m, 2F), -88.28 (m, 2F), -138.49 (m, 2F), -139.10 (m, 4F). Notebook reference = JBP\_4\_78\_6

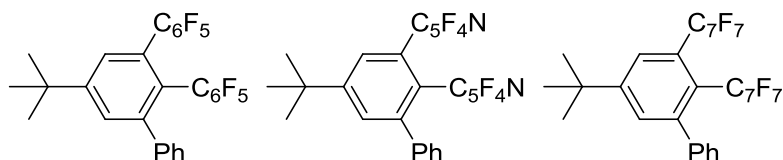
**Mini-scale Model Reaction Setup.** For smaller test reactions, the bis(cyclopentadienone) monomer (15 mg, 0.017 mmol) was weighed into an NMR tube sealed with a J-Young valve. Phenylacetylene (40 mg, 0.39 mmol) and solvent (about 10 drops) was added. The tube is sealed under a nitrogen purge and heated in an oil bath. Once the reaction changes from orange-red to yellow in color, the reaction was analyzed by adding some  $\text{C}_6\text{D}_6$  and collecting the NMR spectrum directly.

**Model Reaction Setup.** CPD- $\text{C}_6\text{F}_5$  (100 mg, 0.111 mmol), phenylacetylene (122  $\mu\text{L}$ , 1.113 mmol), and the solvent (4 mL) are added to a small beaker. The solution in the beaker is transferred to a Schlenk tube using a pipette and the beaker is rinsed with more solvent (1 mL). Then, the Schlenk tube is vacuum degassed (freeze—pump—thaw cycles) to remove oxygen, and then placed in an oil bath. The samples are analyzed periodically using aliquot analysis method A for the reactions in dichlorobenzene, toluene, xylene,  $\text{Mg}(\text{ClO}_4)_2$  in diglyme and xylene, as the solvent. Aliquot analysis method B was used for the reactions in trifluoroethanol and where as aliquot analysis method C was used for the test reactions in *m*-cresol, pentafluorophenol, and trifluoroethanol. The reaction is followed by  $^{19}\text{F}$  NMR. As the reaction occurs, the pair of *para*-fluorine signals found at -149.5 ppm and another pair of triplets at -152 ppm characteristic of the bis(cyclopentadienone) monomer begin to disappear as a new set of

triplets grow in at -153.7 ppm. The disappearance of starting material and intermediate peaks indicate the reaction is complete. The color is also indicative as to whether or not the reaction is complete. The cyclopentadienone chromophore is red-orange and the reaction turns to a pale yellow color corresponding to completion by NMR.



This NMR is shown in Figure 3-2. mp 135-265 °C.  $^1\text{H}$  NMR (400 MHz,  $\text{CDCl}_3$ )  $\delta$  (ppm): 7.64 (d, 1H), 7.62 (d, 2H), 7.60 (d, 1H), 7.49 (d, 1H), 7.45 (d, 1H), 7.43 (d, 1H), 7.40 (d, 1H), 7.14 (d, 10H), 1.43 (s, 18H), 1.42 (s, 18H).  $^{19}\text{F}$  NMR (367 MHz,  $\text{CDCl}_3$ )  $\delta$  (ppm): -137.7 to -138.9 (m), -140.3 (m), -140.7 (m, ), -153.7 (t, 1F), -153.8 (t, 1F), -154.0 (t, 1F), -154.1 (t, 1F), -161.9 (m), -162.4 (m, ). Notebook reference = JBP\_4\_101\_7 or JBP\_155\_12.



**$\text{C}_{16}\text{H}_{16}\text{Ar}_2$  (Ar =  $\text{C}_6\text{F}_5$ ,  $\text{C}_5\text{F}_4\text{N}$ , or  $\text{C}_7\text{F}_7$ ).** A Schlenk tube was charged with  $\text{C}_9\text{H}_{10}\text{Ar}_2\text{O}$  (Ar =  $\text{C}_6\text{F}_5$ ,  $\text{C}_5\text{F}_4\text{N}$ , or  $\text{C}_7\text{F}_7$ ) (100 mg, 0.21 mmol) and phenylacetylene (0.22 g, 2.1 mmol). Solvent (3 mL) was added to the Schlenk tube. After degassing (freeze-pump-thaw cycles), the solution was heated in an oil bath until the reaction was complete as determined by NMR aliquot Method A. Solvent and excess phenylacetylene were removed by rotary evaporation. Silica gel chromatography (10 cm x 25 mm, hexanes) afforded a white solid. In the case of Ar =  $\text{C}_5\text{F}_4\text{N}$ , the product precipitated from the reaction solution upon cooling and was isolated by filtration.

**Ar = C<sub>6</sub>F<sub>5</sub>** (94%) <sup>19</sup>F NMR (367 MHz, CDCl<sub>3</sub>) δ (ppm): -139.00 to -139.11 (m, 2F), -140.68 to -140.79 (m, 2F), -153.75 (t, 1F), -154.09 (t, 1F), -161.77 (m, 2F), -162.28 (m, 2F). MS (APCI positive, *m/z*) calcd [M-H]<sup>+</sup> (found) 542.1087 (542.1102). Notebook JBP\_2\_67\_14 or JBP\_4\_70.

**Ar = C<sub>5</sub>F<sub>4</sub>N** (98%) <sup>1</sup>H NMR (400 MHz, CDCl<sub>3</sub>) δ (ppm): This material is insoluble in CDCl<sub>3</sub> and DMSO. The spectra were recorded in a THF/C<sub>6</sub>D<sub>6</sub> mixture. <sup>19</sup>F NMR (367 MHz, THF and C<sub>6</sub>D<sub>6</sub>) δ (ppm): -92.1 (m, 2F), -92.4 (m, 2F), -141.7 (m, 2F), -143.8 (m, 2F). The identity of the compound was confirmed by X-ray diffraction analysis (see below). Notebook reference = JBP\_2\_75\_13 or JBP\_4\_110\_3.

**Ar = C<sub>7</sub>F<sub>7</sub>** (96%) <sup>19</sup>F NMR (367 MHz, CDCl<sub>3</sub>) δ (ppm): -56.7 (m, 6F), -137.4 (m, 2F), -138.9 (m, 2F), -140.1 (m, 2F), -140.8 (m, 2F). Notebook reference = JBP\_3\_69\_4 or JBP\_4\_109\_3.

**General Crystallographic Procedure.** Orange prisms of ketone **10** were obtained by cooling of a hexane solution to -10 °C. Colorless rods of arene **12** were obtained by cooling a hexane solution to -10 °C. Dr. Carla Sleboznick collected, solved, and refined the data for the remainder of the compounds, following the same procedures described in Chapter 2. Neither **10** nor **12** had special crystallographic issues that need further discussion. Data is archived in CIF format at Virginia Tech.

## Chapter 4. Highly Fluorinated DAPPs by Diels-Alder Polycondensation

### 4.1 Introduction

Since Nafion<sup>TM</sup> was first reported, fluorine-containing polymers have been extensively explored for high performance applications.<sup>209,210</sup> The unique interfacial properties and thermal stability of fluoropolymers make them ideal for high performance materials including microelectronic coatings and proton exchange membranes.<sup>110-112,211</sup> However, the high cost and limited versatility of fluorinated monomers associated with fluoropolymer synthesis (other than simple fluoroethylenes) limit the overall success of these materials.

Aromatic polymers could provide alternatives, but there is a trade-off between thermal stability and solubility / processability. Polyphenylenes have the necessary thermal stability, but solubility and processing are problematic. Aromatics with backbone heteroatoms such as poly(arylene ethers) or polysulfones are also viable, but the heteroatoms used to impart solubility can also weaken overall stability. Diels-Alder polyphenylenes provide a nice compromise with structural features that enable solubility without compromising other physical properties. DAPPs have recently been investigated for proton exchange membrane applications with a thermally stable aromatic backbone and a more versatile monomer synthesis, as described in Chapter 1.

This dissertation describes my efforts to combine the properties of fluoropolymers and DAPPs. Chapter 1 provided a general review of the published background. Chapter 2 described the design and synthesis of our “modular” or “second generation” fluorinated CPD monomer synthesis. Chapter 3 described a study of reactivity and our efforts to increase reactivity through structural modifications and catalysis. This chapter reports the synthesis of the polymers, which are glassy materials, soluble in common solvents, with impressive thermal properties.

## 4.2 Experimental

General procedures. Solvents for polymerization experiments were vacuum-distilled from calcium hydride. Dialkyne monomers were purified by sublimation just before each experiment. CPD monomer synthesis was reported in Chapter 2. Monomers **1** and **2** were purified by column chromatography and dried thoroughly just before polymerization. These compounds exist as inseparable mixtures of regioisomers as described in Chapter 2.



Characterization. Molecular weights were determined by GPC in THF on a Waters size exclusion chromatography (SEC) instrument at 40 °C with an inline multiple angle laser light scattering detector and calibration by polystyrene standards. Molecular weights were also confirmed by end group analysis (NMR).  $^{19}\text{F}$  and  $^1\text{H}$  NMR data was collected on a Varian Unity 400 spectrometer in  $\text{CDCl}_3$  using long relaxation delays (5 s) and signal averaging (240 transients) to obtain reliable integration data in proton spectra. Thermal analysis with TA Instruments Q-100 differential scanning calorimetry (DSC) determined thermal transition temperatures in a nitrogen atmosphere [10 °C/min]. Thermal stability was measured by a TA Instruments TGA Q500 with a temperature ramp of 10 °C/min up to 800 °C.

Polymer synthesis (conventional heating by oil bath). *m*-Cresol (4.0 mL) was added under a nitrogen counterstream to a Schlenk tube charged with dialkyne (0.15 mmol) combined with CPD monomer (0.15 mmol) under a purge of nitrogen gas. The reaction was vacuum degassed (two freeze-pump-thaw cycles), refilled with a nitrogen atmosphere, and heated in an oil bath regulated by a JKEM temperature controller.

Polymer synthesis (microwave heating). The microwave apparatus is a Milestone START™ Labstation. *m*-Cresol (4.0 mL) was added to a 12 mL Teflon reactor vessel charged with CPD monomer (0.15 mmol) and dialkyne (0.15 mmol). First, the microwave was heated to the reaction temperature with a ramp program (15 minutes to reach the desired temperature at a power of 800 W). The reaction was then maintained at temperature for the remainder of the reaction time with 500 W, using the instrument's infrared temperature sensor to control the application of microwave radiation.

There are two ways to monitor the reaction for conversion. One is to look for the CCH signal of the terminal alkyne end group in the <sup>1</sup>H NMR spectrum, but this method requires a complete workup (i.e., precipitation) to remove most of the cresol solvent. The problem with precipitation is that there may be some fractionation of the sample and then the spectrum is not representative of the reaction mixture. Instead we found, by comparing several NMR spectra with SEC data for samples with varying molecular weight, that there is a characteristic sharp signal within the spectrum of the CPD monomer that diminishes with increasing molecular weight (Figure 4-1). With <sup>19</sup>F NMR, one only needs to add some benzene-d<sub>6</sub> (0.3 mL) to an aliquot of reaction mixture (0.25 mL). High conversion is also accompanied by a color change. The CPD chromophore is red-orange and the reaction turns a pale yellow or ivory color upon completion. The polymer product was precipitated from methanol and dried in a vacuum oven at 90 °C to yield white, yellow, or brown solids, depending on the reaction conditions.

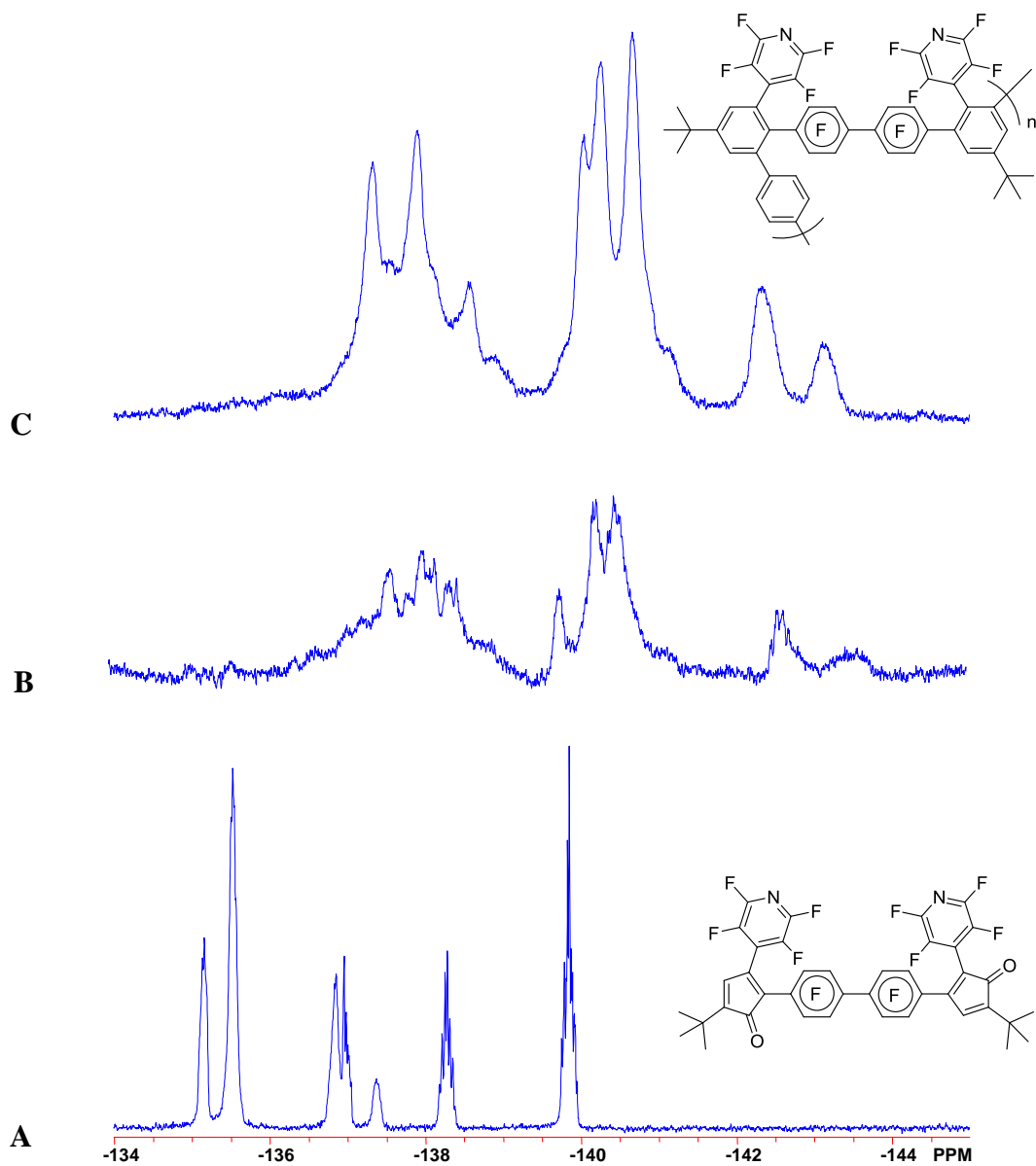
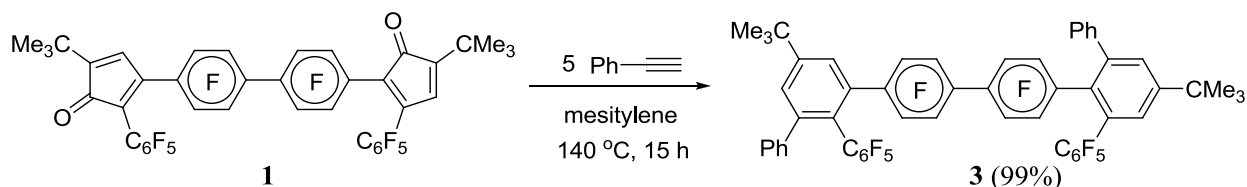


**Figure 4-1.** The polymerization reaction progress is monitored by  $^{19}\text{F}$  NMR. Fluorine signals representative of starting material from -135 ppm to -140 ppm (A) shift upfield to -137 to -144 as the polymerization occurs (B). Sharp peaks at -139.8 ppm in (B) disappears. Spectrum B represents a polymer with  $M_n = 8 \text{ kg/mol}$  and C represents a polymer with  $M_n = 15 \text{ kg/mol}$ . The mixture of isomers are depicted arbitrarily.

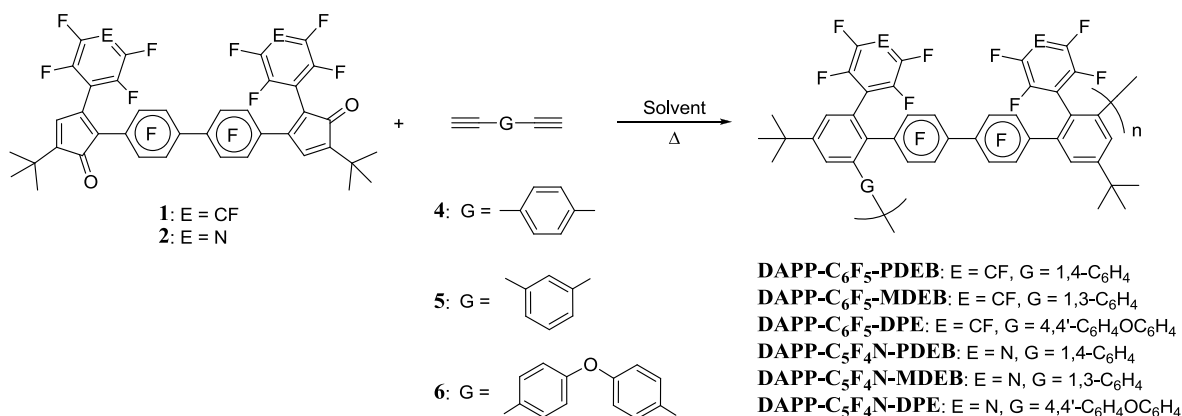
## 4.3 Results and Discussion

4.3.1 From Models to Polymers. As shown in Chapter 3 (Section 3.2), monomer **1** reacts with phenylacetylene to form two new benzene rings (Scheme 4-1 below). High conversion to the diarylated **3** (>98%) was easily obtained and the reaction was clean, despite the complication of having a mixture regioisomers. This model reaction is also useful in providing chemical shift data for subsequent NMR spectroscopic analysis of our polymers. Each new benzene ring must have two “new” aromatic NMR signals (see Figure 3-2), half of which are in a unique downfield region of the spectrum (ca. 7.62 ppm) where there are no interferences.



**Scheme 4-1.** CPDs react with monofunctional phenylacetylene for a simple model reaction.

Fluorinated Diels-Alder polyphenylenes (DAPPs) were synthesized with monomers **1** and **2** in stoichiometric combination with from *para*-diethynylbenzene (**4**), *meta*-diethynylbenzene (**5**), and bis(4-ethynylphenyl) ether (**6**) as shown in Scheme 4-2.



**Scheme 4-2.** Fluorinated DAPPs are synthesized from CPDO-C<sub>6</sub>F<sub>5</sub> and CPDO-C<sub>5</sub>F<sub>4</sub>N and a variety of dialkynes.

4.3.2 End Group Analysis. Much of the discussion in this dissertation centers around optimizing model and polymerization reactions to increase molecular weights in polymeric products. Even though we used  $^{19}\text{F}$  NMR to determine “complete” conversion qualitatively, quantitative end group analysis required the use of  $^1\text{H}$  NMR, where we had well-resolved, unambiguously assigned signals that we could integrate cleanly (Figure 4-2). The spectrum shows the “new” aromatic CH signals at ca. 7.5 ppm (c), in agreement with the model chemistry described in the previous section. The symmetrical *p*-phenylene units arising from the *p*-diethynylbenzene monomer are found at 7.1 ppm (d). Since the reaction occurs with 1:1 stoichiometry to obtain the highest molecular weight, there should be one CPDO end group (vinyl CH at 6.8 ppm (e)) for every alkyne end group (3.1 ppm (a) in Figure 4-2). The integration of CPDO to alkyne is typically 1:1, as expected since the reaction ratio is also 1:1. However, the integration of CPDO end groups is not as reliable because any remaining solvent, such as *m*-cresol, can interfere with integration. Ultimately it was most convenient to integrate the alkyne end group relative to the *tert*-butyl protons for the polymer chain (1.4 ppm (b) in Figure 4-2) to estimate the number-average molecular weight. The *tert*-butyl protons from the CPDO end groups (1.2 ppm (f)) are not perfectly resolved but do not contribute much error to that determination. The number-average molecular weights obtained from end group analysis are similar to the results determined by SEC. As described below, technical problems with SEC made end group analysis our primary method for estimating molecular weights.

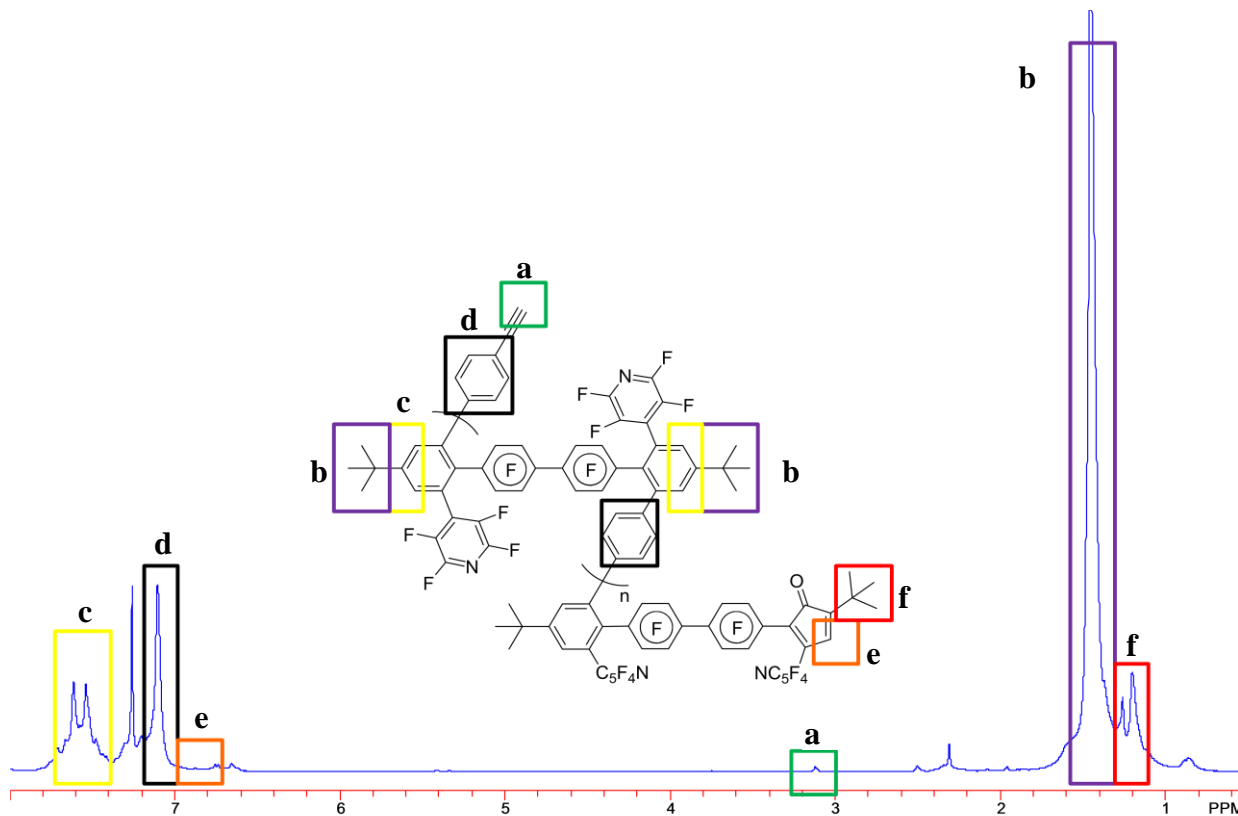


**Figure 4-2. Number-average molecular weight can be calculated by integration.**

4.3.3 Testing the Step-Growth Model. The Carothers equation for step-growth polycondensation is shown in eq 1.<sup>212</sup> This equation provides the degree of polymerization for a specific fractional monomer conversion to polymer.  $X_n$  is the number average degree of polymerization, also known as DP, and  $p$  corresponds to the extent or conversion in the polymerization (eq 2).  $N_o$  is the number of molecules present initially and  $N$  is the number of unreacted molecules, so  $p$  is the effective conversion (eq 2). Step-growth condensation requires a high monomer conversion to achieve high molecular weights or high degree of polymerization. If conversion is only 98%,  $p = 0.98$  and the highest attainable degree of polymerization is 50. Therefore, conversion should be higher than 99% to obtain polymers with  $X_n > 100$ .

$$X_n = \frac{1}{(1 - p)} \quad (1)$$

$$p = \frac{N_o - N}{N_o} \quad (2)$$

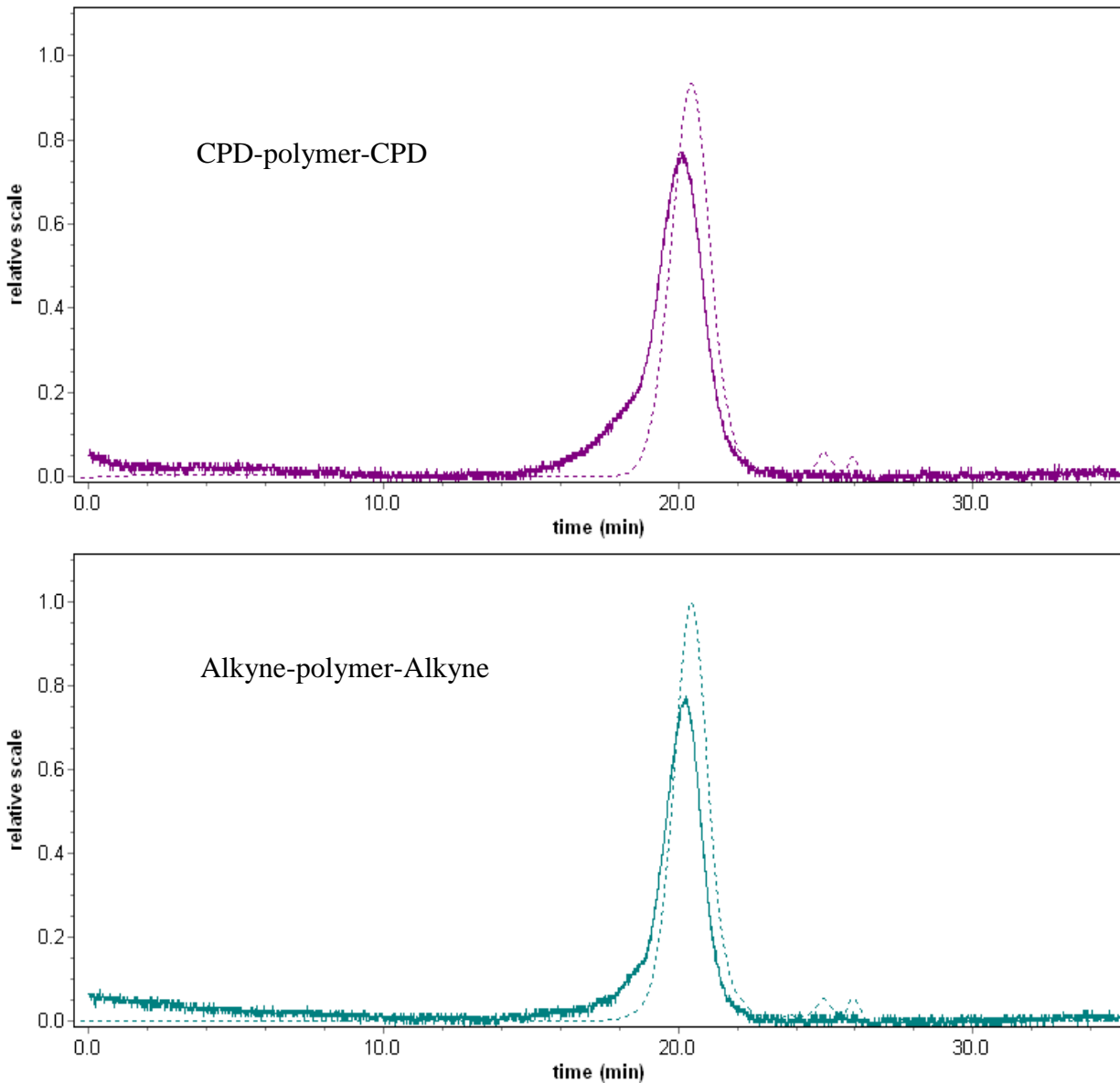
The Carothers equation can be manipulated to determine the degree of polymerization with an imbalance of stoichiometry, where  $r$  is the stoichiometric ratio of the reactants,  $N_a$  is the number of moles of AA monomer,  $N_b$  is the number of moles of the monomer, BB (eq 3). Here monomer BB is assumed to be in excess, so that  $r < 1$ . Excess reactant decreases the degree of polymerization (eq 4), even at complete conversion (as  $p$  tends toward 1, eq 5). For example, if BB is present in a 25% molar excess, the highest obtainable  $X_n$  is 9. Therefore, exactly one to one stoichiometry provides the highest molecular weight.

$$r = \frac{N_a}{N_b} \quad (3)$$

$$X_n = \frac{(1 + r)}{(1 + r - 2rp)} \quad (4)$$

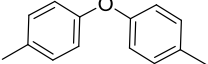
$$X_n = \frac{(1 + r)}{(1 - r)} \quad (5)$$

To ensure the reaction followed the laws of step-growth condensation, the monomers were reacted with an imbalanced stoichiometric ratio. Excess (25%) of monomer **2** was polymerized with *p*-diethynylbenzene at 145 °C by conventional heating. The theoretical degree of polymerization is 9 for  $p = 1$  and  $r = 0.8$ , while the experimentally determined value is 11 (the repeat unit weight is about 1000 and the measured  $M_n$  is 11 kg/mol). This result also shows that we can make oligomers with defined  $M_n$ . Figure 4-3 demonstrates the oligomers have similar molecular weights.



**Figure 4-3.** SEC shows oligomers with excess CPD end groups have the same molecular weight as oligomers with alkyne end groups. These polymers were synthesized by reacting 4:5 (top) and 5:4 (bottom) equivalence of CPD-C<sub>3</sub>F<sub>4</sub>N: PDEB at 140 °C respectively.

#### 4.3.4 Equivalent-Stoichiometric Polymerizations.

Table 4-1. A series of experiments show similar molecular weight data for several polymerizations.								
CPD Group	Dialkyne Linker	Temp (°C)	M <sub>n</sub> [SEC]	X <sub>n</sub> [SEC]	M <sub>n</sub> [NMR]	X <sub>n</sub> [NMR]	M <sub>w</sub> [SEC]	PDI [SEC]
X = C <sub>6</sub> F <sub>5</sub>		120	NA <sup>a</sup>	NA <sup>a</sup>	5000	5	NA <sup>a</sup>	NA <sup>a</sup>
X = C <sub>5</sub> F <sub>4</sub> N		120	17200	18	10500	11	25500	1.5
X = C <sub>5</sub> F <sub>4</sub> N		140	18300	20	14900	16	26200	1.4
X = C <sub>5</sub> F <sub>4</sub> N		150	18700	20	16500	17	27500	1.5
X = C <sub>5</sub> F <sub>4</sub> N		170	15600	17	NA <sup>b</sup>	NA <sup>b</sup>	29900	1.9
X = C <sub>5</sub> F <sub>4</sub> N		160	12000	12	NA <sup>b</sup>	NA <sup>b</sup>	20800	1.4

a: This sample was analyzed before we started to use SEC regularly.

b: End group analysis could not be used because we suspected decomposition of end groups.

Table 4-1 summarizes molecular weight data obtain for polymers prepared by conventional heating. The polymerizations typically afford 60-80% product after isolation by precipitation, purification by precipitation, and drying in a vacuum oven. While weight-average molecular weights in excess of 25 kg/mol seem like a promising result, one must remember that DAPPs have relatively rigid structures with high repeat-unit molecular weights and relatively few

degrees of freedom; each repeat unit weighs approximately 950 g/mol. Based on published work,<sup>137</sup> DAPPs generally need to have  $X_n$  values of at least 50 before the polymer will have useful properties, such as the ability to form a stable, solvent-cast film. Our attempts to cast films from THF and other solvents failed. Only brittle glasses were observed.

Some of the polymers we made could not be studied by end group analysis because decomposition had obviously occurred; the end groups were not detectable by NMR, even though the substances were soluble and responded well to SEC analysis. Careful examination of the size-exclusion chromatograms also suggests decomposition at high polymerization temperatures. The light-scattering (LS) detector shows a broadening on the left (low retention volume side) of the main peak. Because the time axis has a logarithmic relationship to molecular weight, and because the response of the LS detector also scales with molecular weight, this “shoulder” represents very high molecular weight species, possibly evidence of coupling or cross-linking side-reactions. The absence of the broadening in the refractive index (RI) detector, which is more sensitive to lower molecular weight species, indicates that the concentration of the high molecular weight material is very low (Fig. 4-4). However, if the reaction is subjected to excessively high temperatures (above 170 °C), the SEC begins to show a dramatic increase in the  $M_w/M_n$  ratio which supports the formation microgel, aggregated, or crosslinked polymers.

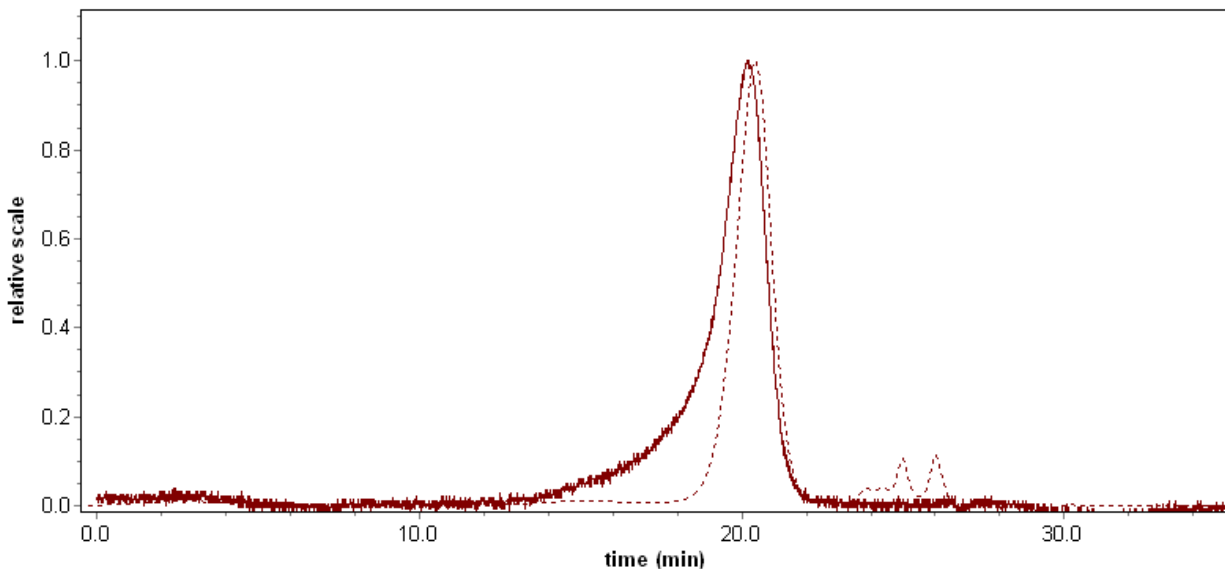


**Figure 4-4. A SEC trace indicates the presence of a low concentration of high molecular weight material.**

Side reactions are not entirely limited to high-temperature reactions. An increase in reaction time, past the disappearance of the sharp signal in the  $^{19}\text{F}$  spectrum, does not result in an increase the polymers' molecular weights, but the SEC LS trace continues to broaden. Closer examination of the NMR spectra also reveals byproduct formation with unexpected peaks between 3.5 to and 5.5 ppm. Two small signals near 5.4 ppm can even be seen in the spectrum shown in Figure 4-2. These and other signals in the 3.5-5.5 ppm range become more pronounced with higher reaction temperature. We have not been able to assign these signals, despite considerable effort to try various model reactions and many speculative discussions. Intentionally polymerized phenylacetylene reacted with CPD produces similar peaks in the 3.5-5.5 ppm region, but they are not an exact match.

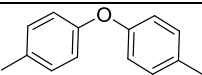
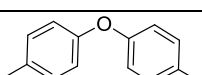
Figure 4-3 also shows some of the same byproduct for oligomer formation. There is obviously more broadening for the CPD-terminated oligomer compared to the alkyne-terminated oligomer. This might suggest the CPD could be responsible for the decomposition, but there is no other experimental evidence supporting this notion.

Under the more extreme conditions (above 160 °C) a brown residue forms on the side of the reaction flask. This precipitate is intractable in common organic solvents and was not analyzed further. Obviously, side reactions could interfere with the stoichiometric balance, so we wanted to understand them as well as we could. Several studies were designed to try to replicate the formation of the byproduct. However, they were all relatively unsuccessful. The CPD monomers are stable above 200 °C according to TGA and they withstand extended heating (in pure form, or in *m*-cresol solution) at 160 °C according to NMR spectroscopic analysis. Dialkynes are also stable to 160 °C, but one must ensure that no acid is present. Alkynes can couple oxidatively (Glaser coupling), but that reaction generally requires a transition metal catalyst. The side reaction only occurs with the presence of both the CPD and dialkyne monomers together, with or without solvent. The cause of byproduct formation remains unknown and is key to understanding how to produce high molecular weight polymers by this method.

The polymers are also unstable towards NMP or DMAc. Polymers react with NMP to form brown solutions with a gel-like consistency at room temperature in a matter of hours. Model reactions indicate a very slow reaction in DMAc (see Chapter 3) to also form solutions with gel-like consistency with heat applied (180 °C). The perfluoropyridyl side group is unstable with respect to DMAc and other nucleophiles. New peaks appear at ca. -161 ppm in the <sup>19</sup>F NMR indicating substitution has occurred.

*Microwave Heating.* The optimization experiments described in Chapter 3 encouraged us to try some new polymerization techniques. CPD monomers were reacted with dialkyne monomers in *m*-cresol with microwave heating. The reactions appeared to be cleaner based on visual inspection (no brown material, products colored either ivory or white after reprecipitation). Unfortunately, the microwave polymers could not be analyzed by SEC because the materials

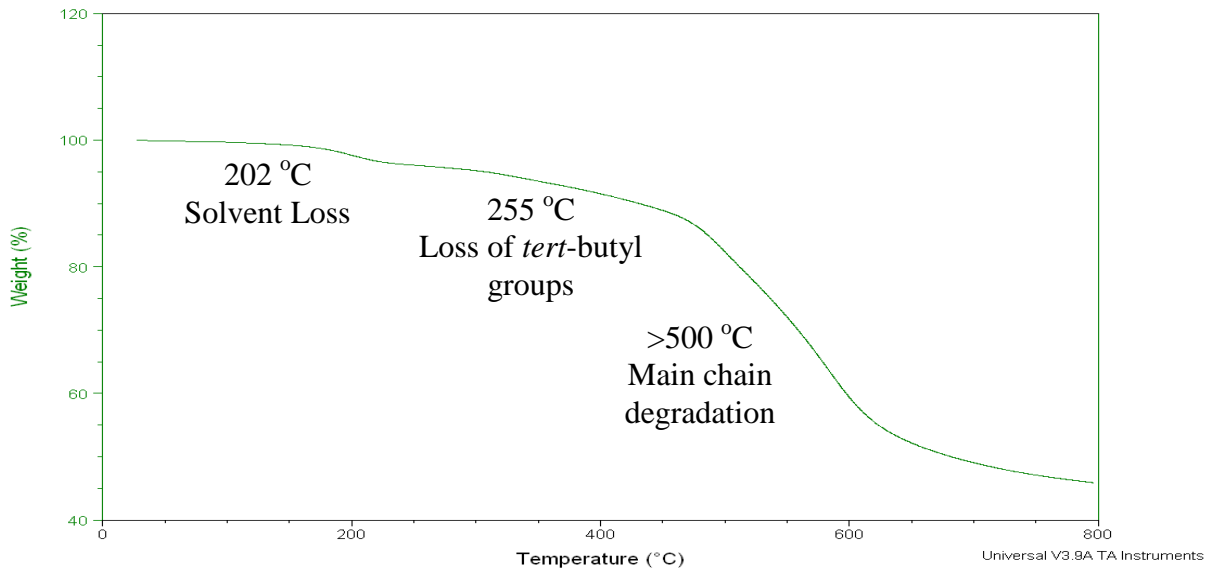
were “sticking to the columns.” Although the NMR spectra did not indicate any difference in overall structure between conventional heating and microwave heating, the new materials did behave differently. The polymers are still mostly soluble in common organic solvents including dichloromethane, chloroform, hexanes, acetone, etc. But higher yields were obtained (80% rather than 60%) and the polymer solutions form a thin residue on the sides of glass containers, possibly indicating emerging film-forming characteristics. The products obtained by microwave heating do not show the mysterious signals in the NMR spectrum, even up to reaction temperatures of 180 °C. Furthermore the reactions are visibly cleaner with the absence of the brown precipitate on the side of the reaction vessel with microwave heating. Thus we found ourselves in a predicament: Many subjective indicators suggested microwave heating was superior, but we were not able to obtain SEC data, and preliminary NMR end-group analyses did not suggest any increase in molecular weights as compared to polymers made by conventional heating. We could still at best make oligomers with  $X_n \sim 8$  to 20 (Table 4-2). As of this writing, our opinion is that this is the best we can hope for with this monomer system, using *m*-cresol as the solvent at pressures in the range of 1-5 atm.

Table 4-2. Microwave heating produces polymers with relatively low molecular weights compared to conventional heating.			
CPD Pendant Group	Dialkyne Linker	$\Delta$ (°C)	$M_n$ [NMR]
X= C <sub>5</sub> F <sub>4</sub> N		140	7500
X= C <sub>5</sub> F <sub>4</sub> N		180	20900
X= C <sub>5</sub> F <sub>4</sub> N		140	NA
X= C <sub>6</sub> F <sub>5</sub>		140	8300
X= C <sub>6</sub> F <sub>5</sub>		140	NA

NA = Decomposition occurred for the polymer samples. The materials formed a brown gel.

#### 4.4 Thermal characterization

4.4.1 Thermo-Gravimetric Analysis (TGA). Fluorinated DAPPs show good thermal stability up to approximately 220 °C. The trace shown in Figure 4-5 is typical of our results. Small amounts of solvent are lost from 185-205 °C. The weight loss beginning at 255 °C corresponds to the loss of *tert*-butyl groups (13-14%). Main chain degradation (35-40%) occurs above 500 °C in all samples. A black residue (35-40%) remains up to 800 °C.



**Figure 4-5. Thermal stability was measured under N<sub>2</sub> up to 800 °C.**

4.4.2 Differential Scanning Calorimetry (DSC). Glass transition temperatures are difficult to determine for rigid polymers, including polyphenylenes. The anticipated limited chain mobility for the rigid polymer prevents the determination of glass transition in most samples. Even if there is evidence of a slight endothermic transition, the slope is very small and the  $T_g$  may not be well pronounced. The scan shown in Figure 4-6a represents a sample with a low molecular weight ( $M_n = 7500$ ), where chain-end effects can become dominant. The second heating cycle suggests the glass transition temperature is approximately 90 °C. The same endothermic transition occurs in the cooling cycle at 87 °C (Figure 4-6b). But in several other samples having higher molecular weights, no  $T_g$  was observed calorimetrically.

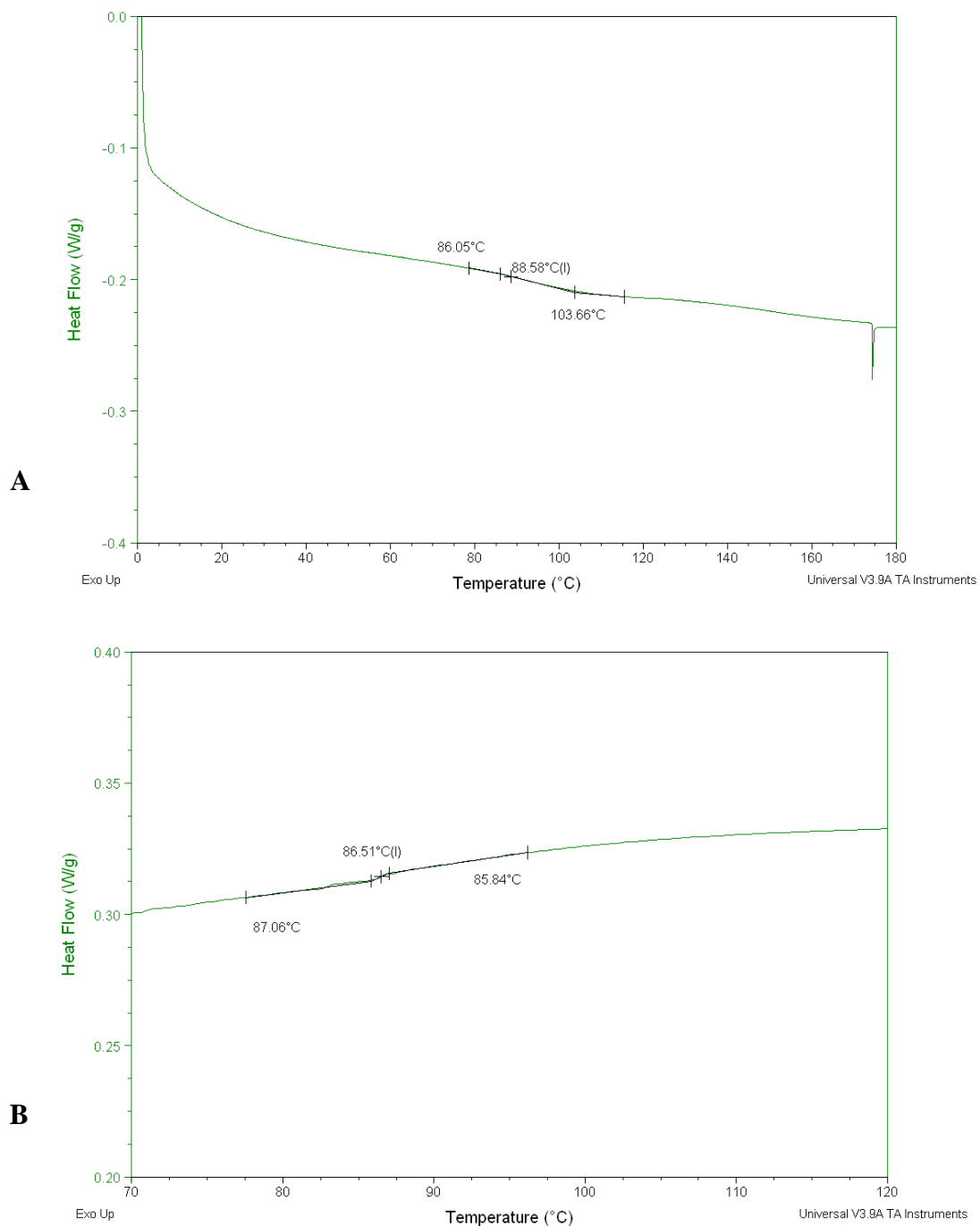


**Figure 4-6. DSC (10 °C/min up to 200 °C) might suggest the presence of a glass transition temperature with the second heating cycle (top, A) confirmed by the cooling cycle (bottom, B).**

When a glass transition temperature is difficult to determine, DMA can be useful for more easily characterizing the transition temperature. However, these fluorinated DAPPs do not form

functional films. Polymer solutions from THF, dichloroethane, dichloromethane, and several other solvents evaporate to form cracked, brittle films.

#### **4.5 Conclusions**

The synthesis and characterization of highly fluorinated DAPPs by Diels-Alder condensation was reported. Molecular weights can be controlled by stoichiometric imbalance up to approximately 9 repeat units. The highly fluorinated DAPPs exhibit weight average molecular weights up to 30 kg/mol and DP up to 25. These materials form cracked brittle films and are not suitable for membrane applications. Unfortunately, even with 1:1 stoichiometry, the molecular weights are limited to that molecular weight range because there is an unknown side reaction that occurs between the two monomers. SEC shows the formation of a low concentration of a high molecular material even under mild conditions. Higher temperatures and longer reaction times increase the concentration of this unknown material.

#### **Acknowledgements**

I would like to thank Mark Flynn and Dr. Rebecca Brown for GPC measurements and extend gratitude to Brian Hickory and Professor Gordon Yee for useful discussions. This work is possible thanks to the Virginia Tech Chemistry Department and The Petroleum Research Fund.

## Chapter 5. Conclusions and Future Work

### 5.1 Summary and Conclusions

The overall aims of my research were (1) to demonstrate a novel synthesis of highly fluorinated Diels-Alder polyphenylenes, and (2) to use that synthetic method to learn how fluorinated aromatic content affects polymer properties. I successfully developed a “modular” monomer synthesis and prepared several fluoroaromatic CPD monomers. Optimized conditions generally gave 50% yields of the desired CPD monomer over three steps. In the course of this work, I discovered interesting and unusual alkali counterion ( $\text{Li}^+$ ,  $\text{Na}^+$ , and  $\text{K}^+$ ) effects on nucleophilic aromatic substitution reactions. These studies enabled me to solve a synthetic problem with one of our monomers by switching from NaH to LiTMP as the base in a key step.

Subsequently, I used reacted my fluorinated CPD monomers with dialkynes to form soluble, wholly aromatic fluorinated polyphenylenes. The DA condensation formed polymers with  $M_n$  up to 30 kg/mol (DP = 25) and a two-step thermal stability profile. Use of a dialkyne monomer containing a flexible oxygen linkage does not afford flexible films at the low molecular weights that we were able to obtain. Chain entanglement does not occur at these molecular weights, and the polymers have poor film forming properties as a result. The current reaction conditions for these polymers will not afford higher molecular weights.

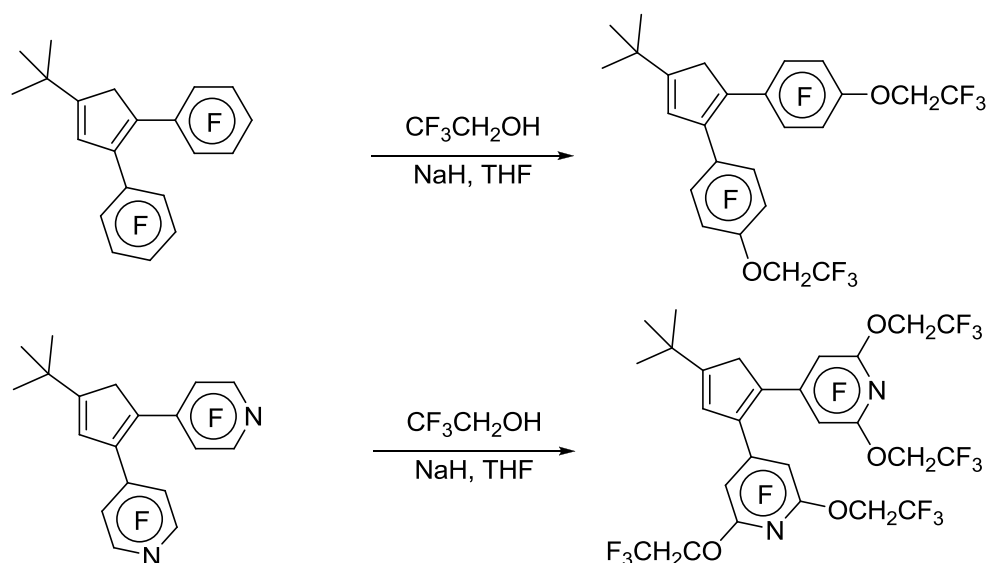
However, oligomers are readily obtained with either CPD end groups or alkyne end groups with reproducible molecular weights. A stoichiometric imbalance (4:5) yields oligomers with DP = 9 and  $M_n = 10$  kg/mol. The novel polymers contain very high *fluoroaromatic* content, especially compared to previously reported literature.

## 5.2 Recommendations for future work

5.2.1 Achieving Higher Molecular Weights. Membrane applications require higher molecular weight formation. We think these polymers will be useful for gas separation, water purification, or fuel cell applications, so we still hold out hope that we can double our molecular weights. Elucidation of the side reaction is the next logical step to obtaining polymers with high molecular weights. The side reaction ultimately limits the molecular weight by reducing the stoichiometric ratio. However, sometimes the logical step is not the best next step because it cannot realistically be achieved.

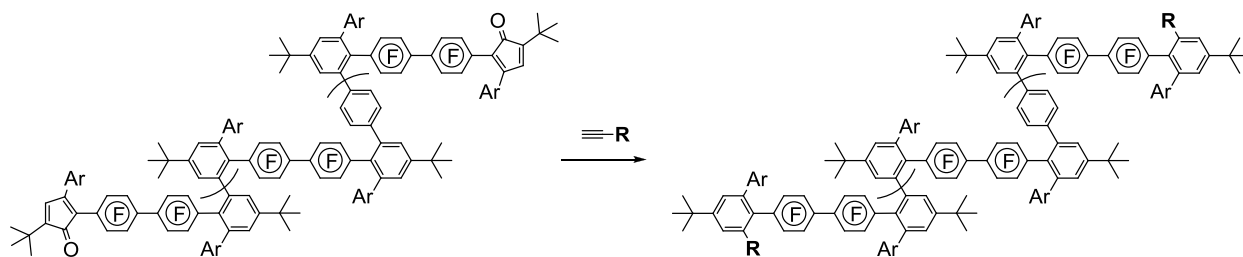
On the other hand, high molecular weight might be obtainable at very low temperatures (80 °C in trifluoroethanol with microwave heating) with the associated disadvantage of a very long reaction time. As a side note, DA reactions are also catalyzed by high pressure, but I did not investigate the effect of pressure on the polymerization because this lab is poorly suited for those experiments. We may be able to collaborate to attempt high pressure experiments.

5.2.2 Post-modification. These materials were made with functionality for post-modification in mind. I carried out preliminary model reactions (Scheme 5-1) to demonstrate that nucleophiles can easily substitute the *para* positions of the perfluorophenyl side group or the *ortho* positions of the perfluoropyridyl side groups selectively under mild conditions. Prof. Deck is working on exploring the scope of this reaction through a collaboration with Roanoke College.



**Scheme 5-1.** The pendant fluoroaromatic groups can be used as sites for postfunctionalization.

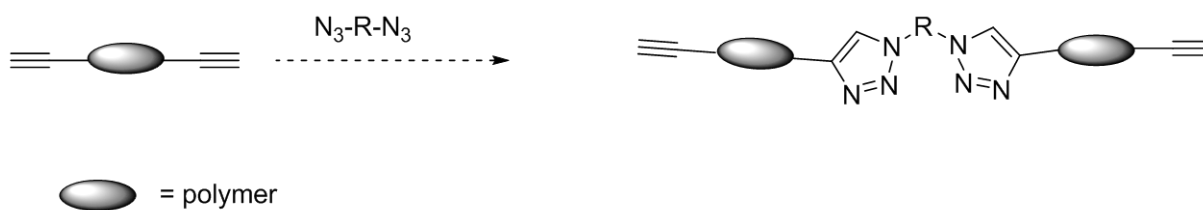
5.2.3 Telomer Approaches. Fluorinated DAPPs with  $X_n = 10$  can easily be synthesized with 25% excess of one monomer. I propose endcapping a CPD-terminated oligomer with an alkyne designed for copolymerization. For example, if the endcapping molecule has both an alkyne group and another functional unit (R), the material could be used to make a variety of new fluorinated polymers (Scheme 5-2). For example, if R was phenol, the polymer could be highly fluorinated material endcapped with a functional group. The disadvantage of this method is the fluorinated DAPPs are sensitive to nucleophiles like OH groups (see previous section!) but there is more chemistry than nucleophilic substitution to be explored. The CPD end groups could also react with



**Scheme 5-2.** A monofunctional alkyne could react as an endcapping agent.

Oligomers could also be crosslinked into more advanced materials with multifunctional alkyne monomers. Perhaps this material could be spin coated onto a surface and crosslinked similar to Dow SilK™ resins.<sup>143,213</sup> These rigid rod oligomers could be used to enhance thermal stability or high modulus reinforcing units for multiblock synthesis.

The alkyne-terminated oligomers could be especially useful. Lee<sup>105</sup> reported thermal curing of alkyne terminated polymers. This method was discussed in Section 1.2 in Chapter 1. Thermal curing of the alkyne end groups could produce a thermally stable, film-forming material. Click chemistry could also enhance the polymer properties. Bisalkyne-terminated oligomers could be reacted with diazide compounds to form longer polymer chains (Scheme 5-3).<sup>214</sup>



**Scheme 5-3. The alkyne terminated oligomer could be thermally cured or linked with other difunctional compounds (such as N<sub>3</sub>-R-N<sub>3</sub>).**

5.2.4 Triarylated Monomers. I have demonstrated that triarylated tert-butylcyclopentadienes (Figure 5-1) could be synthesized under forcing conditions. I carried out preliminary synthetic studies to show that an analogous difunctional CPD monomer could be made with the more reactive perfluoroarene and LiTMP. The material was made on an NMR scale and tested by mass spectrometry (APCI neg [M-H]<sup>-</sup> : calc. 1134.142 found. 1134.1469), but the product was not completely characterized.

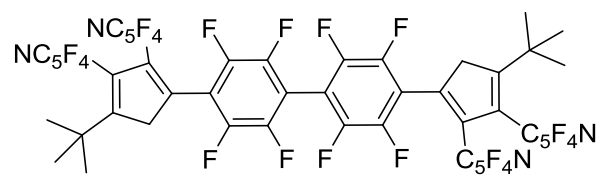


**Figure 5-1. The triarylated bisdiene monomer precursor was synthesized on a preliminary (NMR) scale.**

## References

- (1) Babudri, F.; Farinola, G.; Naso, F.; Ragni, R. *Chem. Commun.* **2007**, *10*, 1003-1022.
- (2) Gladysz, J. A.; Curran, D. A. *Tetrahedron* **2002**, *58*, 3823-3825.
- (3) Gladysz, J. A. *Angew. Chem.* **2005**, *44*, 5766-5768.
- (4) Lawrence, J.; Yamaguchi, T. *Journal of Membrane Science* **2008**, *325*, 633-640.
- (5) Kovacic, P.; Jones, M. *Chem. Rev.* **1987**, *87*, 357-379.
- (6) Kovacic, P.; Kyriakis, A. *J. Am. Chem. Soc.* **1963**, *85*, 454-458.
- (7) Hassan, J.; Sevignon, M.; Gozzi, C.; Schultz, E.; Lemaire, M. *Chem. Rev.* **2002**, *102*, 1359-1469.
- (8) Akagi, K. *Journal of Polymer Science: Part A: Polymer Chemistry* **2009**, *47*, 2463-2485.
- (9) Yang, S.-H.; Hsu, C.-S. *Journal of Polymer Science: Part A: Polymer Chemistry* **2009**, *47*, 2713-2733.
- (10) Heidenhain, S. B.; Sakamoto, Y.; Suzuki, T.; Miura, A.; Fujikawa, H.; Mori, T.; Tokito, S.; Taga, Y. *J. Am. Chem. Soc.* **2000**, *122*, 10240-10241.
- (11) Bilow, N.; Miller, L. J. *Journal of Macromolecular Science Part A* **1967**, *1*, 183-197.
- (12) Abe, M.; Tokita, M.; Watanabe, J.; Sakai, Y.; Yamamoto, T. *J. Appl. Polym. Sci.* **2009**, *111*, 2426-2435.
- (13) Kaeriyama, K. *Plast. Eng.* **1998**, *49*, 33-60.
- (14) Grimsdale, A. C.; Mullen, K. *Adv. Polym. Sci.* **2006**, *199*, 1-82.
- (15) Grigoras, M.; Mercore(Teodor), V.; Cianga, I.; Yagci, Y. *Macromolecular Symposia* **2008**, *263*, 38-46.
- (16) Morrison, R. T.; Boyd, R. N. *Organic Chemistry*; 4th ed.; Allyn and Bacon: Boston, 1983.
- (17) Aeiyaeh, S.; Soubiran, P.; Lacaze, P. C. *Synth. Met.* **1989**, *32*, 103-112.
- (18) Endres, F.; Borissenko, N.; El, A., S. *ACS Symp. Ser.* **2007**, *950*, 28-35.
- (19) Fanta, P. *Chem. Rev.* **1945**, *38*, 139-196.
- (20) Babudri, F.; Cardone, A.; Farinola, G.; Gianluca, M.; Naso, F. *Tetrahedron* **1998**, *54*, 14609-14616.
- (21) Silvestri, F.; Marrocchi, A. *International Journal of Molecular Science* **2010**, *11*, 1471-1508.
- (22) Ma, H.; Schollwock, U. *J. Phys. Chem. A* **2010**, *114*, 5439-5444.
- (23) Voskerician, G.; Weder, C. *Adv. Polym. Sci.* **2005**, *177*, 209-248.
- (24) Takahashi, A.; Rho, Y.; Higashihara, T.; Ahn, B.; Ree, M.; Ueda, M. *Macromolecules* **2010**, *43*, 4843-4852.
- (25) Ewbank, P. C.; Laird, D.; McCullough, R. D. *Organic Photovoltaics* **2008**, 3-55.
- (26) Inganas, O.; Zhang, F.; Andersson, M. R. *Acc. Chem. Res.* **2009**, *42*, 1731-1739.
- (27) James, D. K.; Tour, J. M. *Top. Curr. Chem.* **2005**, *257*, 33-62.
- (28) Liang, Y.; Wang, H.; Yuan, S.; Lee, Y.; Gan, L.; Yu, L. *J. Mater. Chem.* **2007**, *17*, 2183-2194.
- (29) Goodson, F. E.; Wallow, T. I.; Novak, B. M. *Macromolecules* **1998**, *31*, 2047-2056.
- (30) Schluter, A. *Journal of Polymer Science: Part A: Polymer Chemistry* **2001**, *39*, 1533-1556.
- (31) Kandre, R.; Schluter, A. *Macromol. Rapid Commun.* **2008**, *29*, 1661-1665.
- (32) Sahkulubey, E. L.; Durmaz, Y.; Demirel, A.; Yagei, Y. *Macromolecules* **2010**, *43*, 2732-2738.
- (33) Kandre, R.; Kutzner, F.; Schlaad, H.; Schluter, A. *Macromol. Chem. Phys.* **2005**, *206*, 1610-1618.

- (34) Sakamoto, J.; Rehahn, M.; Wegner, G.; Schluter, A. *Macromol. Rapid Commun.* **2009**, *30*, 653-687.
- (35) Toshimitsu, T. In *US Patent & Trademark Office*; Sughrue Mion, P., Ed.; Nitto Denko Corporation: 2006.
- (36) Crouch, D.; Skabara, P.; Lohr, J.; McDouall, J.; Heeney, M.; McCulloch, I.; Sparrowe, D.; Shkunov, M.; Coles, S.; Horton, P.; Hursthouse, M. *Chem. Mater.* **2005**, *17*, 6567-6578.
- (37) Wang, Y.; Watson, M. *J. Am. Chem. Soc.* **2006**, *128*, 2536-2537.
- (38) Yu, C.-Y.; Chen, C.-P.; Chan, S.-H.; Hwang, G.-W.; Ting, C. *Chem. Mater.* **2009**, *21*, 3262-3269.
- (39) Babudri, F.; Farinola, G.; Naso, F. *Synlett* **2009**, *17*, 2740-2748.
- (40) Helgesen, M.; Krebs, F. *Macromolecules* **2010**, *43*, 1253-1260.
- (41) Cardone, A.; Martinelli, C.; Pinto, V.; Babudri, F.; Losurdo, M.; Bruno, G.; Cosma, P.; Naso, F.; Farinola, G. *Journal of Polymer Science: Part A: Polymer Chemistry* **2010**, *48*, 285-291.
- (42) Farinola, G.; Cardone, A.; Babudri, F.; Martinelli, C.; Naso, F.; Bruno, G.; Losurdo, M. *Materials* **2010**, *3*, 3077-3091.
- (43) Nichele, T. Z.; Monteiro, A. L. *Tetrahedron Lett.* **2007**, *48*, 7472-7475.
- (44) John, J.; Tour, J. *J. Am. Chem. Soc.* **1994**, *116*, 5011-5012.
- (45) Marvel, C. S.; Hartzell, G. E. *J. Am. Chem. Soc.* **1959**, *81*, 448-452.
- (46) Carey, F.; Sundberg, R. *Advanced Organic Chemistry: Part A: Structure and Mechanisms*; 4th ed.; Kluwer Academic Publisher, 2000.
- (47) Anslyn, E.; Dougherty, D. *Modern Physical Organic Chemistry*; University Science Books, 2005.
- (48) Lowry, T.; Richardson, K. *Mechanism and Theory in Organic Chemistry*; Addison-Wesley, 1981.
- (49) Lozano, A.; Jimeno, M.; Abajo, J.; Campa, J. *Macromolecules* **1994**, *27*, 7164-7170.
- (50) Bloom, P.; Jones, C. I.; Sheares, V. *Macromolecules* **2005**, *38*, 2159-2166.
- (51) Kim, Y.; Chung, I.; Kim, S. *Macromolecules* **2003**, *36*, 3809-3811.
- (52) Williams, F. J.; Donahue, P. E. *J. Org. Chem.* **1977**, *42*, 3414.
- (53) Markezich, R. L.; Zamek, O. S. *J. Org. Chem.* **1977**, *42*, 3431.
- (54) Markezich, R. L.; Zamek, O. S.; Donahue, P. E.; Williams, F. J. *J. Org. Chem.* **1977**, *42*, 3435.
- (55) Takekoshi, T.; Wirth, J. G.; Heath, D. R.; Kochanowski, J. E.; Manello, J. S.; Webber, M. *J. J. Polym. Sci., Part A: Polym. Chem.* **1980**, *18*, 3069.
- (56) Edson, J.; Knauss, D. *J. Polym. Sci., Part A: Polym. Chem.* **2004**, *42*, 6353-6363.
- (57) Knauss, D.; Edson, J. *Polymer* **2006**, *47*, 3996-4003.
- (58) Chung, I.; Kim, S. *J. Am. Chem. Soc.* **2001**, *123*, 11071-11072.
- (59) Liu, B.; Robertson, G.; Guiver, M.; Sun, Y.; Liu, Y.; Lai, J.; Mikhailenko, S.; Kaliaguine, S. *J. Polym. Sci., Part B: Polym. Phys.* **2006**, *44*, 2299-2310.
- (60) Gauderon, R.; Plummer, C.; Hilborn, J. *Macromolecules* **1998**, *31*, 501-507.
- (61) Knauss, D.; Bender, J. *J. Polym. Sci., Part A: Polym. Chem.* **2002**, *40*, 3046-3054.
- (62) Hedrick, J.; Twieg, R.; Matray, T.; Carter, K. *Macromolecules* **1993**, *26*, 4833-4839.
- (63) Rusanov, A.; Keshtov, M.; Belomoina, N.; Likhatchev, D. *High Perform. Polym.* **2005**, *17*, 449-465.
- (64) Klein, D.; Korleski, J.; Harris, F. *J. Polym. Sci., Part A: Polym. Chem.* **2001**, *39*, 2037-2042.

- (65) Herbert, C.; Bass, R.; Watson, K.; Connell, J. *Macromolecules* **1996**, *29*, 7709-7716.
- (66) Brooke, G.; Matthews, R. *J. Chem. Soc., Perkin Trans. 1* **1979**, *2*, 372-375.
- (67) Chambers, R.; Hassan, M.; Hoskin, P.; Kenwright, A.; Richmond, P.; Sandford, G. *J. Fluorine Chem.* **2001**, *111*, 135-146.
- (68) Chambers, R.; Waterhouse, J.; Williams, D. *J. Chem. Soc., Perkin Trans. 2* **1976**, *5*, 585-588.
- (69) Chambers, R.; Musgrave, W.; Waterhouse, J.; Williams, D.; Burdon, J.; Hollyhead, W.; Tatlow, J. *J. Chem. Soc., Chem. Commun.* **1974**, *6*, 239-240.
- (70) Anslyn, E.; Dougherty, D. *Modern Physical Organic Chemistry*; University Science Books: Sausalito, CA, 2006.
- (71) Dubois, M.; Guerin, K.; Giraudet, J.; Pilichowski, J.; Thomas, P.; Delbe, K.; Mansot, J.; Hamwi, A. *Polymer* **2005**, *46*, 6736-6745.
- (72) Zhang, W.; Dubois, M.; Guerin, K.; Hamwi, A. *J. Fluorine Chem.* **2007**, *128*, 1402-1409.
- (73) Zhang, W.; Dubois, M.; Guerin, K.; Hamwi, A. *Polymer* **2007**, *48*, 3961-3973.
- (74) Kharitonov, A.; Kharitonova, L. *International Union of Pure and Applied Chemistry* **2009**, *81*, 451-471.
- (75) Brown, P.; Nicholas, J. In *Eur. Pat. Appl.*; Co., B. P., Ed. 1985; Vol. EP 144220.
- (76) Brown, P.; Nicholas, J. In *Eur. Pat. Appl.*; Co., B. P., Ed. 1985; Vol. EP 120056.
- (77) Fear, E.; Thrower, J. In *European Patent Organization*; London, T. P. O., Ed. Britain, 1968; Vol. GB1100261 (A).
- (78) Thrower, J.; White, M. *Polymer Preprints* **1966**, *7*, 1077-1083.
- (79) Takemura, H.; Nakashima, S.; Kon, N.; Inazu, T. *Tetrahedron Lett.* **2000**, *41*, 6105-6109.
- (80) Nova, A.; Reinhold, M.; Perutz, R. N.; Macgregor, S.; McGrady, J. *Organometallics* **2010**, *29*, 1824-1831.
- (81) Nova, A.; Erhardt, S.; Jasim, N.; Perutz, R. N.; Macgregor, S.; McGrady, J.; Whitwood, A. *J. Am. Chem. Soc.* **2008**, *130*, 15499-15511.
- (82) Clot, E.; Megret, C.; Eisenstein, O.; Perutz, R. N. *J. Am. Chem. Soc.* **2009**, *131*, 7817-7827.
- (83) Deck, P. A.; Lane, M. J.; Montgomery, J. L.; Slebodnick, C.; Fronczek, F. R. *Organometallics* **2000**, *19*, 1013-1024.
- (84) Woody, K.; Bullock, J.; Parkin, S.; Watson, M. *Macromolecules* **2007**, *40*, 4470-4473.
- (85) Deck, P. A.; Maiorana, C. R. *Macromolecules* **2001**, *34*, 9-13.
- (86) Prakash, G.; Yudin, A. *Chem. Rev.* **1997**, *97*, 757-786.
- (87) Omotowa, B.; Shreeve, J. *Organometallics* **2000**, *19*, 2664-2670.
- (88) Kim, J.; Kang, J.; Kim, J.; Lee, J. *J. Polym. Sci., Part A: Polym. Chem.* **2003**, *41*, 1497-1503.
- (89) Goodwin, A.; Mercer, F.; McKenzie, M. *Macromolecules* **1997**, *30*, 2767-2774.
- (90) Ding, J.; Liu, F.; Li, M.; Day, M.; Zhou, M. *J. Polym. Sci., Part A: Polym. Chem.* **2002**, *40*, 4205-4216.
- (91) Irvin, J.; Neef, C.; Kane, K.; Cassidy, P.; Tullos, G.; St. Clair, A. *J. Polym. Sci., Part A: Polym. Chem.* **1992**, *30*, 1675-1679.
- (92) Lee, H.; Hong, H.; Kim, Y.; Choi, S.; Hong, M.; Lee, H.; Kim, K. *Electrochim. Acta* **2004**, *49*, 2315-2323.
- (93) Banerjee, S.; Maier, G. *Chem. Mater.* **1999**, *11*, 2179-2184.
- (94) Maier, G. *Prog. Polym. Sci.* **2001**, *26*, 3-65.
- (95) Fitch, J.; Bucio, E.; Martinez, L.; Macossay, J.; Venumbaka, S.; Dean, N.; Stokley, D.; Cassidy, P. *Polymer Communication* **2003**, *44*, 6431-6434.

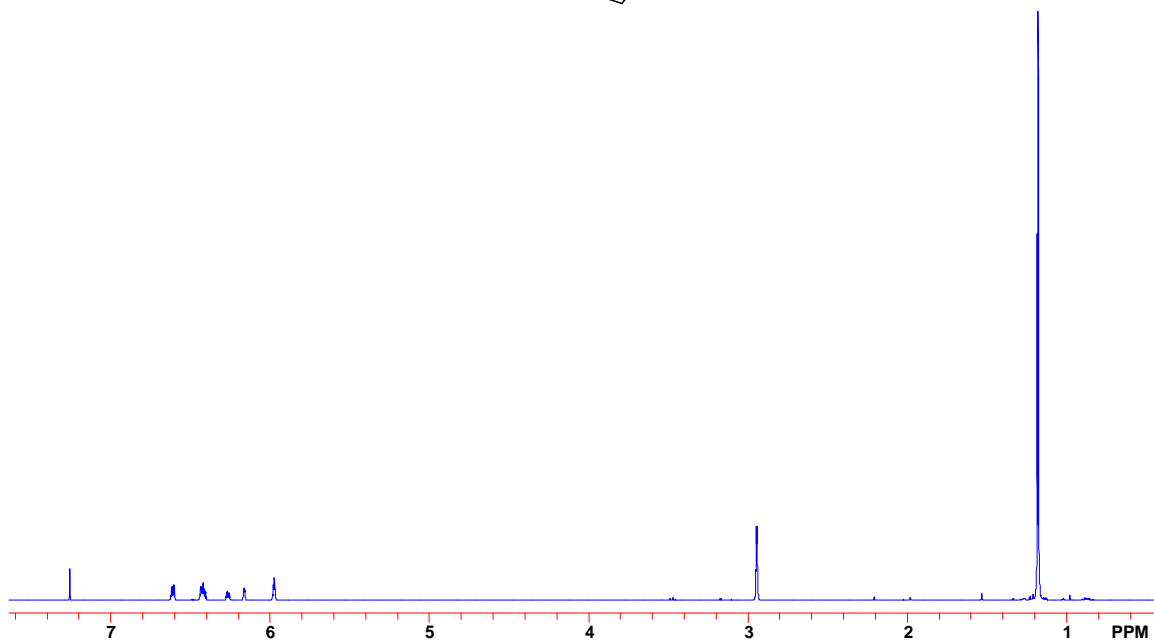
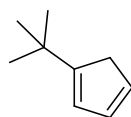
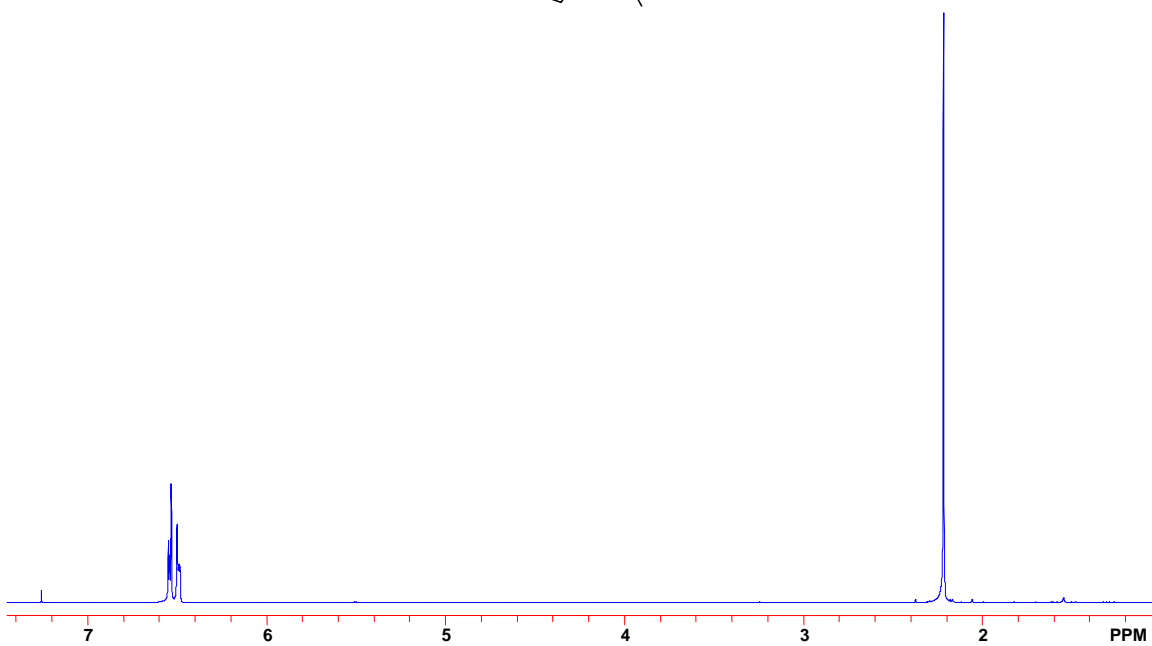
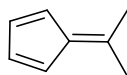
- (96) Reddy, V.; Cassidy, P.; Fitch, J. I.; Lunceford, B.; Person, D. *Polymer* **1996**, *37*, 4873-4875.
- (97) Cassidy, P.; Aminabhavi, T.; Farley, J. *JMS Rev Macromol Chem Phys* **1989**, *C29*, 365-429.
- (98) Lu, Z.; Cheng, L.; Li, J.; Zhang, K.; Yi, S.; Qin, J. *J. Polym. Sci., Part A: Polym. Chem.* **2004**, *42*, 925-932.
- (99) Xiao, S.; Wang, J.; Jin, K.; Jian, X.; Peng, Q. *Polymer* **2003**, *44*, 7369-7376.
- (100) Long, T.; Swager, T. *J. Am. Chem. Soc.* **2003**, *125*, 14113-14119.
- (101) Lu, J.; Miyatake, K.; Hlil, A.; Hay, A. *Macromolecules* **2001**, *34*, 5860-5867.
- (102) Hougham, G.; Tesoro, G.; Shaw, J. *Macromolecules* **1994**, *27*, 3642-3649.
- (103) Kim, D.; Robertson, G.; Guiver, M.; Lee, Y. *J. Membr. Sci.* **2006**, *281*, 111-120.
- (104) Ghassemi, H.; McGrath, J.; Zawodzinski, T., Jr. *Polymer* **2006**, *47*, 4132-4139.
- (105) Lee, H.; Lee, E.; Lee, M.; Oh, M.; Ahn, J.; Han, S.; Kim, H. *J. Polym. Sci., Part A: Polym. Chem.* **1998**, *36*, 2881-2887.
- (106) Bloom, P.; Sheares, V. *Macromolecules* **2005**, *34*, 1627-1633.
- (107) Bloom, P.; Sheares, V. *J. Polym. Sci., Part A: Polym. Chem.* **2001**, *39*, 3505-3512.
- (108) Ghassemi, H.; McGrath, J. *Polymer* **2004**, *5847*, 5847-5854.
- (109) Velasco, V.; Zolotukhin, M.; Guzman-Gutierrez, M.; Morales, S.; Fomine, S.; Carreon-Castro, M.; Salmon, M.; Scherf, U. *Macromolecules* **2008**, *41*, 8504-8512.
- (110) Ameduri, B. *Well-Architected Fluoropolymers*; Elsevier: Amsterdam, Netherlands, 2004.
- (111) Hougham, G.; Cassidy, P.; Johns, K., Davidson, T., Eds.; Kluwer/Plenum Publisher: New York, NY, 1999, p 408.
- (112) Scheirs, J. *Modern Fluoropolymers: High Performance Polymers for Diverse Applications*; Wiley: New York, NY, 1997.
- (113) Kameshima, H.; Nemoto, N.; Endo, T. *Journal of Polymer Science: Part A: Polymer Chemistry* **2001**, *39*, 3143-3150.
- (114) Pu, H.; Wang, L.; Pan, H.; Wan, D. *Journal of Polymer Science: Part A: Polymer Chemistry* **2010**, *48*, 2115-2122.
- (115) Kerres, J.; Xing, D.; Schonberger, F. *J. Polym. Sci., Part B: Polym. Phys.* **2006**, *44*, 2311-2325.
- (116) Zhu, Q.; Han, C. C. *Polymer* **2007**, *48*, 3624-3631.
- (117) Mitov, S.; Vogel, B.; Roduner, E.; Zhang, H.; Zhu, X.; Gogel, V.; Jorissen, L.; Hein, M.; Xing, D.; Schonberger, F.; Kerres, J. *Fuel Cells* **2006**, *6*, 413-424.
- (118) Mitov, S.; Delmer, O.; Kerres, J.; Roduner, E. *Helv. Chim. Acta* **2006**, *89*, 2354-2370.
- (119) Patel, P.; Hull, T. R.; McCabe, R. W.; Flath, D.; Grasmeder, J.; Percy, M. *Polym. Degrad. Stab.* **2010**, *95*, 709-718.
- (120) Iojoiu, C.; Marechal, M.; Chabert, F.; Sanchez, J. Y. *Fuel Cells* **2005**, *5*, 344-354.
- (121) Stille, J.; Plummer, L. *J. Org. Chem.* **1961**, *26*, 4026-4029.
- (122) Stille, J. K.; Plummer, L. *J. Org. Chem.* **1961**, *26*, 4026-4029.
- (123) Murphy, E.; Wudl, F. *Prog. Polym. Sci.* **2010**, *35*, 223-251.
- (124) Murphy, E.; Bolanos, E.; Schaffner-H, C.; Wudl, F.; Nutt, S.; Auad, M. *Macromolecules* **2008**, *41*, 5203-5209.
- (125) Reed, J. A.; Schilling, C. L.; Tarvin, R. F.; Rettig, T. A.; Stille, J. K. *J. Org. Chem.* **1969**, *34*.

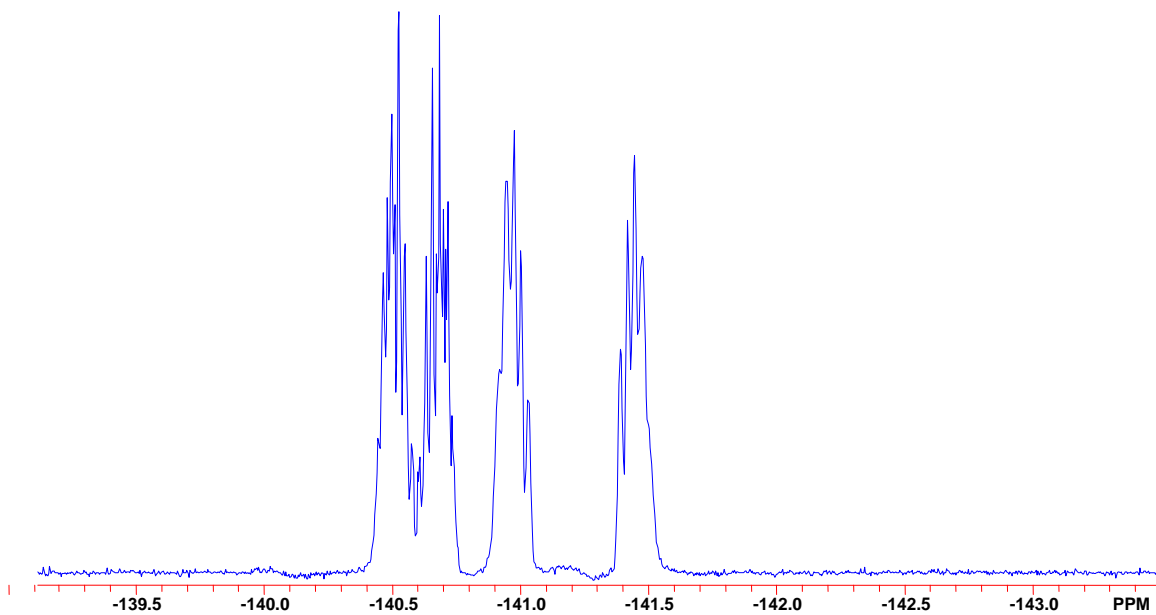
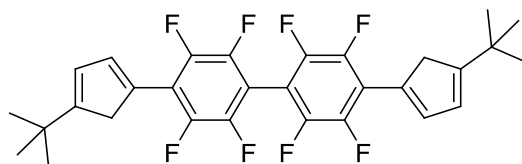
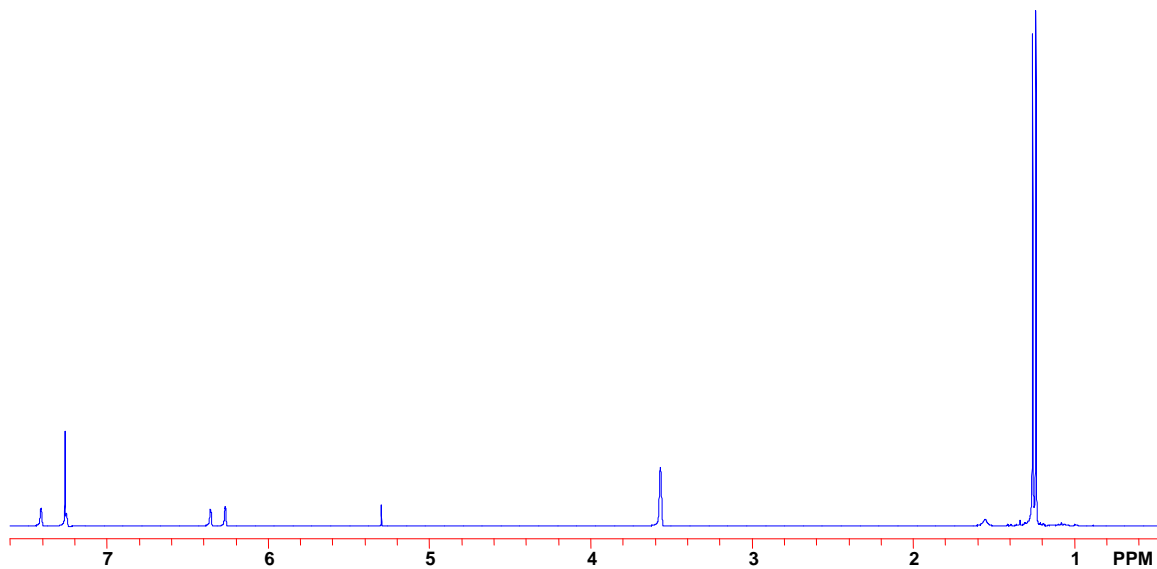
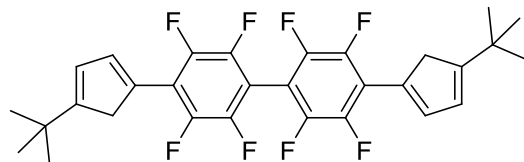
- (126) Stille, J. K.; Rakutis, R. O.; Mukamal, H.; Harris, F. W. *Macromolecules* **1968**, *1*, 431-436.
- (127) Braham, J. N.; Hodgins, T.; Katto, T.; Kohl, R. T.; Stille, J. K. *Macromolecules* **1978**, *11*, 343-346.
- (128) Schilling, C. L.; Reed, J., J.; Stille, J. K. *Macromolecules* **1969**, *2*, 85-88.
- (129) Braham, J.; Hodgins, T.; Katto, T.; Kohl, R.; Stille, J. *Macromolecules* **1978**, *11*, 343-346.
- (130) Stille, J. K.; Noren, G. K. *Macromolecules* **1972**, *5*, 49-55.
- (131) Hibbs, M. R.; Fujimoto, C.; Cornelius, C. *Macromolecules* **2009**, *42*, 8316-8321.
- (132) Stille, J. K.; Noren, G. K. *Macromolecules* **1972**, *5*, 49-55.
- (133) VanKerckhove, H. F.; Gilliams, Y. K.; Stille, J. K. *Macromolecules* **1972**, 541-546.
- (134) Harris, F. W.; Stille, J. K. *Macromolecules* **1968**, *1*, 463-464.
- (135) Rusanov, A. L.; Likhachev, D.; Kozlova, O. V.; Harris, F. W. *Prog. Polym. Sci.* **2006**, *31*, 749-810.
- (136) Kraiman, E. In *USPO*; Pont, D., Ed. USA, 1959; Vol. 2890206.
- (137) Kumar, U.; Neenan, T. *Macromolecules* **1995**, *28*, 124-130.
- (138) Wiesler, U.; Mullen, K. *Chem. Commun.* **1999**, *22*, 2293-2294.
- (139) Zhi, L.; Wu, J.; Li, J.; Stepputat, M.; Kolb, U.; Mullen, K. *Adv. Mater.* **2005**, *17*, 1492-1496.
- (140) Schmaltz, B.; Weil, T.; Mullen, K. *Adv. Mater.* **2009**, *21*, 1067-1078.
- (141) Morgenroth, F.; Kubel, C.; Muller, M.; Wisler, U.; Berresheim, A.; Wagner, M.; Mullen, K. *Carbon* **1998**, *36*, 833-837.
- (142) Godschalx, J. P.; Romer, D. R.; So, Y. H.; Lysenko, Z.; Mills, M. E.; Buske, G. R.; Townsend, I. P.; Smith, J., D.; Martin, S.; DeVries, R.; Organization, U. S. P., Ed.; The Dow Chemical Company: United States, 1999; Vol. 5965679.
- (143) Martin, S.; Godschalx, J. P.; Mills, M. E.; Shaffer, I., E.; Townsend, I., P. *Adv. Mater.* **2000**, *12*, 1769-1778.
- (144) Fujimoto, C.; Hickner, M.; Cornelius, C.; Loy, D. *Macromolecules* **2005**, *38*, 5010-5016.
- (145) Cornelius, C. In *USPTO Patent Full-Text and Image Database*; Corporation, S., Ed. United States, 2003.
- (146) James, J., C.; Cornelius, C.; Marand, E. *Polymer* **2009**, *50*, 3220-3224.
- (147) Bernardo, P.; Drioli, E.; Golemme, G. *Industrial & Engineering Chemistry Research* **2009**, *48*, 4638-4663.
- (148) Fujimoto, C.; Loy, D.; Wheeler, D.; Jamison, G.; Cornelius, C. *Polymer Preprints* **2002**, *43*, 1376.
- (149) Loy, D.; Fujimoto, C.; Wheeler, D.; Jamison, G.; Cornelius, C. *Abstracts of Papers, 224th ACS National Meeting, Boston, MA, United States, August 18-22 2002*.
- (150) Ogliaruso, M. A.; Romanelli, M. G.; Becker, E. I. *Chem. Rev.* **1965**, *65*, 261-367.
- (151) Dua, S. S.; Jukes, A. E.; Gilman, H. *J. Organomet. Chem.* **1968**, *12*, 24-26.
- (152) Nesmeyanov, A. N.; Zol'nikova, G. P.; Babakhina, G. M.; Kritskaya, I. I.; Yakobson, G. G. *Zhurnal Obshchei Khimiii* **1973**, *43*, 2007-2012.
- (153) Deck, P. A. *Coord. Chem. Rev.* **2006**, *250*, 1032-1055.
- (154) Deck, P. A.; McCauley, B. D.; Slebodnick, C. *J. Organomet. Chem.* **2006**, *691*, 1973-1983.
- (155) Warren, A. D.; Tetterton, K. F.; Slebodnick, C.; Deck, P. A. *manuscript in preparation*.
- (156) Dilthey, W.; Schommer, W. J. *Journal fuer Praktische Chemie (Leipzig)* **1933**, *136*, 293-298.

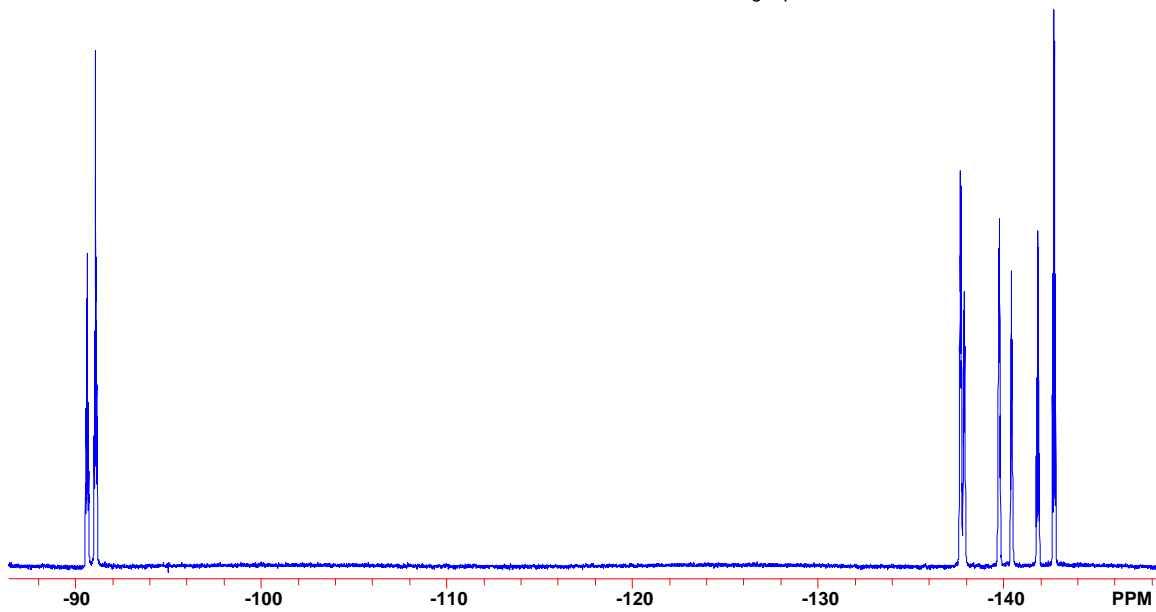
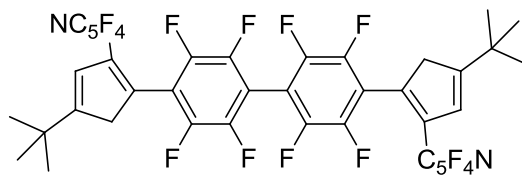
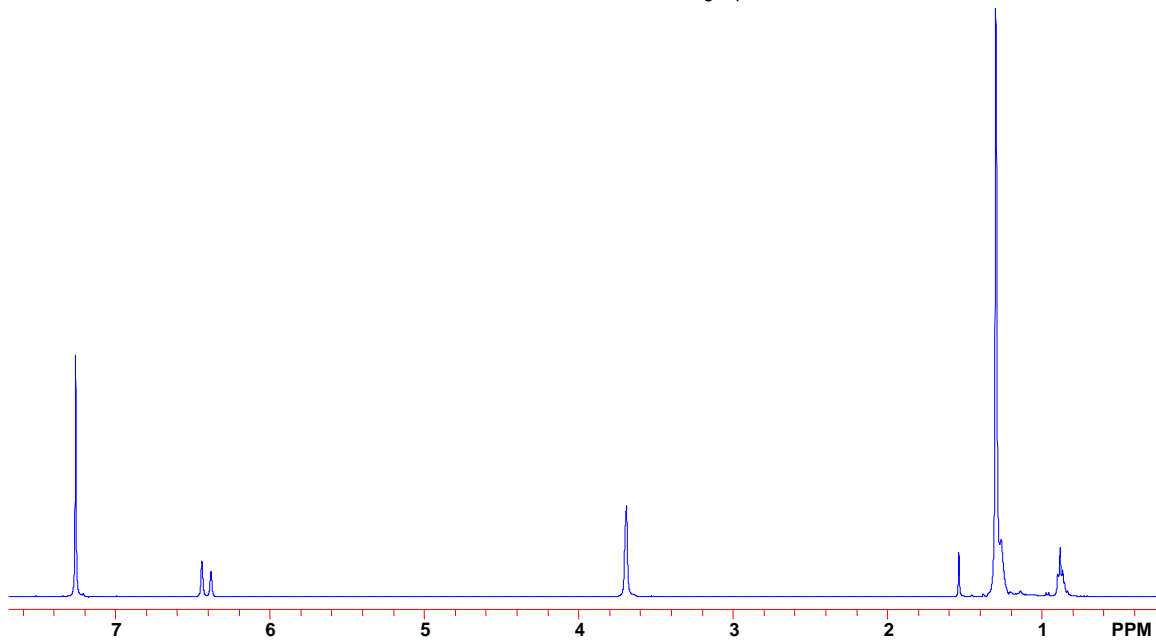
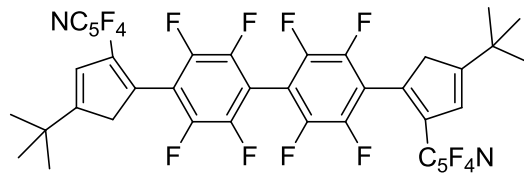
- (157) Sen, S., Virginia Polytechnic Institute and State University, 2008.
- (158) Deck, P.; Hickory, B. *Abstracts of Papers, 230th ACS National Meeting, Washington, DC, United States*. **2005**.
- (159) Vladimirskaya, N. B.; Koshutin, V. I.; Smirnov, V. A. *Zh. Org. Khim.* **1975**, *11*, 212.
- (160) Deck, P. A.; Kroll, C. E.; Hollis, W. G.; Fronczek, F. R. *J. Organomet. Chem.* **2001**, *637-639*, 107-115.
- (161) Pangborn, A. B.; Giardello, M. A.; Grubbs, R. H.; Rosen, R. K.; Timmers, F. J. *Organometallics* **1996**, *15*, 1518-1520.
- (162) Freiesleben, W. *Angew. Chem.* **1963**, *75*, 576.
- (163) Craig, D.; Shipman, J.; Kiehl, J.; Widmer, F.; Fowler, R.; Hawthorne, A. *J. Am. Chem. Soc.* **1954**, *76*, 4573-5.
- (164) Moore, W. R.; King, B. J. *J. Org. Chem.* **1971**, *36*, 1882-1886.
- (165) Lappert, M. F.; Slade, M. J.; Singh, A.; Atwood, J. L.; Rogers, R. D.; Shakir, R. *J. Am. Chem. Soc.* **1983**, *105*, 302-304.
- (166) Gehrhus, B.; Hitchcock, P. H.; Kennedy, A. R.; Lappert, M. F.; Mulvey, R. E.; Rodger, P. J. A. *J. Organomet. Chem.* **1999**, *587*, 88-92.
- (167) Vladimirskaya, N. B.; Koshutin, V. I.; Smirnov, V. A. *Russ. J. Org. Chem.* **1975**, *11*, 212.
- (168) Sheldrick, G. *Acta Crystallogr., Sect. A: Found. Crystallogr.* **2008**, *A64*, 112-122.
- (169) Kiselev, V. D.; Konovalov, A. *J. Phys. Org. Chem.* **2009**, *22*, 466-483.
- (170) Domingo, L. R.; Arno, M.; Andres, J. *J. Org. Chem.* **1999**, *64*, 5867-5875.
- (171) Walborsky, H. M.; Barash, L.; Davis, T. C. *Tetrahedron* **1963**, *19*, 2333-2351.
- (172) Crisp, G.; Gebauer, M. *J. Org. Chem.* **1996**, *61*, 8425-8431.
- (173) Grieco, P.; Beck, J. *Tetrahedron Lett.* **1993**, *34*, 7367-7370.
- (174) Grieco, P.; Collins, J.; Handy, S. *Synlett* **1995**, *11*, 1155-1157.
- (175) Grieco, P.; Nunes, J.; Gaul, M. *J. Am. Chem. Soc.* **1990**, *112*, 4595-4596.
- (176) Kacan, M.; Karabulut, H. *Turkish Journal of Chemistry* **2002**, *26*, 251-254.
- (177) Messer, R.; Fuhrer, C.; Haener, R. *Nucleosides, Nucleotides & Nucleic Acids* **2007**, *26*, 701-704.
- (178) Reetz, M.; Gansaeuer, A. *Tetrahedron* **1993**, *49*, 6025-6030.
- (179) Huang, Y.; Rawal, V. H. *J. Am. Chem. Soc.* **2002**, *124*, 9662-9663.
- (180) Huang, Y.; Unni, A. K.; Thadani, A. N.; Rawal, V. H. *Nature* **2003**, *234*, 146.
- (181) Rawal, V. H.; Thadani, A. N. *Enantioselective cycloaddition reactions catalyzed by hydrogen bonding*; 2nd ed.; Wiley-VCH: Weinheim Germany, 2008.
- (182) Unni, A. K.; Takenaka, N.; Yamamoto, H.; Rawal, V. H. *J. Am. Chem. Soc.* **2005**, *127*, 1336-1337.
- (183) Jorgensen, K. *Eur. J. Org. Chem.* **2004**, 2093-2102.
- (184) Gordillo, R.; Dudding, T.; Anderson, C.; Houk, K. *Org. Lett.* **2007**, *9*, 501-503.
- (185) Seebach, D.; Beck, A.; Heckel, A. *Angew. Chem. Int. Ed.* **2001**, *40*, 92-138.
- (186) Anderson, C.; Dudding, T.; Gordillo, R.; Houk, K. *Org. Lett.* **2008**, *10*, 2749-2752.
- (187) Connon, S. *Chem. Commun.* **2008**, *22*, 2499-2510.
- (188) Merino, P.; Marques-Lopez, R.; Tejero, T.; Herrera, R. *Synthesis* **2010**, *1*, 1-26.
- (189) Shen, J.; Tan, C.-H. *Organic & Biomolecular Chemistry* **2008**, *6*, 3229-3236.
- (190) Wittkopp, A.; Schreiner, P. *Chemistry of Dienes and Polyenes* **2000**, *2*, 1029-1088.
- (191) Lindstroem, U. M. *Chem. Rev.* **2002**, *102*, 2751-2771.
- (192) Wijnen, J. W.; Zavarise, S.; Engberts, J. *J. Org. Chem.* **1996**, *61*, 2001-2005.
- (193) Otto, S.; Blokzijl, W.; Engberts, J. *J. Org. Chem.* **1994**, *59*, 5372-5376.

- (194) Meijer, A.; Otto, S.; Engberts, J. *J. Org. Chem.* **1998**, *63*, 8989-8994.
- (195) Kong, S.; Evanseck, J. *J. Am. Chem. Soc.* **2000**, *122*, 10418-10427.
- (196) Rideout, D. C.; Breslow, R. *J. Am. Chem. Soc.* **1980**, *102*, 7816-7817.
- (197) Mbofufu, E. B.; Engberts, J. *J. Phys. Org. Chem.* **2007**, *20*, 764-770.
- (198) Blokzijl, W.; Blandamer, M. J.; Engberts, J. *J. Am. Chem. Soc.* **1991**, *113*, 4241-4246.
- (199) Kappe, C. O. *Angew. Chem.* **2004**, *43*, 6250-6284.
- (200) Schanche, J. *Molecular Diversity* **2003**, *7*, 293-300.
- (201) Hoogenboom, R.; Schubert, U. S. *Macromol. Rapid Commun.* **2007**, *28*, 368-386.
- (202) Baar, M.; Falcone, D.; Gordon, C. J. *Chem. Educ.* **2010**, *87*.
- (203) Perreux, L.; Loupy, A. *Tetrahedron* **2001**, *57*, 9199-9223.
- (204) Loupy, A.; Maurel, F.; Sabatie-Gogova, A. *Tetrahedron* **2003**, *60*, 1683-1691.
- (205) Hoz, A.; Diaz-Ortiz, A.; Moreno, A. *Chem. Soc. Rev.* **2005**, *34*, 164-178.
- (206) Baghurst, D. R.; Mingos, D. M. *J. Chem. Soc., Chem. Commun.* **1992**, *9*, 674-677.
- (207) Zhang, X.; Hayward, D. O.; Mingos, D. M. *Chem. Commun.* **1999**, *11*, 975-976.
- (208) Gedye, R. N.; Rank, W.; Westaway, K. C. *Can. J. Chem.* **1991**, *69*, 706-711.
- (209) Rikukawa, M. *Maku* **2003**, *28*, 14-20.
- (210) Hickner, M.; Ghassemi, H.; Kim, Y.; Einsla, B.; McGrath, J. *Chem. Rev.* **2004**, *104*, 4587-4611.
- (211) Ramharack, R.; Nguyen, T. *Journal of Polymer Science: Part C: Polymer Letters* **1987**, *25*, 93-98.
- (212) Odian, G. In *Principles of Polymerization*; Fourth Edition ed.; John Wiley & Sons: Hoboken, New Jersey, 2004, p 105-111.
- (213) Godschalx, J. P.; Romer, D. R.; So, Y. H.; Lysenko, Z.; Mills, M. E.; Buske, G. R.; Townsend, I., P.; Smith, J., D.; Martin, S.; DeVries, R.; The Dow Chemical Company, U., Ed. USA, 1999; Vol. US 5965679.
- (214) Qin, A.; Lam, J.; Tang, B. *Chem. Soc. Rev.* **2010**, *39*, 2522-2544.

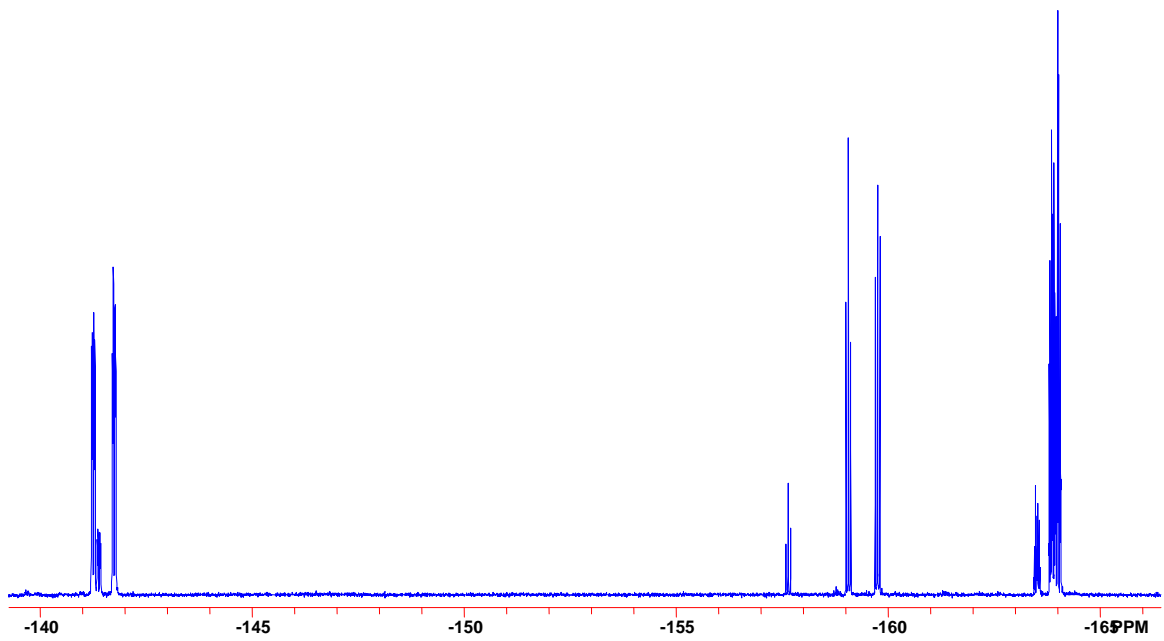
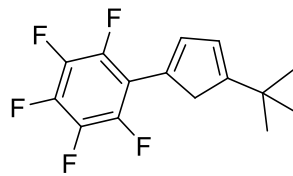
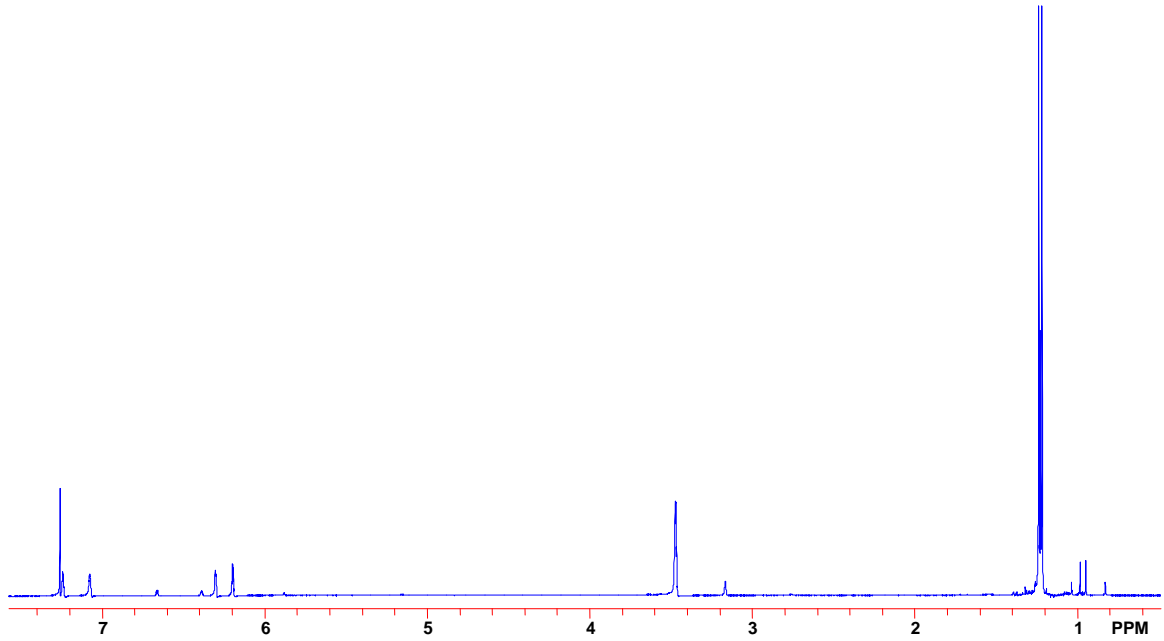
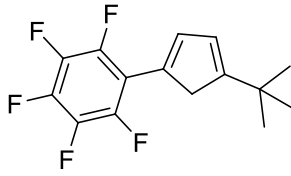
## Appendix A. NMR Spectra

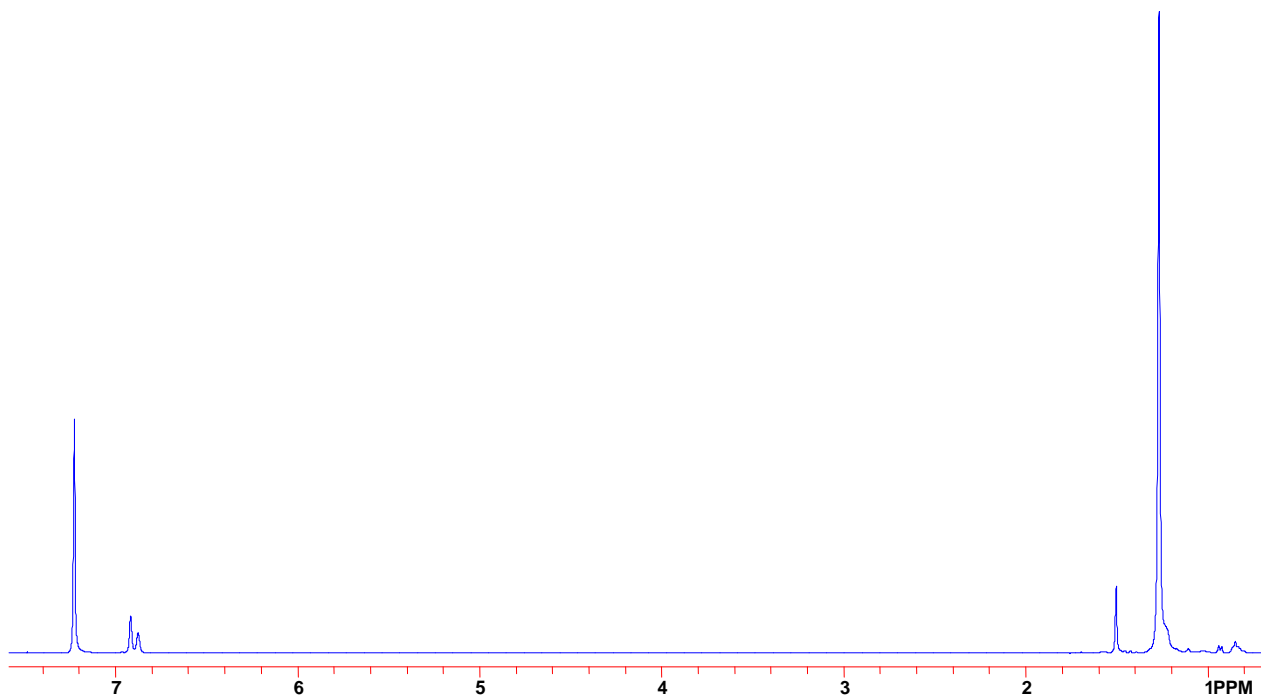
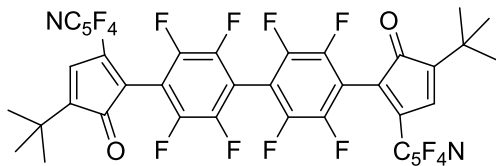


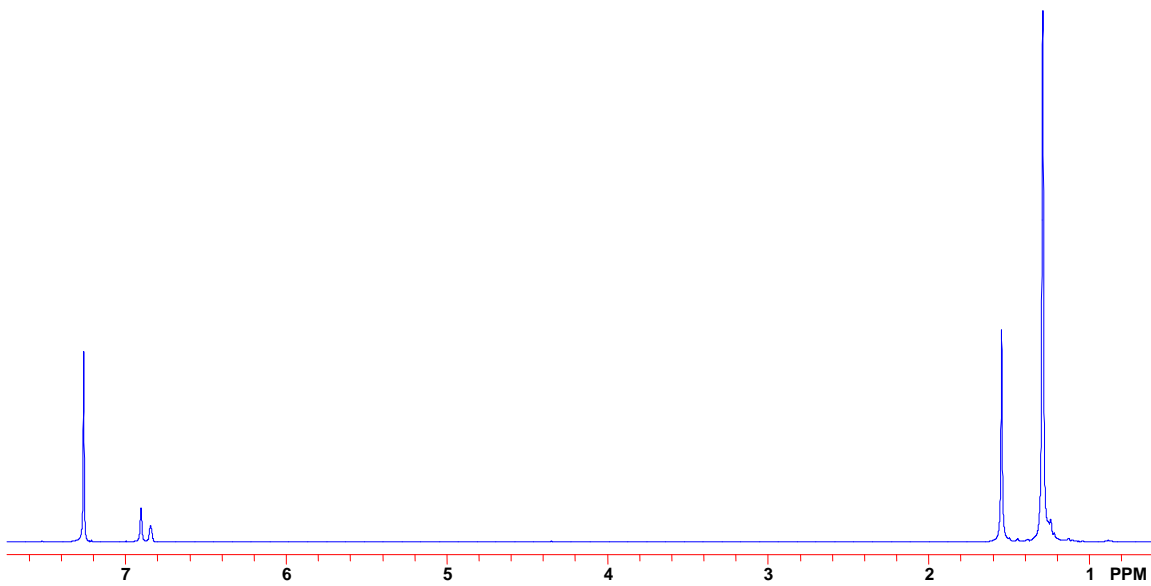
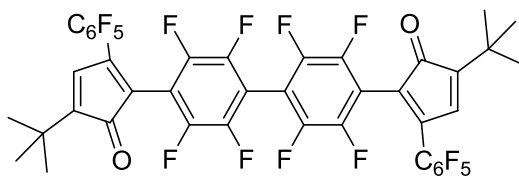
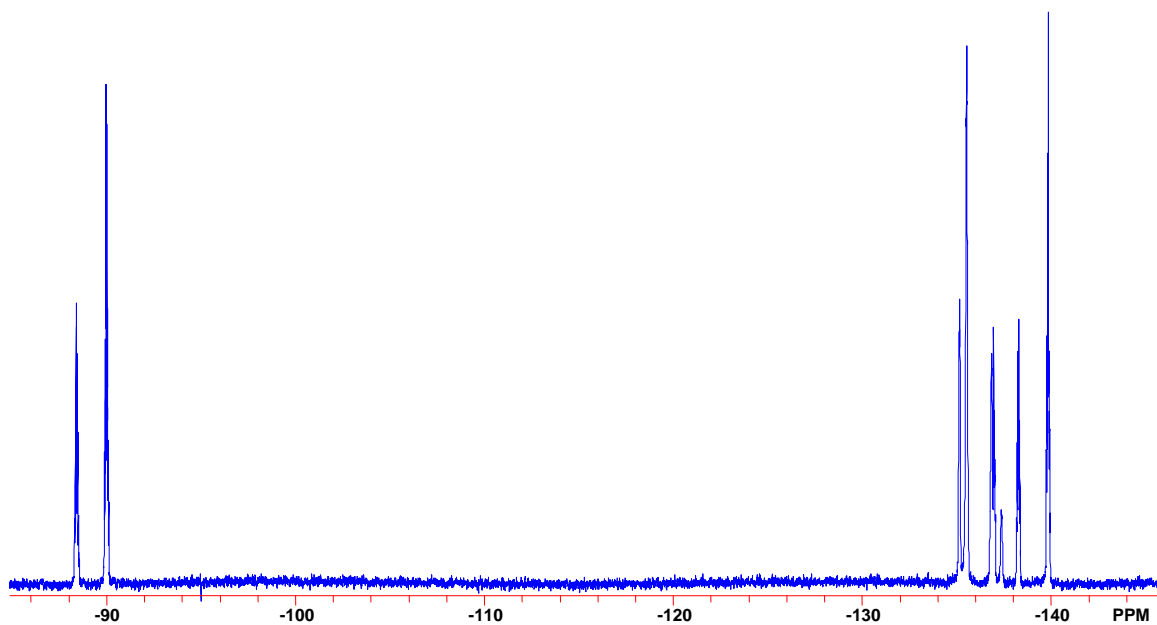
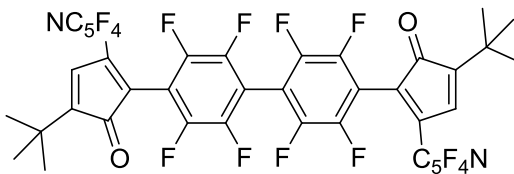


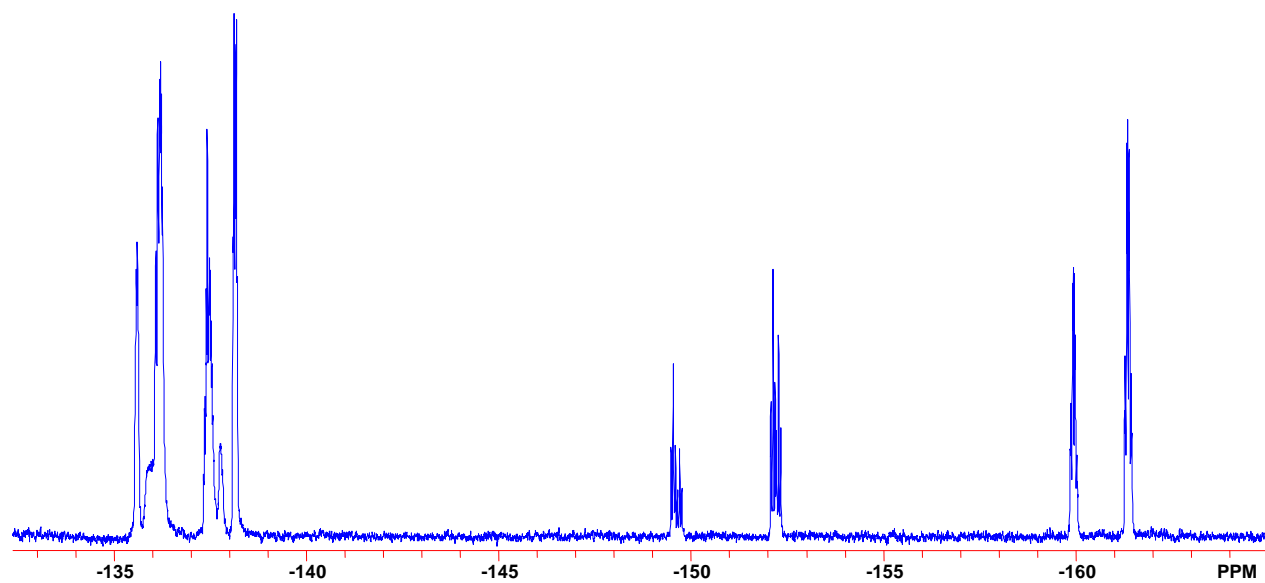
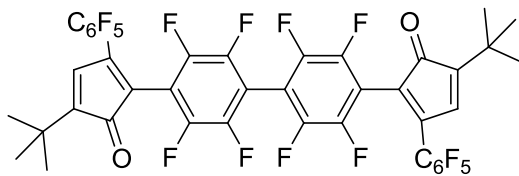


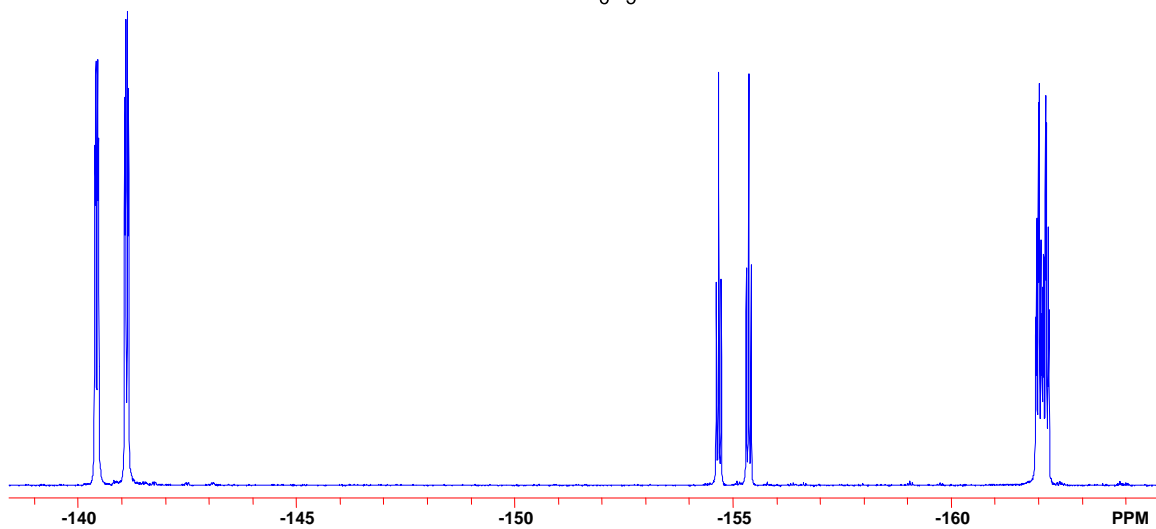
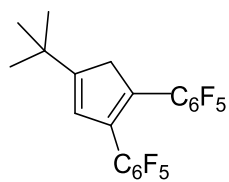
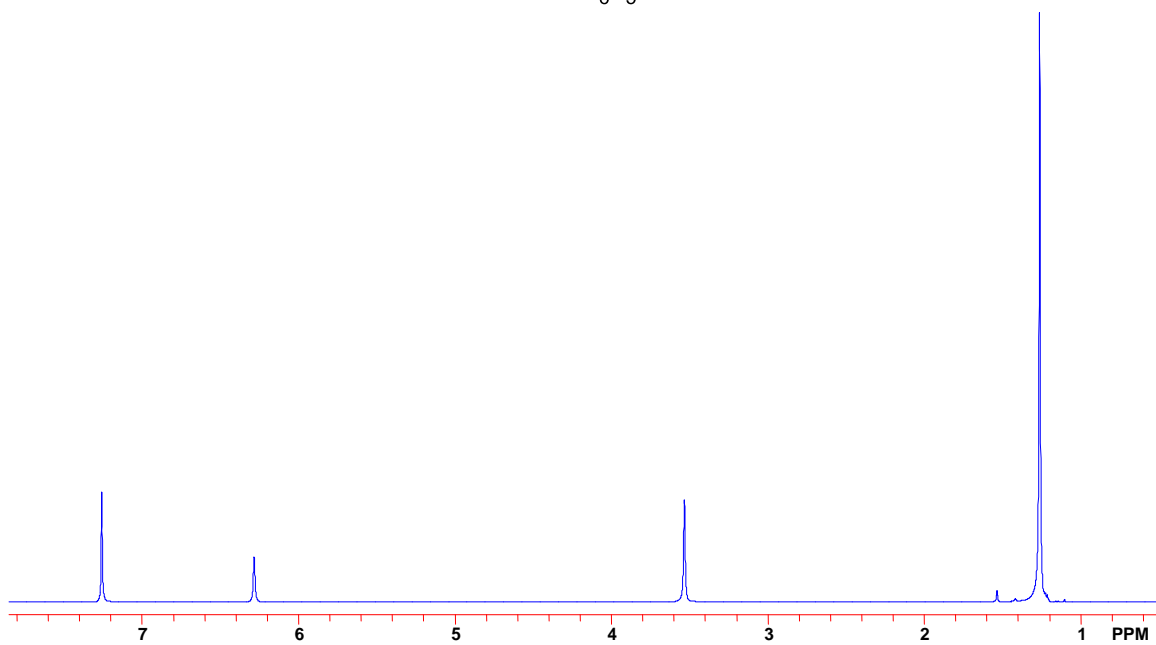
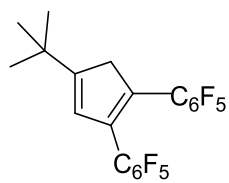


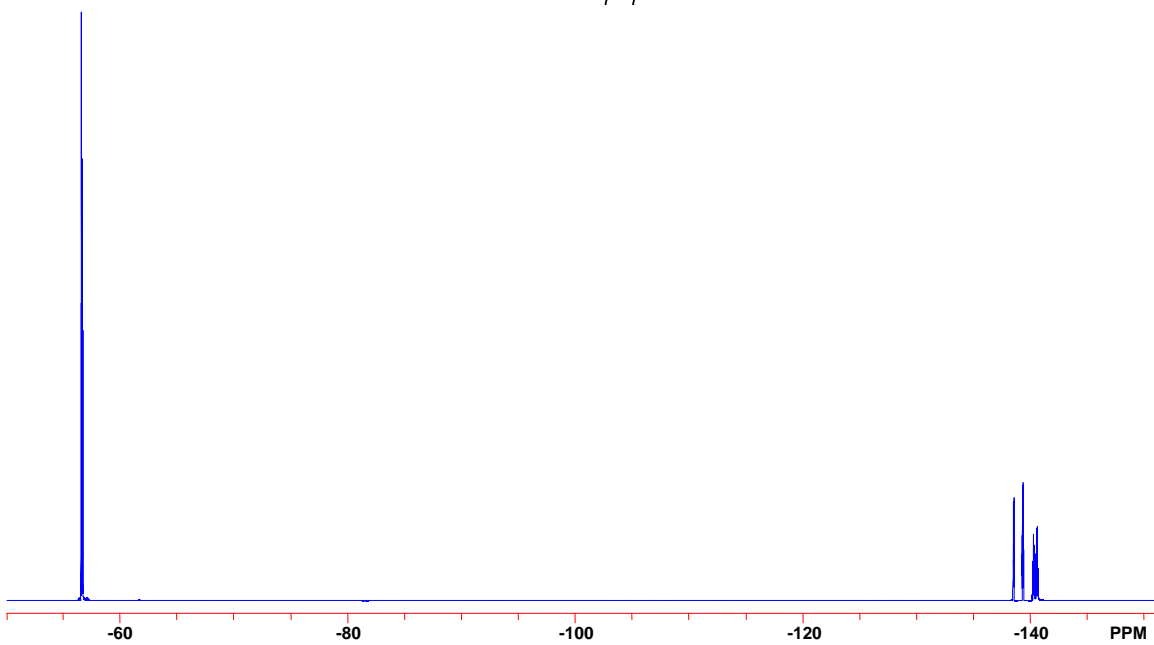
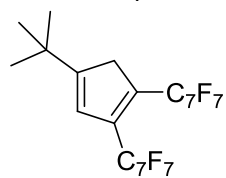
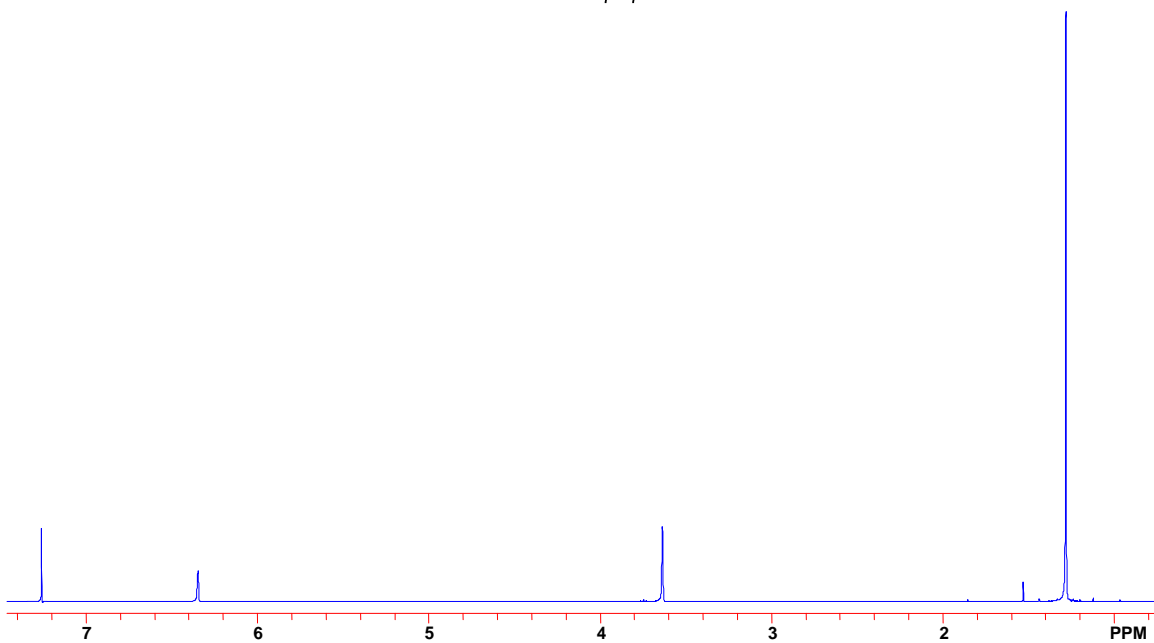
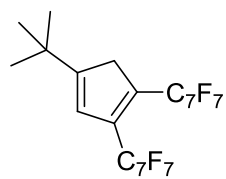


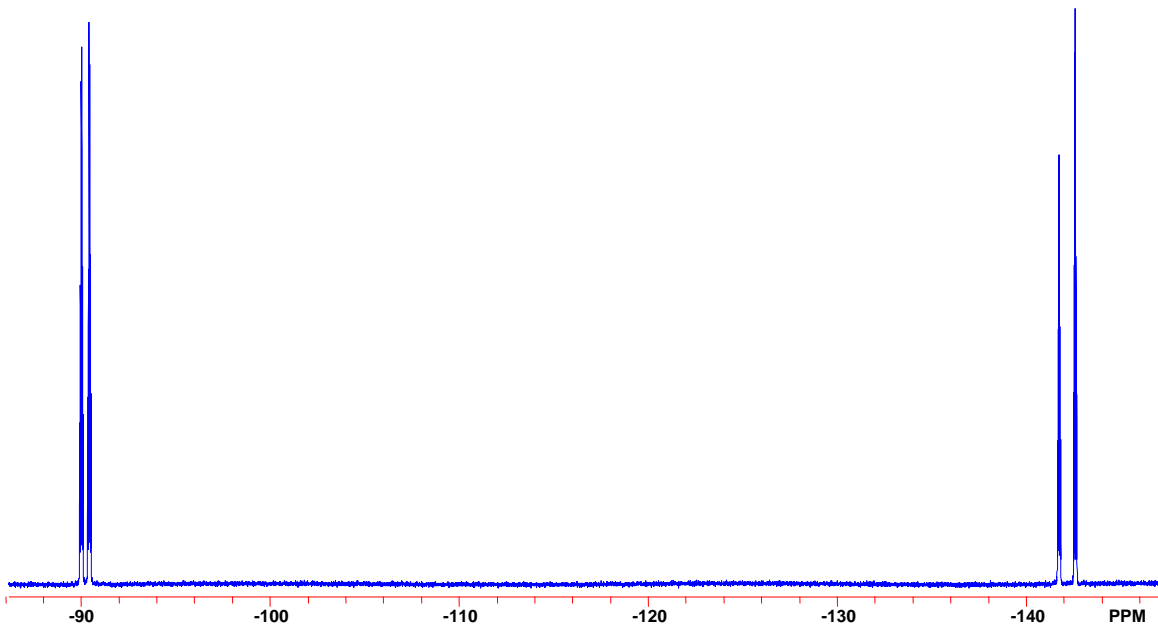
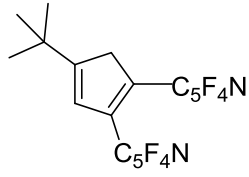
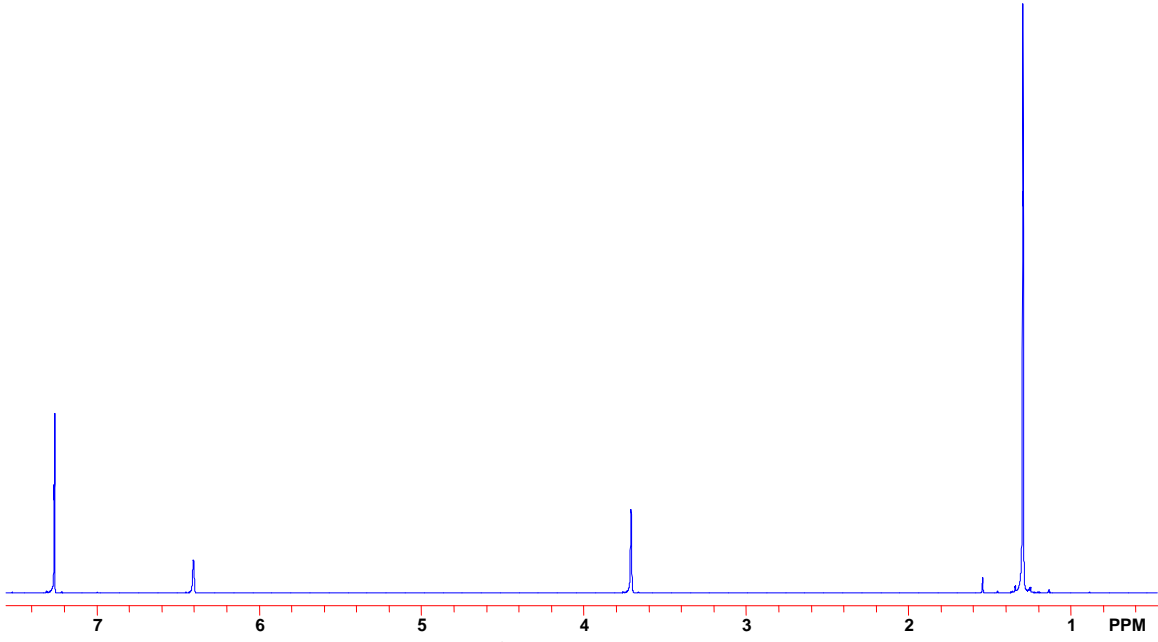
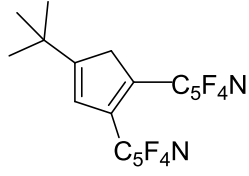


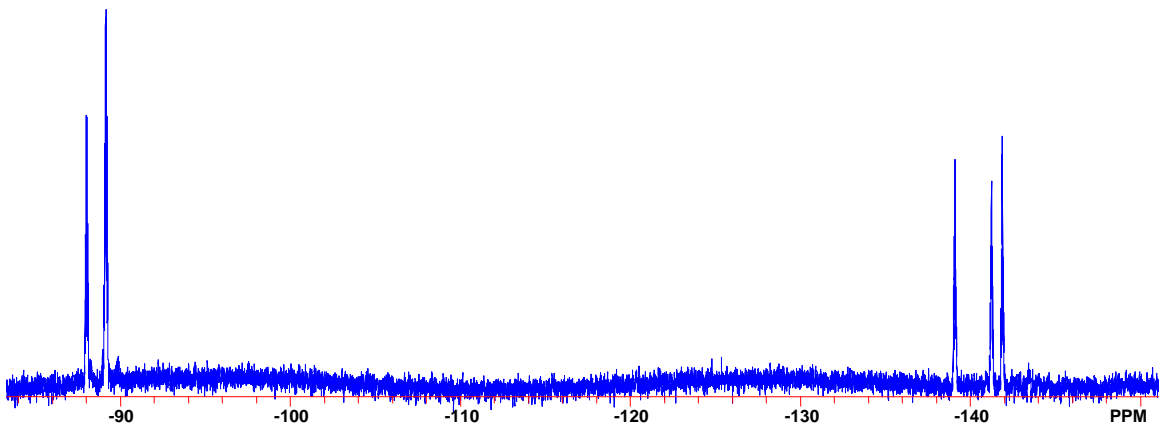
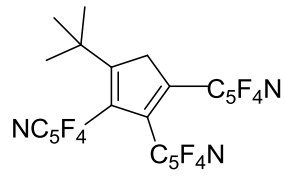
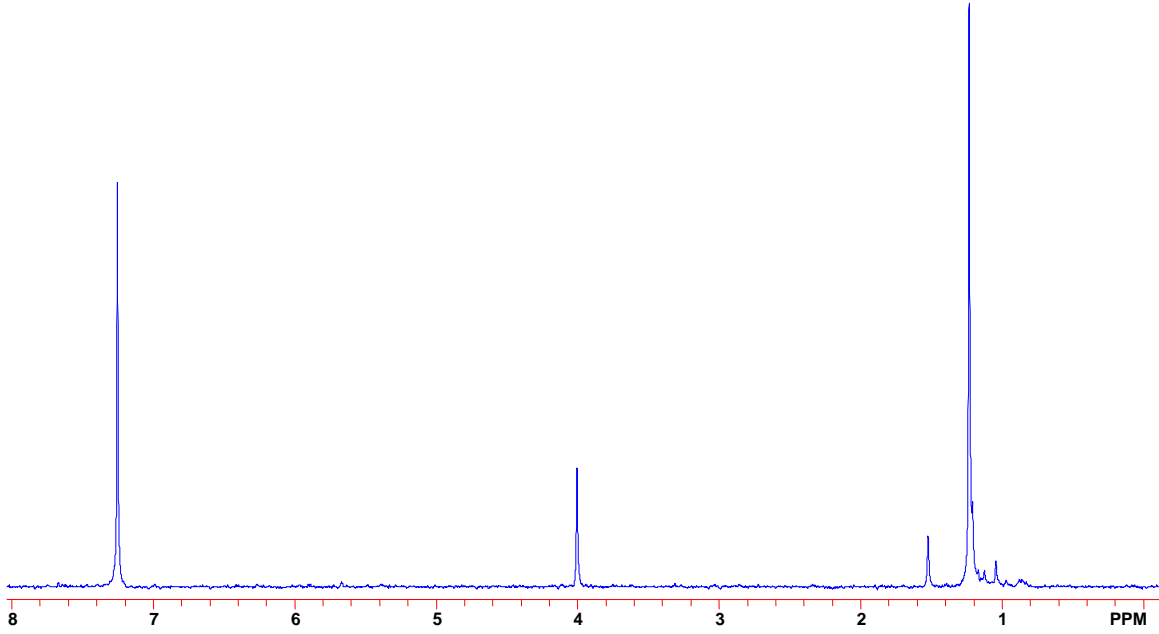
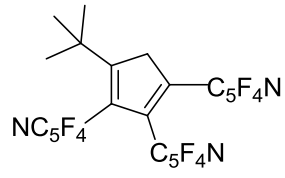


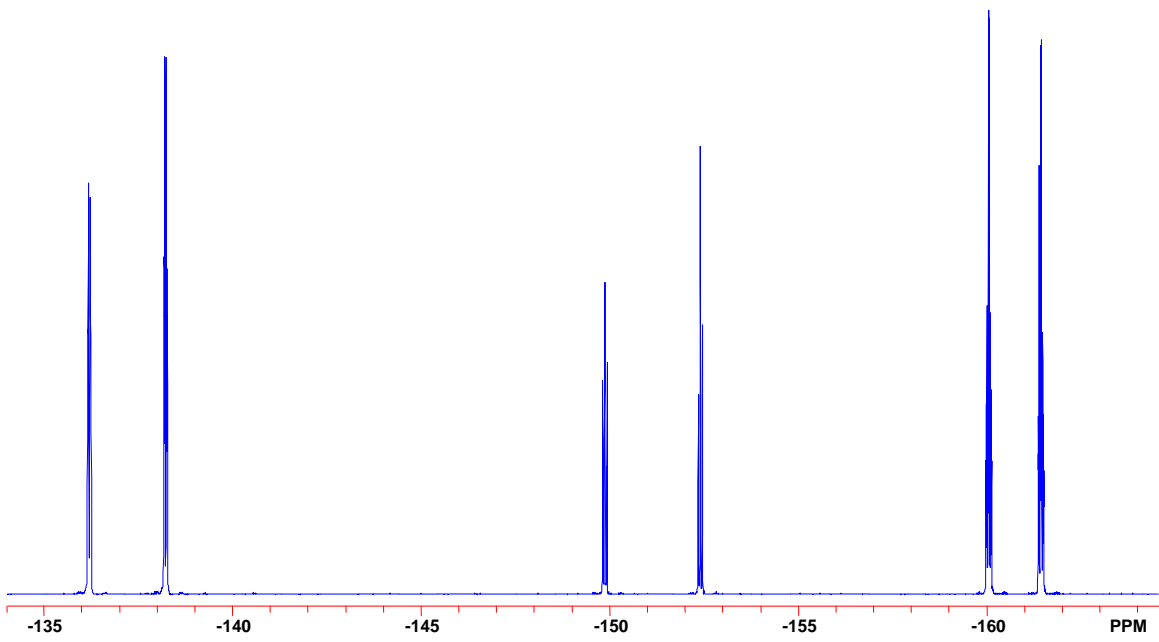
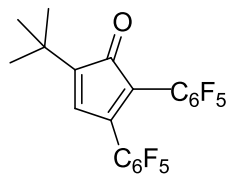
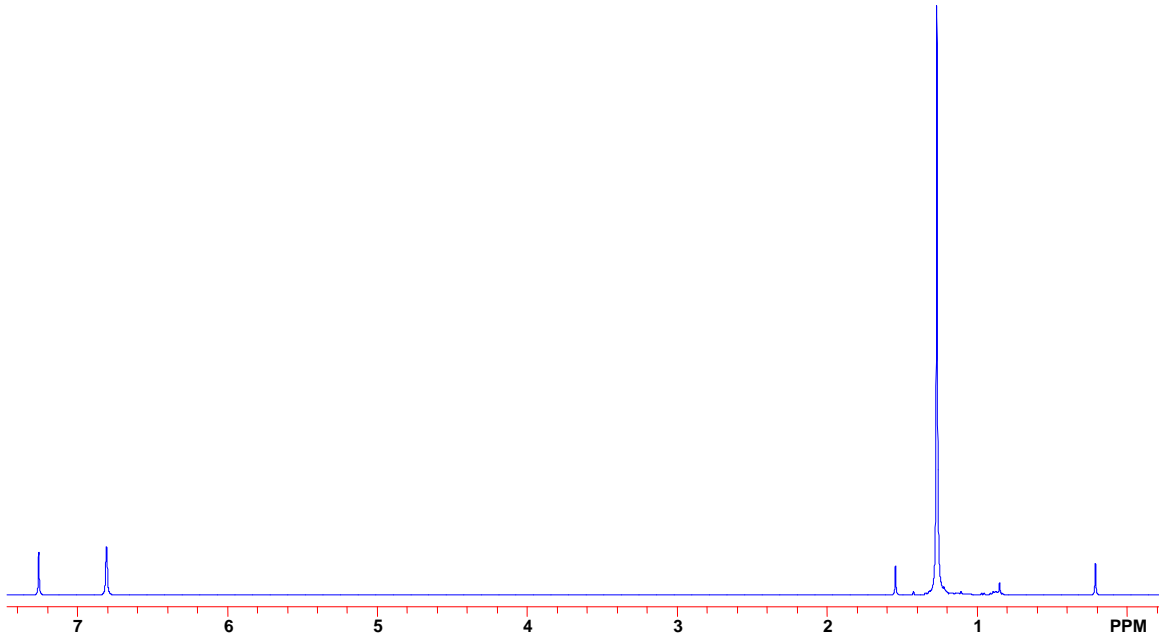
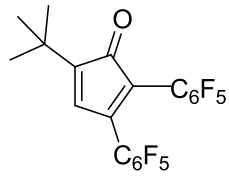


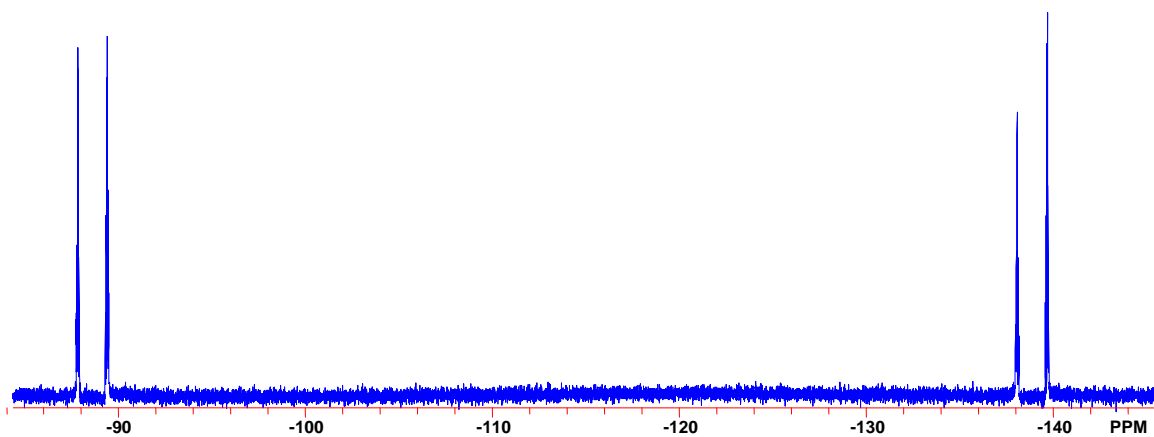
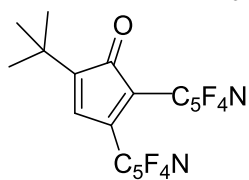
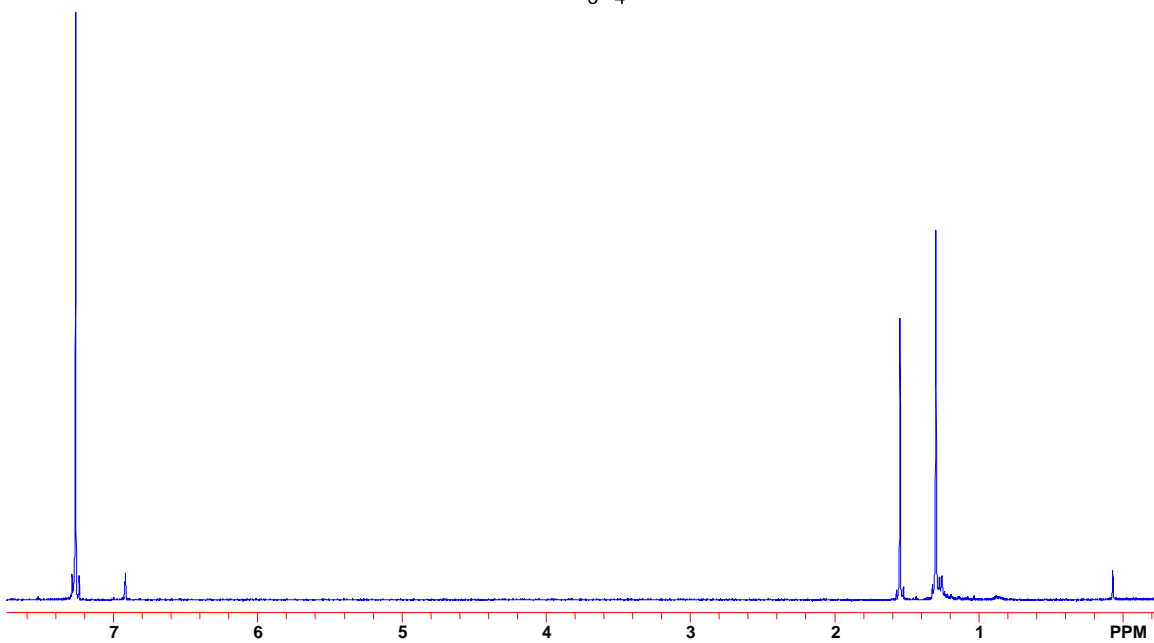
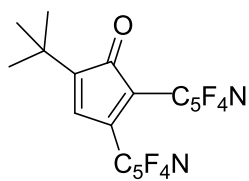


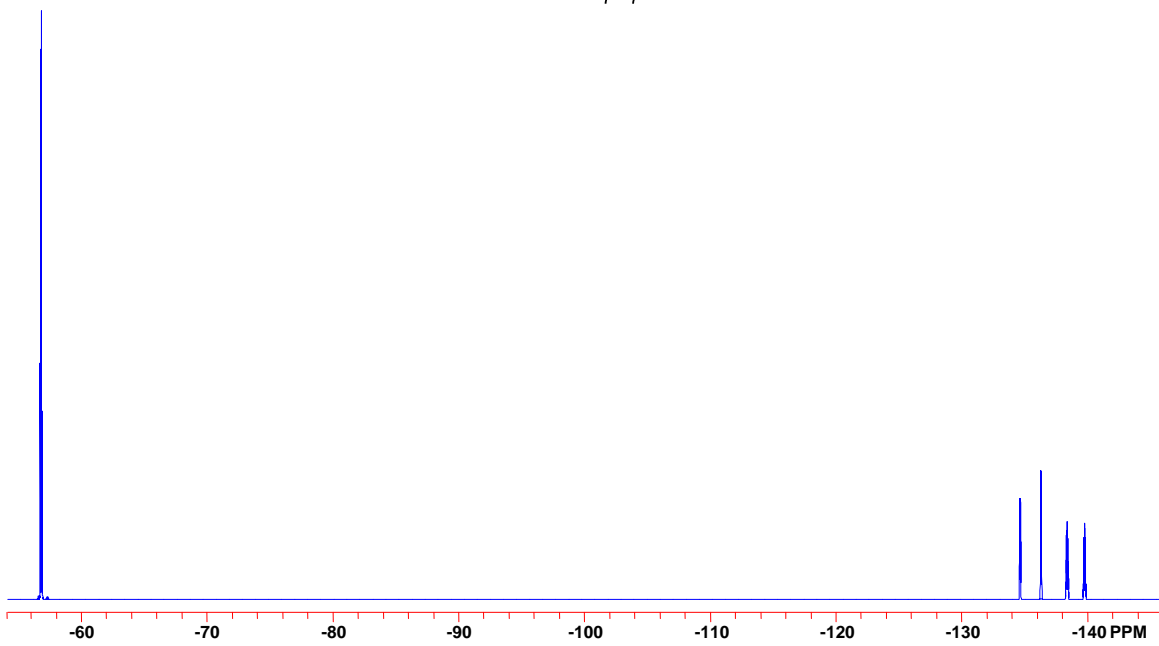
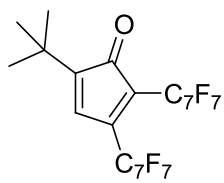
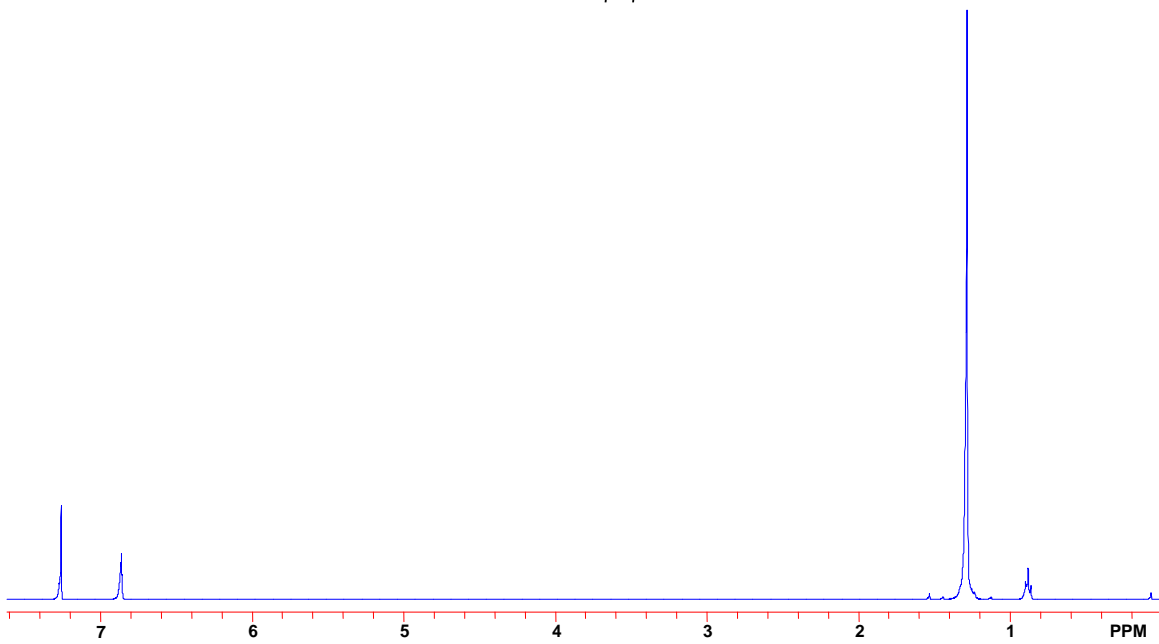
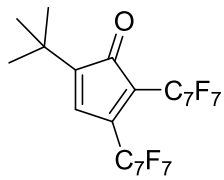


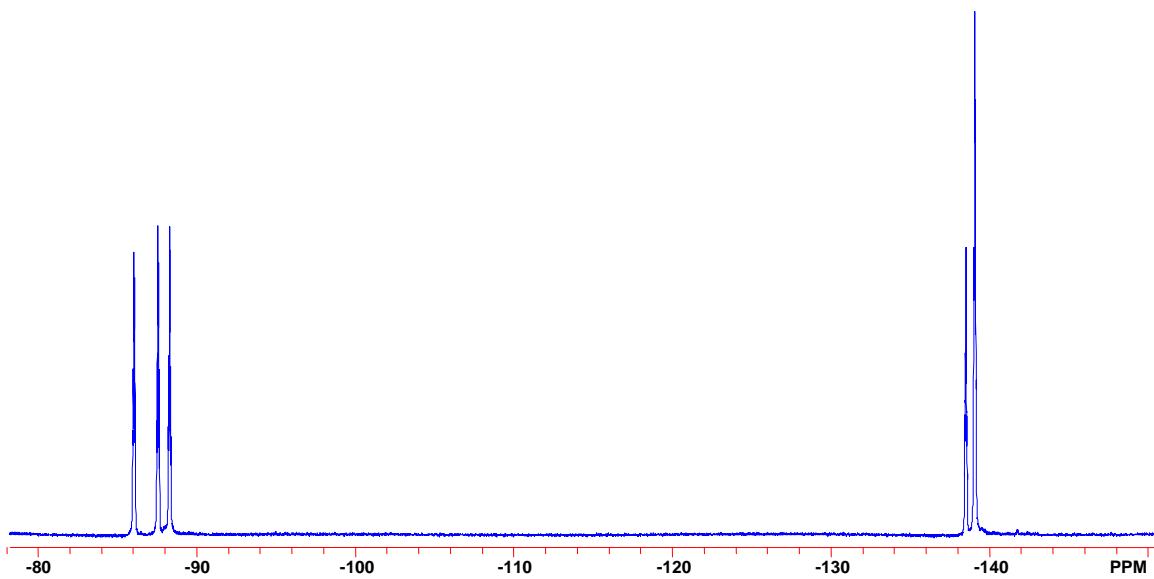
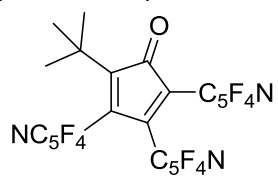
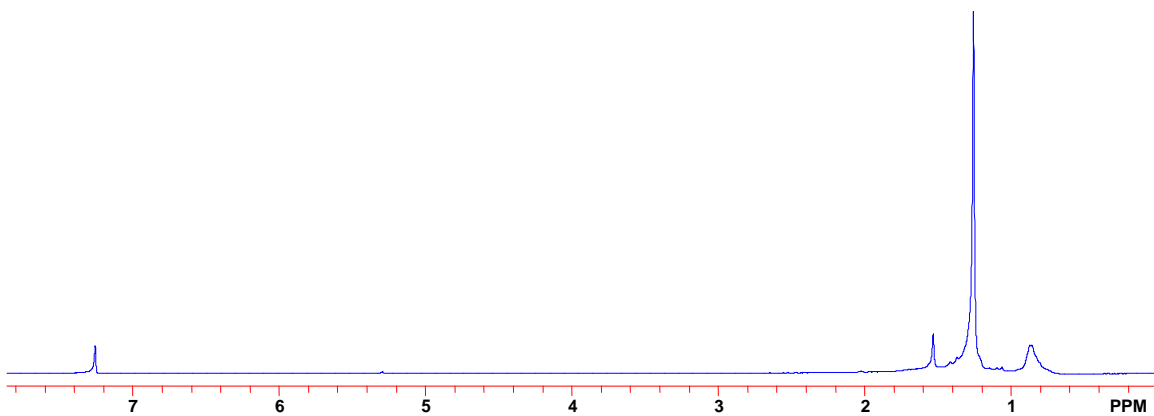
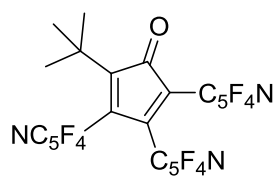


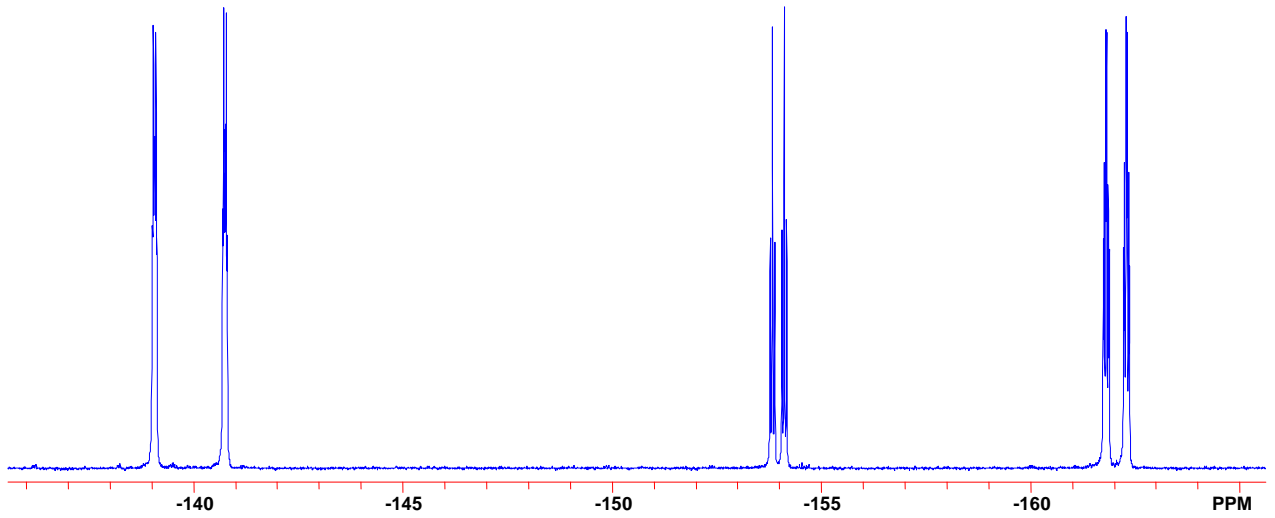
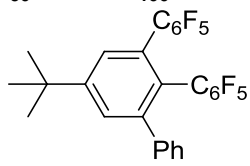
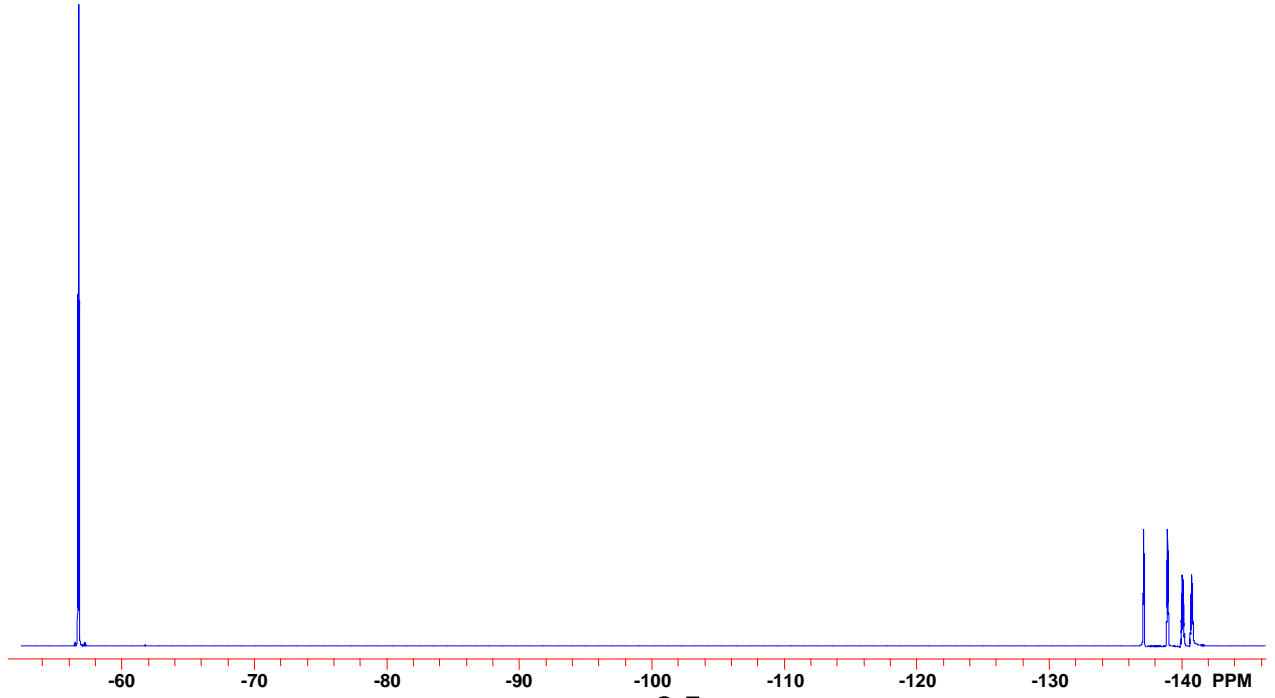
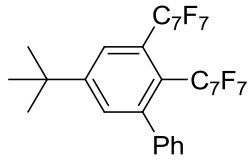


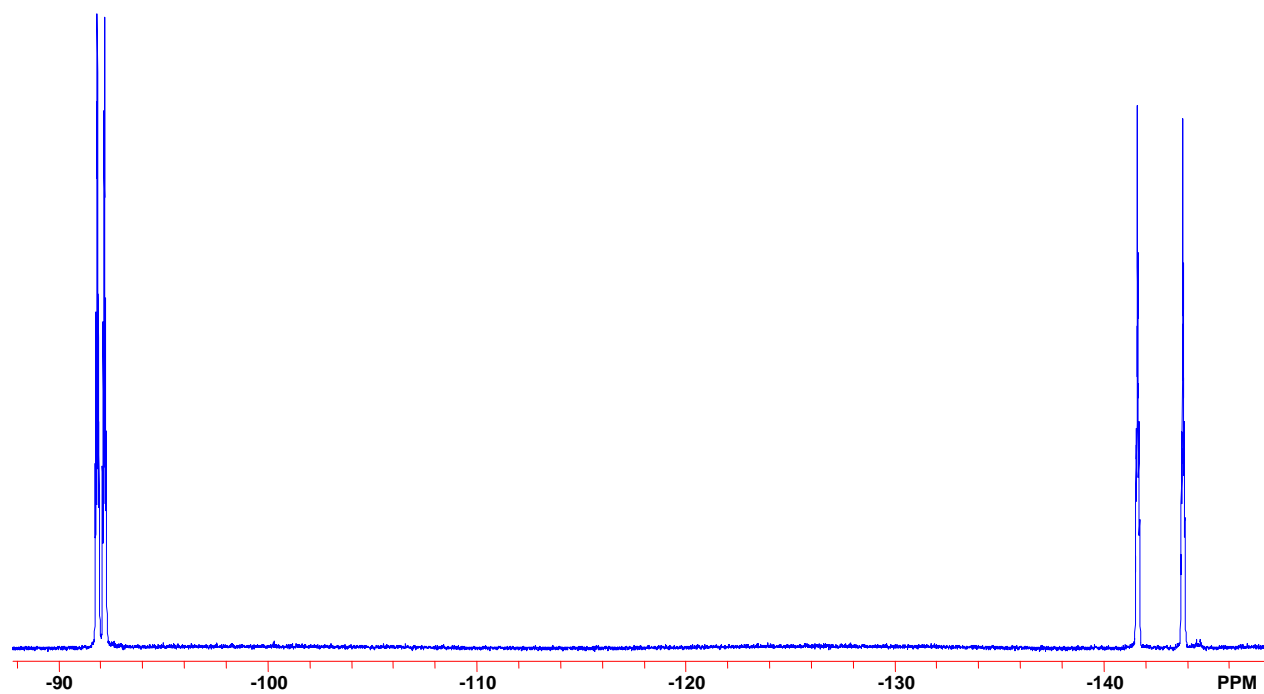
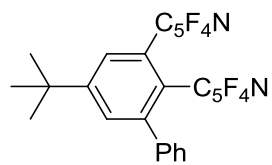












## Appendix B. Copyright Permission

### SPRINGER LICENSE TERMS AND CONDITIONS

Aug 06, 2010

---

---

This is a License Agreement between Jessica P Evans ("You") and Springer ("Springer") provided by Copyright Clearance Center ("CCC"). The license consists of your order details, the terms and conditions provided by Springer, and the payment terms and conditions.

**All payments must be made in full to CCC. For payment instructions, please see information listed at the bottom of this form.**

License Number	2480951224443
License date	Aug 02, 2010
Licensed content publisher	Springer
Licensed content publication	Molecular Diversity
Licensed content title	Microwave synthesis solutions from personal chemistry
Licensed content author	Jon-Sverre Schanche
Licensed content date	Jun 1, 2003
Volume number	7
Issue number	2
Type of Use	Thesis/Dissertation
Portion	Figures
Author of this Springer article	No
Order reference number	
Title of your thesis / dissertation	Synthesis of Highly Fluorinated Diels-Alder Polyphenylenes
Expected completion date	Aug 2010
Estimated size(pages)	150
Total	0.00 USD
Terms and Conditions	

#### Introduction

The publisher for this copyrighted material is Springer Science + Business Media. By clicking "accept" in connection with completing this licensing transaction, you agree that the following terms and conditions apply to this transaction (along with the Billing and

Payment terms and conditions established by Copyright Clearance Center, Inc. ("CCC"), at the time that you opened your Rightslink account and that are available at any time at <http://myaccount.copyright.com>).

#### Limited License

With reference to your request to reprint in your thesis material on which Springer Science and Business Media control the copyright, permission is granted, free of charge, for the use indicated in your enquiry. Licenses are for one-time use only with a maximum distribution equal to the number that you identified in the licensing process.

This License includes use in an electronic form, provided it is password protected or on the university's intranet, destined to microfilming by UMI and University repository. For any other electronic use, please contact Springer at ([permissions.dordrecht@springer.com](mailto:permissions.dordrecht@springer.com) or [permissions.heidelberg@springer.com](mailto:permissions.heidelberg@springer.com))

The material can only be used for the purpose of defending your thesis, and with a maximum of 100 extra copies in paper.

Although Springer holds copyright to the material and is entitled to negotiate on rights, this license is only valid, provided permission is also obtained from the (co) author (address is given with the article/chapter) and provided it concerns original material which does not carry references to other sources (if material in question appears with credit to another source, authorization from that source is required as well). Permission free of charge on this occasion does not prejudice any rights we might have to charge for reproduction of our copyrighted material in the future.

#### Altering/Modifying Material: Not Permitted

However figures and illustrations may be altered minimally to serve your work. Any other abbreviations, additions, deletions and/or any other alterations shall be made only with prior written authorization of the author(s) and/or Springer Science + Business Media. (Please contact Springer at [permissions.dordrecht@springer.com](mailto:permissions.dordrecht@springer.com) or [permissions.heidelberg@springer.com](mailto:permissions.heidelberg@springer.com))

#### Reservation of Rights

Springer Science + Business Media reserves all rights not specifically granted in the combination of (i) the license details provided by you and accepted in the course of this licensing transaction, (ii) these terms and conditions and (iii) CCC's Billing and Payment terms and conditions.

#### Copyright Notice:

Please include the following copyright citation referencing the publication in which the material was originally published. Where wording is within brackets, please include verbatim.

"With kind permission from Springer Science+Business Media: <book/journal title, chapter/article title, volume, year of publication, page, name(s) of author(s), figure

number(s), and any original (first) copyright notice displayed with material>."

Warranties: Springer Science + Business Media makes no representations or warranties with respect to the licensed material.

#### Indemnity

You hereby indemnify and agree to hold harmless Springer Science + Business Media and CCC, and their respective officers, directors, employees and agents, from and against any and all claims arising out of your use of the licensed material other than as specifically authorized pursuant to this license.

#### No Transfer of License

This license is personal to you and may not be sublicensed, assigned, or transferred by you to any other person without Springer Science + Business Media's written permission.

#### No Amendment Except in Writing

This license may not be amended except in a writing signed by both parties (or, in the case of Springer Science + Business Media, by CCC on Springer Science + Business Media's behalf).

#### Objection to Contrary Terms

Springer Science + Business Media hereby objects to any terms contained in any purchase order, acknowledgment, check endorsement or other writing prepared by you, which terms are inconsistent with these terms and conditions or CCC's Billing and Payment terms and conditions. These terms and conditions, together with CCC's Billing and Payment terms and conditions (which are incorporated herein), comprise the entire agreement between you and Springer Science + Business Media (and CCC) concerning this licensing transaction. In the event of any conflict between your obligations established by these terms and conditions and those established by CCC's Billing and Payment terms and conditions, these terms and conditions shall control.

#### Jurisdiction

All disputes that may arise in connection with this present License, or the breach thereof, shall be settled exclusively by the country's law in which the work was originally published.

Other terms and conditions:

v1.2

**Gratis licenses (referencing \$0 in the Total field) are free. Please retain this printable license for your reference. No payment is required.**

**If you would like to pay for this license now, please remit this license along with your payment made payable to "COPYRIGHT CLEARANCE CENTER" otherwise you will be invoiced within 48 hours of the license date. Payment should be in the form of a check or money order referencing your account number and this invoice number RLNK10824792.**

**Once you receive your invoice for this order, you may pay your invoice by credit card. Please follow instructions provided at that time.**

**Make Payment To:  
Copyright Clearance Center  
Dept 001  
P.O. Box 843006  
Boston, MA 02284-3006**

**If you find copyrighted material related to this license will not be used and wish to cancel, please contact us referencing this license number 2480951224443 and noting the reason for cancellation.**

**Questions? [customer care@copyright.com](mailto:customer care@copyright.com) or +1-877-622-5543 (toll free in the US) or +1-978-646-2777.**